TG—1069
JUNE 1969
Copy No. 27

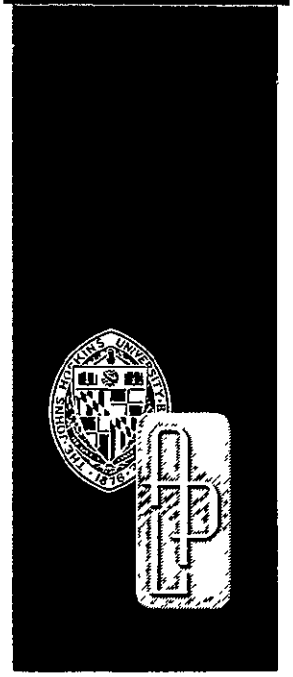

Technical Memorandum

INVESTIGATION OF THE EARTH'S GRAVITATIONAL EFFECTS ON THE MOTION OF NEAR EARTH SATELLITES

by S. M. YIONOULIS

W12-004

THE JOHNS HOPKINS UNIVERSITY ▪ APPLIED PHYSICS LABORATORY

TG–1069
JUNE 1969

Technical Memorandum

INVESTIGATION OF THE EARTH'S GRAVITATIONAL EFFECTS ON THE MOTION OF NEAR EARTH SATELLITES

by S. M. YIONOULIS

This work was supported by the National Aeronautics and Space Administration, Office of Space Science and Applications, under Task I of Contract NOw 62–0604–C.

THE JOHNS HOPKINS UNIVERSITY • APPLIED PHYSICS LABORATORY
8621 Georgia Avenue, Silver Spring, Maryland 20910
Operating under Contract NOw 62-0604-c with the Department of the Navy

THE JOHNS HOPKINS UNIVERSITY
APPLIED PHYSICS LABORATORY
SILVER SPRING MARYLAND

ABSTRACT

The accuracy with which the earth's gravitational field can be defined from an analysis of satellite data is strongly dependent upon the satellite constellation used. The constellation selected must satisfy several criteria. The objective of this study was to produce quantitative information on the effects of the geopotential harmonics on the motion of satellites for a large variety of orbits. This data can then be used to investigate satellite constellations which will yield useful geodetic information.

THE JOHNS HOPKINS UNIVERSITY
APPLIED PHYSICS LABORATORY
SILVER SPRING MARYLAND

TABLE OF CONTENTS

THE JOHNS HOPKINS UNIVERSITY
APPLIED PHYSICS LABORATORY
SILVER SPRING MARYLAND

I. INTRODUCTION

In future satellite geodesy programs to improve on the current models of the geopotential, additional satellite orbits will be needed. Some of the present models of the earth's gravity potential contain over 200 coefficients. It is fairly obvious that as more terms are added to the model the problem of separating out their individual effects becomes increasingly difficult. Separation of these harmonic effects is strongly dependent on the orbital characteristics of the satellites used in the analysis. Therefore serious consideration should be given to the problem of defining a satellite constellation to be utilized in a satellite geodesy program.

There are several factors to be considered in selecting this satellite constellation. Since the major expense of a satellite geodesy program is in the cost of the satellites and their launch vehicles, it is important that the constellation consist of the minimum number of satellites that is needed to adequately determine the geopotential model. This implies that maximum use of existing satellite data should be made. Additional satellites therefore should be selected to complement the existing data, which are of sufficient quantity and quality.

The main objective of this paper is to provide quantitative information on the contributions of the harmonics in the earth's gravitational field to the motion of a near-earth satellite. The harmonics through 20th degree and order are considered. This provides information necessary in selecting a constellation to be used in a satellite geodesy program. Most of the

analyses are contained in the Appendices. The notation used is given in section II and the main results are discussed in section III.

II. DEFINITIONS AND NOTATIONS

x,y,z = inertial cartesian components of the satellite

r,φ,λ = spherical radius, latitude, and longitude of the satellite

H,C,L = components in a right handed coordinate system with axes in the three directions
1 - radius vector from Earth's C.G. to instantaneous position of the satellite
2 - negative angular momentum vector direction
3 - component of satellite velocity perpendicular to radius vector and lying in the orbital plane of the theoretically computed orbit

a = semi-major axis of the satellite orbit

e = eccentricity

i = inclination

ω = argument of perigee

Ω = longitude of ascending node

f = true anomaly

β = $f + \omega$

M = mean anomaly

E = eccentric anomaly

$\bar{n}$ = mean motion

Λ_G = right ascension of Greenwich

$U(r,\varphi,\lambda)$ = potential function

μ = gravitational constant for the Earth ($= 398601.5\ km^3/sec^2$)

$P_\ell^m(\sin\varphi)$ = associated Legendre polynomial of degree ℓ and order m

C_ℓ^m, S_ℓ^m = unnormalized coefficients associated with the spherical harmonics of degree and order (ℓ,m).

$N_{\ell m}$ = normalization used for spherical harmonics

$$N_{\ell m} = \left[\frac{(\ell-m)!\ (2\ell+1)\ (2-\delta_{om})}{(\ell+m)!}\right]^{1/2}$$

$$\delta_{om} = \begin{cases} 0 \text{ for } m \neq 0 \\ 1 \text{ for } m = 0 \end{cases}.$$

R_e = near equatorial radius of the earth (=6378.144 km)

Zero subscripts are used to designate parameters associated with a reference orbit.

III. DISCUSSION OF RESULTS

In selecting a satellite constellation to be used in a program to determine a model of the earth's gravity field, it is important to understand the physical effects each harmonic in the geopotential expansion will have on the satellite's motion. Studies have already been made on using resonant orbits for a geodetic program [1,2]. Resonance occurs when the satellite orbital frequency becomes commensurate with an integer multiple of the earth's sidereal rate. This results in greatly amplified motions of the satellite due to those harmonics which are in resonance, thus allowing for a more accurate determination of their coefficients. However this approach would require a considerably larger satellite constellation, since a given orbit can be selected to resonate with only a relatively small subset of the geopotential harmonics. As the major cost in a satellite geodesy program is in the satellites and their launch vehicles, the use of resonant orbits becomes undesirable, financially.

It is important, however, in future attempts to improve the geopotential model to incorporate data from satellites which are more sensitive to the effects of the earth's gravity field, particularly to the higher order harmonics. This can be achieved through the use of very low altitude orbits. Until recently, these orbits were not useful because of the unpredictableness of atmospheric drag which contaminated the data. Considerable effort has been put into the development of a thrust package to be incorporated into the design of a satellite which would counteract the effects of all non-gravitational forces acting on the satellite [3]. This device would make feasible the use of low-altitude orbits as well as simplify

the analysis required to reduce the tracking data received. Since the effects of radiation are also eliminated, the inclusion of this package on satellites at all altitudes would be desirable.

To study the effects the harmonics in the geopotential expansion will have on the motion of a satellite, their contributions are derived in a coordinate system moving in inertial space. The origin is located at the satellite as defined by a reference orbit. The vector difference between the true position and the position as defined by the reference orbit is partitioned into the H, C, L components of this system. (Definitions are given in section II.) Contributions of the geopotential harmonics in this system are derived in Appendix B. The final results given in equations (B.22) - (B.24) are restated here for discussion purposes.

$$H_{\ell m} = \frac{\mu}{n^2 R_e^2}\left[\frac{1}{(1-e^2)}\right]^{\frac{\ell+2}{2}}\left(\frac{R_e}{a}\right)^{\ell+2}\sum_{p=0}^{\ell}\sum_{k=-\infty}^{\infty} I_{\ell mp}^{(0,0)}(i)\, F_{\ell,G_1,p,k}^{(H)}(e)\, S_{\ell,m,p,k} \qquad (B.22)$$

$$C_{\ell m} = \frac{\mu}{n^2 R_e^2}\left[\frac{1}{(1-e^2)}\right]^{\frac{\ell+2}{2}}\left(\frac{R_e}{a}\right)^{\ell+2}\sum_{p=0}^{\ell}\sum_{k=-\infty}^{\infty}\left[2\cos i\, I_{\ell mp}^{(1,0)}(i) - m \sin i\, I_{\ell mp}^{(0,1)}(i)\right] F_{\ell,G_2,p,k}^{(C)}(e)\, S_{\ell-1,m,p,k} \qquad (B.23)$$

$$L_{\ell m} = \frac{\mu}{n^2 R_e^2}\left[\frac{1}{(1-e^2)}\right]^{\frac{\ell+2}{2}}\left(\frac{R_e}{a}\right)^{\ell+2}\sum_{p=0}^{\ell}\sum_{k=-\infty}^{\infty} I_{\ell mp}^{(0,0)}(i)\, F_{\ell,G_1,p,k}^{(L)}(e)\,(-1)\,\bar{S}_{\ell,m,p,k} \qquad (B.24)$$

From the definition of β_1 in Appendix A, equation (A.21), we made the substitution

$$\frac{1 + \beta_1^2}{1 - \beta_1^2} = (1 - e^2)^{-1/2}$$

in the above expressions. The S-functions are defined as

$$S_{\ell mpk} = (-1)^{\left[\frac{\ell-m}{2}\right]} \left\{ \begin{bmatrix} \overline{C}_\ell^m \\ -\overline{S}_\ell^m \end{bmatrix} \begin{matrix} (\ell-m)\text{even} \\ (\ell-m)\text{odd} \end{matrix} \cos\left[(\ell-2p+k)M + (\ell-2p)\omega + m(\Omega-\Lambda_G)\right] \right.$$
$$\left. + \begin{bmatrix} \overline{S}_\ell^m \\ \overline{C}_\ell^m \end{bmatrix} \begin{matrix} (\ell-m)\text{even} \\ (\ell-m)\text{odd} \end{matrix} \sin\left[(\ell-2p+k)M + (\ell-2p)\omega + m(\Omega-\Lambda_G)\right] \right\} \quad \text{(A.28)}$$

For a given satellite orbit (to the accuracy of the solutions), the time dependence of the solutions are contained in these S-functions. They encompass all possible frequencies that can be generated by a harmonic of degree ℓ, and order m. The summing index k denotes those frequencies generated by terms of order e^k and higher. For each frequency the inclination and eccentricity dependence can be factored into the I and F functions, respectively. The I-function is defined in equations (A.18) and (A.19) The F-functions are given in equations (B.26)-(B.28). Because of their complexity they will not be rewritten here. The frequency contributions are imbedded in the F-functions. From their given form, it is apparent that the amplitude of the contribution of each oscillation is inversely proportional to its corresponding frequency. Therefore, in general,

the low frequency terms associated with each harmonic will be the major contributors to the satellite's motion. Thus by examining in detail the amplitudes of these low frequency terms, significant insight into the effects of the geopotential harmonics on the satellite's motion can be obtained. With the given partitioning of the inclination and eccentricity effects, one can investigate a much larger variety of orbits.

The possible frequencies that arise for a given ℓ and m can be written as

$$(\ell-2p+k)\,\dot{M} + (\ell-2p)\,\dot{\omega} + m\,(\dot{\Omega}-\dot{\Lambda}_G) \qquad (1)$$

As a general rule, the larger amplitudes are associated with the low frequency terms which occur when $k = 0$. This follows from the fact that k incorporates those frequencies which result from the eccentricity effects of the harmonics. (It should be noted that these low frequencies associated with the harmonics of a given order m and of the same parity in degree ℓ will be identical. This is the main reason why it is difficult to separate any two of these harmonics using data from only a single satellite.)

In the H and L equations (B.22) and (B.24), the low frequencies investigated were for values of $\ell-2p$ equal to 0 and 1. The inclination dependences in these components are identical and the graphs associated with this function are given in Appendix C where

$$F_2 = I^{(0,0)}_{\ell mp}(i) \qquad (2)$$

Each graph contains one or more plots of F_2 versus inclination for a specified value of m for the range $0^\circ \leq i \leq 180^\circ$. Each curve corresponds to a different value of ℓ and the set of curves in each graph consists of those ℓ values which yield the same low frequency terms for the given m. This grouping is helpful in selecting orbital inclinations which will give good separation of the harmonics represented. The graphs indicate that the contributions of the harmonics of order 13 and higher for satellites with orbital inclinations less than 40° and greater than 150° will be negligible.

The inclination dependence in the C component is given by

$$F_1 = 2 \cos i \, I^{(1,0)}_{\ell mp}(i) - m \sin i \, I^{(0,1)}_{\ell mp}(i) \qquad (3)$$

Similar graphs of this function are presented in Appendix D for values of ℓ-2p-1 equal to 0 and 1. Since the inclination functions are independent of k, the values generated are applicable for the frequencies corresponding to all values of k.

To obtain meaningful information on the effects of varying eccentricity, it is necessary to consider simultaneously the semi-major axis contributions. This is accomplished by requiring that the perigee altitude remain constant for all eccentricity values considered. You can then express $\underline{a}$ as a function of $\underline{e}$ and the fixed perigee altitude. For computational purposes we arbitrarily fixed the perigee altitude at 638 km so that

$$\frac{a}{R_e} = \frac{1.1}{(1-e)}$$

By also defining

$$\left.\begin{aligned} G_1 &= (\ell-2p)\frac{\dot{\omega}}{\bar{n}} + m\left(\frac{\dot{\Omega}-\dot{\Lambda}_G}{\bar{n}}\right) \\ G_2 &= (\ell-2p-1)\frac{\dot{\omega}}{\bar{n}} + m\left(\frac{\dot{\Omega}-\dot{\Lambda}_G}{\bar{n}}\right) \end{aligned}\right\} \tag{4}$$

the explicit dependence of the functions on m, $\dot{\omega}$, $\dot{\Omega}$, and $\dot{\Lambda}_G$ are contained in a single parameter. The final form of the functions plotted for each component is given by

$$F(H) = \frac{1}{(1.1)^{\ell+2}}\left(\frac{1-e}{1+e}\right)^{\frac{\ell+2}{2}} F^{(H)}_{\ell,G_1,p,k}(e) \tag{5}$$

$$F(C) = \frac{1}{(1.1)^{\ell+2}}\left(\frac{1-e}{1+e}\right)^{\frac{\ell+2}{2}} F^{(C)}_{\ell,G_2,p,k}(e) \tag{6}$$

$$F(L) = \frac{1}{(1.1)^{\ell+2}}\left(\frac{1-e}{1+e}\right)^{\frac{\ell+2}{2}} F^{(L)}_{\ell,G_1,p,k}(e) \tag{7}$$

In Appendix E these functions are plotted versus e for the range $0 < e \leq 0.5$. The parameters G_1 and G_2 take on values in the range $-0.1 \leq G_1, G_2 \leq -1.5$ in increments of 0.2. G_2 appears only in the C component, G_1 is contained in the H and L expressions. The same values of $\ell-2p$ were used with k set equal to zero. Each graph contains a set of curves associated with a given value of ℓ and each curve is generated for a constant value

of G_i . (i = 1 or 2, depending on which function is being plotted.) In plotting the functions, a distinct symbol was used for each value of G_i . This relationship is presented in Table 1.

The use of the G_i parameters increases the amount of information contained in each graph. However, to relate these graphs to a particular harmonic requires an additional computation to obtain the appropriate values of G_i . Equations (4) give the formulas needed. The range of values used for G_i should cover the majority of orbits of interest for investigating useful satellite constellations for geodetic studies. The effects of a different value of the semi-major axis can be incorporated by multiplying the approriate number from the graphs by

$$K_a = \left[\frac{1.1\ R_e}{a(1-e)}\right]^{\ell+2} \tag{8}$$

The magnitudes of the functions decrease monotonically as the eccentricity increases, for a majority of the cases plotted. We also evaluated the functions for $k = -1$. These results yielded increasing magnitudes as e increased, however their maximum values were much smaller. These computations are not included in this report.

The information contained in this report is by no means sufficient to base the selection of a satellite constellation to be used in a geodesy program. There are many other factors that must be considered. For example, as mentioned earlier, satellite and launch vehicle costs, and usefulness of existing data influence the selection. Equally important is the coverage

Table 1. Symbols used to designate the value of G_1 and G_2 corresponding to each curve in Appendix E.

G_1 , G_2	Symbol
-0.1	◇
-0.3	⧖
-0.5	☆
-0.7	+
-0.9	×
-1.1	△
-1.3	⬭
-1.5	□

available and quality of data obtainable for a given orbit. However, proper analysis of these data can yield valuable information for purposes of orbit selection.

Acknowledgments

I would like to acknowledge the assistance of Mr. Robert Yuhasz in deriving some of the results contained in this paper and Mr. Martin Sturmanis, for programming the computed functions. This work was supported under NASA contract I440.

REFERENCES

1. Douglass, B. C., Palmiter, M. T., Gedeon, G. S., "Resonant Satellite Geodesy Study," TRW Report No. 09128.6001-R000, 1968.

2. Winn, C. Byron, "The Selection of a Satellite System for Determining the Geopotential," paper presented at AAS/AIAA Astrodynamics Specialist Conference, Jackson, Wyoming; September 3-5, 1968.

3. Lange, Benjamin, "The Drag-Free Satellite," AIAA Journal, Vol. 2 No. 5, September 1964.

4. Kaula, W. M., Theory of Satellite Geodesy, Blaisdell Publishing Co. (1966).

5. Smart, W. M., Celestial Mechanics, John Wiley and Sons, Inc., New York, N. Y.

APPENDIX A

Expansion of the Gravitational Potential

The earth's gravitational potential is defined in terms of a series expansion in spherical harmonics.

$$U = \frac{\mu}{r}\left\{1 + \sum_{\ell=2}^{\infty}\sum_{m=0}^{\ell}\left(\frac{R_e}{r}\right)^{\ell} P_\ell^m(\sin\varphi)\left[C_\ell^m \cos m(\lambda - \Lambda_G) + S_\ell^m \sin m(\lambda - \Lambda_G)\right]\right\} \qquad (A.1)$$

The notation used is given in section II. In examining the gravitational effects on the motion of a near-earth satellite, a normalization factor is introduced for the surface spherical harmonics which is reflected in the determined values of their corresponding coefficients $(\bar{C}_\ell^m, \bar{S}_\ell^m)$. We have chosen the normalization which makes the integral of the square of each harmonic over the surface of a sphere to be 4π [4]. This is given by

$$N_{\ell m} = \left[\frac{(\ell-m)!\,(2\ell+1)\,(2-\delta_{om})}{(\ell+m)!}\right]^{1/2} \qquad (A.2)$$

where

$$\delta_{om} = \begin{cases} 0 \text{ for } m \neq 0 \\ 1 \text{ for } m = 0 \end{cases}$$

thus

$$\bar{C}_\ell^m = \frac{1}{N_{\ell m}} C_\ell^m$$

$$\bar{S}_\ell^m = \frac{1}{N_{\ell m}} S_\ell^m \qquad (A.3)$$

The mean equatorial radius of the earth, R_e, is used to define the unit of

length, and the unit of time is $(2\pi)^{-1}$ times the Schuler period. This time transformation is given by

$$\tau = \sqrt{\frac{\mu}{R_e^3}}\, t \tag{A.4}$$

The gravitational constant, μ, expressed in these units is unity. Incorporating the above changes, equation (A.1) becomes

$$U = \frac{1}{R_e}\left(\frac{R_e}{r}\right)\left\{1 + \sum_{\ell=2}^{\infty}\sum_{m=0}^{\ell} N_{\ell m}\left(\frac{R_e}{r}\right)^{\ell} P_\ell^m(\sin\varphi)\left[\bar{C}_\ell^m \cos m(\lambda-\Lambda_G) + \bar{S}_\ell^m \sin m(\lambda-\Lambda_G)\right]\right\} \tag{A.5}$$

which is partitioned further into a central term and perturbations about this term:

$$U = \frac{1}{R_e}\left(\frac{R_e}{r}\right) + V \tag{A.6}$$

Transforming to the kepler elements, V can be expanded into a form more useful for a perturbational analysis. For a harmonic of given degree and order, (ℓ,m), we define the complex function

$$\psi_\ell^m = u_\ell^m + j\, v_\ell^m \tag{A.7}$$

where

$$\begin{cases} u_\ell^m = P_\ell^m(\sin\varphi)\cos m(\lambda-\Lambda_G) \\ v_\ell^m = P_\ell^m(\sin\varphi)\sin m(\lambda-\Lambda_G) \end{cases} \tag{A.8}$$

such that

$$V_\ell^m = \frac{1}{R_e}\left(\frac{R_e}{r}\right)^{\ell+1} N_\ell^m \left[\bar{C}_\ell^m \mathcal{R}_e\{\psi_\ell^m\} + \bar{S}_\ell^m \mathcal{I}_m\{\psi_\ell^m\}\right]$$
$$V = \sum_{\ell=2}^{\infty} \sum_{m=0}^{\ell} V_\ell^m \qquad (A.9)$$

From spherical geometry we have that

$$\begin{cases} \sin\varphi = \sin i \sin\beta \\ \cos\varphi \cos(\lambda-\Omega) = \cos\beta \\ \cos\varphi \sin(\lambda-\Omega) = \cos i \sin\beta \end{cases} \qquad (A.10)$$

Also, the Legendre polynomials can be rewritten as

$$P_\ell^m(\sin\varphi) = \cos^m\varphi \, T_\ell^m(\sin\varphi) \qquad (A.11)$$

where

$$T_\ell^m(\sin\varphi) = \frac{1}{2^\ell} \sum_{t=0}^{[\frac{\ell-m}{2}]} \frac{(-1)^t (2\ell-2t)! \, [\sin i \sin\beta]^{\ell-m-2t}}{t!\,(\ell-t)!\,(\ell-m-2t)!} \qquad (A.12)$$

and

$$[\tfrac{\ell-m}{2}] = \begin{cases} \frac{\ell-m}{2} & \text{for } \ell-m \text{ even} \\ \frac{\ell-m-1}{2} & \text{for } \ell-m \text{ odd} \end{cases}$$

Incorporating equations (A.10) and (A.11) into (A.7) yields

$$\psi_\ell^m = T_\ell^m(\sin\varphi)\,[\cos\beta + j\cos i \sin\beta]^m \; e^{jm(\Omega-\Lambda_G)} \qquad (A.13)$$

Now, replacing

$$\begin{cases} \sin\beta = \left(\frac{-j}{2}\right)\left[e^{j\beta} - e^{-j\beta}\right] \\ \\ \cos\beta = \left(\frac{1}{2}\right)\left[e^{j\beta} + e^{-j\beta}\right] \end{cases} \tag{A.14}$$

into eq. (A.13) and expanding, we obtain

$$\psi_{\ell}^{m} = \frac{1}{2^{\ell}} \sum_{t=0}^{\left[\frac{\ell-m}{2}\right]} (-1)^{t} \frac{(2\ell-2t)!\,\sin^{\ell-m-2t} i}{t!\,(\ell-t)!\,(\ell-m-2t)!} \left(\frac{-j}{2}\right)^{\ell-m-2t}$$

$$\sum_{s=0}^{m} \sum_{c=0}^{\ell-m-2t} (-1)^{c} \cos^{2(m-s)}\frac{i}{2} \sin^{2s}\frac{i}{2} \binom{m}{s}\binom{\ell-m-2t}{c} \exp j\{[\ell-2(t+s+c)]\beta + m(\Omega-\Lambda_{G})\} \tag{A.15}$$

The above equation can be rewritten so as to collect the coefficients of each argument of the function $\exp j\{[\ell-2(t+s+c)]\beta+m(\Omega-\Lambda_{G})\}$. Let

$$p = t+s+c\ , \tag{A.16}$$

where $0 \le p \le \ell$. In adding the summation on p we can eliminate one of the other summations. In this case we set $s = p-t-c$ and eliminate the summation on s. Finally,

$$\psi_\ell^m = (-j)^{\ell-m} \sum_{p=0}^{\ell} I^{(0,0)}_{\ell,m,p}(i) \exp j\{[\ell - 2p](f+\omega) + m(\Omega - \Lambda_G)\} \tag{A.17}$$

where

$$I^{(g,h)}_{\ell mp}(i) = N_\ell^m \sum_t \frac{(2\ell-2t)!\,(\sin\frac{i}{2}\cos\frac{i}{2})^{\ell-m-2t-g}}{t!\,(\ell-t)!\,(\ell-m-2t-g)\;2^{\ell+g}}$$

$$\sum_c (-1)^c \binom{\ell-m-2t-g}{c} \binom{m-h}{s} \cos\frac{i}{2}^{2(m-s-h)} \sin\frac{i}{2}^{2s} \tag{A.18}$$

and

$$0 \le t \le \left\{ \begin{array}{l} p;\ p \le [\frac{\ell-m-g}{2}] \\ [\frac{\ell-m-g}{2}];\ p \ge [\frac{\ell-m-g}{2}] \end{array} \right\}$$

$$\left\{ \begin{array}{l} 0\ ;\ p-t \le m-h \\ p-t-m+h\ ;\ p-t \ge m-h \end{array} \right\} \le c \le \left\{ \begin{array}{l} \ell-m-2t-g\ ;\ p-t \ge \ell-m-2t-g \\ p-t\ ;\ p-t \le \ell-m-2t-g \end{array} \right\} \tag{A.19}$$

The additional parameters g and h are introduced into the definition in order to facilitate the computation of the forces derived from the potential.

We now need to expand the functions of r and f as a series in the mean anomaly, M. Utilizing the derivations given in [5] we can obtain

$$r^{-h} e^{jqf} = \left(\frac{1+\beta_1^2}{1-\beta_1^2}\right)^h a^{-h} \sum_{Q=-\infty}^{\infty} E^{(e)}_{\ell,p,Q,h}\, e^{j(q+Q)M} \tag{A.20}$$

where

$$q = \ell - 2p \tag{A.21}$$

$$\beta_1 = \frac{e}{1 + (1-e^2)^{1/2}}$$

and

$$E^{(e)}_{\ell,p,Q,h} = \begin{cases} \frac{1}{2}\left[A_{q,0}\, A_0 + \sum_{\alpha=1} (-1)^{\alpha} \beta_1^{\alpha} (A_\alpha\, A_{q+\alpha,0} + B_\alpha\, A_{q-\alpha,0})\right] & \text{for } Q+q=0 \\ A_0 \frac{q}{Q+q} J_Q\,[(Q+q)e] + \sum_{\alpha=1} (-1)^{\alpha} \frac{\beta_1^{\alpha}}{Q+q} [(q+\alpha)A_\alpha J_{Q-\alpha}[(Q+q)e] & \\ \qquad + (q-x)\, B_\alpha J_{Q+\alpha}[(Q+q)e]] \quad \text{for } Q+q \neq 0 & \end{cases} \tag{A.22}$$

$$\begin{cases} A_0 = (1-\beta_1^2)^{-q}\, F\left(q+h,\ q-h+1;\ 1;\ \frac{-\beta_1^2}{1-\beta_1^2}\right) \\ A_\alpha = (1-\beta_1^2)^{q}\, C_\alpha^{-(q+h)}\, F\left(-q+h,\ -q-h+1,\ \alpha+1;\ \frac{-\beta_1^2}{1-\beta_1^2}\right) \\ B_\alpha = (1-\beta_1^2)^{-q}\, C_\alpha^{(q-h)}\, F\left(q+h,\ q-h+1,\ \alpha+1;\ \frac{-\beta_1^2}{1-\beta_1^2}\right) \\ A_{d,0} = \begin{cases} -e & \text{if } d = \pm 1 \\ 0 & \text{if } d \neq \pm 1 \end{cases} \end{cases} \tag{A.23}$$

$$J_n(x) = \frac{(\frac{x}{2})^n}{n!} \sum_{k=0} (-1)^k \left(\frac{x}{2}\right)^{2k} \frac{n!}{k!(n+k)!} \tag{A.24}$$

$$F(-a,-b,c;x) = 1 + \sum_{k=1} C_k^{\,a}\, C_k^{\,b} \frac{k!}{C(c+1)\cdots(c+k-1)}\, x^k \ , \tag{A.25}$$

$$C_k^a = \frac{a(a-1)\cdots(a-k+1)}{k!} \tag{A.26}$$

Equation (A.20) is valid for all integer values of q and k. Eq. (A.24) is just the definition of the Bessel functions of the first kind and eq. (A.25) is one form of the hypergeometric series. With these expressions, we can now write the perturbing potential for a given ℓ and m.

$$V_\ell^m = \frac{1}{R_e}\left(\frac{R_e}{a}\right)^{\ell+1}\left(\frac{1+\beta_1^2}{1-\beta_1^2}\right)^{\ell+1}\sum_{p=0}^{\infty}\sum_{Q=-\infty}^{\infty} I_{\ell mp}^{(0,0)(i)} E_{\ell,p,Q,\ell+1}^{(e)} S_{\ell mpQ} \tag{A.27}$$

where

$$S_{\ell mpQ} = (-1)^{\left[\frac{\ell-m}{2}\right]}\left\{\begin{bmatrix}\overline{C}_\ell^m\\ -\overline{S}_\ell^m\end{bmatrix}\begin{matrix}(\ell-m)\text{ even}\\ (\ell-m)\text{ odd}\end{matrix}\cos\{[\ell-2p+Q]M + (\ell-2p)\omega + m(\Omega-\Lambda_G)\}\right.$$
$$\left. + \begin{bmatrix}\overline{S}_\ell^m\\ \overline{C}_\ell^m\end{bmatrix}\begin{matrix}(\ell-m)\text{ even}\\ (\ell-m)\text{ odd}\end{matrix}\sin\{[\ell-2p+Q]M + (\ell-2p)\omega + m(\Omega-\Lambda_G)\}\right\} \tag{A.28}$$

APPENDIX B

Derivation of H, C, L Equations

The effects of the geopotential harmonics on the motion of a near-earth satellite are derived in a coordinate system moving in inertial space. The origin of this system is located at the satellite's position as defined by a reference orbit. We denote the true satellite position vector by $\bar{r}$ and use a zero subscript to characterize those orbital parameters defined by the reference orbit. We now define

$$\overline{\Delta r} = \bar{r} - \bar{r}_o = H\,\hat{h} + C\,\hat{\mathcal{C}} + L\,\hat{\ell} \tag{B.1}$$

where

$$\begin{cases} \hat{h} = \dfrac{\bar{r}_o}{|\bar{r}_o|} \\[2ex] \hat{\mathcal{C}} = \dfrac{\dfrac{d\bar{r}_o}{d\beta_o} \times \bar{r}_o}{\left|\dfrac{d\bar{r}_o}{d\beta_o} \times \bar{r}_o\right|} \\[2ex] \hat{\ell} = \dfrac{\bar{r}_o \times \left(\dfrac{d\bar{r}_o}{d\beta_o} \times \bar{r}_o\right)}{\left|\bar{r}_o \times \left(\dfrac{d\bar{r}_o}{d\beta_o} \times \bar{r}_o\right)\right|} \end{cases} \tag{B.2}$$

The H, C, L - space, so defined, is an orthogonal right-handed coordinate system. It is assumed that errors in defining the reference orbit are due to errors in the geopotential harmonic coefficients, denoted by $\Delta\bar{C}^m_\ell$ and

$\Delta\bar{S}^m_\ell$, and are of the order $0\,(10^{-6})$. A first order perturbation theory is used, therefore terms which contain $\bar{C}^m_\ell\,\Delta\bar{C}^m_\ell$, $\bar{S}^m_\ell\,\Delta\bar{C}^m_\ell$, etc. are omitted.

The radius vector in inertial cartesian coordinates is

$$r = x\,\hat{i} + y\,\hat{j} + z\,\hat{k} \tag{B.3}$$

Setting $x = x_o + \Delta x$, etc. in eq. (B.3) and substituting into (B.1) gives

$$H\,\hat{h} + C\,\hat{\xi} + L\,\hat{\ell} = \Delta x\,\hat{i} + \Delta y\,\hat{j} + \Delta z\,\hat{k} \tag{B.4}$$

or

$$\begin{pmatrix} H \\ C \\ L \end{pmatrix} = \begin{pmatrix} \hat{h}\cdot\hat{i} & \hat{h}\cdot\hat{j} & \hat{h}\cdot\hat{k} \\ \hat{\xi}\cdot\hat{i} & \hat{\xi}\cdot\hat{j} & \hat{\xi}\cdot\hat{k} \\ \hat{\ell}\cdot\hat{i} & \hat{\ell}\cdot\hat{j} & \hat{\ell}\cdot\hat{k} \end{pmatrix} \begin{pmatrix} \Delta x \\ \Delta y \\ \Delta z \end{pmatrix} \tag{B.5}$$

In spherical coordinates

$$\begin{cases} x = r\cos\varphi\sin\lambda \\ y = r\cos\varphi\sin\lambda \\ z = r\sin\varphi \end{cases} \tag{B.6}$$

Setting $r = r_o + \Delta r$, etc. into (B.6), one can obtain

$$\begin{pmatrix} \Delta x \\ \Delta y \\ \Delta z \end{pmatrix} = \begin{pmatrix} \cos\varphi_\odot\cos\lambda_\odot & -r_o\sin\varphi_o\cos\lambda_\odot & -r_\odot\cos\varphi_\odot\sin\lambda_o \\ \cos\varphi_\odot\sin\lambda_\odot & -r_\odot\sin\varphi_o\sin\lambda_\odot & r_\odot\cos\varphi_\odot\cos\lambda_\odot \\ \sin\varphi_o & r_o\cos\varphi_o & 0 \end{pmatrix} \begin{pmatrix} \Delta r \\ \Delta\varphi \\ \Delta\lambda \end{pmatrix} \tag{B.7}$$

Substituting (B.7) into (B.5) and simplifying yields

$$\begin{pmatrix} H \\ C \\ L \end{pmatrix} = \begin{pmatrix} 1 & 0 & 0 \\ 0 & -r_o \dfrac{\cos i_o}{\cos \varphi_\odot} & r_o \sin i_o \cos \beta_o \\ 0 & r_\odot \dfrac{\sin i_o \cos \beta_\odot}{\cos \varphi_\odot} & r_\odot \cos i_\odot \end{pmatrix} \begin{pmatrix} \Delta r \\ \Delta\varphi \\ \Delta\lambda \end{pmatrix} \tag{B.8}$$

or taking the inverse of the matrix

$$\begin{pmatrix} \Delta r \\ \Delta\varphi \\ \Delta\lambda \end{pmatrix} = \begin{pmatrix} 1 & 0 & 0 \\ 0 & \dfrac{-\cos i_o}{r_o \cos \varphi_\odot} & \dfrac{\sin i_o \cos \beta_\odot}{r_\odot \cos \varphi_\odot} \\ 0 & \dfrac{\sin i_\odot}{r_o \cos^2 \varphi_o} & \dfrac{\cos i_o}{r_o \cos^2 \varphi_o} \end{pmatrix} \begin{pmatrix} H \\ C \\ L \end{pmatrix} \tag{B.9}$$

At this point in the analysis there are two ways in which one can proceed. The first approach results in a set of differential equations relating the H, C, L coordinates to the geopotential harmonics. To obtain these equations we start with the equations of motion of a satellite in spherical coordinates.

$$\begin{cases} \ddot{r} - r(\dot{\varphi})^2 - r\cos^2\varphi\,(\dot{\lambda})^2 + \dfrac{L}{r^2} = -\dfrac{\partial V}{\partial r} \\ \dfrac{d}{dt}\left[r^2\dot{\varphi}\right] + r^2 \sin\varphi\cos\varphi\,(\dot{\lambda})^2 = -\dfrac{\partial V}{\partial \varphi} \\ \dfrac{d}{dt}\left[r^2\cos^2\varphi\,(\dot{\lambda})\right] = -\dfrac{\partial V}{\partial \lambda} \end{cases} \tag{B.10}$$

In the above we again make the substitution

$$\begin{cases} r = r_\odot + \Delta r \\ \varphi = \varphi_\odot + \Delta\varphi \\ \lambda = \lambda_\odot + \Delta\lambda \\ V = V_\odot + \Delta V \end{cases} \tag{B.11}$$

and expand to first order in the differential elements. The zeroth order term in the equations cancel since they are the defining equations of our reference orbit. The resulting first order equations are

$$\begin{cases} \Delta\ddot{r} - 2r_\odot\dot{\varphi}_\odot(\Delta\dot{\varphi}) - 2r_\odot\cos^2\varphi_\odot(\dot{\lambda}_\odot)(\Delta\dot{\lambda}) - [(\dot{\varphi})^2 + \cos^2\varphi_\odot(\dot{\lambda}_\odot)^2 + \frac{2}{r_\odot^3}]\,\Delta r \\ \qquad + r_\odot \sin 2\varphi_\odot(\dot{\lambda})^2\,\Delta\varphi = \frac{\partial\Delta V}{\partial r_\odot} \\ \frac{d}{dt}\{r_\odot^2(\Delta\dot{\varphi}) + 2r_\odot(\dot{\varphi}_\odot)\Delta r\} + r_\odot^2(\dot{\lambda}_\odot)\sin 2\varphi_\odot(\Delta\dot{\lambda}) + r_\odot(\dot{\lambda}_\odot)^2 \sin 2\varphi_\odot\,\Delta r \\ \qquad + r_\odot^2(\dot{\lambda}_\odot)^2\cos 2\varphi_\odot\,\Delta\varphi = \frac{\partial\Delta V}{\partial\varphi_\odot} \\ \frac{d}{dt}\{r_\odot^2\cos^2\varphi_\odot(\Delta\dot{\lambda}) - r_\odot^2\sin 2\varphi_\odot(\dot{\lambda}_\odot)\,\Delta\varphi + 2r_\odot(\dot{\lambda}_\odot)\cos^2\varphi_\odot\Delta r\} = \frac{\partial\Delta V}{\partial\lambda_\odot} \end{cases} \tag{B.12}$$

In these equations the reference orbit can be approximated by an ellipse. Therefore substituting equation (B.9) into (B.12) and simplifying gives

$$\ddot{H} - [(\dot{\beta})^2 + \frac{2}{r_o^3}] H - 2 \dot{r}_o(\dot{\beta}) \frac{d}{dt} (\frac{L}{r_o}) = \frac{\partial \Delta V}{\partial r_\odot}$$

$$\ddot{L} - \frac{\ddot{r}_o}{r_o} L + 2(\dot{\beta}_\odot) \dot{H} + 2 [\frac{\dot{r}_o}{r_o} \dot{\beta}_\odot + \ddot{\beta}_\odot] H = \frac{1}{r_o} \frac{\partial \Delta V}{\partial \beta_o}$$

$$\ddot{C} + [(\dot{\beta})^2 - \frac{\ddot{r}_o}{r_o}] C = - \frac{1}{r_o \sin\beta_o} \frac{\partial \Delta V}{\partial i_o} \qquad (B.13)$$

Solutions to these equations are best obtained via numerical integration techniques.

The problem of solving coupled second order differential equations however can be avoided. This alternate approach provides solutions better suited for the objectives of this paper. We first define the H, C, L coordinates as a function of differential kepler elements. The satellite radius as a function of the osculating kepler elements is given by

$$r = a (1-e \cos E) \qquad (B.14)$$

where the eccentric anomaly, E , is related to M , the mean anomaly through Kepler's equation

$$E - e \sin E = M \qquad (B.15)$$

These equations yield

$$\Delta r = \frac{r}{a} \Delta a + \frac{a e \sin f}{(1-e^2)^{1/2}} \Delta M - a \cos f \Delta e$$

From equations (A.10) in Appendix A and

$$\cos f = \frac{\cos E - e}{1 - e \cos E} \quad , \tag{B.17}$$

which relates the true anomaly, f to the eccentric anomaly, we obtain

$$\begin{cases} \Delta\varphi = \dfrac{\sin i \cos \beta}{\cos \varphi} \Delta\beta + \dfrac{\cos i \sin \beta}{\cos \varphi} \Delta i \\ \Delta\lambda = \Delta\Omega + \dfrac{\cos i}{\cos^2 \varphi} \Delta\beta - \dfrac{\cos \beta \sin \varphi}{\cos^2 \varphi} \Delta i \\ \Delta\beta = \Delta\omega + \dfrac{a^2(1-e^2)^{1/2}}{r^2} \Delta M + \dfrac{\sin f}{(1-e^2)} \left[\dfrac{a(1-e^2)}{r} + 1\right] \Delta e \end{cases} \tag{B.18}$$

Substitution of equations (B.16) and (B.18) into (B.8) yields

$$\begin{cases} H = \dfrac{r}{a} \Delta a + \dfrac{ae \sin f}{[1-e^2]^{1/2}} \Delta M - a \cos f \, \Delta e \\ C = r \left[\sin i \cos \beta \, \Delta\Omega - \sin \beta \, \Delta i\right] \\ L = r \left[\Delta\omega + \cos i \, \Delta\Omega + \dfrac{a^2(1-e^2)^{1/2}}{r^2} \Delta M\right] \end{cases} \tag{B.19}$$

These differential kepler elements also represent the contributions of the errors in the force model used to generate the reference orbit Their coefficients in the above equations can be evaluated using a set of mean kepler elements. The differential kepler elements are related to errors in the geopotential model through a perturbation on Lagrange's planetary

equations of motion. To first order they can be written as

$$\begin{cases} \dot{\Delta a} = \dfrac{2}{n(1-e^2)^{1/2}} \left[e \sin f \, \Delta R + \dfrac{a(1-e^2)}{r} \Delta S \right] \\ \dot{\Delta e} = \dfrac{(1-e^2)^{1/2}}{na} \left[\sin f \, \Delta R + (\cos E + \cos f) \, \Delta S \right] \\ \dot{\Delta i} = \dfrac{1}{na(1-e^2)^{1/2}} \dfrac{r}{a} \cos \beta \, \Delta W \\ \sin i \, \dot{\Delta \Omega} = \dfrac{1}{na(1-e^2)^{1/2}} \dfrac{r}{a} \sin \beta \, \Delta W \\ \dot{\Delta \omega} = \dfrac{(1-e^2)^{1/2}}{nae} \left[-\cos f \, \Delta R + \left(\dfrac{r}{a(1-e^2)} + 1 \right) \sin f \, \Delta S \right] - \cos i \, \dot{\Delta \Omega} \\ \dot{\Delta M} = -\dfrac{3}{2} \dfrac{n}{a} \Delta a - \dfrac{2r}{na^2} \Delta R - (1-e^2)^{1/2} \left[\dot{\Delta \omega} + \cos i \, \dot{\Delta \Omega} \right] \end{cases} \tag{B.20}$$

where

$$\begin{cases} \Delta R = \dfrac{\partial \Delta V}{\partial r} \\ \Delta S = \dfrac{1}{r} \dfrac{\partial \Delta V}{\partial \beta} \\ \Delta W = \dfrac{1}{r \sin \beta} \dfrac{\partial \Delta W}{\partial i} \end{cases} \tag{B.21}$$

Using the results obtained in Appendix A, equations (B.20) are integrated and then substituted into (B.19). After collecting terms with the same frequency, the final expressions become

$$H_{\ell m} = \frac{\mu}{n^2 R_e^2} \left(\frac{1+\beta_1^2}{1-\beta_1^2}\right)^{\ell+2} \left(\frac{R_e}{a}\right)^{\ell+2} \sum_{p=0}^{\ell} \sum_{k=-\infty}^{\infty} I_{\ell m p}^{(0,0)} F_{\ell, G_1, p, k}^{(H)(e)} S_{\ell,m,p,k} \tag{B.22}$$

$$C_{\ell m} = \frac{\mu}{n^2 R_e^2} \left(\frac{1+\beta_1^2}{1-\beta_1^2}\right)^{\ell+2} \left(\frac{R_e}{a}\right)^{\ell+2} \sum_{p=0}^{\ell} \sum_{k=-\infty}^{\infty} \left[2 \cos i \, I_{\ell m p}^{(1,0)} - m \sin i \, I_{\ell m p}^{(0,1)}\right] F_{\ell, G_2, p, k}^{(C)(e)} S_{\ell-1,m,p,k} \tag{B.23}$$

$$L_{\ell m} = \frac{\mu}{n^2 R_e^2} \left(\frac{1+\beta_1^2}{1-\beta_1^2}\right)^{\ell+2} \left(\frac{R_e}{a}\right)^{\ell+2} \sum_{p=0}^{\ell} \sum_{k=-\infty}^{\infty} I_{\ell m p}^{(0,0)} F_{\ell, G_1, p, k}^{(L)(e)} (-1) \bar{S}_{\ell,m,p,k} \tag{B.24}$$

$S_{\ell,m,p,k}$ is defined in equation (A.28). $\bar{S}_{\ell,m,p,k}$ denotes the derivative with respect to its argument.

$$\begin{cases} G_1 = (\ell-2p) \dfrac{\dot{e}}{n} + m \left(\dfrac{\dot{\Omega}-\dot{\Lambda}_G}{n}\right) \\ G_2 = (\ell-2p-1) \dfrac{\dot{e}}{n} + m \left(\dfrac{\dot{\Omega}-\dot{\Lambda}_G}{n}\right) \end{cases} \tag{B.25}$$

$$\begin{aligned} F_{\ell,p,G_1,k}^{(H)(e)} = \sum_{Q=-\infty}^{\infty} \Bigg[& \frac{1}{2} \{[(2p+1)\sqrt{1-e^2}\, E_{\ell-1,p,Q+1,\ell+2} - (\ell-2p) E_{\ell-1,p,Q+1,\ell+1}] E_{1,0,k-(Q+1),0} \\ & - [(2\ell-2p+1)\sqrt{1-e^2}\, E_{\ell+1,p,Q-1,\ell+2} + (\ell-2p) E_{\ell+1,p,Q-1,\ell+1}] E_{-1,0,k-(Q-1),0} \} \\ & - e E_{\ell,p,Q,\ell+1} \{[\tfrac{3}{2}\ell-p+1] E_{1,0,k-(Q+1),0} - [\tfrac{1}{2}\ell+p+1] E_{-1,0,k-(Q-1),0}\} \\ & + \{\frac{e}{2} \frac{(\ell+1)}{\sqrt{1-e^2}} [E_{\ell+1,p,Q-1,\ell+2} - E_{\ell-1,p,Q+1,\ell+2}] + (\ell-2p) E_{\ell,p,Q,\ell+3}\} \\ & [2 E_{0,0,k-Q,-1} + \frac{3}{2} \frac{e}{\sqrt{1-e^2}} \frac{[E_{1,0,k-(Q+1),0} - E_{-1,0,k-(Q+1),0}]}{[(\ell-2p+Q) + G_1]}\} \Bigg] \frac{1}{[(\ell-2p+Q) + G_1]} \end{aligned} \tag{B.26}$$

$$F^{(C)}_{(e)\,\ell,G_2,p,k} = \frac{\sqrt{1-e^2}}{2} \sum_{Q=-\infty}^{\infty} \{E_{\ell,p,Q-1,\ell+1}\, E_{-1,0,k-(Q-1),-1} - E_{\ell-2,p,Q+1,\ell+1}\, E_{1,0,k-(Q+1),-1}\} \frac{1}{[(\ell-2p-1+Q)+G_2]} \quad (B.27)$$

$$F^{(L)}_{(e)\,\ell,G_1,p,k} = \sum_{Q=-\infty}^{\infty} \Bigg[\{\frac{2(\ell+1)\sqrt{1-e^2}}{[(\ell-2p+Q)+G_1]} E_{\ell,p,Q,\ell+1} - 3\,[\frac{(\ell+1)\beta_1}{(1-\beta_1^2)} (E_{\ell+1,p,Q-1,\ell+2} - E_{\ell-1,p,Q+1,\ell+2}) + (\ell-2p)E_{\ell,p,Q,\ell+3}]\}$$

$$E_{0,0,k-Q,1}$$

$$+ [E_{1,0,k-(Q+1),-1} + \frac{\beta_1}{2(1+\beta_1^2)} (E_{2,0,k-(Q+2),-1} - 3\, E_{0,0,k-Q,-1})]\, [-(2p+1)E_{\ell-1,p,Q-1,\ell+2} + \frac{(\ell-2p)}{\sqrt{1-e^2}}$$

$$E_{\ell-1,p,Q+1,\ell+1}]$$

$$- [E_{-1,0,k-(Q-1),-1} + \frac{\beta_1}{2(1+\beta_1^2)} (E_{-2,0,k-(Q-2),-1} - 3\, E_{0,0,k-Q,-1})][(2\ell-2p+1)E_{\ell+1,p,Q-1,\ell+2} + \frac{(\ell-2p)}{\sqrt{1-e^2}}$$

$$E_{\ell+1,p,Q-1,\ell+1}]$$

$$+ \frac{2\beta_1}{1-\beta_1^2} (\ell-2p)E_{\ell,p,Q,\ell+1} \{E_{1,0,k-(Q+1),-1} - E_{-1,0,k-(Q-1),-1} + \frac{\beta_1}{1+\beta_1^2} (E_{2,0,k-(Q+2),-1} - E_{-2,0,k-(Q-2),-1})\} \Bigg]$$

$$\frac{1}{[(\ell-2p+Q)+G_1]} \quad (B.28)$$

APPENDIX C

Graphs of Inclination Function F_2

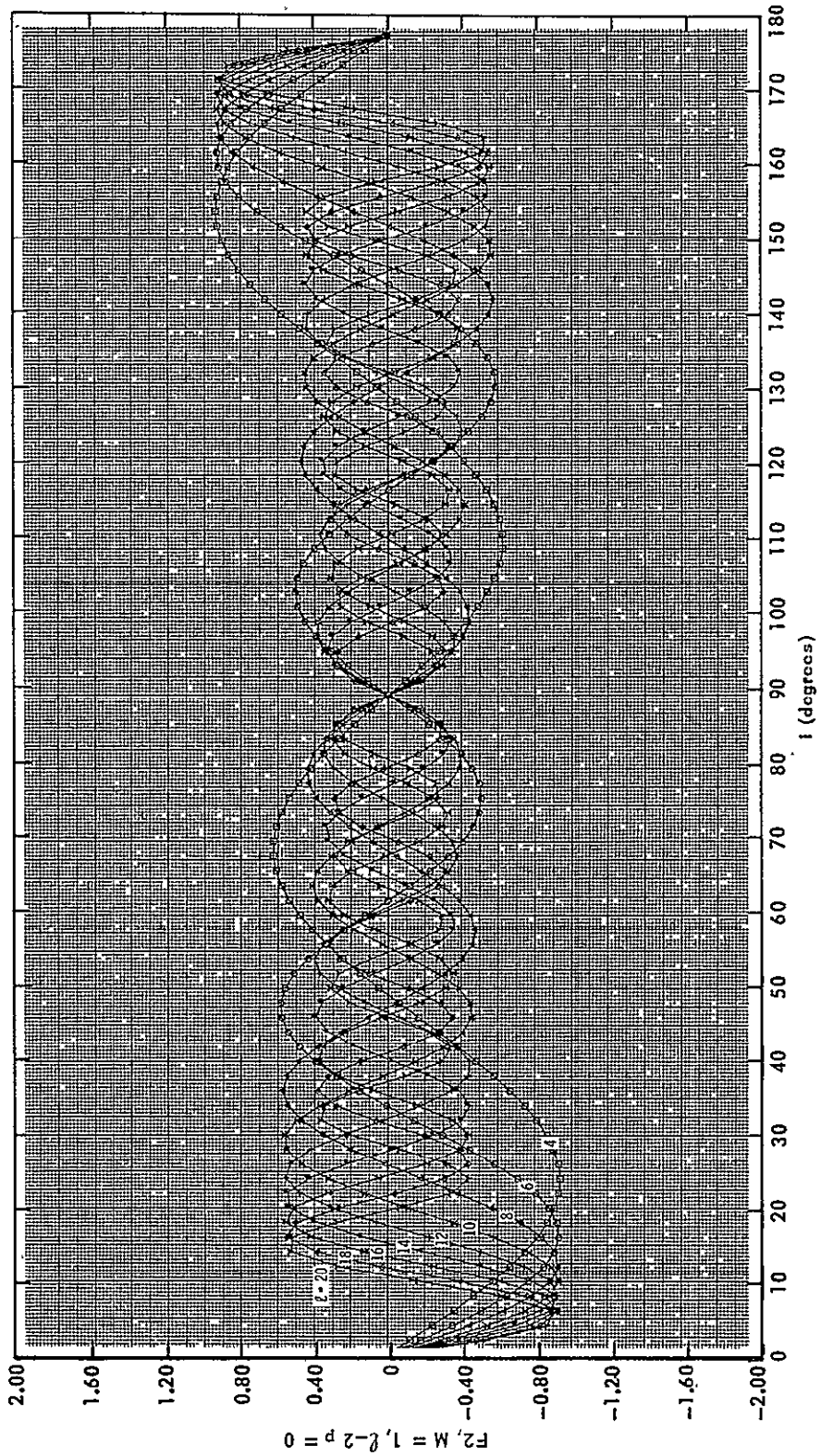

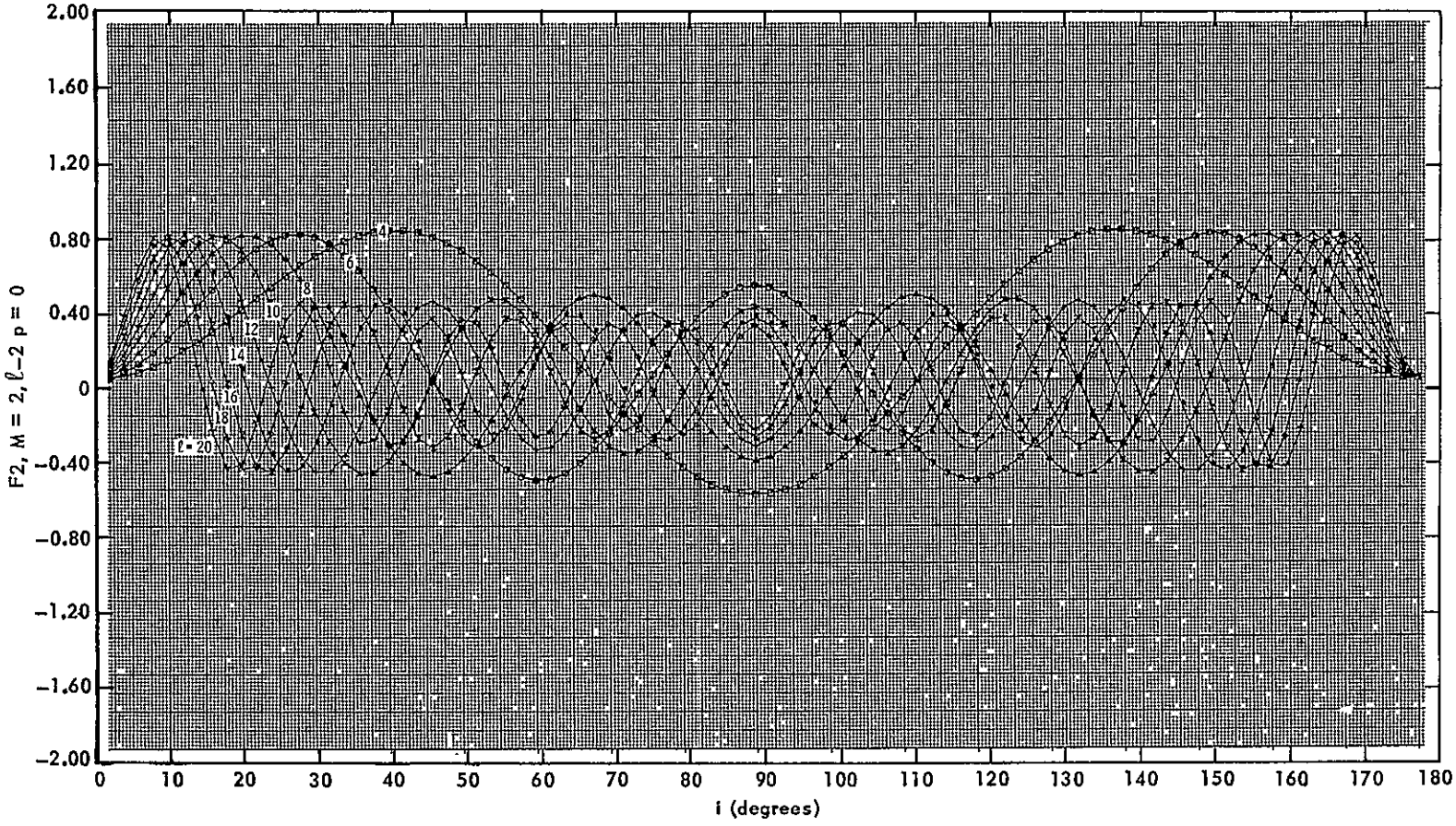
2.00
1.60
1.20
0.80
0.40
0
-0.40
-0.80
-1.20
-1.60
-2.00
F2, M = 2, ℓ-2 p = 0
0
10
20
30
40
50
60
70
80
90
100
110
120
130
140
150
160
170
180
i (degrees)
4
6
8
10
12
14
16
18
ℓ = 20

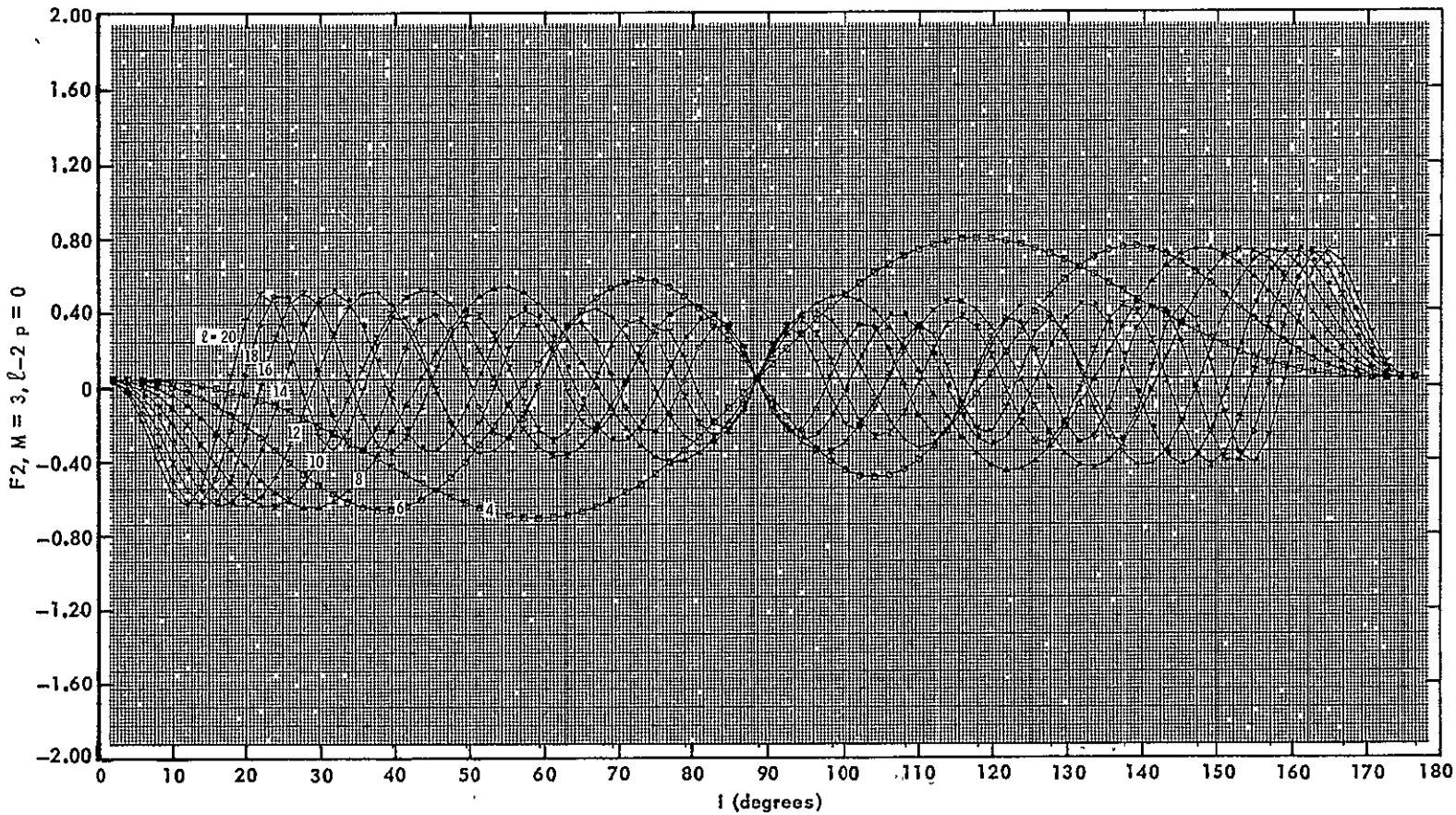
F2, M = 3, ℓ-2 p = 0
2.00
1.60
1.20
0.80
0.40
0
-0.40
-0.80
-1.20
-1.60
-2.00
0
10
20
30
40
50
60
70
80
90
100
110
120
130
140
150
160
170
180
I (degrees)
ℓ = 20
18
16
14
12
10
8
6
4

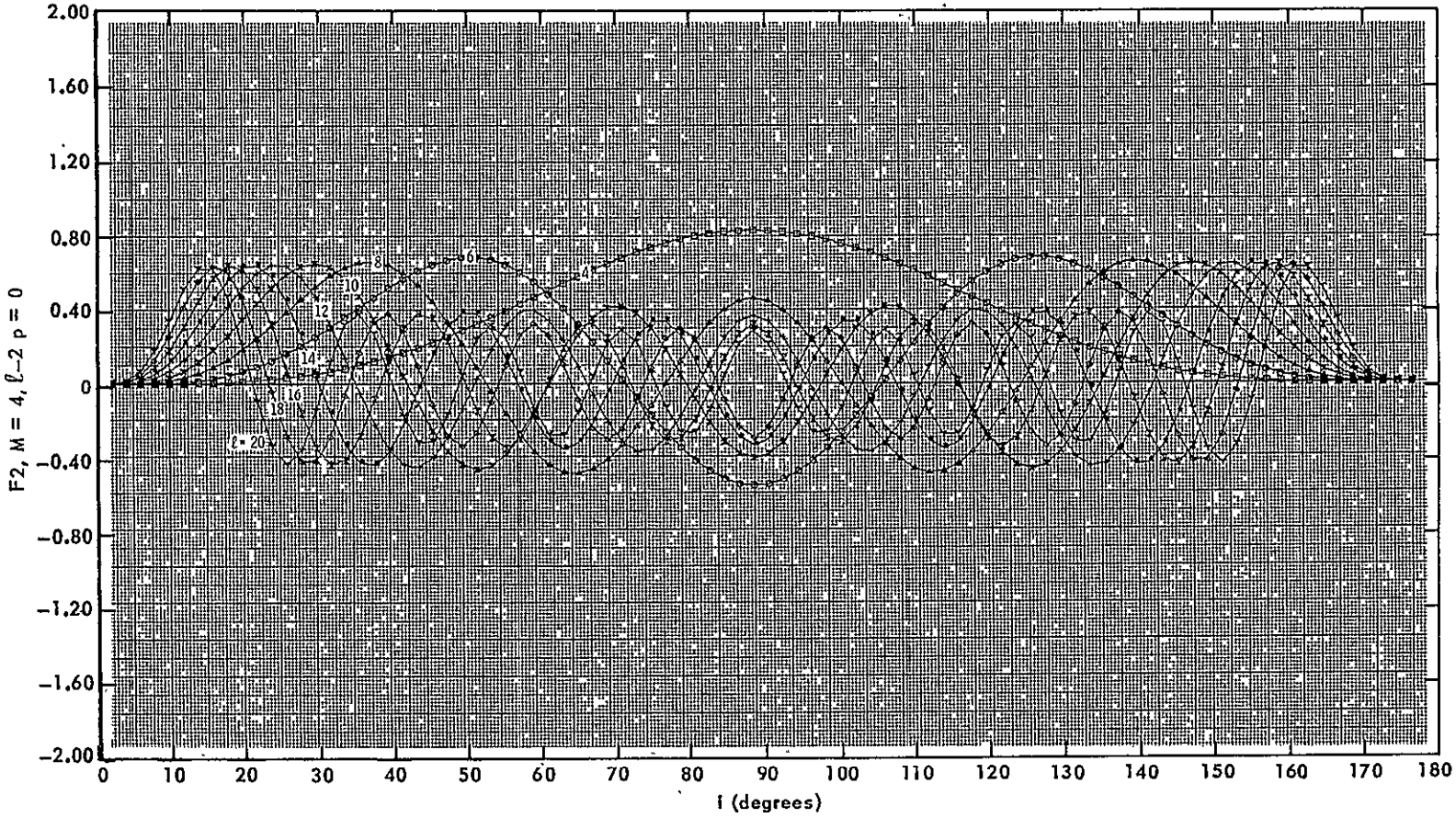
2.00
1.60
1.20
0.80
0.40
0
-0.40
-0.80
-1.20
-1.60
-2.00
F2, M = 4, ℓ-2 p = 0
0
10
20
30
40
50
60
70
80
90
100
110
120
130
140
150
160
170
180
ι (degrees)
ℓ = 2
4
6
8
10
12
14
16
18
20

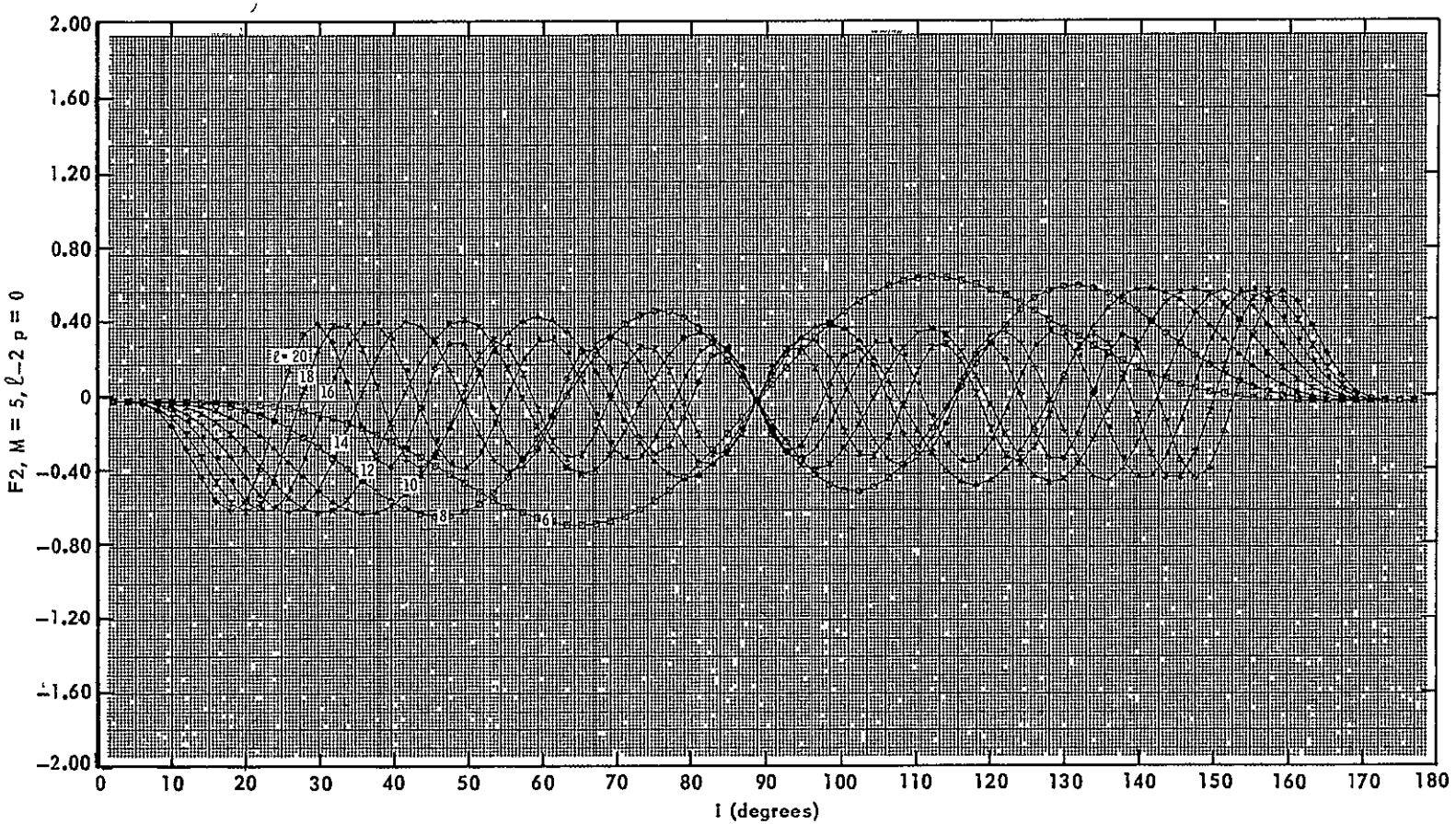
2.00
1.60
1.20
0.80
0.40
0
−0.40
−0.80
−1.20
−1.60
−2.00
F2, M = 5, ℓ−2 p = 0
ℓ = 20
18
16
14
12
10
8
6
0
10
20
30
40
50
60
70
80
90
100
110
120
130
140
150
160
170
180
I (degrees)

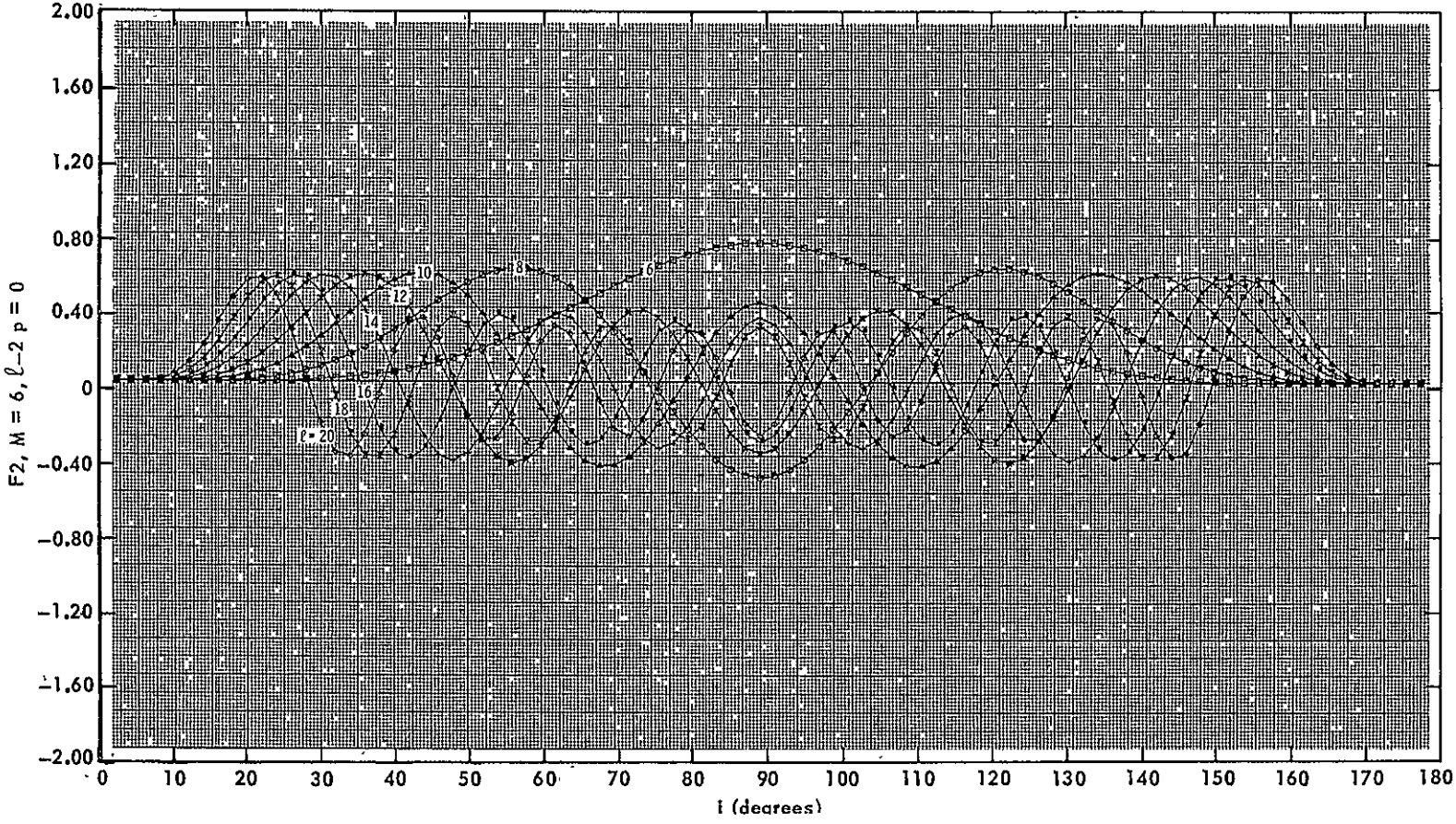
F2, M = 6, ℓ-2 p = 0
2.00
1.60
1.20
0.80
0.40
0
-0.40
-0.80
-1.20
-1.60
-2.00
0
10
20
30
40
50
60
70
80
90
100
110
120
130
140
150
160
170
180
I (degrees)
6
8
10
12
14
16
18
ℓ = 20

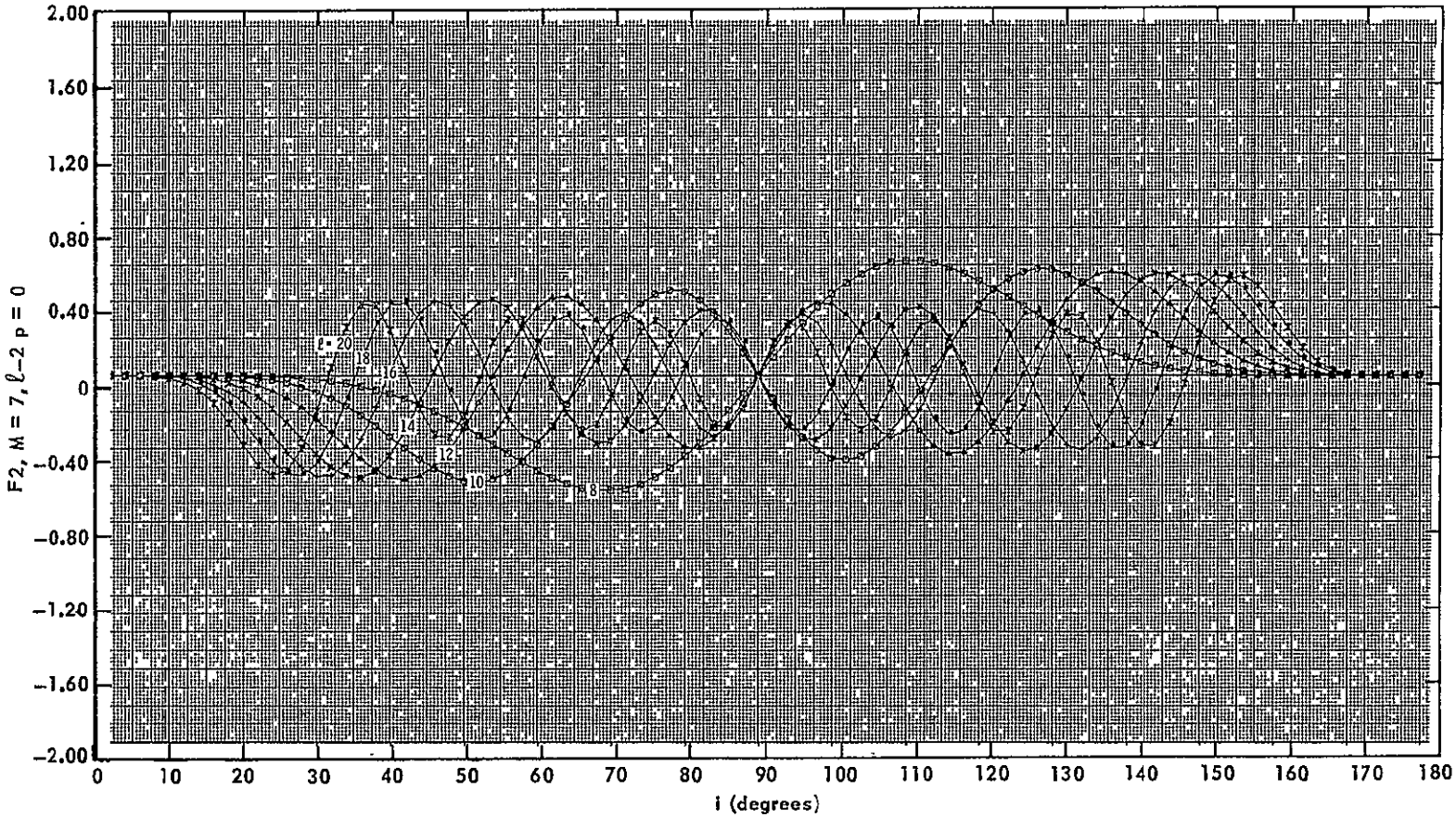
2.00
1.60
1.20
0.80
0.40
0
-0.40
-0.80
-1.20
-1.60
-2.00
F2, M = 7, ℓ-2 p = 0
ℓ = 20
18
16
14
12
10
8
0
10
20
30
40
50
60
70
80
90
100
110
120
130
140
150
160
170
180
i (degrees)

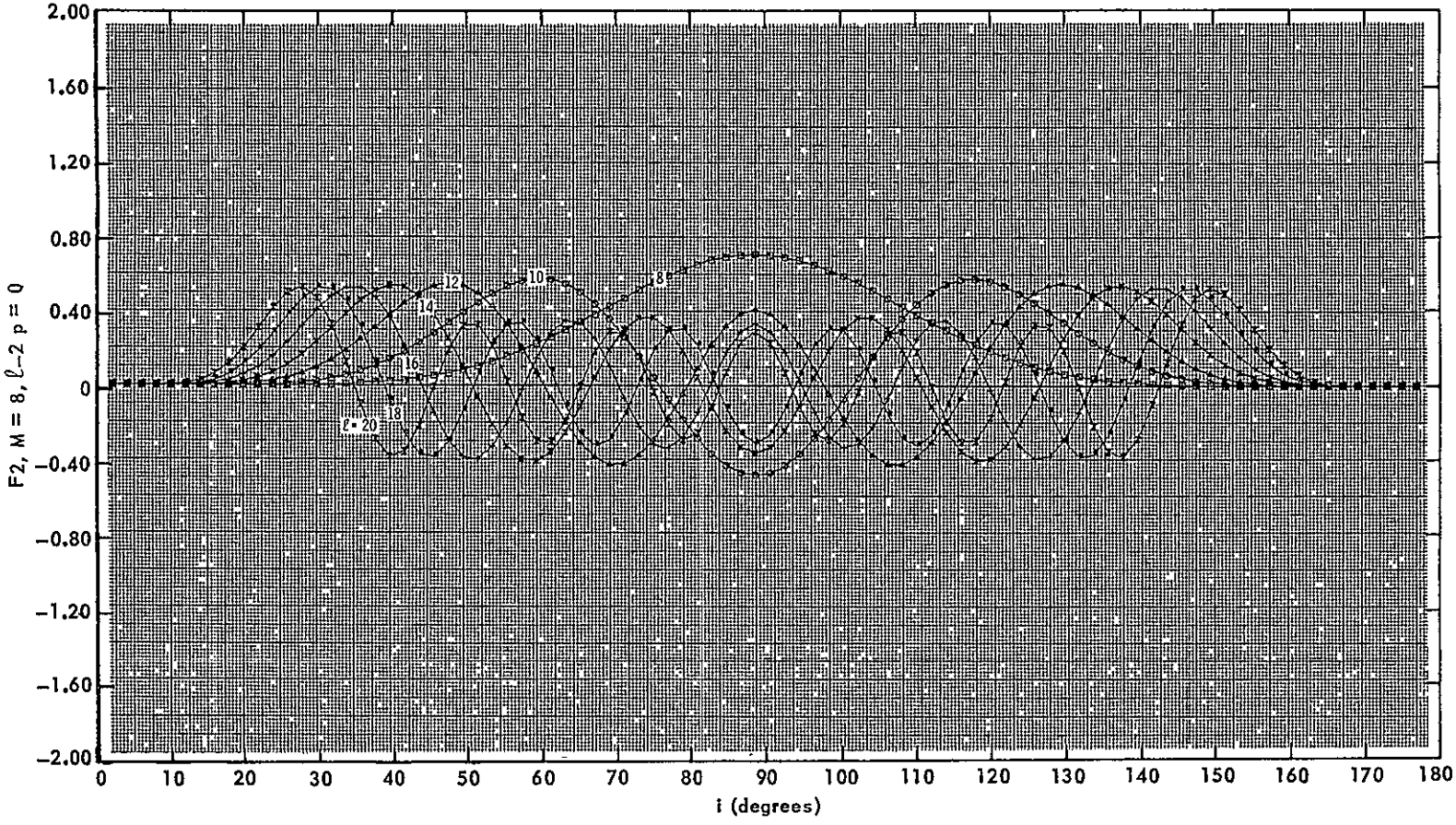
F2, M = 8, ℓ-2 p = 0
2.00
1.60
1.20
0.80
0.40
0
-0.40
-0.80
-1.20
-1.60
-2.00
0
10
20
30
40
50
60
70
80
90
100
110
120
130
140
150
160
170
180
i (degrees)
ℓ = 20
18
16
14
12
10
8

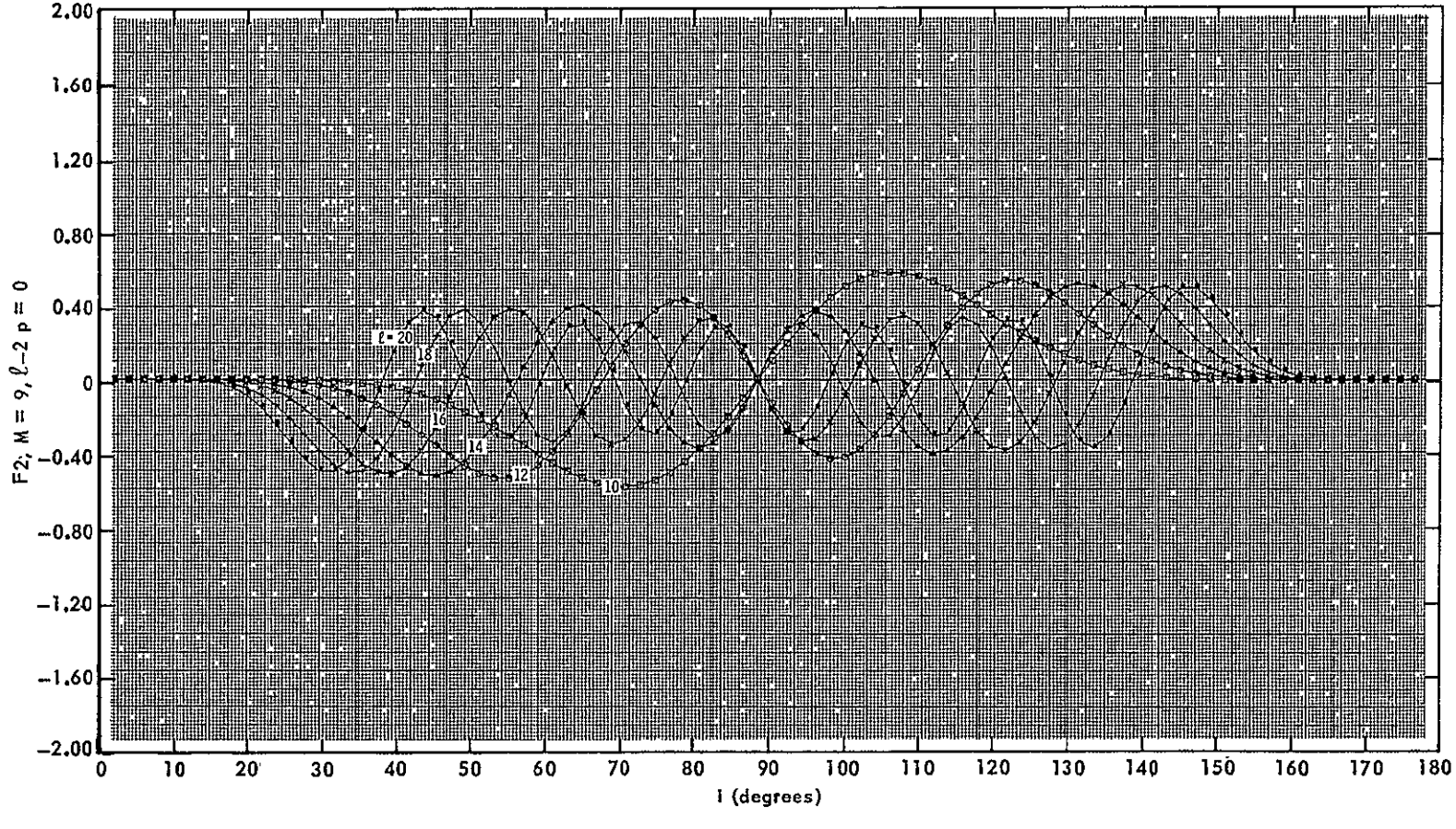
2.00
1.60
1.20
0.80
0.40
0
-0.40
-0.80
-1.20
-1.60
-2.00
F2; M = 9, ℓ-2 p = 0
ℓ = 20
18
16
14
12
10
0
10
20
30
40
50
60
70
80
90
100
110
120
130
140
150
160
170
180
I (degrees)

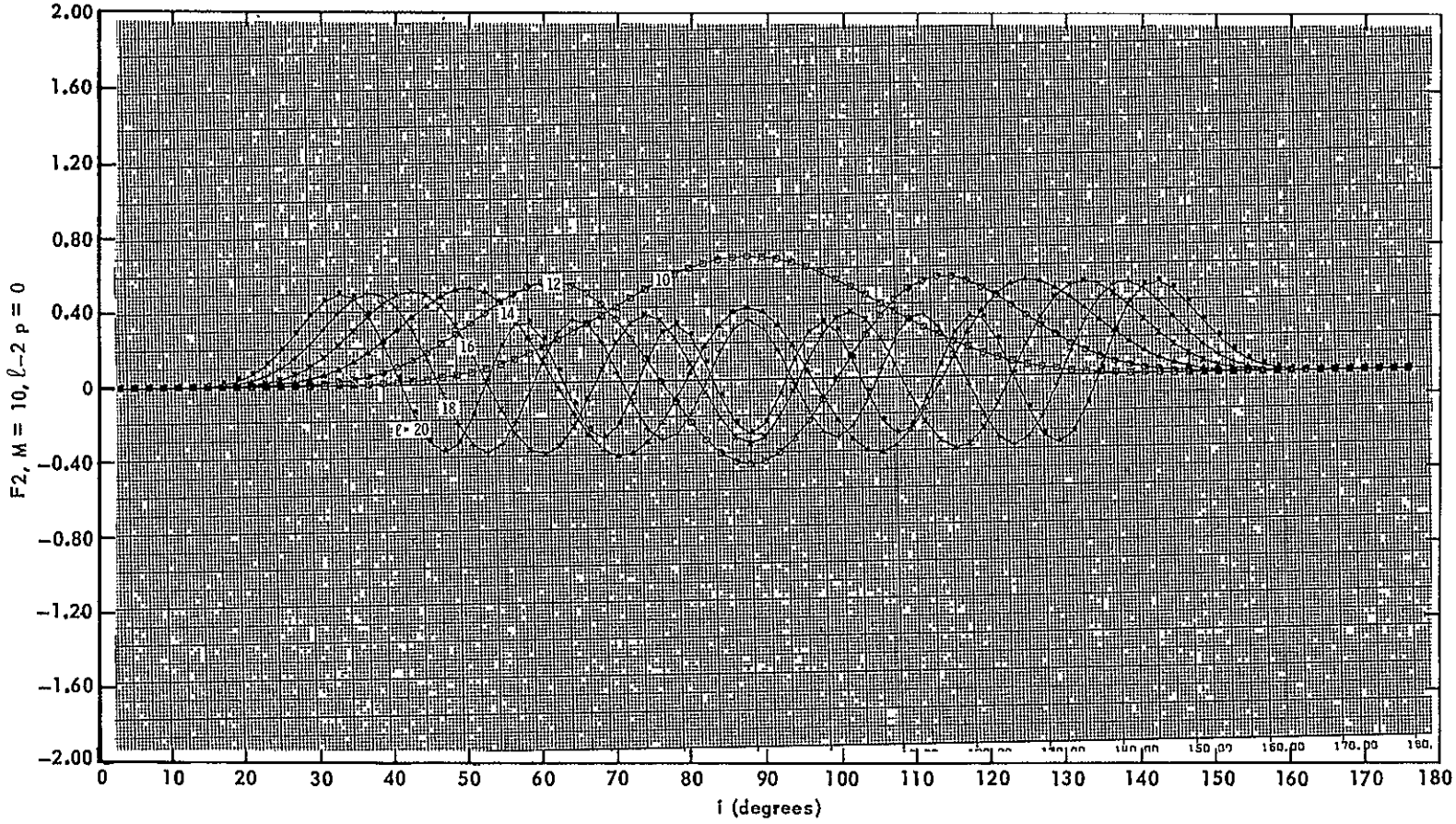
F2, M = 10, ℓ-2 p = 0
2.00
1.60
1.20
0.80
0.40
0
-0.40
-0.80
-1.20
-1.60
-2.00
0
10
20
30
40
50
60
70
80
90
100
110
120
130
140
150
160
170
180
i (degrees)
12
10
14
16
18
p = 20

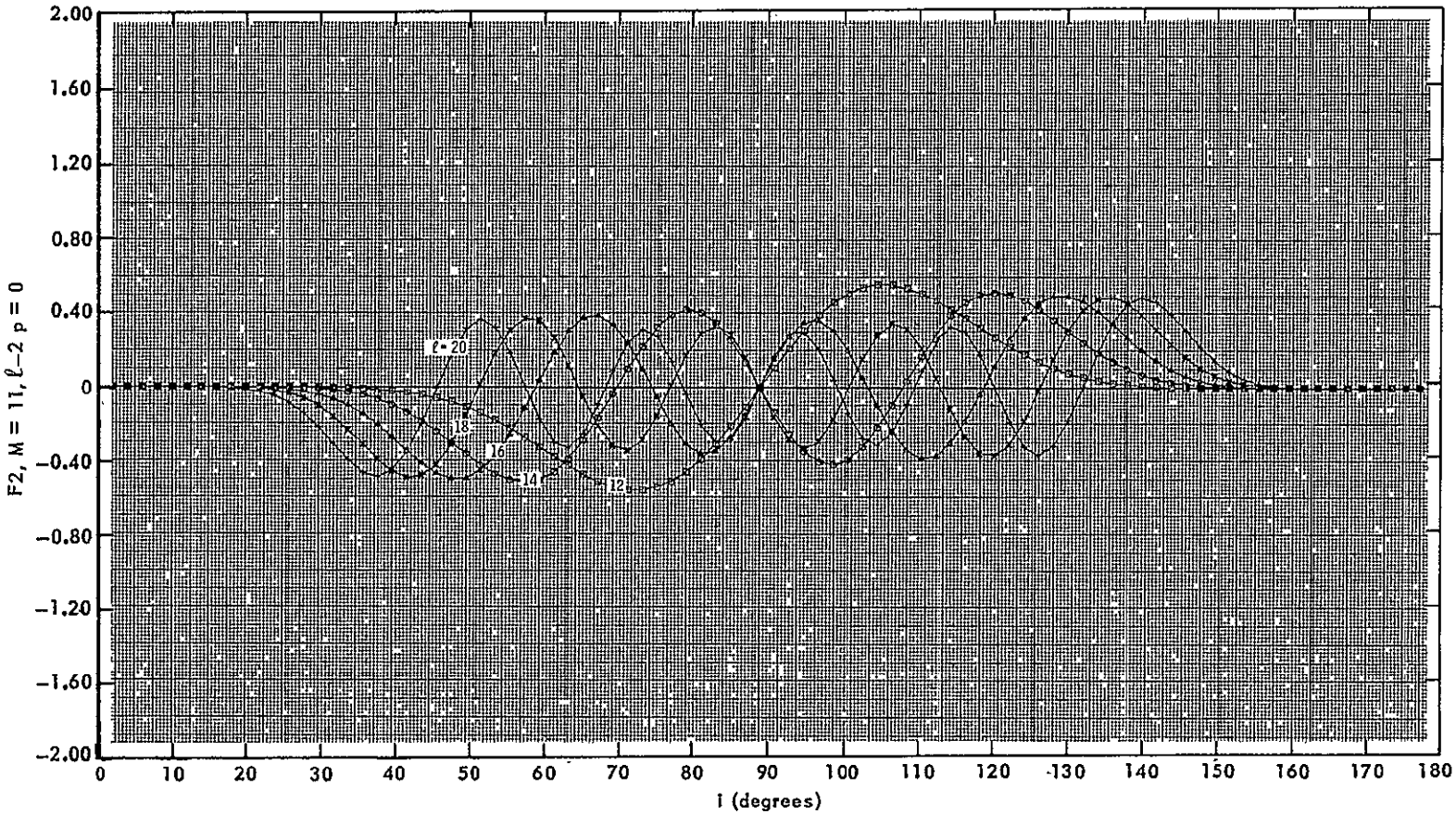
F2, M = 11, ℓ−2 p = 0
2.00
1.60
1.20
0.80
0.40
0
−0.40
−0.80
−1.20
−1.60
−2.00
ℓ = 20
18
16
14
12
0
10
20
30
40
50
60
70
80
90
100
110
120
130
140
150
160
170
180
I (degrees)

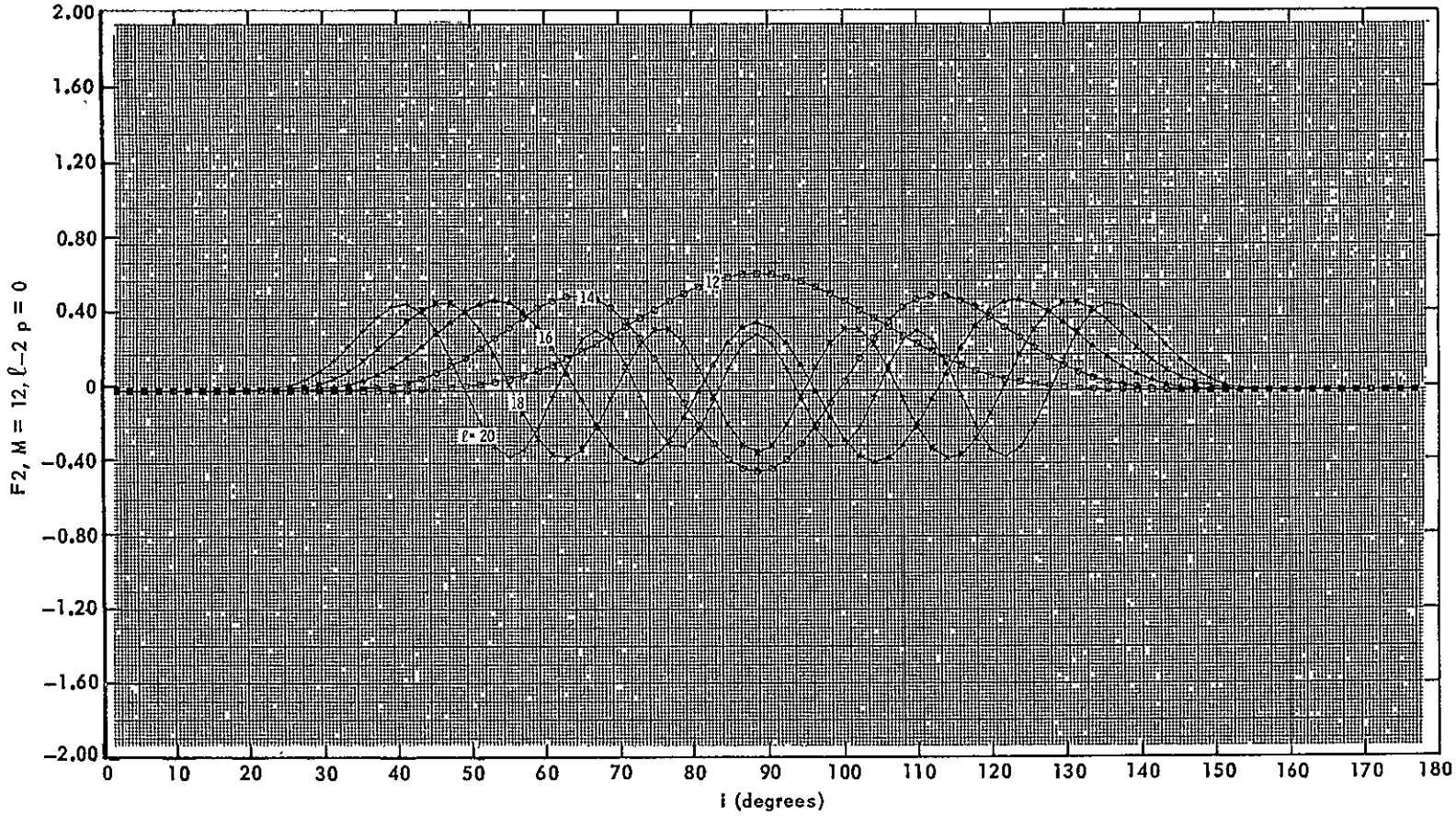
2.00
1.60
1.20
0.80
0.40
0
-0.40
-0.80
-1.20
-1.60
-2.00
F2, M = 12, ℓ-2 p = 0
0
10
20
30
40
50
60
70
80
90
100
110
120
130
140
150
160
170
180
i (degrees)
12
14
16
18
ℓ= 20

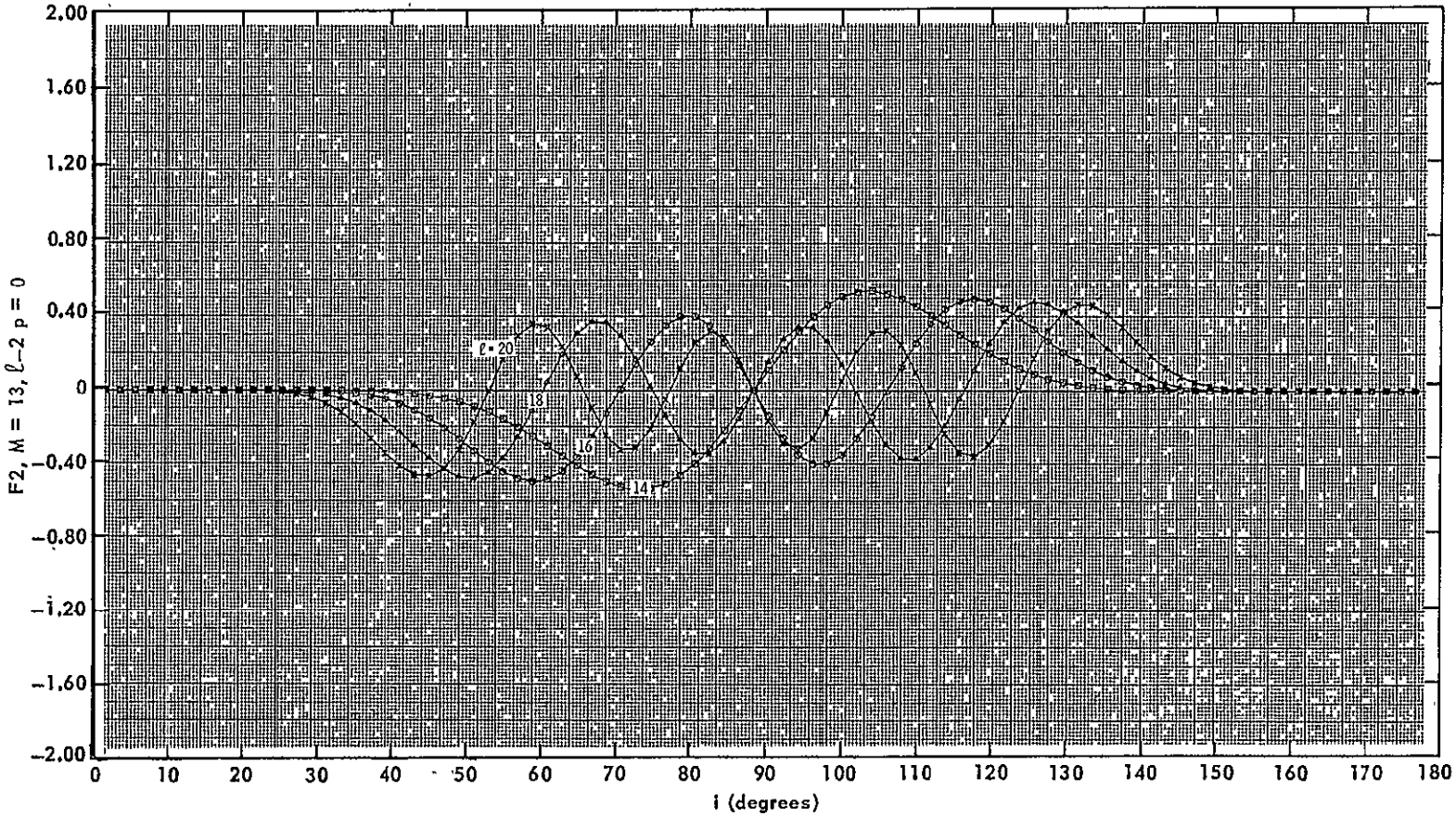
2.00
1.60
1.20
0.80
0.40
0
-0.40
-0.80
-1.20
-1.60
-2.00
F2, M = 13, ℓ-2 p = 0
ℓ = 20
18
16
14
0
10
20
30
40
50
60
70
80
90
100
110
120
130
140
150
160
170
180
i (degrees)

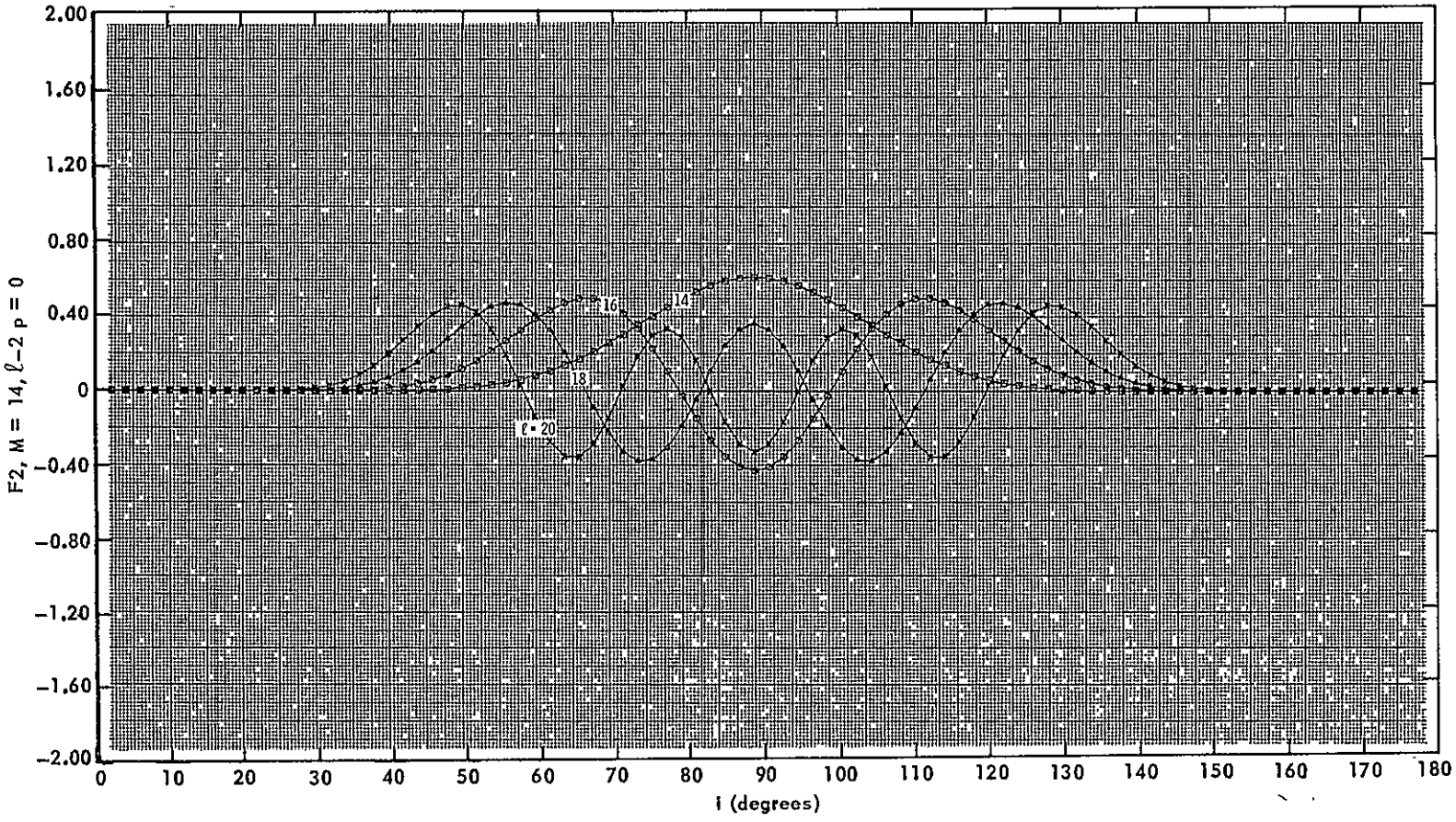
2.00
1.60
1.20
0.80
0.40
0
-0.40
-0.80
-1.20
-1.60
-2.00
F2, M = 14, ℓ-2 p = 0
0
10
20
30
40
50
60
70
80
90
100
110
120
130
140
150
160
170
180
I (degrees)
16
14
18
ℓ = 20

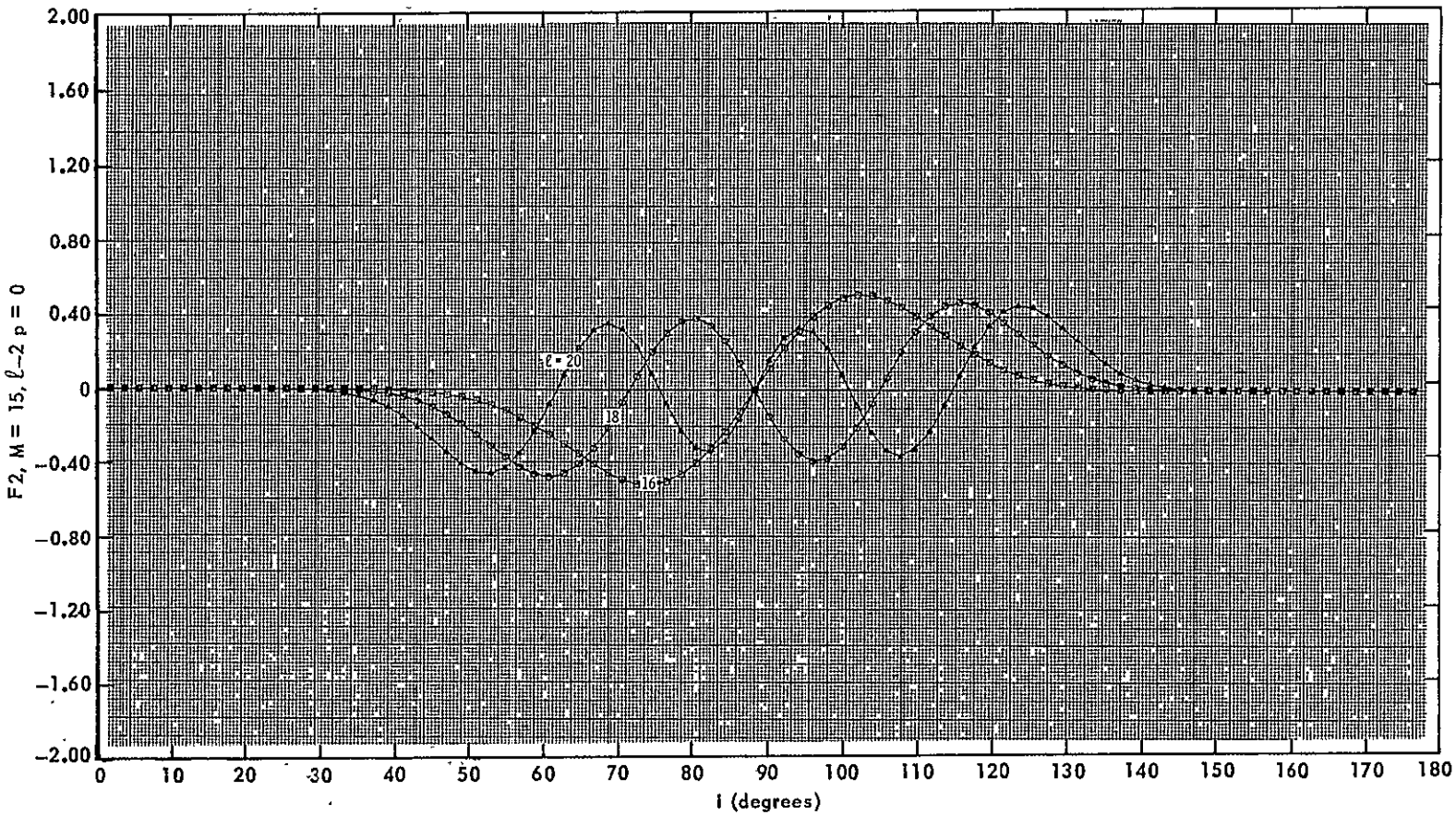
2.00
1.60
1.20
0.80
0.40
0
−0.40
−0.80
−1.20
−1.60
−2.00
F2, M = 15, ℓ−2 p = 0
ℓ = 20
18
16
0
10
20
30
40
50
60
70
80
90
100
110
120
130
140
150
160
170
180
i (degrees)

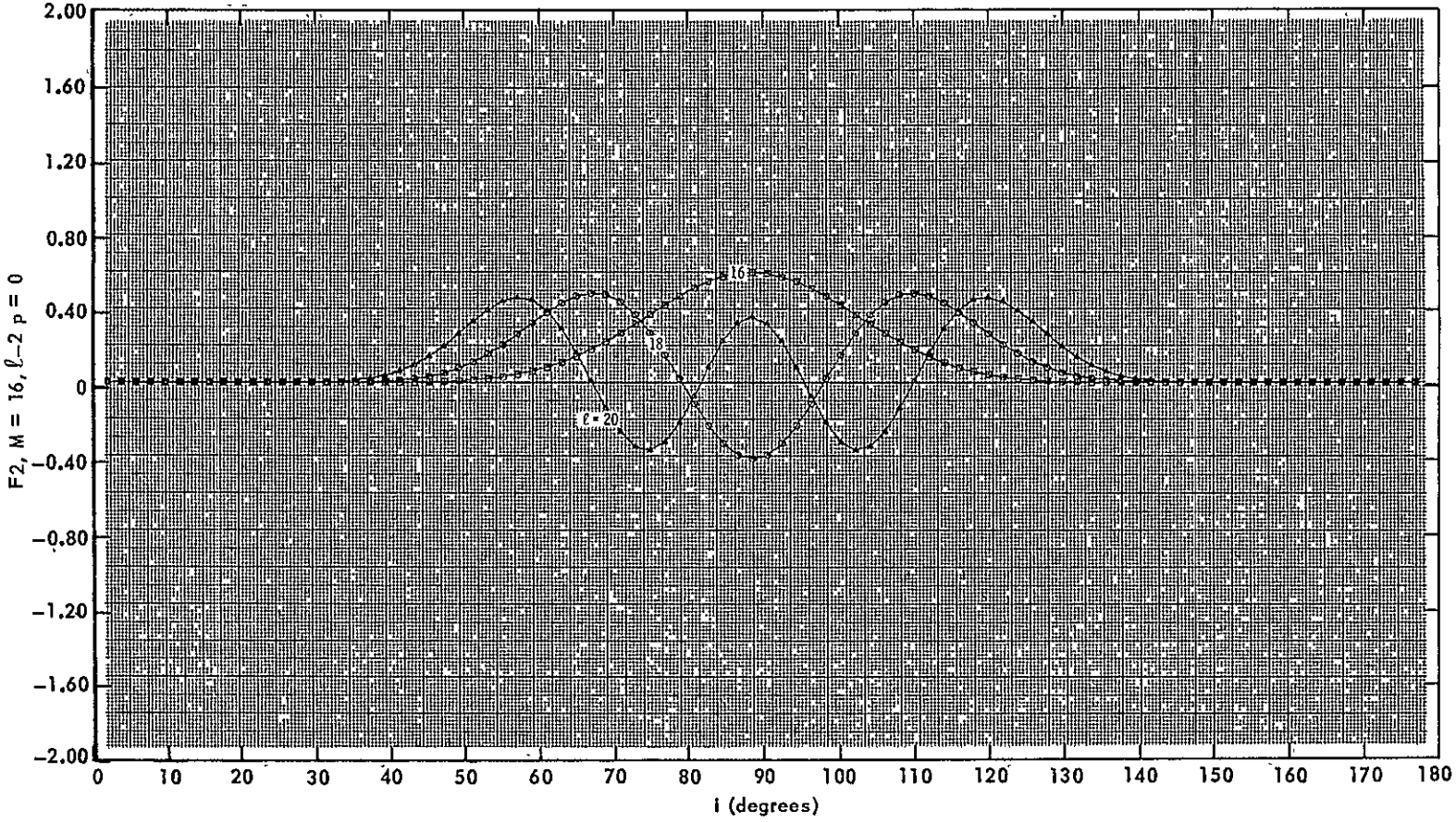
2.00
1.60
1.20
0.80
0.40
0
−0.40
−0.80
−1.20
−1.60
−2.00
F2, M = 16, ℓ−2 p = 0
0
10
20
30
40
50
60
70
80
90
100
110
120
130
140
150
160
170
180
i (degrees)
16
18
ℓ = 20

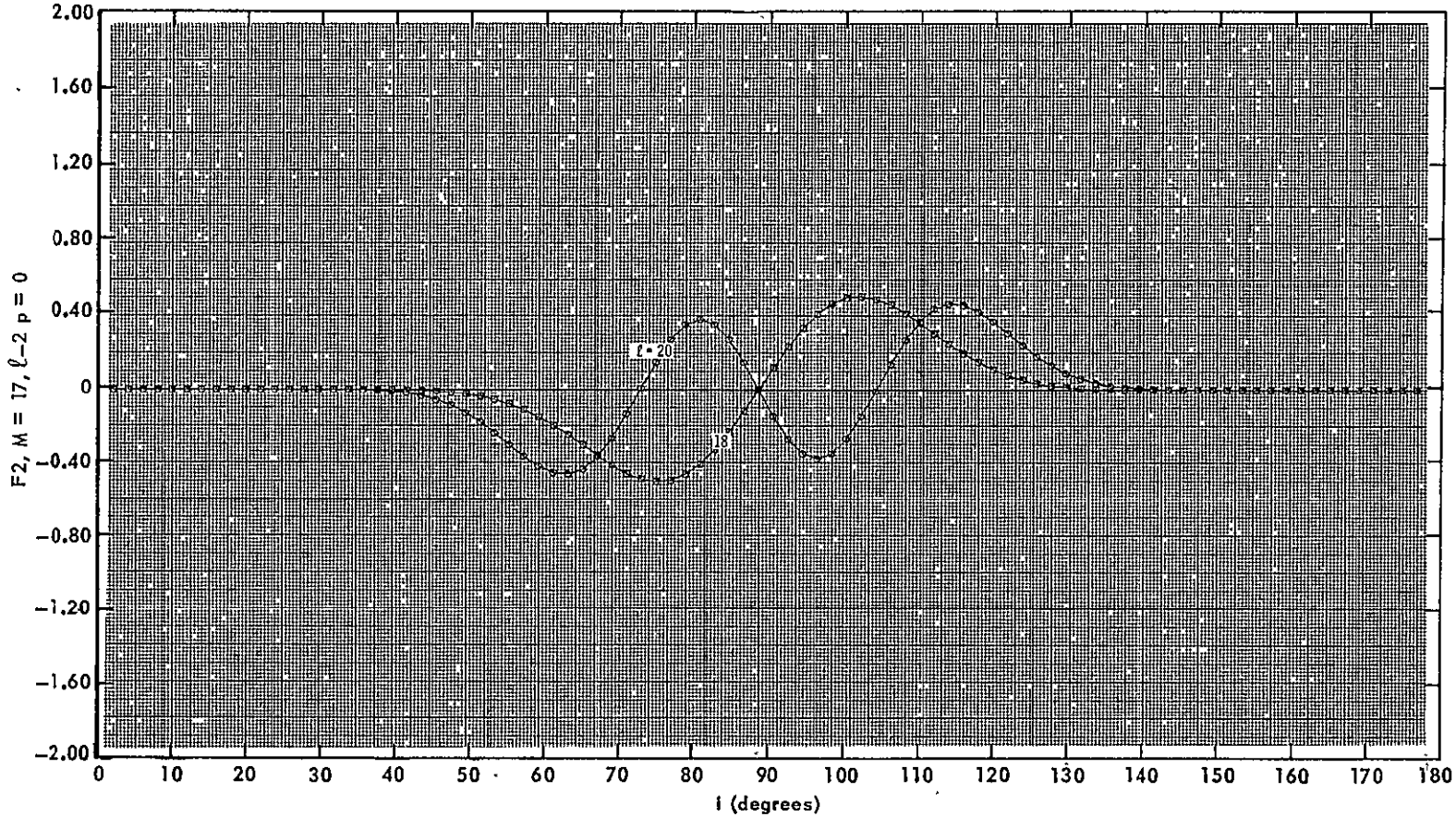
2.00
1.60
1.20
0.80
0.40
0
-0.40
-0.80
-1.20
-1.60
-2.00
F2, M = 17, ℓ-2 p = 0
ℓ = 20
18
0
10
20
30
40
50
60
70
80
90
100
110
120
130
140
150
160
170
180
i (degrees)

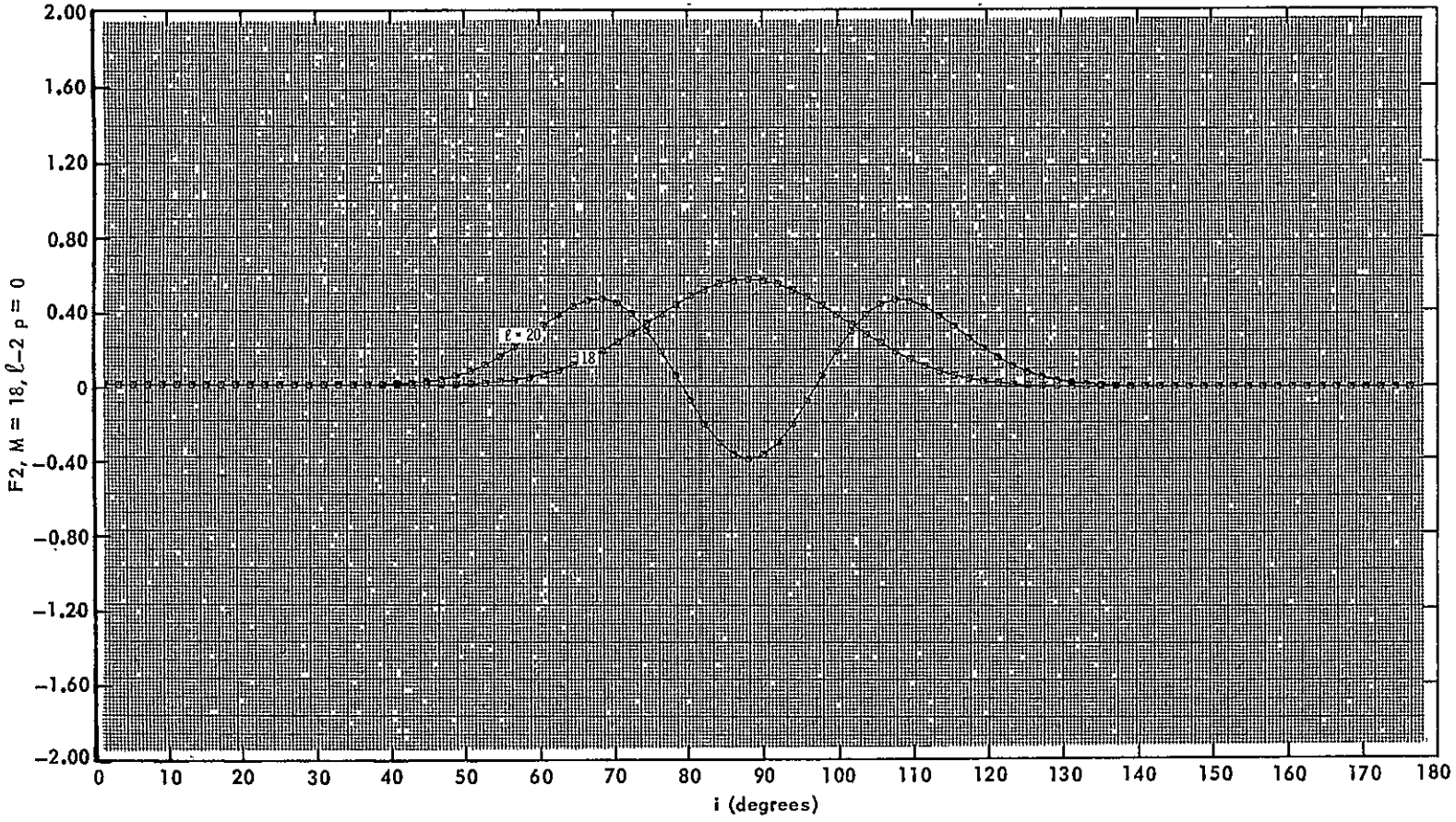
2.00
1.60
1.20
0.80
0.40
0
-0.40
-0.80
-1.20
-1.60
-2.00
F2, M = 18, ℓ-2 p = 0
ℓ = 20
18
0
10
20
30
40
50
60
70
80
90
100
110
120
130
140
150
160
170
180
i (degrees)

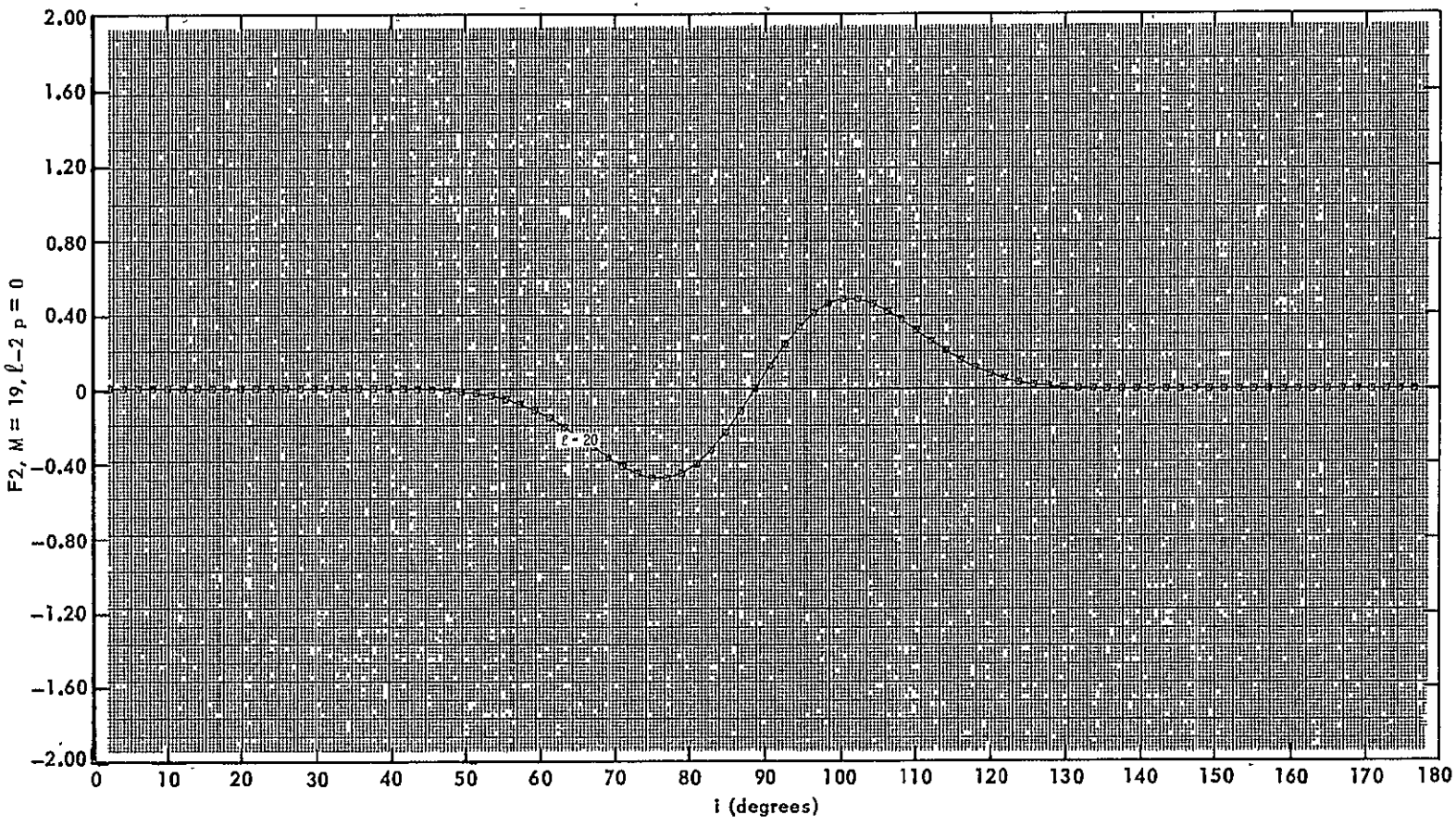
2.00
1.60
1.20
0.80
0.40
0
-0.40
-0.80
-1.20
-1.60
-2.00
F2, M = 19, ℓ-2 p = 0
ℓ = 20
0
10
20
30
40
50
60
70
80
90
100
110
120
130
140
150
160
170
180
i (degrees)

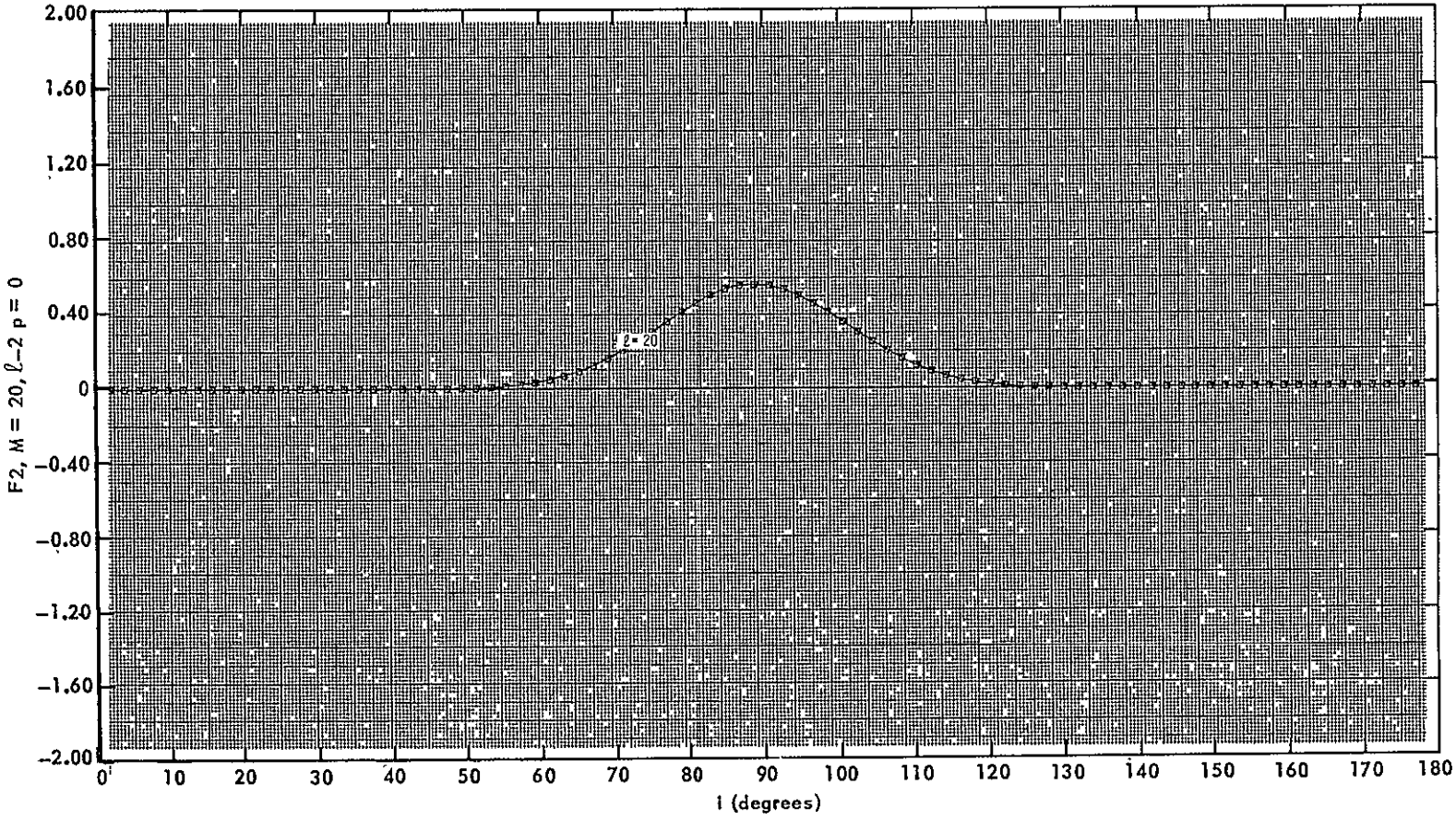
2.00
1.60
1.20
0.80
0.40
0
-0.40
-0.80
-1.20
-1.60
-2.00
F2, M = 20, ℓ-2 p = 0
ℓ = 20
0
10
20
30
40
50
60
70
80
90
100
110
120
130
140
150
160
170
180
i (degrees)

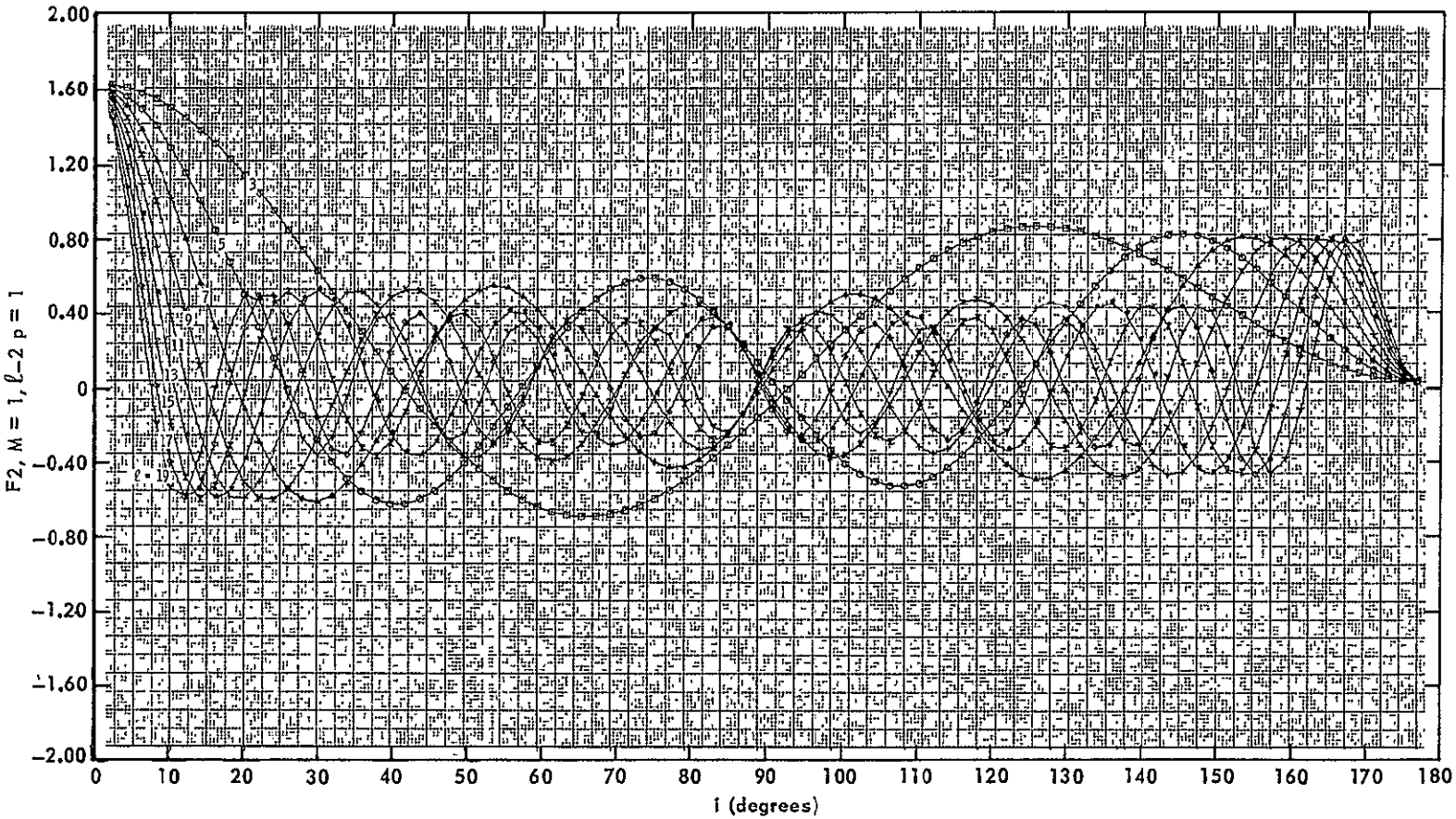
2.00
1.60
1.20
0.80
0.40
0
-0.40
-0.80
-1.20
-1.60
-2.00
F2, M = 1, ℓ-2 p = 1
0
10
20
30
40
50
60
70
80
90
100
110
120
130
140
150
160
170
180
i (degrees)

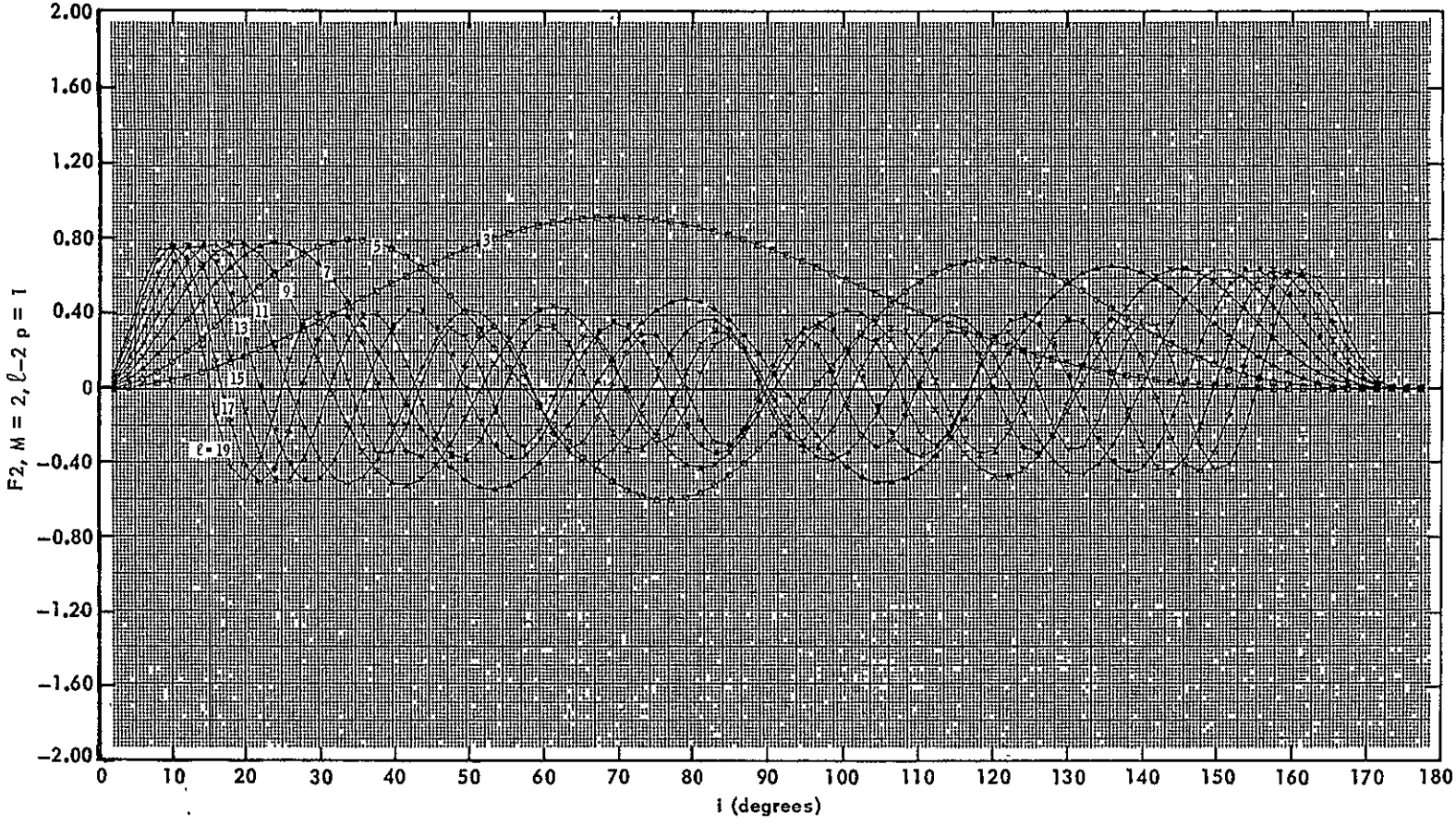
2.00
1.60
1.20
0.80
0.40
0
-0.40
-0.80
-1.20
-1.60
-2.00
F2, M = 2, ℓ-2 p = 1
0
10
20
30
40
50
60
70
80
90
100
110
120
130
140
150
160
170
180
i (degrees)
3
5
7
9
11
13
15
17
ℓ = 19

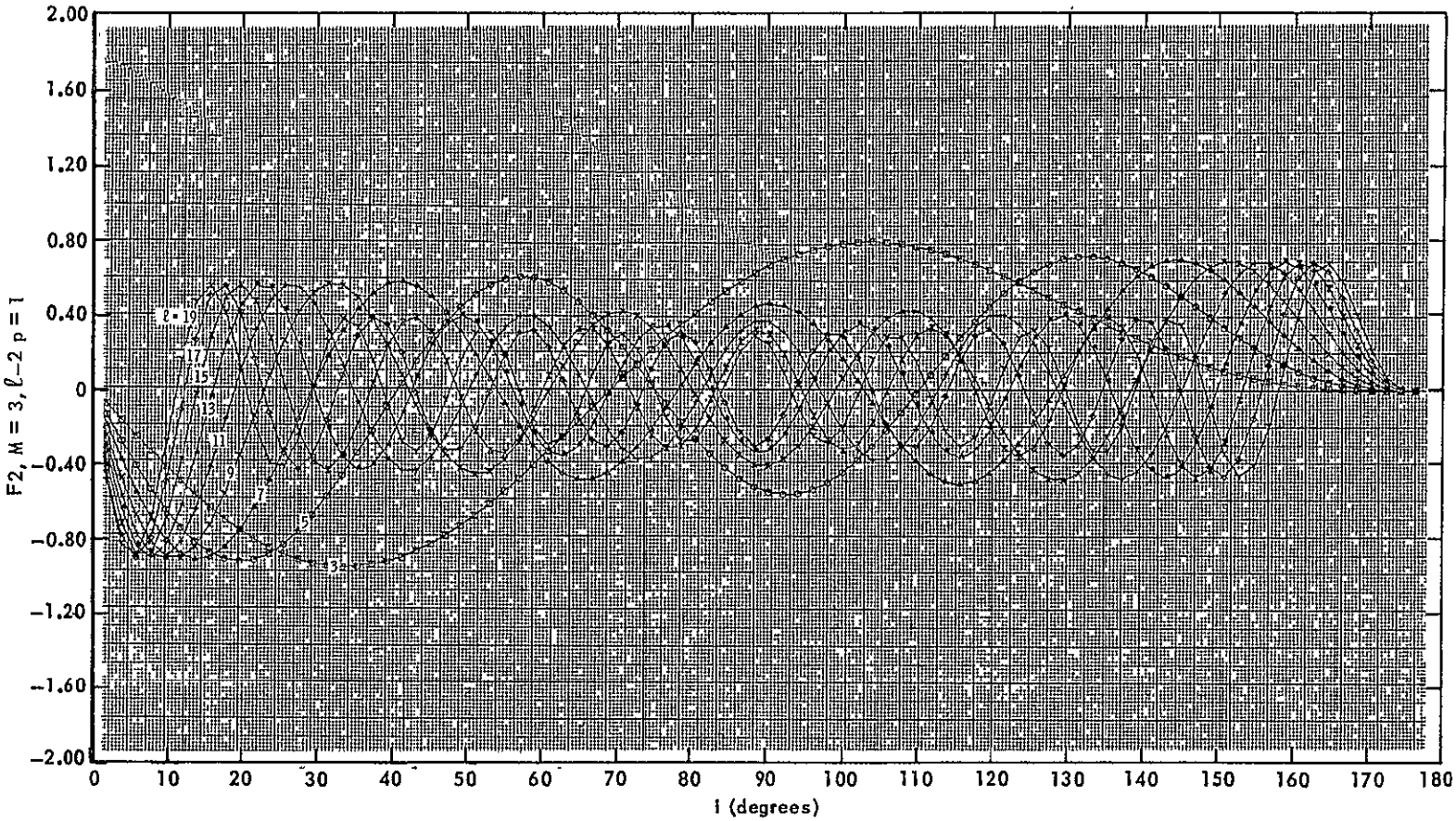
2.00
1.60
1.20
0.80
0.40
0
-0.40
-0.80
-1.20
-1.60
-2.00
F2, M = 3, ℓ-2 p = 1
0
10
20
30
40
50
60
70
80
90
100
110
120
130
140
150
160
170
180
i (degrees)

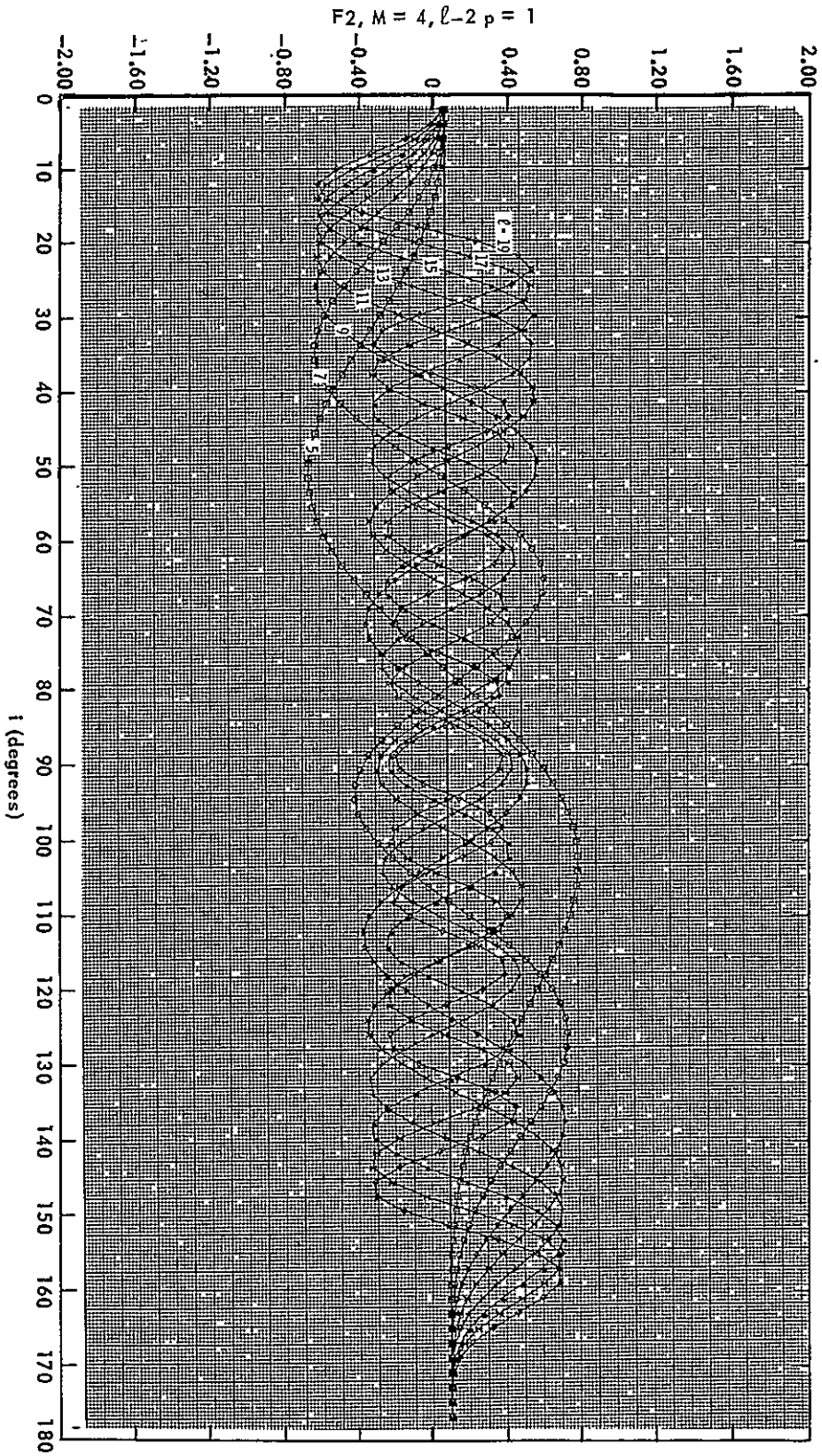
F2, M = 4, ℓ−2 p = 1
−2.00
−1.60
−1.20
−0.80
−0.40
0
0.40
0.80
1.20
1.60
2.00
0
10
20
30
40
50
60
70
80
90
100
110
120
130
140
150
160
170
180
i (degrees)

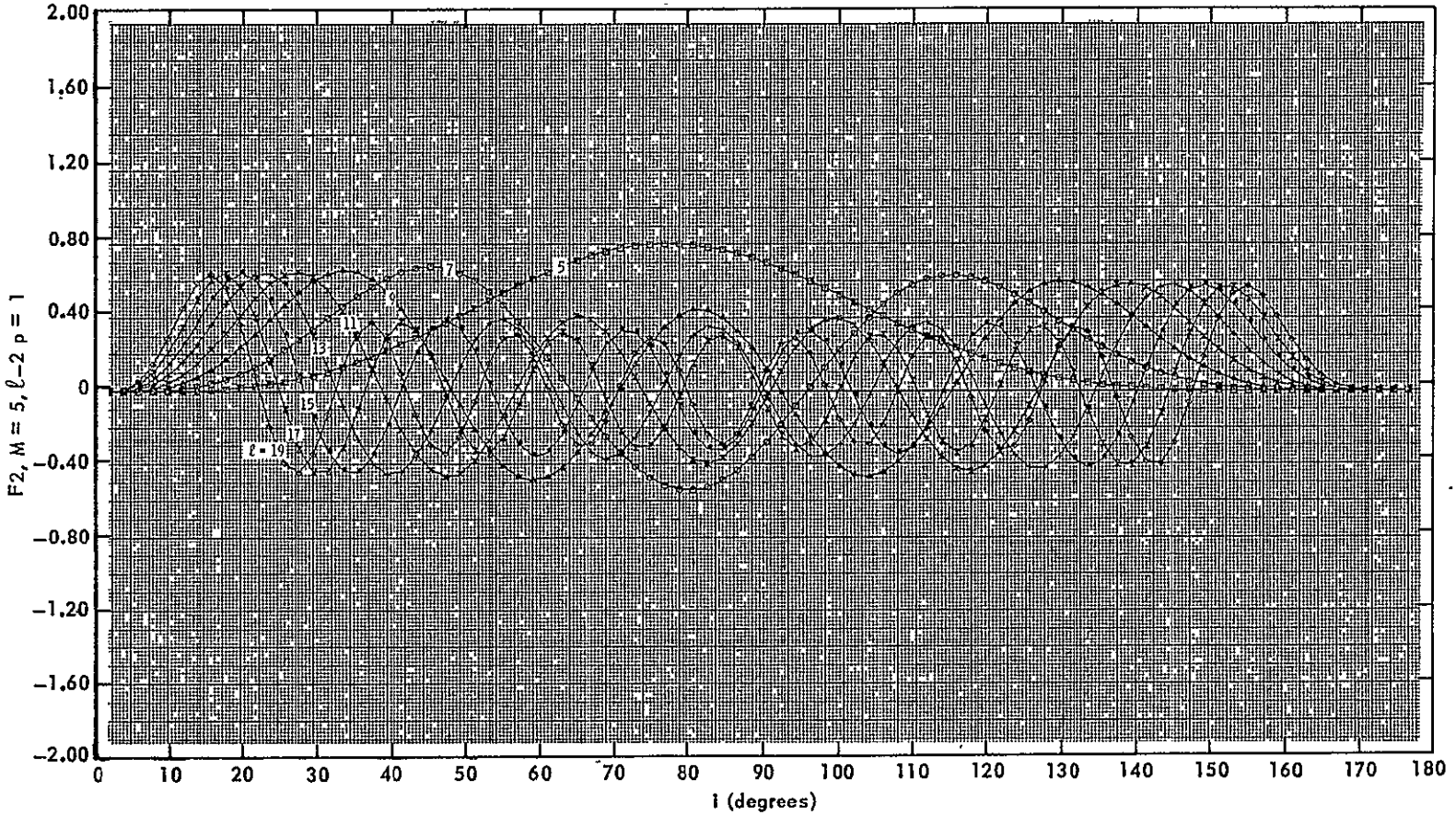
2.00
1.60
1.20
0.80
0.40
0
−0.40
−0.80
−1.20
−1.60
−2.00
F2, M = 5, ℓ−2 p = 1
0
10
20
30
40
50
60
70
80
90
100
110
120
130
140
150
160
170
180
i (degrees)
5
7
9
11
13
15
17
ℓ = 19

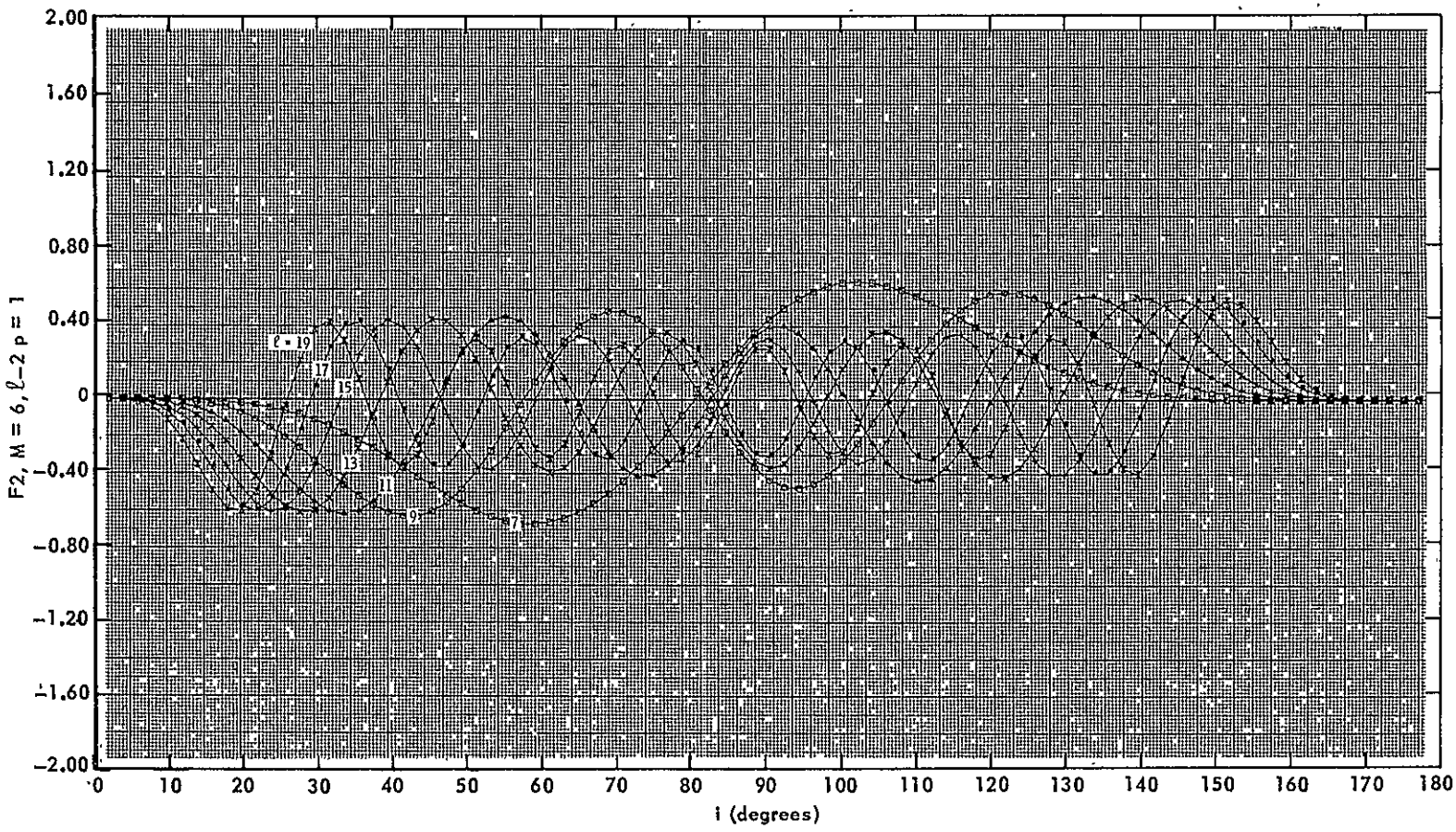
2.00
1.60
1.20
0.80
0.40
0
-0.40
-0.80
-1.20
-1.60
-2.00
F2, M = 6, ℓ-2 p = 1
ℓ = 19
17
15
13
11
9
7
0
10
20
30
40
50
60
70
80
90
100
110
120
130
140
150
160
170
180
i (degrees)

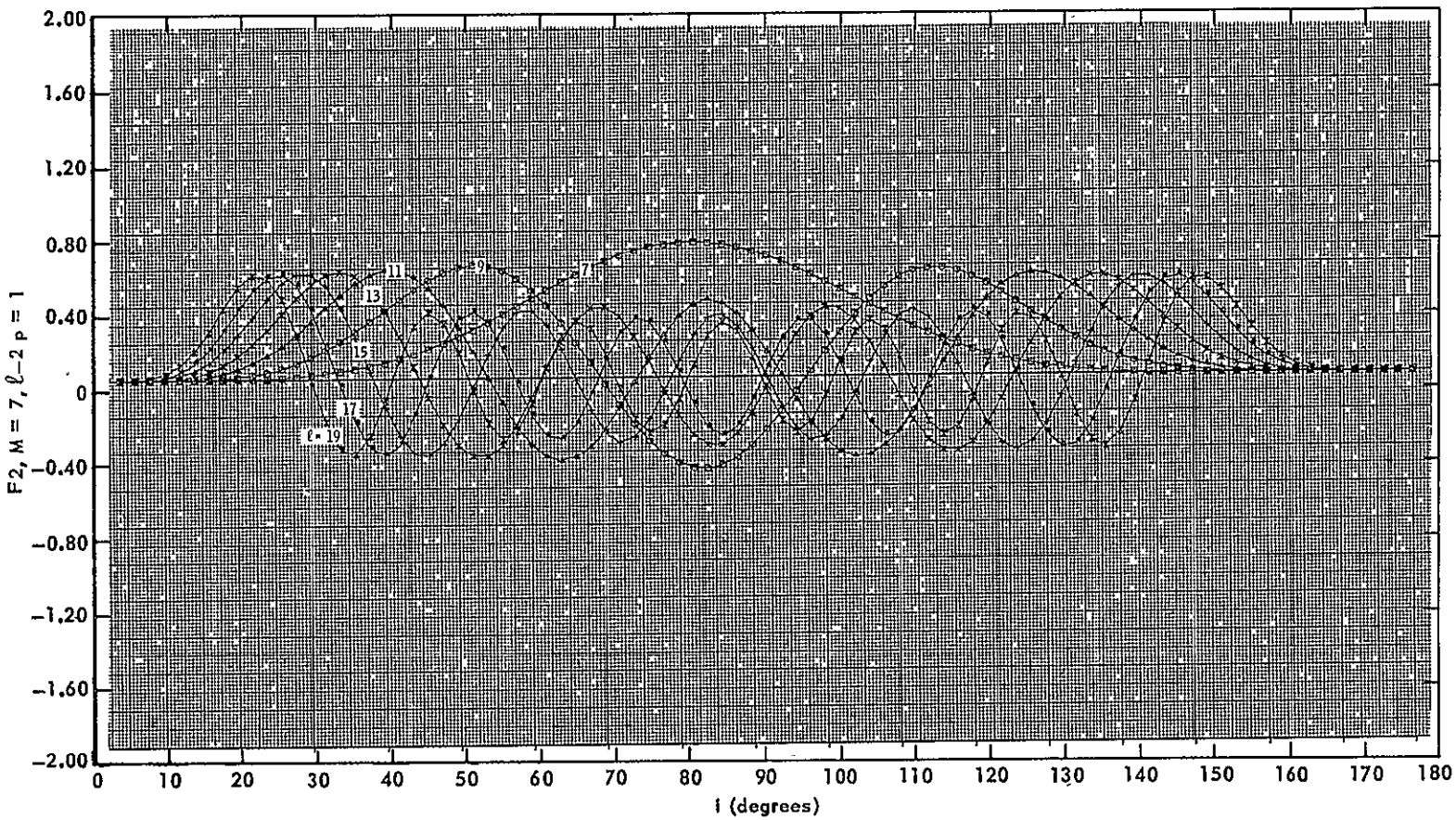
2.00
1.60
1.20
0.80
0.40
0
-0.40
-0.80
-1.20
-1.60
-2.00
F2, M = 7, ℓ−2 p = 1
0
10
20
30
40
50
60
70
80
90
100
110
120
130
140
150
160
170
180
i (degrees)
ℓ = 19
17
15
13
11
9
7

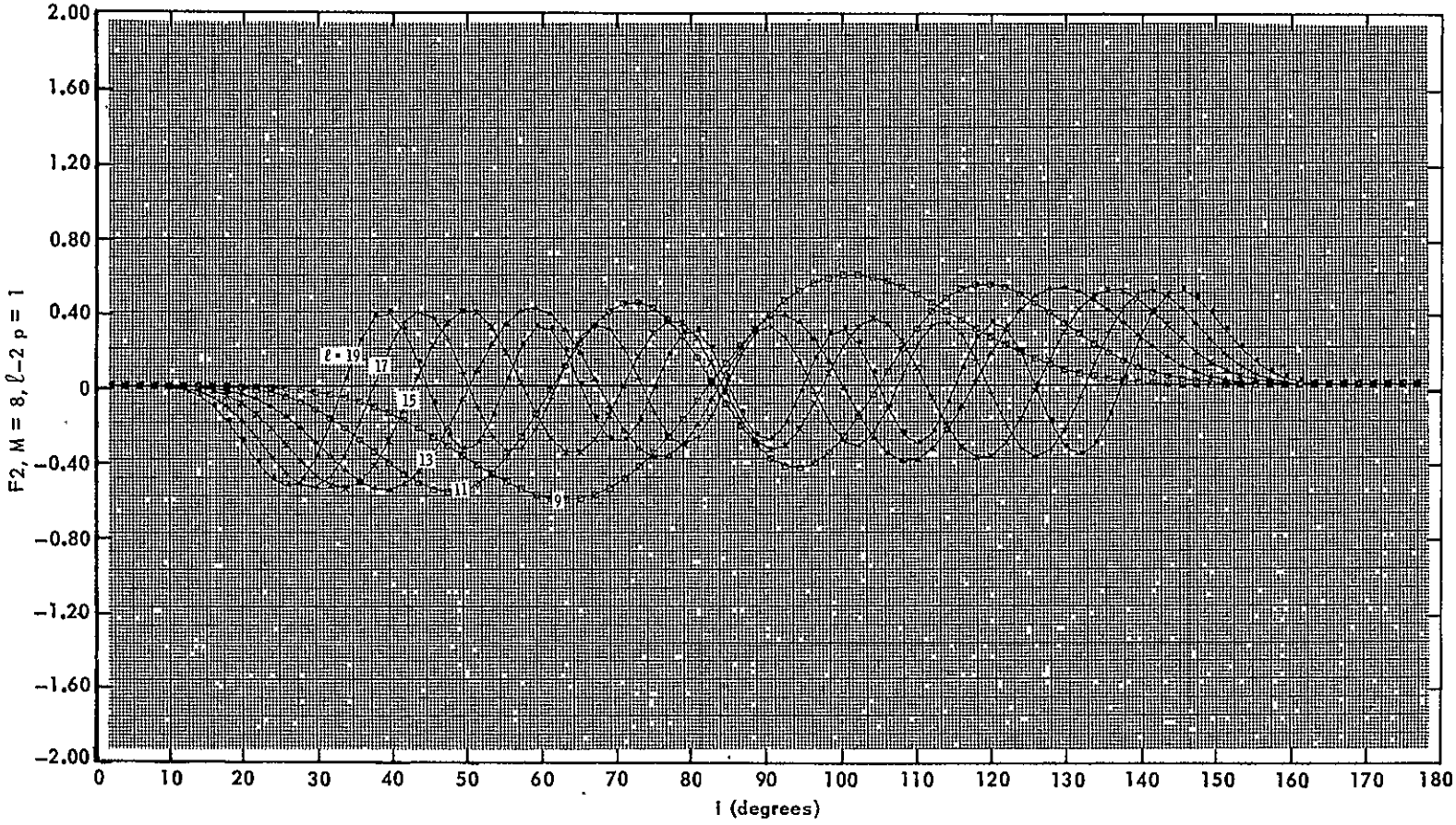
2.00
1.60
1.20
0.80
0.40
0
-0.40
-0.80
-1.20
-1.60
-2.00
F2, M = 8, ℓ-2 p = 1
ℓ = 19
17
15
13
11
9
0
10
20
30
40
50
60
70
80
90
100
110
120
130
140
150
160
170
180
I (degrees)

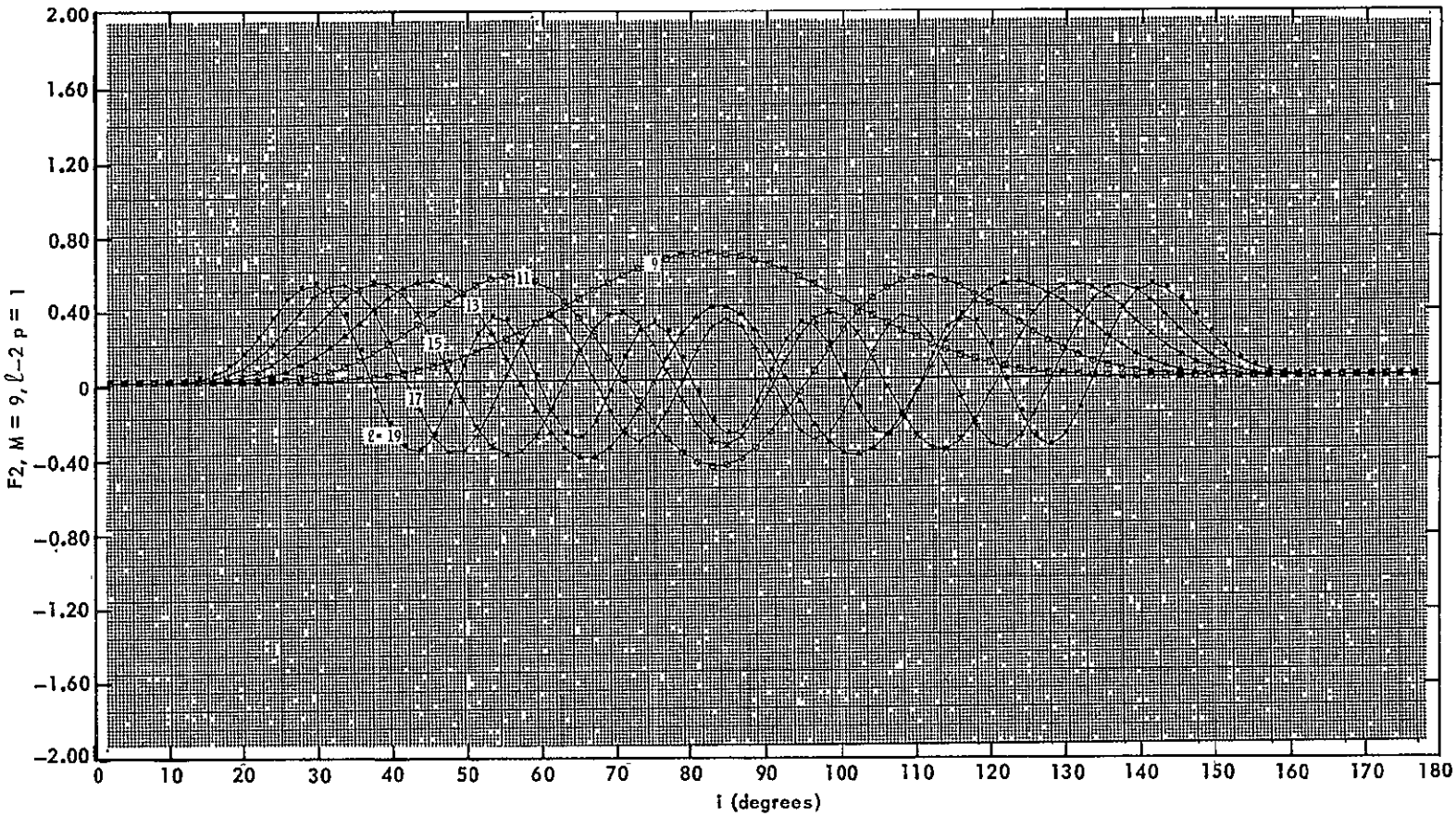
2.00
1.60
1.20
0.80
0.40
0
-0.40
-0.80
-1.20
-1.60
-2.00
F2, M = 9, ℓ-2 p = 1
0
10
20
30
40
50
60
70
80
90
100
110
120
130
140
150
160
170
180
i (degrees)
9
11
13
15
17
19

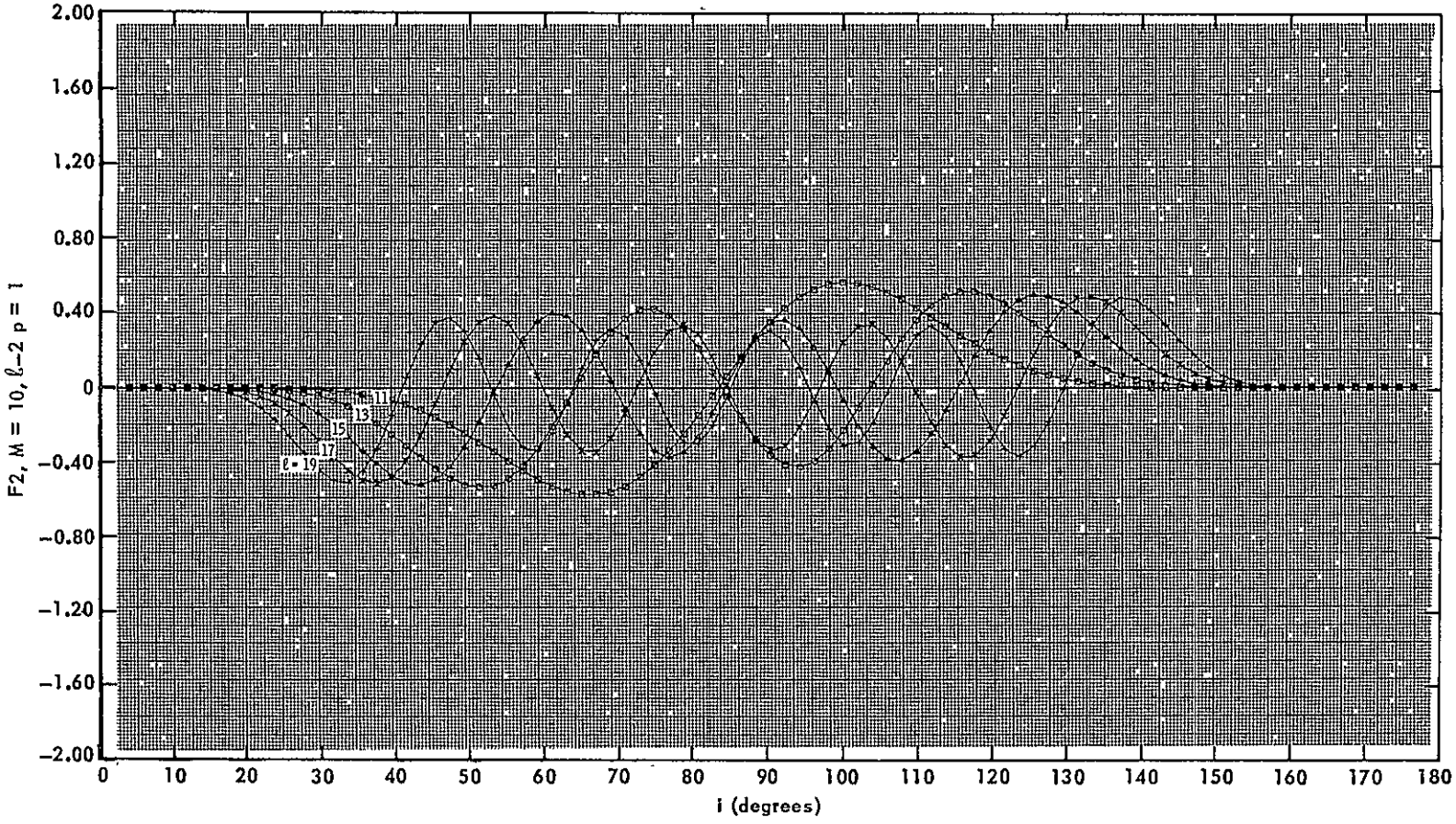
2.00
1.60
1.20
0.80
0.40
0
−0.40
−0.80
−1.20
−1.60
−2.00
F2, M = 10, ℓ−2 p = 1
ℓ = 11
13
15
17
19
0
10
20
30
40
50
60
70
80
90
100
110
120
130
140
150
160
170
180
i (degrees)

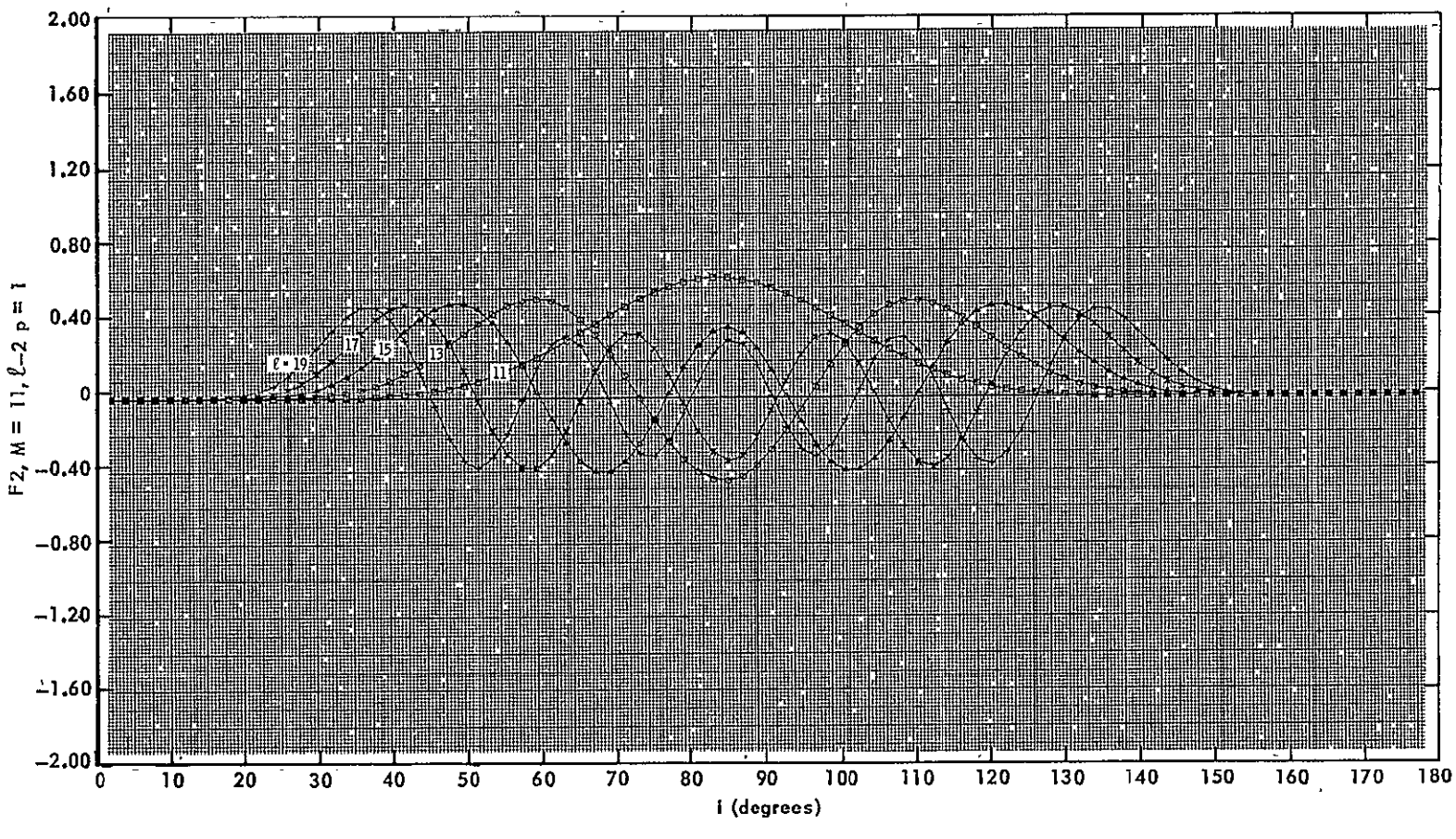
2.00
1.60
1.20
0.80
0.40
0
−0.40
−0.80
−1.20
−1.60
−2.00
F2, M = 11, ℓ−2 p = 1
0
10
20
30
40
50
60
70
80
90
100
110
120
130
140
150
160
170
180
i (degrees)
ℓ = 19
17
15
13
11

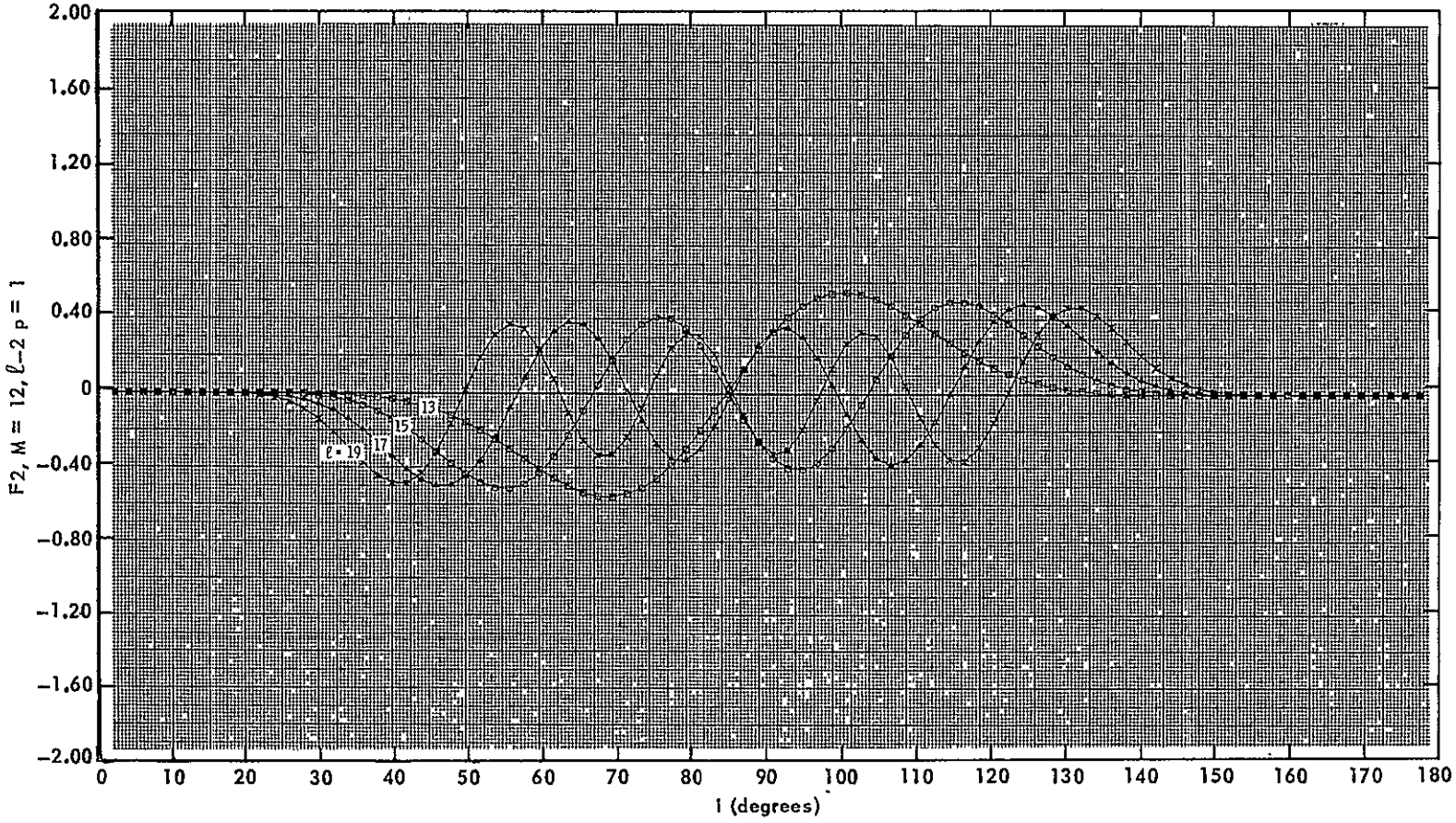
2.00
1.60
1.20
0.80
0.40
0
-0.40
-0.80
-1.20
-1.60
-2.00
F2, M = 12, ℓ-2 p = 1
0
10
20
30
40
50
60
70
80
90
100
110
120
130
140
150
160
170
180
I (degrees)
ℓ = 13
15
17
19

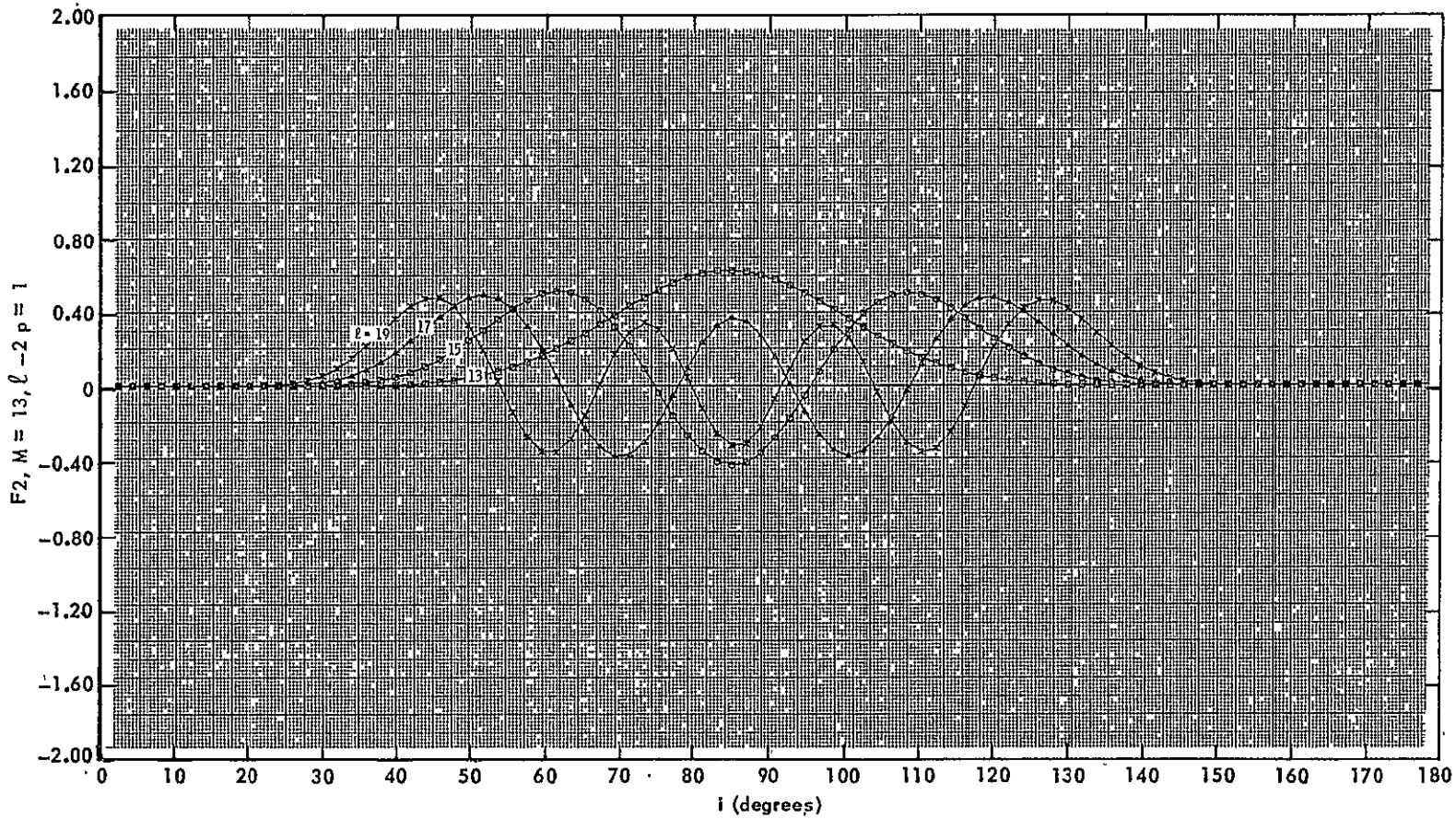
2.00
1.60
1.20
0.80
0.40
0
-0.40
-0.80
-1.20
-1.60
-2.00
F2, M = 13, ℓ -2 p = 1
ℓ = 19
17
15
13
0
10
20
30
40
50
60
70
80
90
100
110
120
130
140
150
160
170
180
i (degrees)

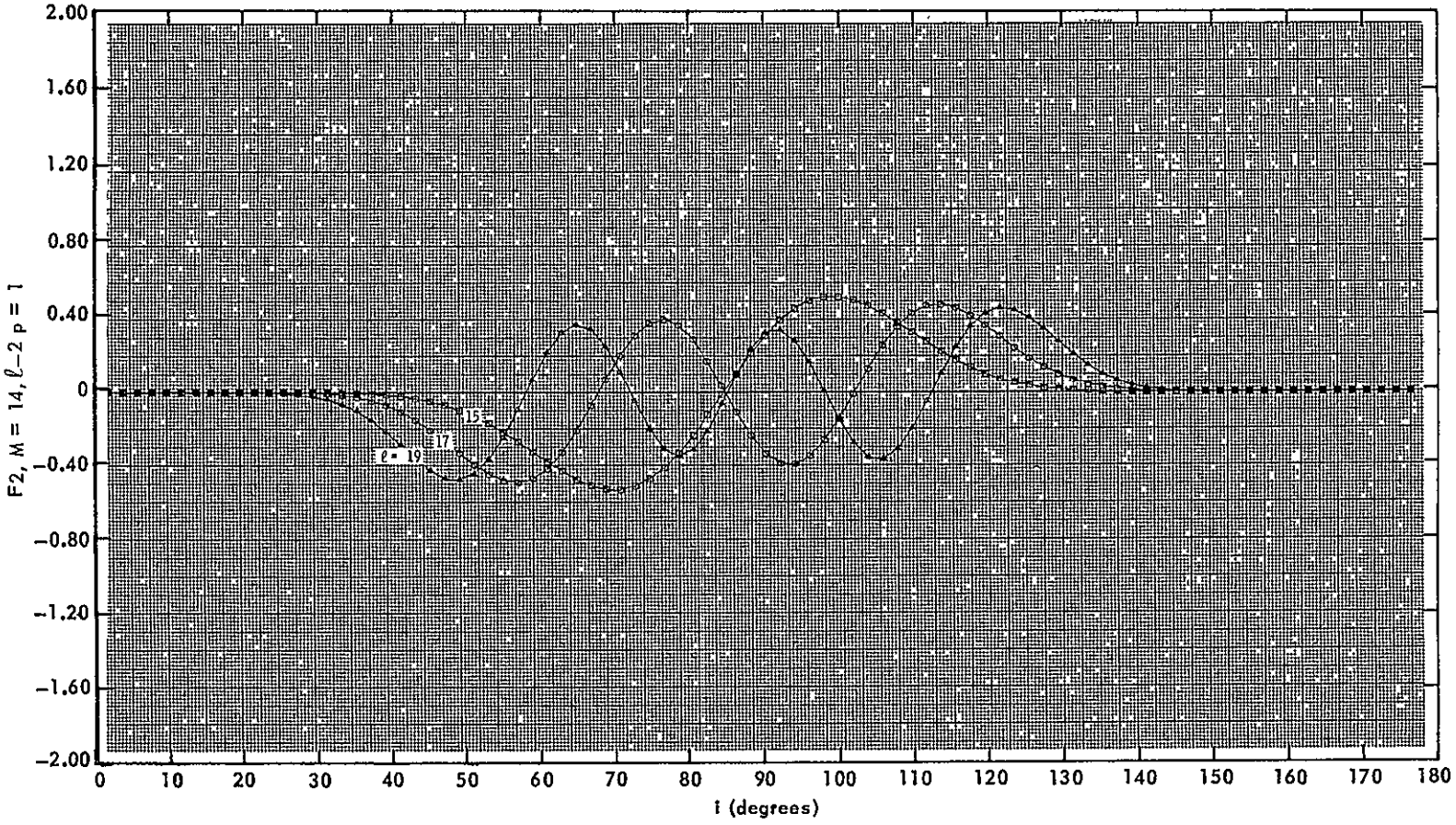
2.00
1.60
1.20
0.80
0.40
0
-0.40
-0.80
-1.20
-1.60
-2.00
F2, M = 14, ℓ-2 p = 1
0
10
20
30
40
50
60
70
80
90
100
110
120
130
140
150
160
170
180
i (degrees)
ℓ = 15
17
19

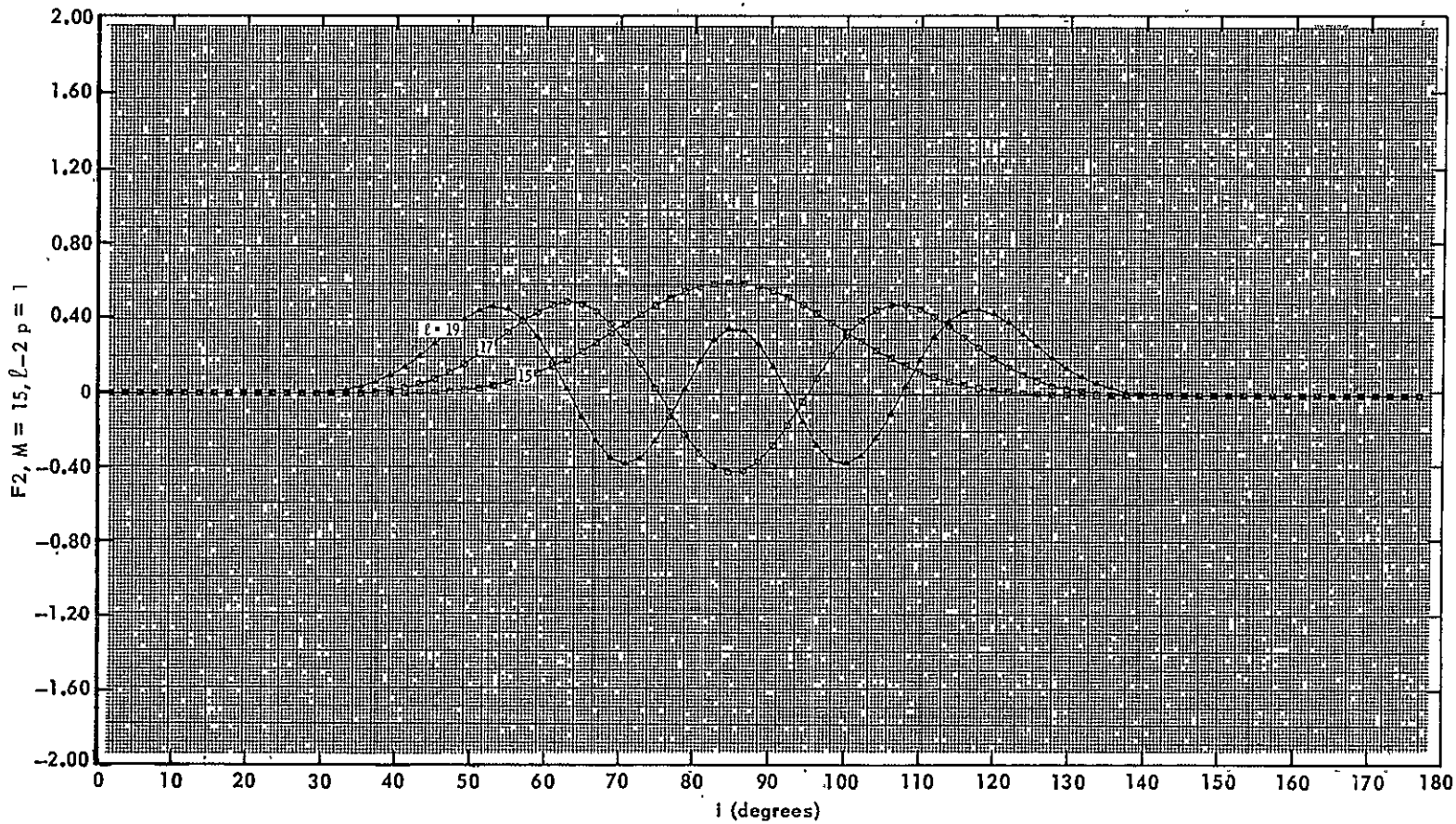
2.00
1.60
1.20
0.80
0.40
0
-0.40
-0.80
-1.20
-1.60
-2.00
F2, M = 15, ℓ-2 p = 1
ℓ = 19
17
15
0
10
20
30
40
50
60
70
80
90
100
110
120
130
140
150
160
170
180
i (degrees)

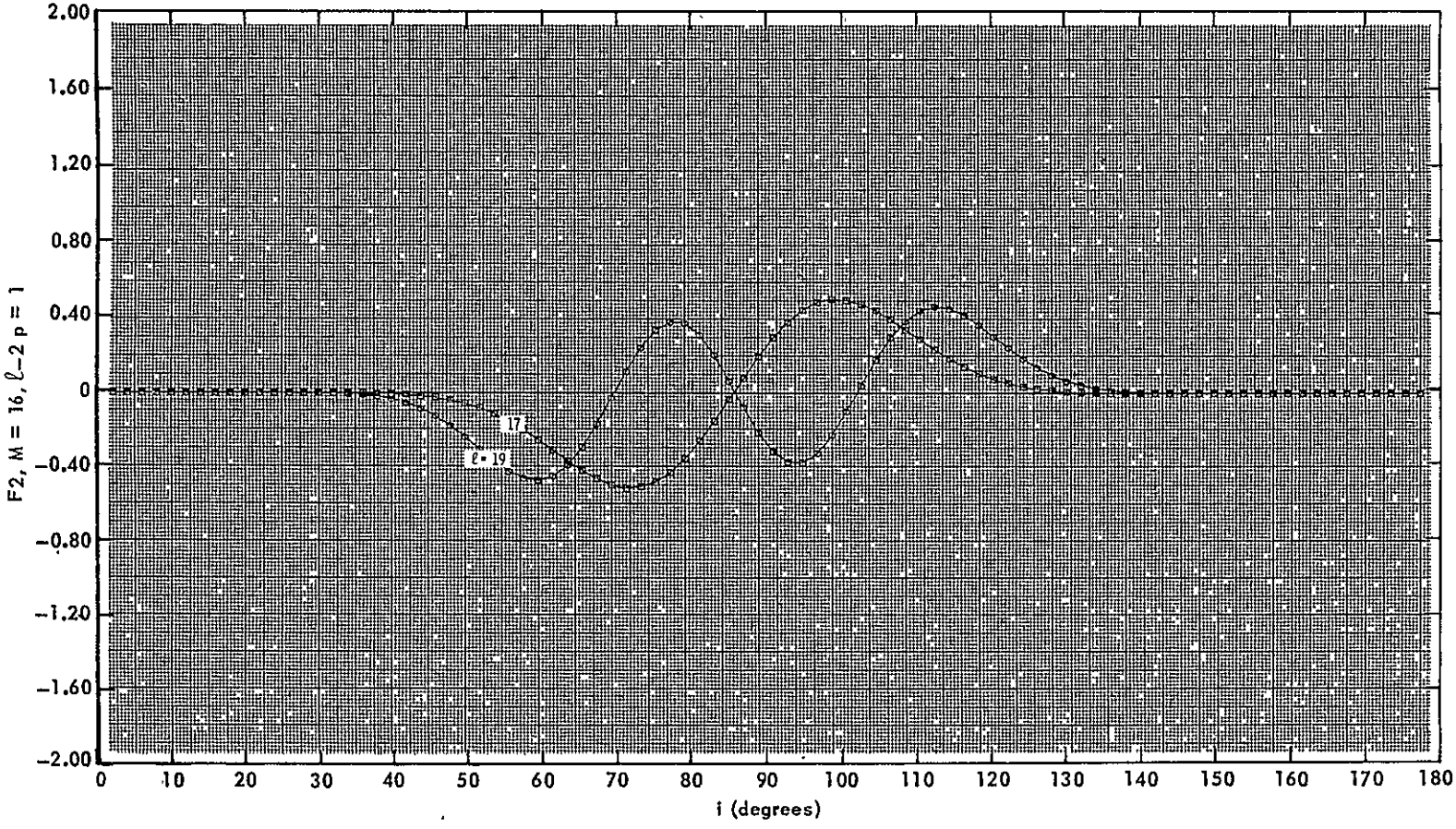
2.00
1.60
1.20
0.80
0.40
0
-0.40
-0.80
-1.20
-1.60
-2.00
F2, M = 16, ℓ-2 p = 1
0
10
20
30
40
50
60
70
80
90
100
110
120
130
140
150
160
170
180
i (degrees)
17
ℓ = 19

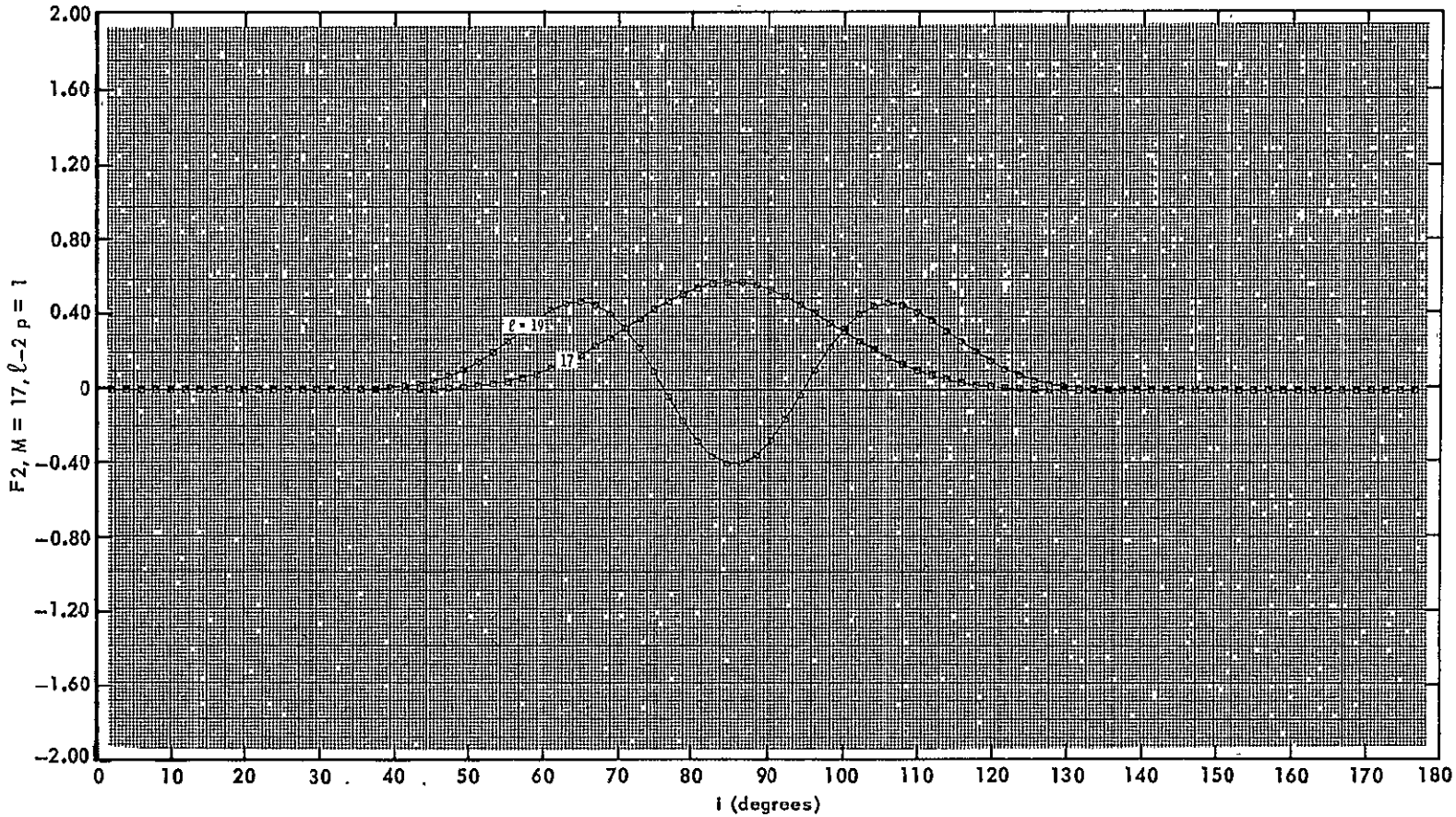
2.00
1.60
1.20
0.80
0.40
0
-0.40
-0.80
-1.20
-1.60
-2.00
F2, M = 17, ℓ-2 p = 1
ℓ = 19
17
0
10
20
30
40
50
60
70
80
90
100
110
120
130
140
150
160
170
180
i (degrees)

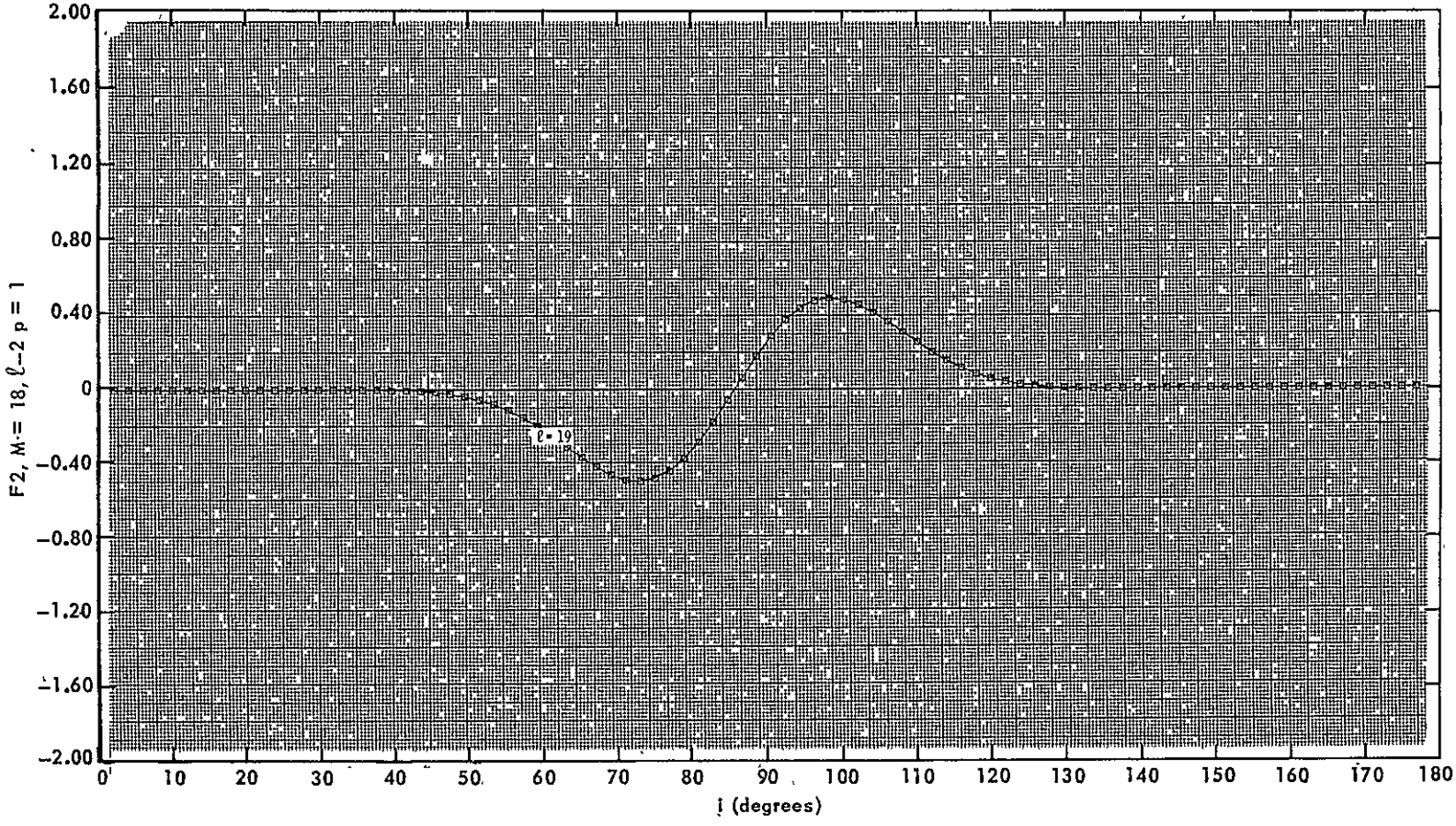
2.00
1.60
1.20
0.80
0.40
0
-0.40
-0.80
-1.20
-1.60
-2.00
F2, M= 18, ℓ-2 p = 1
ℓ = 19
0
10
20
30
40
50
60
70
80
90
100
110
120
130
140
150
160
170
180
I (degrees)

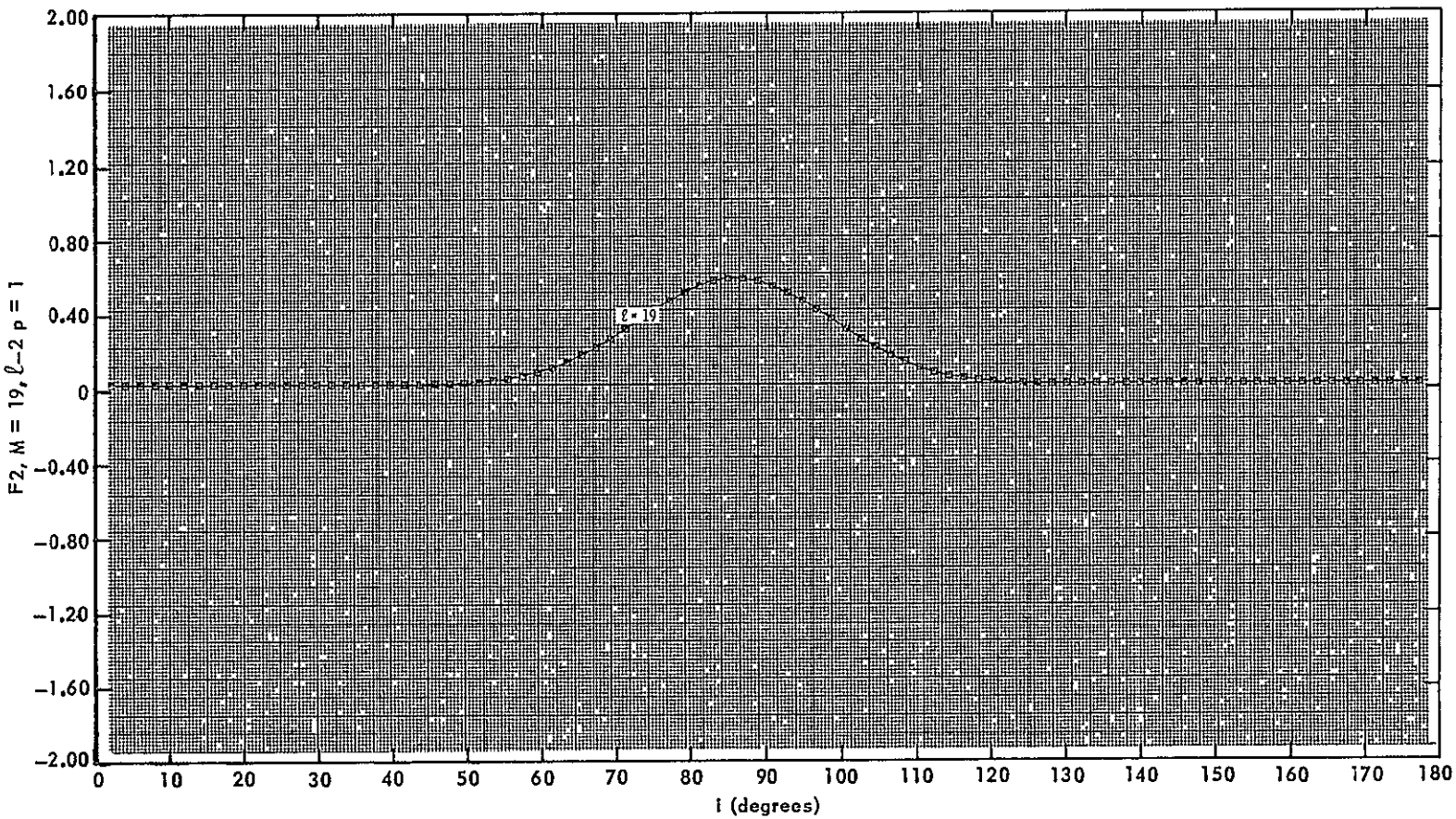
2.00
1.60
1.20
0.80
0.40
0
-0.40
-0.80
-1.20
-1.60
-2.00
F2, M = 19, ℓ-2 p = 1
ℓ = 19
0
10
20
30
40
50
60
70
80
90
100
110
120
130
140
150
160
170
180
i (degrees)

APPENDIX D

Graphs of Inclination Function F_1

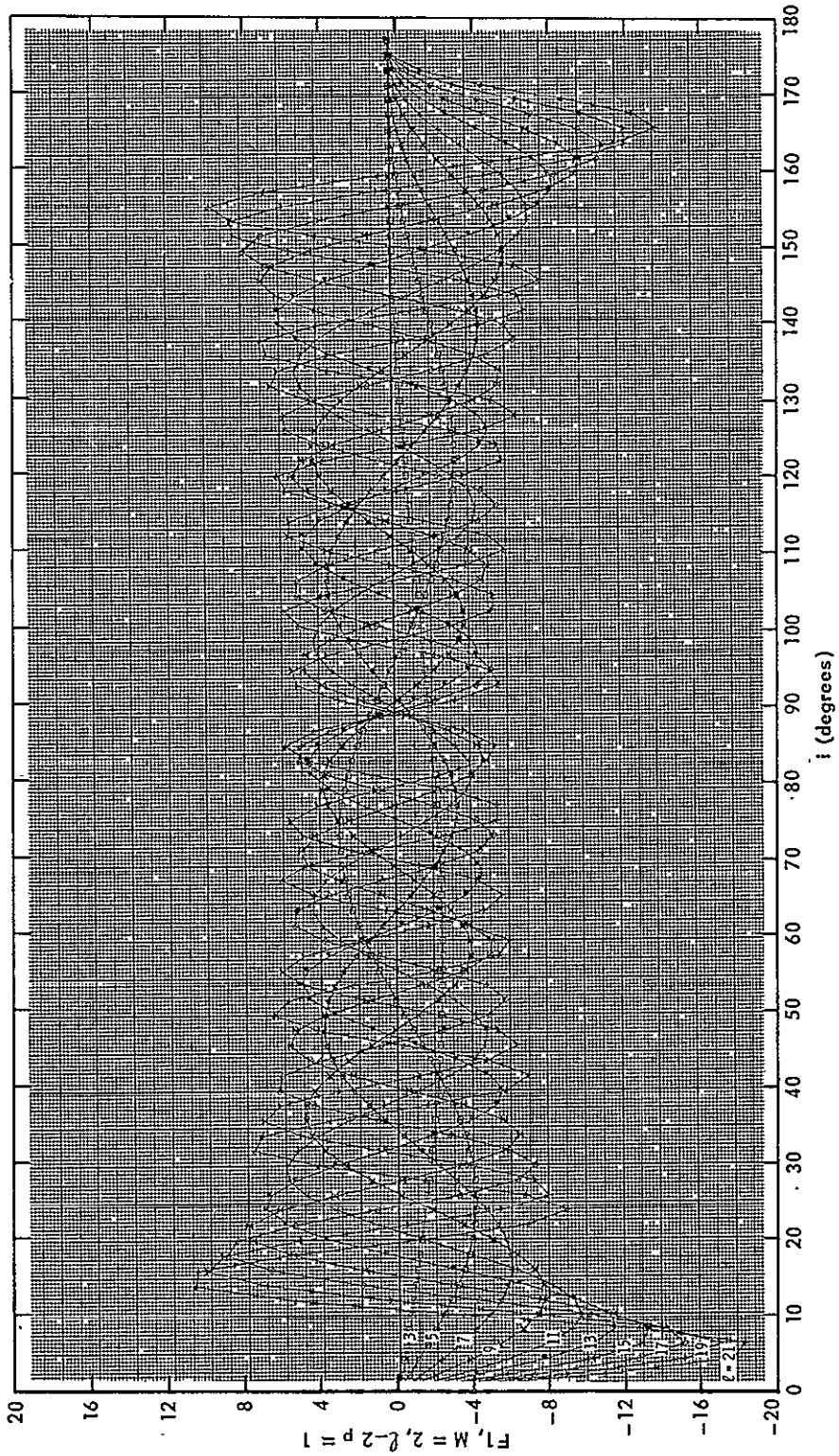

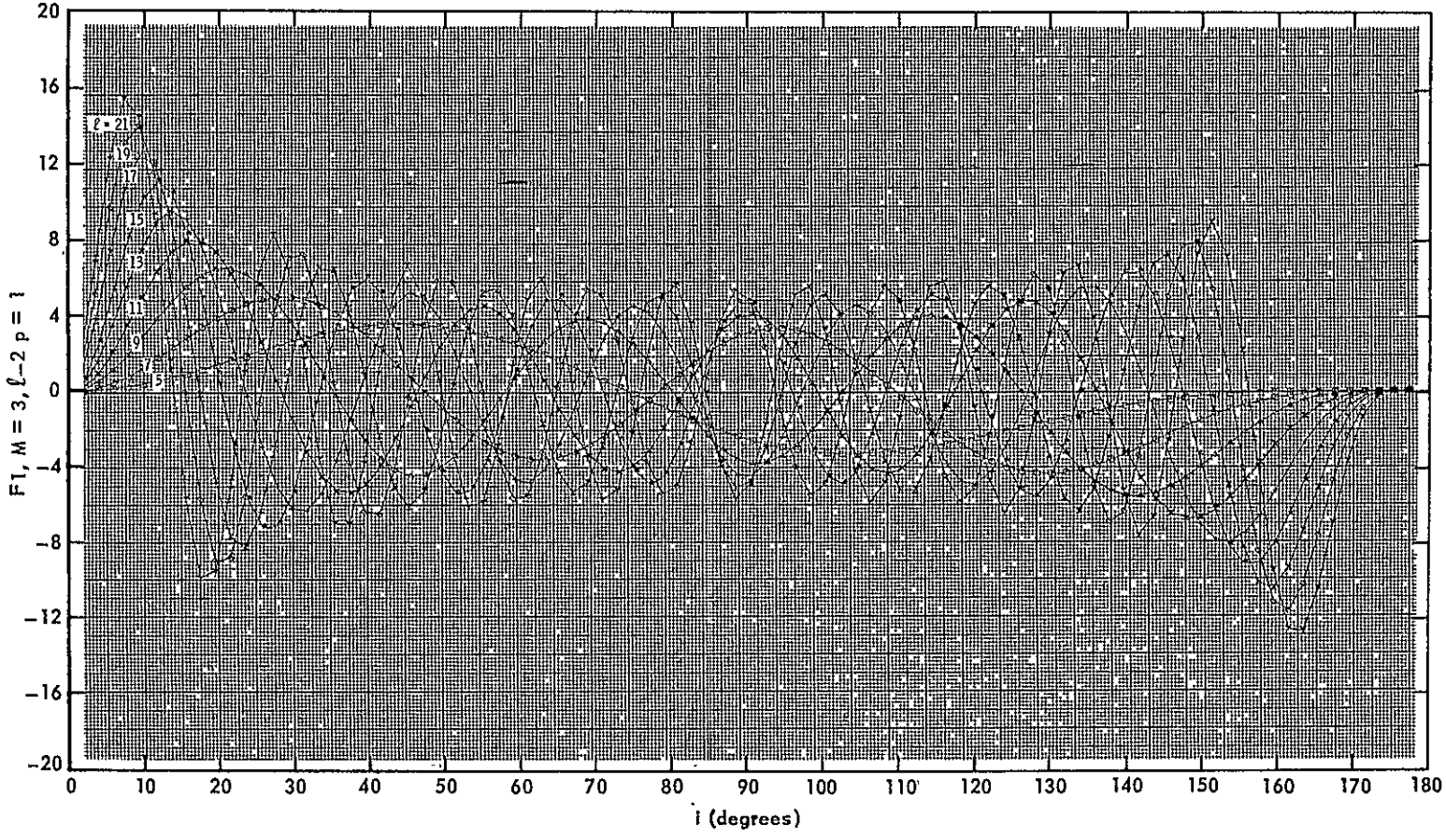
20
16
12
8
4
0
-4
-8
-12
-16
-20
ℓ = 21
19
17
15
13
11
9
7
5
0
10
20
30
40
50
60
70
80
90
100
110
120
130
140
150
160
170
180
i (degrees)
F1, M = 3, ℓ-2 p = 1

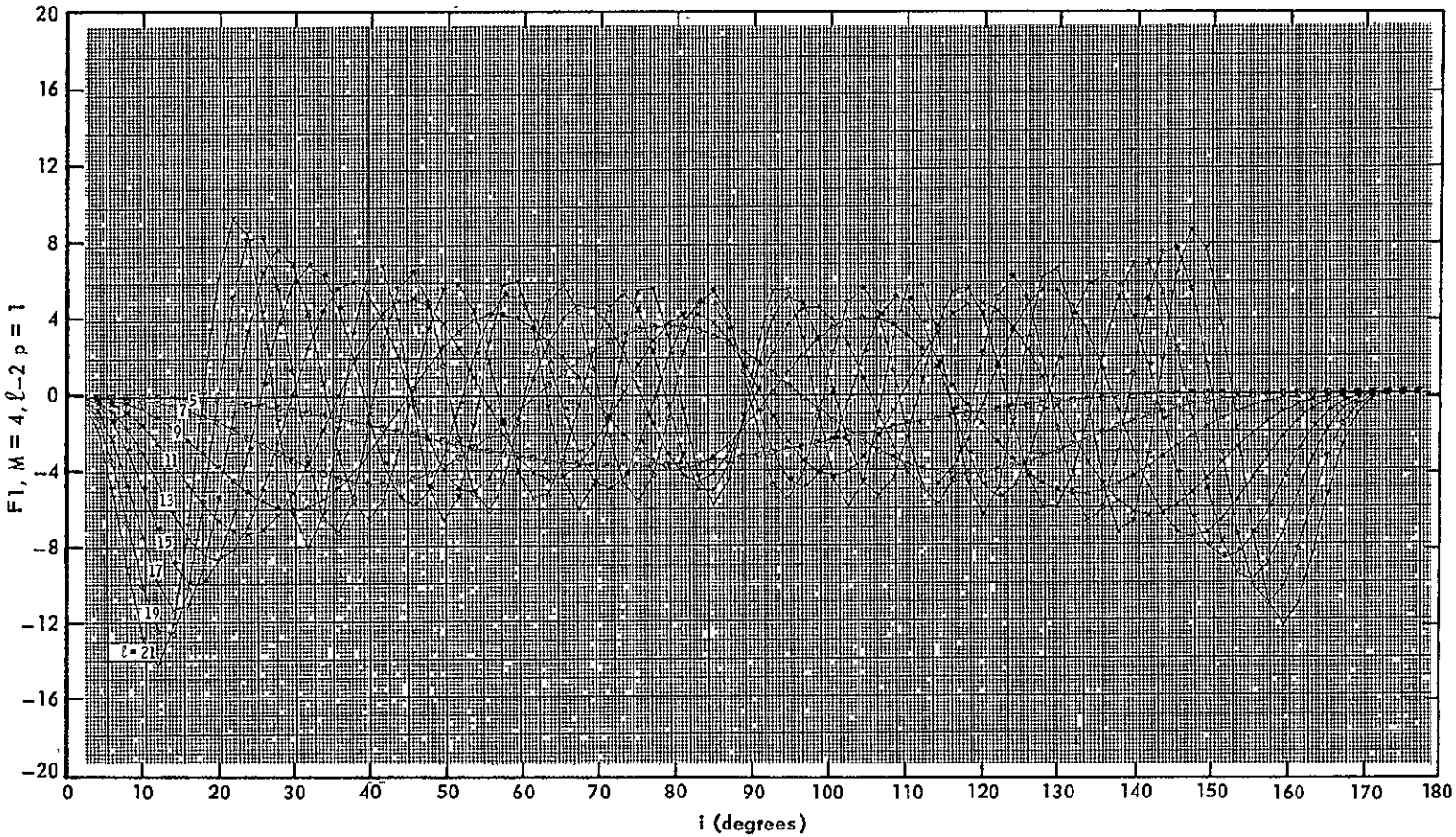
20
16
12
8
4
0
-4
-8
-12
-16
-20
0
10
20
30
40
50
60
70
80
90
100
110
120
130
140
150
160
170
180
i (degrees)
F1, M = 4, ℓ-2 p = 1
ℓ = 5
7
9
11
13
15
17
19
ℓ = 21

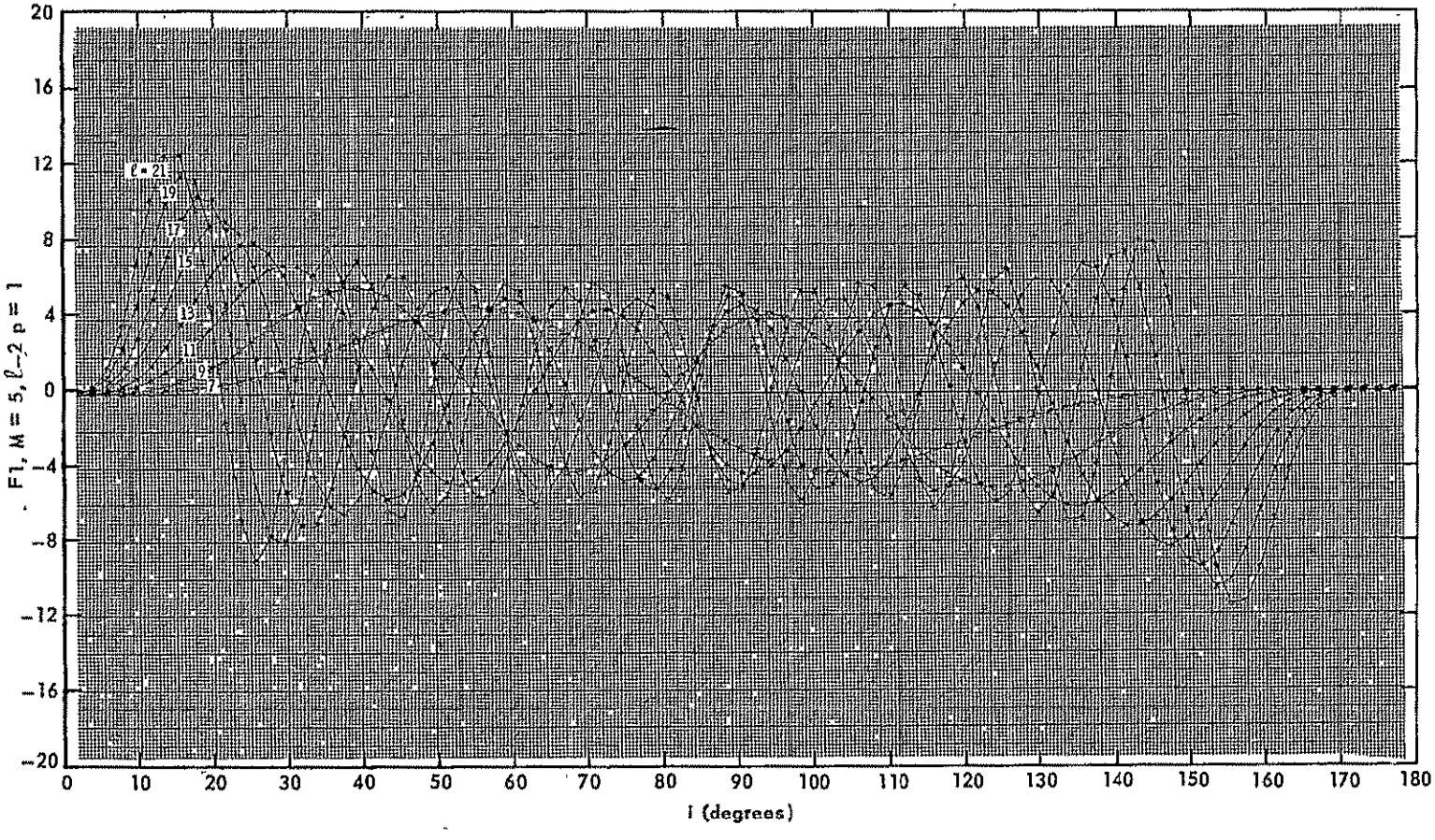
20
16
12
8
4
0
-4
-8
-12
-16
-20
0
10
20
30
40
50
60
70
80
90
100
110
120
130
140
150
160
170
180
ℓ = 21
19
17
15
13
11
9
7
F1, M = 5, ℓ-2 p = 1
I (degrees)

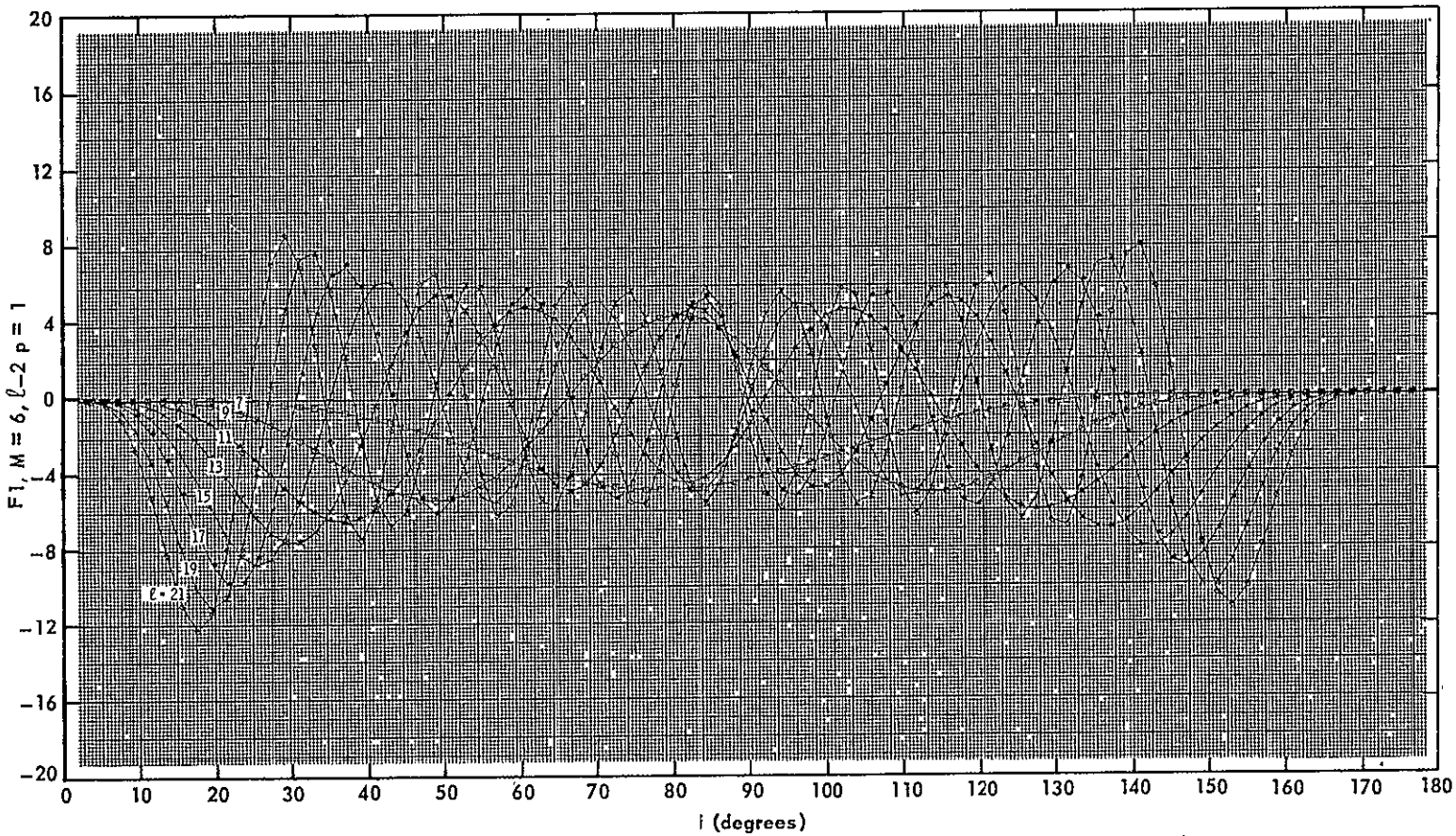
20
16
12
8
4
0
-4
-8
-12
-16
-20
0
10
20
30
40
50
60
70
80
90
100
110
120
130
140
150
160
170
180
i (degrees)
F1, M = 6, ℓ-2 p = 1
9
7
11
13
15
17
19
ℓ = 21

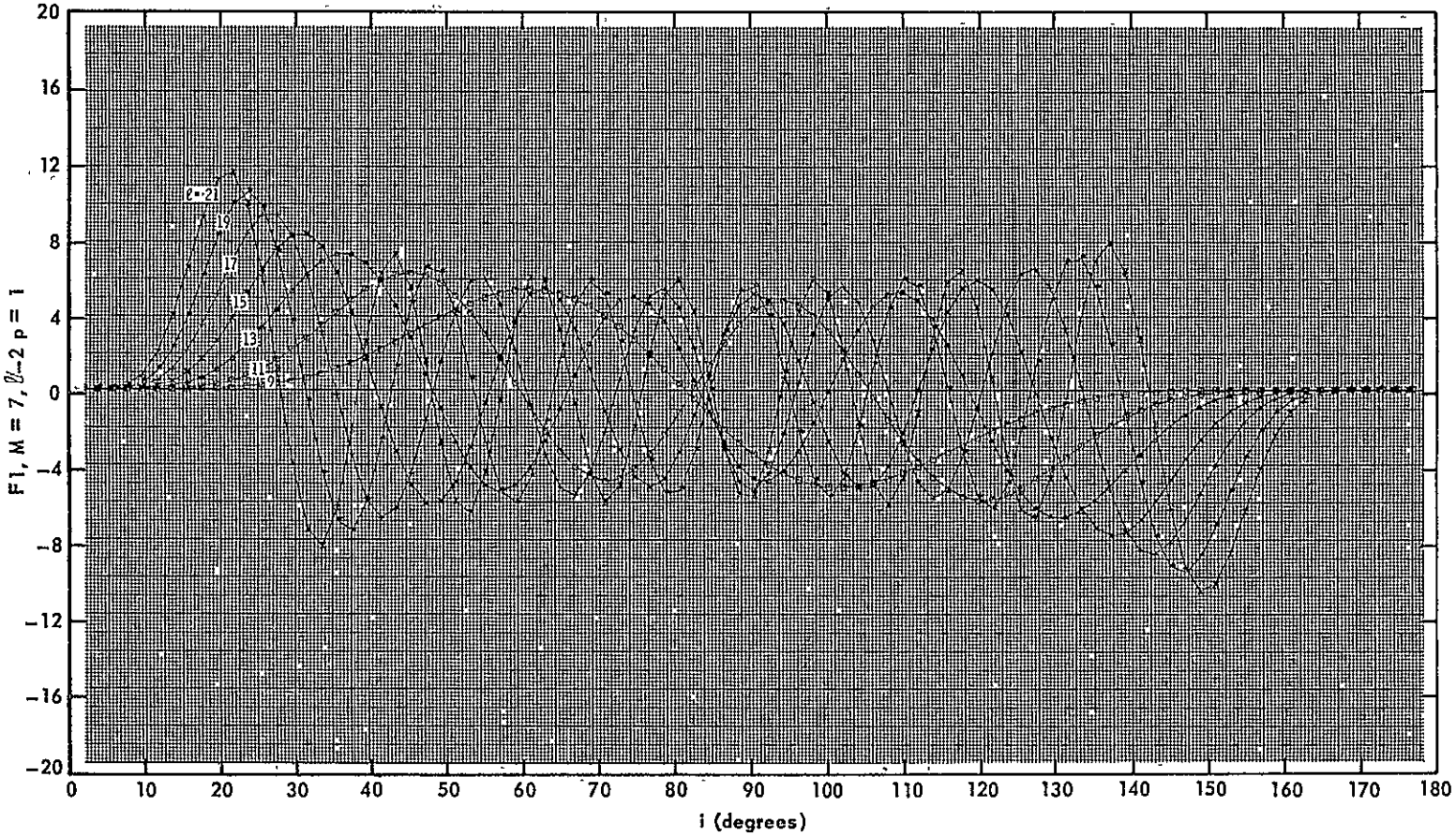
20
16
12
8
4
0
-4
-8
-12
-16
-20
0
10
20
30
40
50
60
70
80
90
100
110
120
130
140
150
160
170
180
i (degrees)
F1, M = 7, β=2 p = 1
ℓ=21
19
17
15
13
11
9

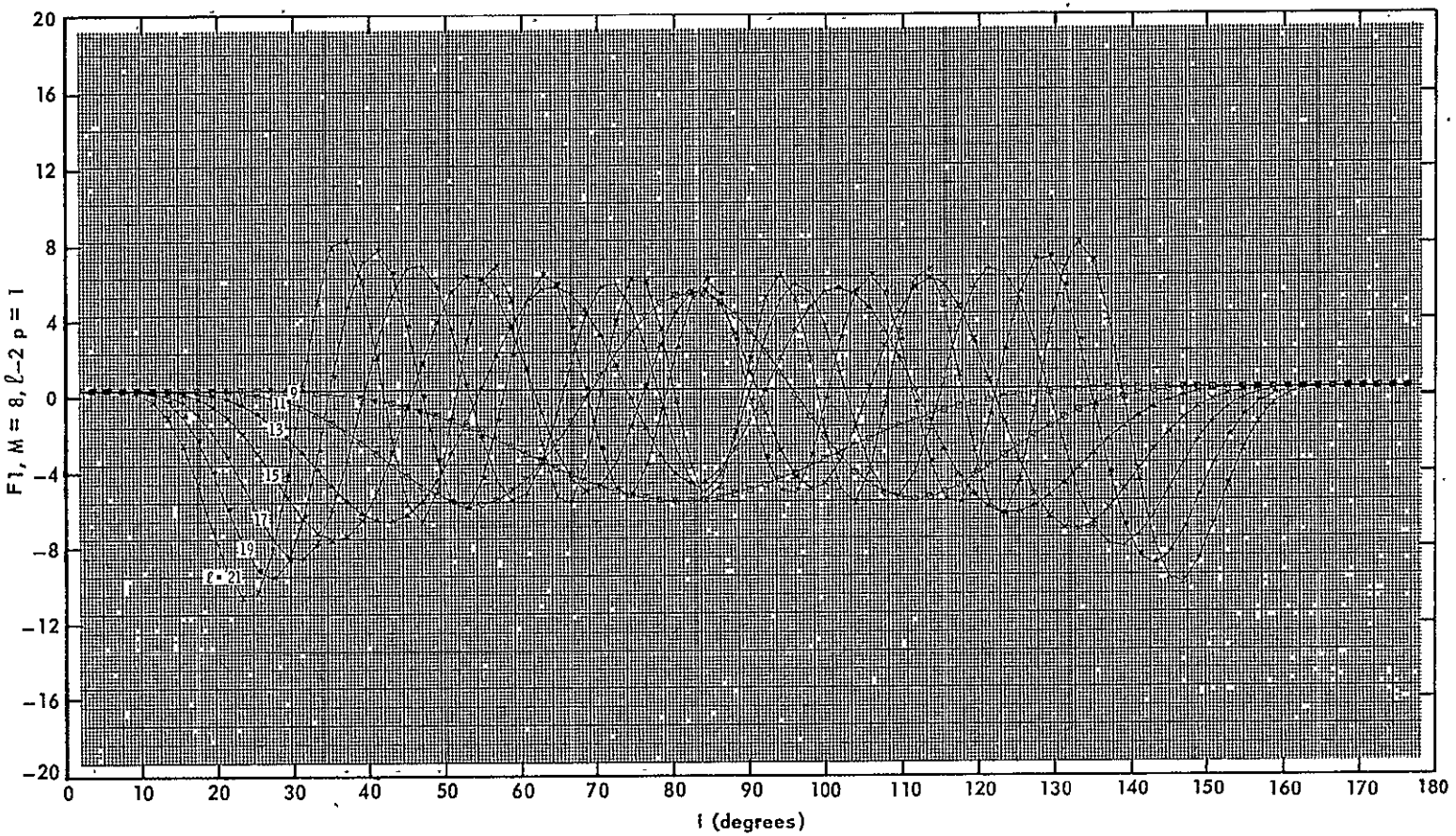
20
16
12
8
4
0
−4
−8
−12
−16
−20
0
10
20
30
40
50
60
70
80
90
100
110
120
130
140
150
160
170
180
F1, M = 8, ℓ−2 p = 1
ℓ (degrees)
9
11
13
15
17
19
ℓ = 21

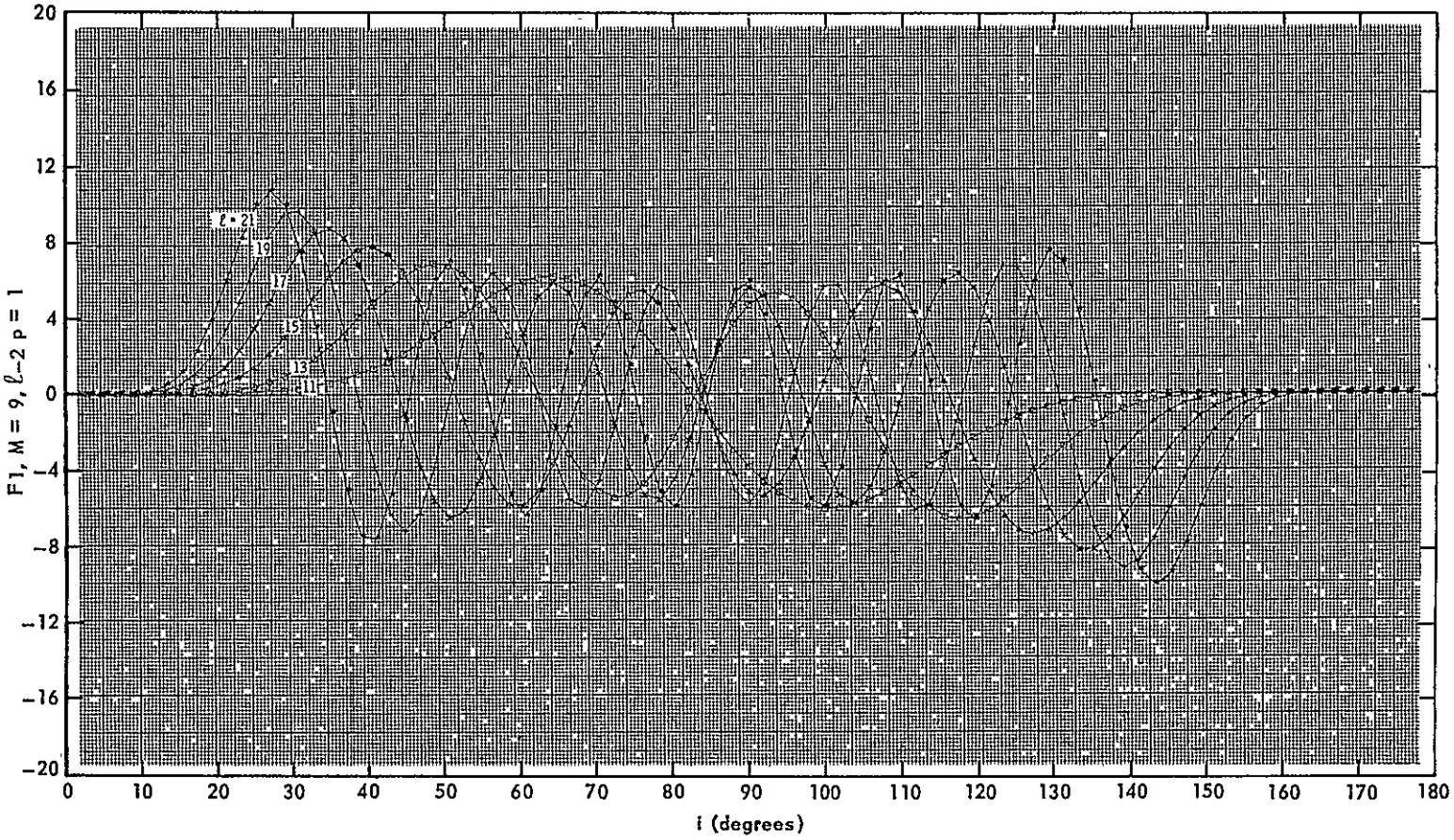
20
16
12
8
4
0
−4
−8
−12
−16
−20
0
10
20
30
40
50
60
70
80
90
100
110
120
130
140
150
160
170
180
i (degrees)
F1, M = 9, ℓ−2 p = 1
ℓ = 21
19
17
15
13
11

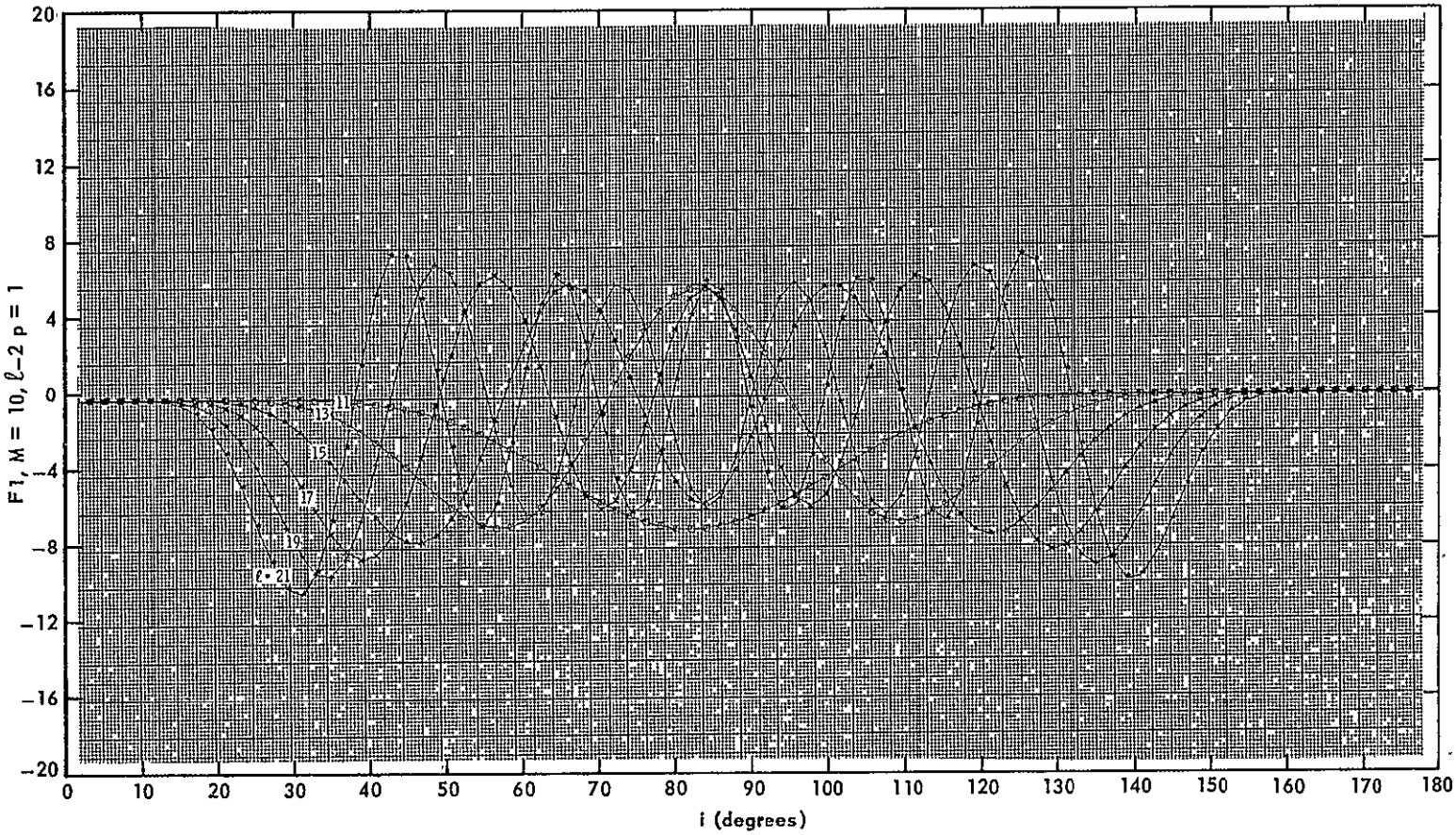
20
16
12
8
4
0
−4
−8
−12
−16
−20
0
10
20
30
40
50
60
70
80
90
100
110
120
130
140
150
160
170
180
i (degrees)
F1, M = 10, ℓ−2 p = 1
11
13
15
17
19
ℓ = 21

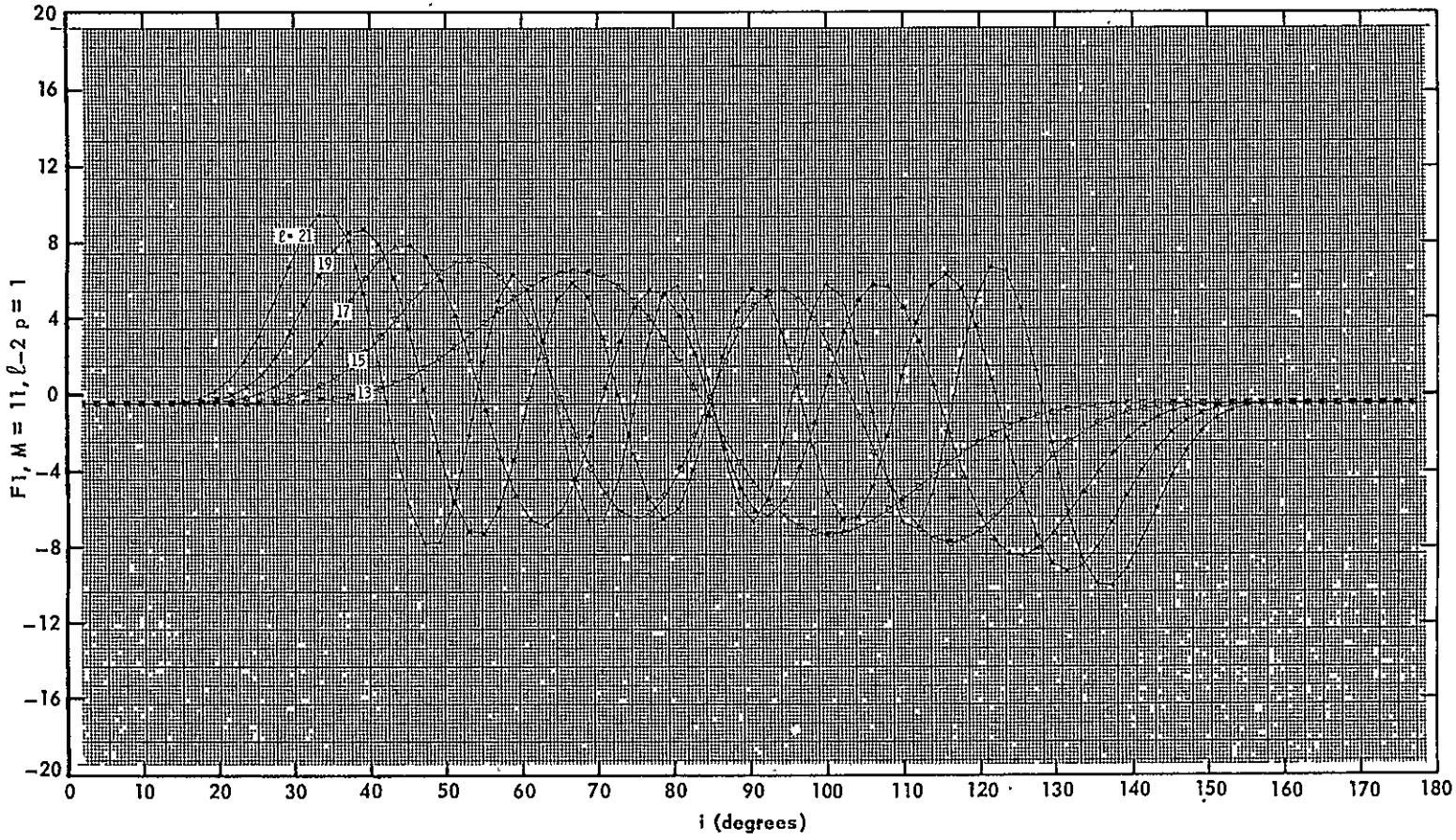
20
16
12
8
4
0
-4
-8
-12
-16
-20
0
10
20
30
40
50
60
70
80
90
100
110
120
130
140
150
160
170
180
ℓ = 21
19
17
15
13
F1, M = 11, ℓ-2 p = 1
i (degrees)

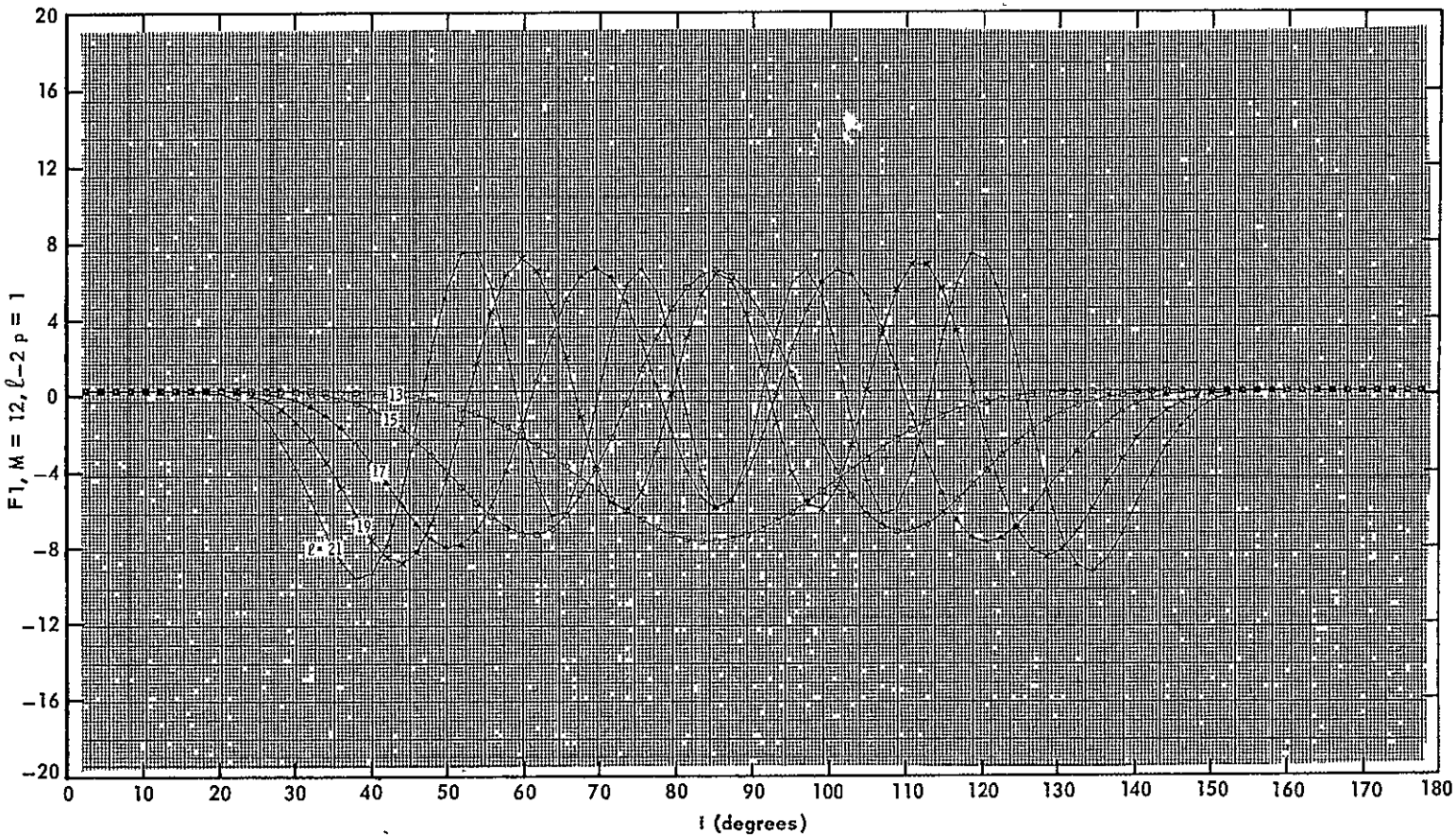
F1, M = 12, ℓ−2 p = 1
20
16
12
8
4
0
−4
−8
−12
−16
−20
0
10
20
30
40
50
60
70
80
90
100
110
120
130
140
150
160
170
180
I (degrees)
13
15
17
19
21

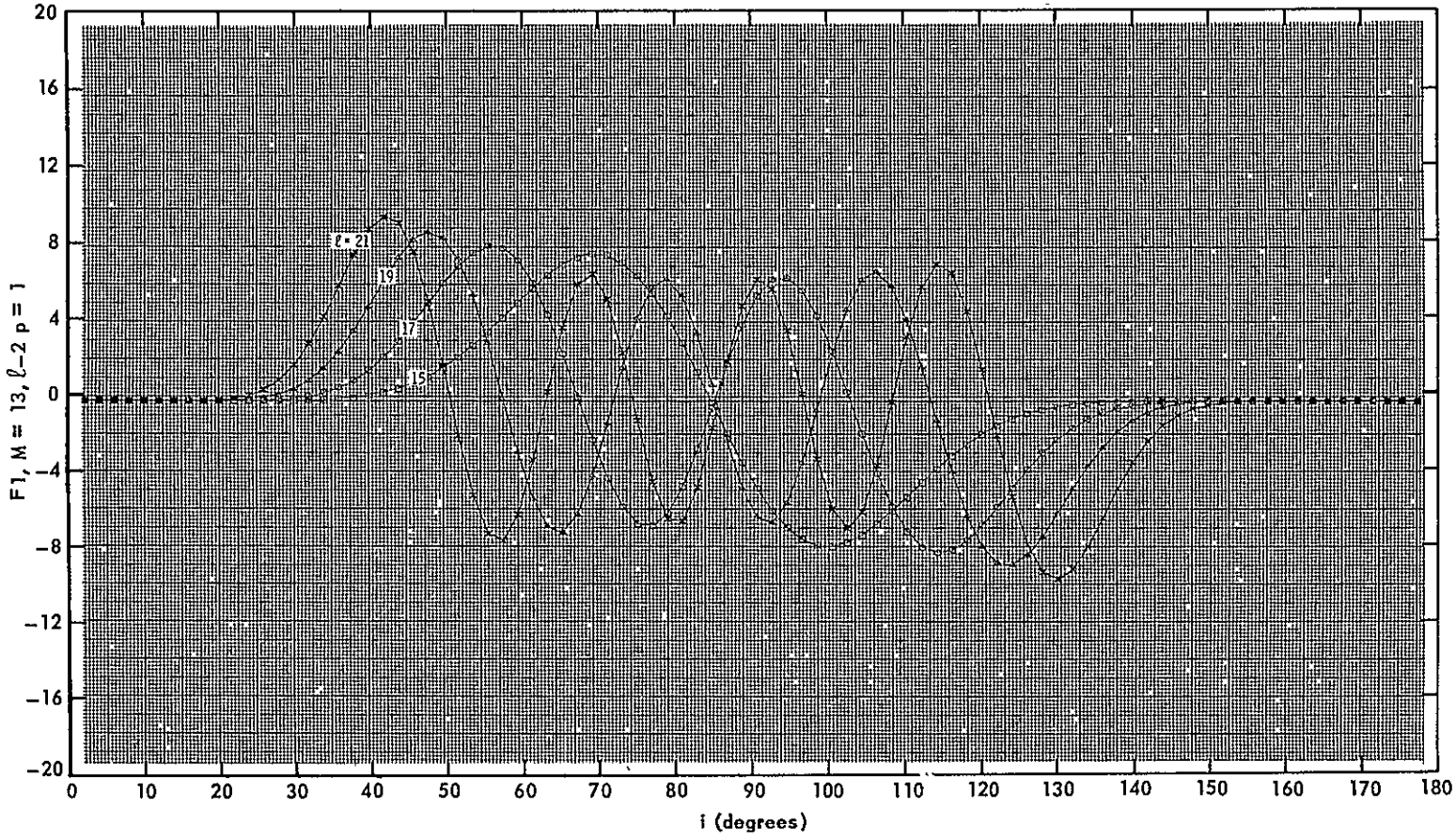
20
16
12
8
4
0
−4
−8
−12
−16
−20
0
10
20
30
40
50
60
70
80
90
100
110
120
130
140
150
160
170
180
i (degrees)
F1, M = 13, ℓ−2 p = 1
ℓ = 21
19
17
15

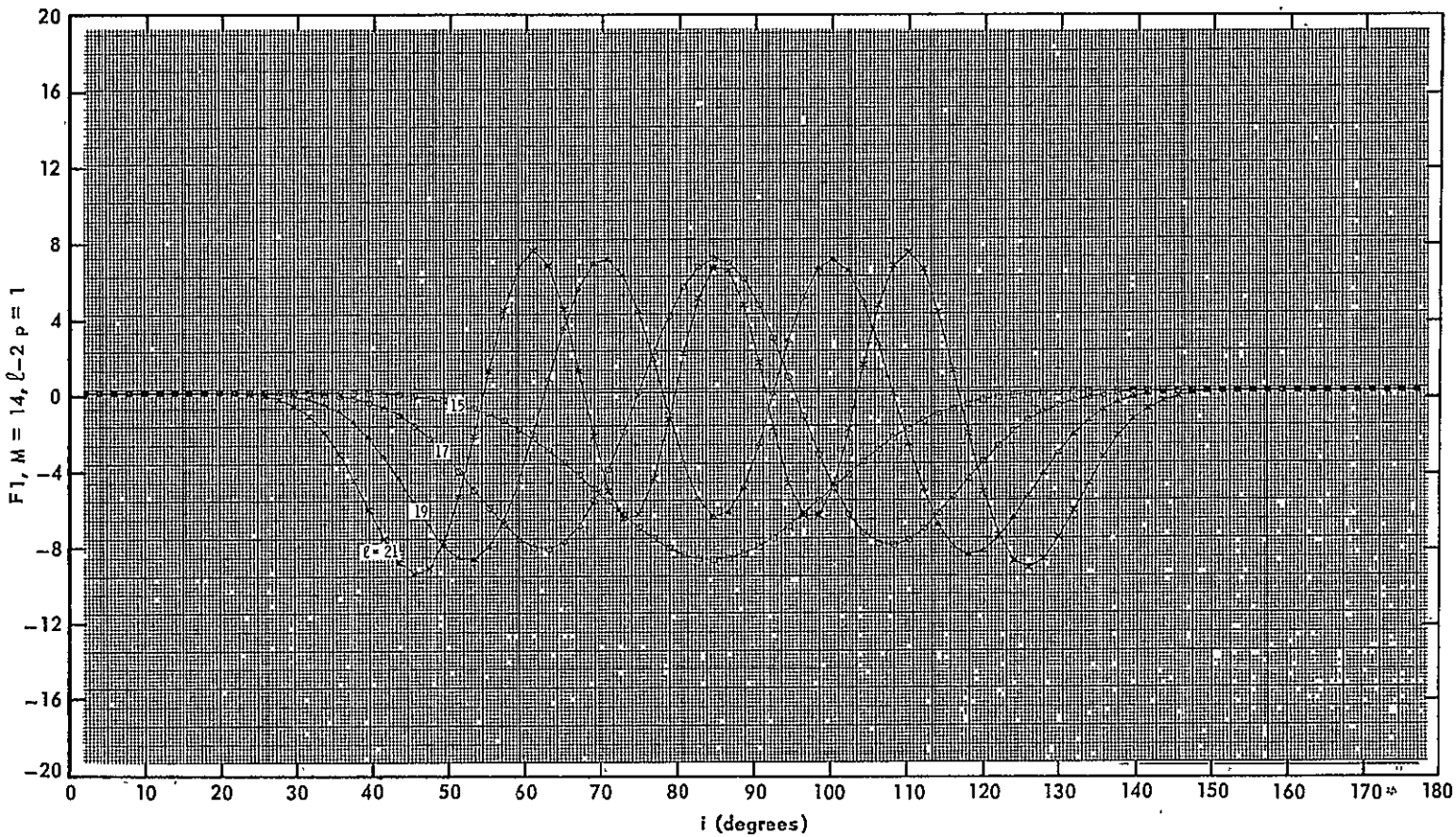
F1, M = 14, ℓ-2 p = 1
i (degrees)
ℓ = 15
17
19
ℓ = 21
20
16
12
8
4
0
-4
-8
-12
-16
-20
0
10
20
30
40
50
60
70
80
90
100
110
120
130
140
150
160
170
180

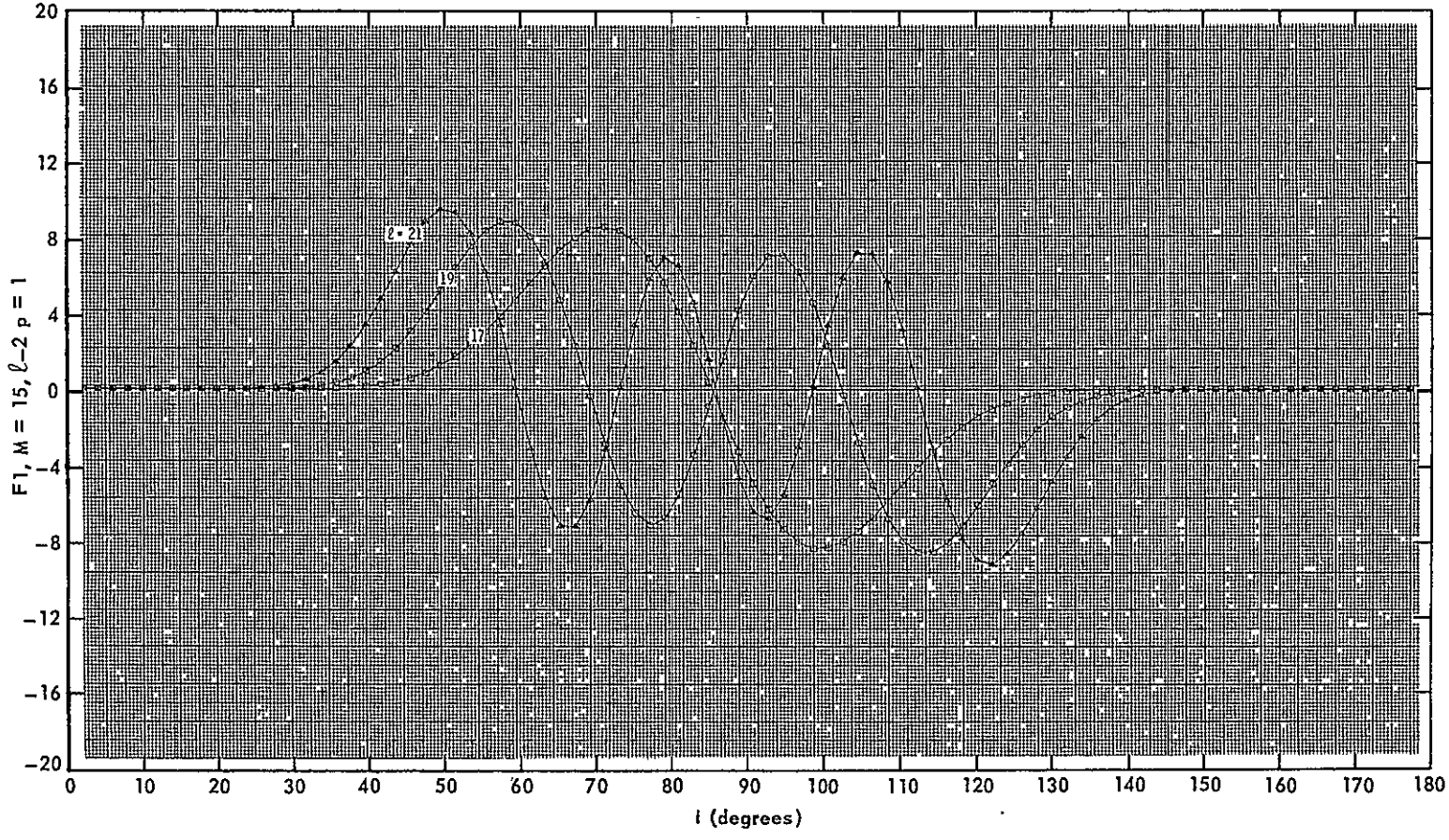
20
16
12
8
4
0
-4
-8
-12
-16
-20
0
10
20
30
40
50
60
70
80
90
100
110
120
130
140
150
160
170
180
F1, M = 15, ℓ-2 p = 1
ℓ = 21
19
17
l (degrees)

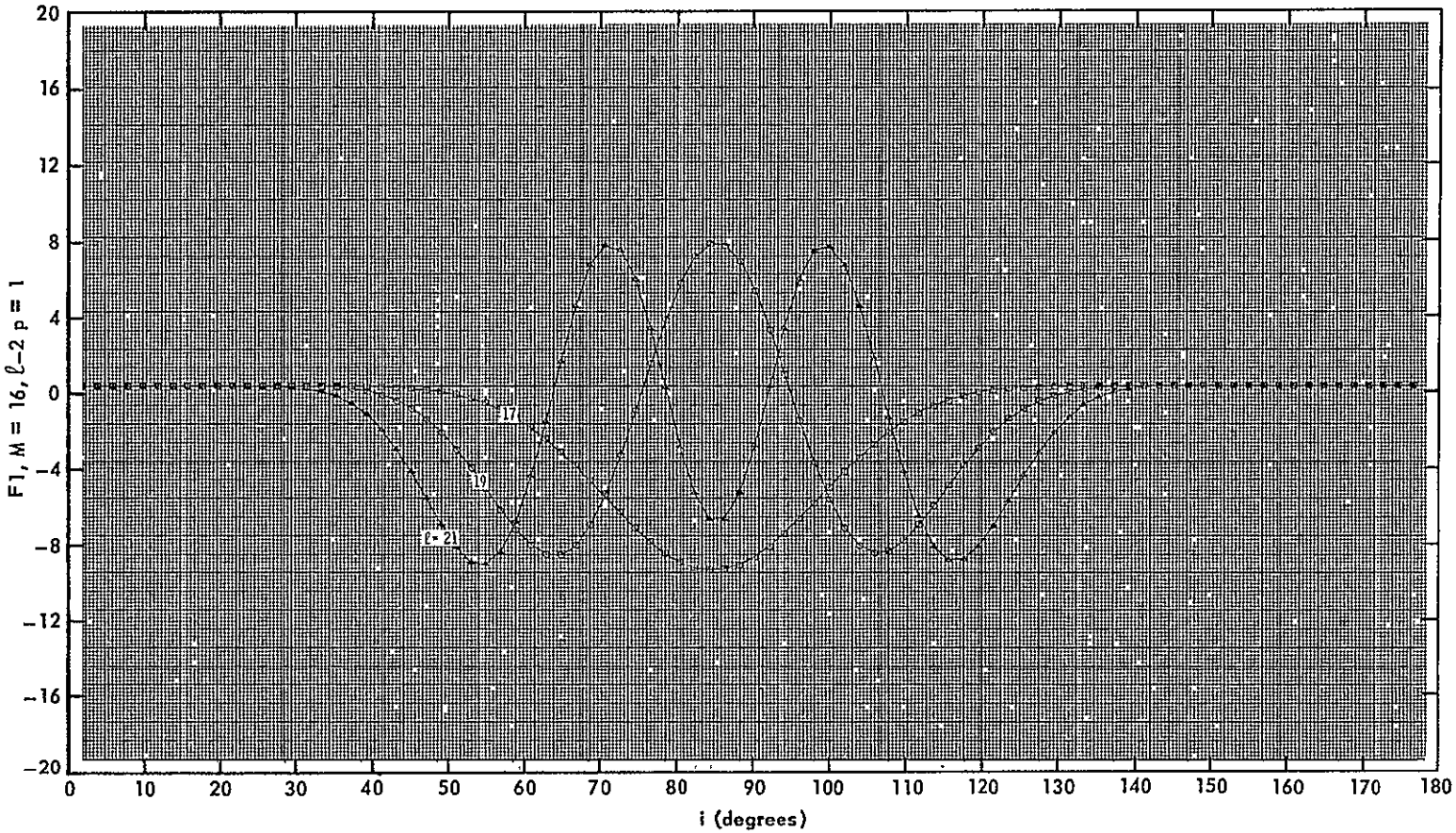
20
16
12
8
4
0
-4
-8
-12
-16
-20
F1, M = 16, ℓ-2 p = 1
0
10
20
30
40
50
60
70
80
90
100
110
120
130
140
150
160
170
180
i (degrees)
ℓ= 17
ℓ= 19
ℓ= 21

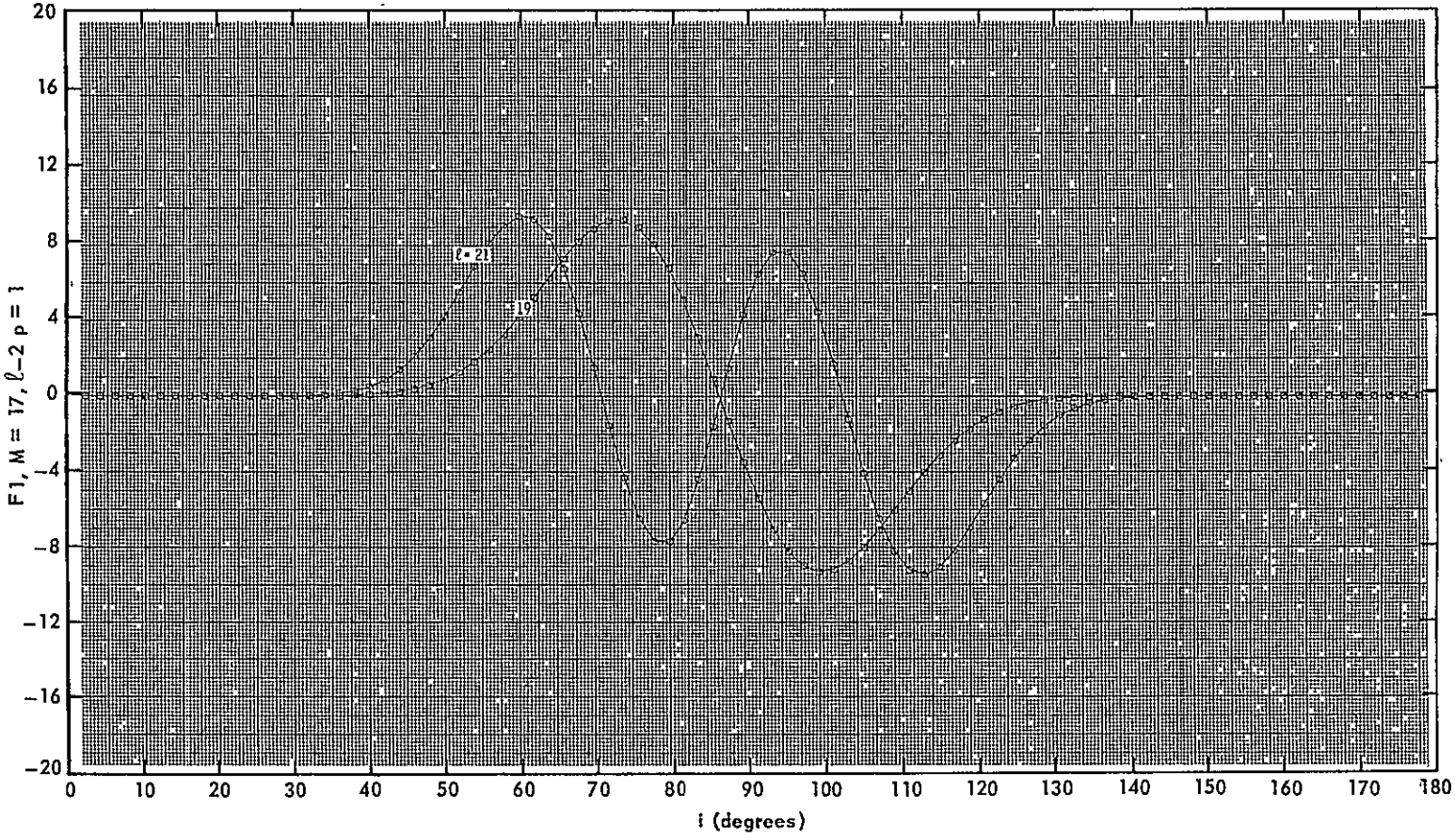
20
16
12
8
4
0
-4
-8
-12
-16
-20
0
10
20
30
40
50
60
70
80
90
100
110
120
130
140
150
160
170
180
F1, M = 17, ℓ-2 p = 1
i (degrees)
ℓ = 21
19

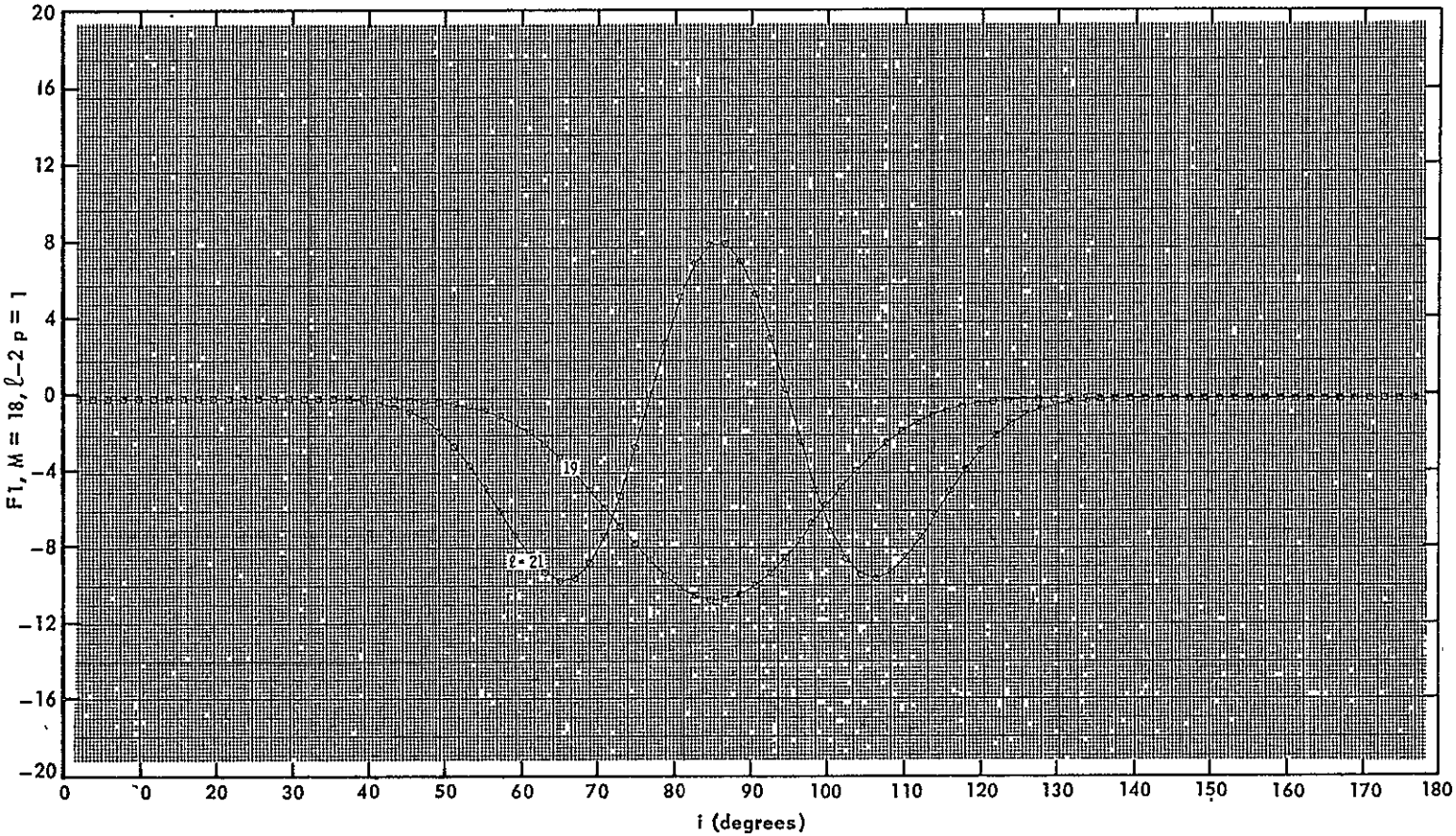
20
16
12
8
4
0
-4
-8
-12
-16
-20
0
10
20
30
40
50
60
70
80
90
100
110
120
130
140
150
160
170
180
F1, M = 18, ℓ-2 p = 1
i (degrees)
19
ℓ = 21

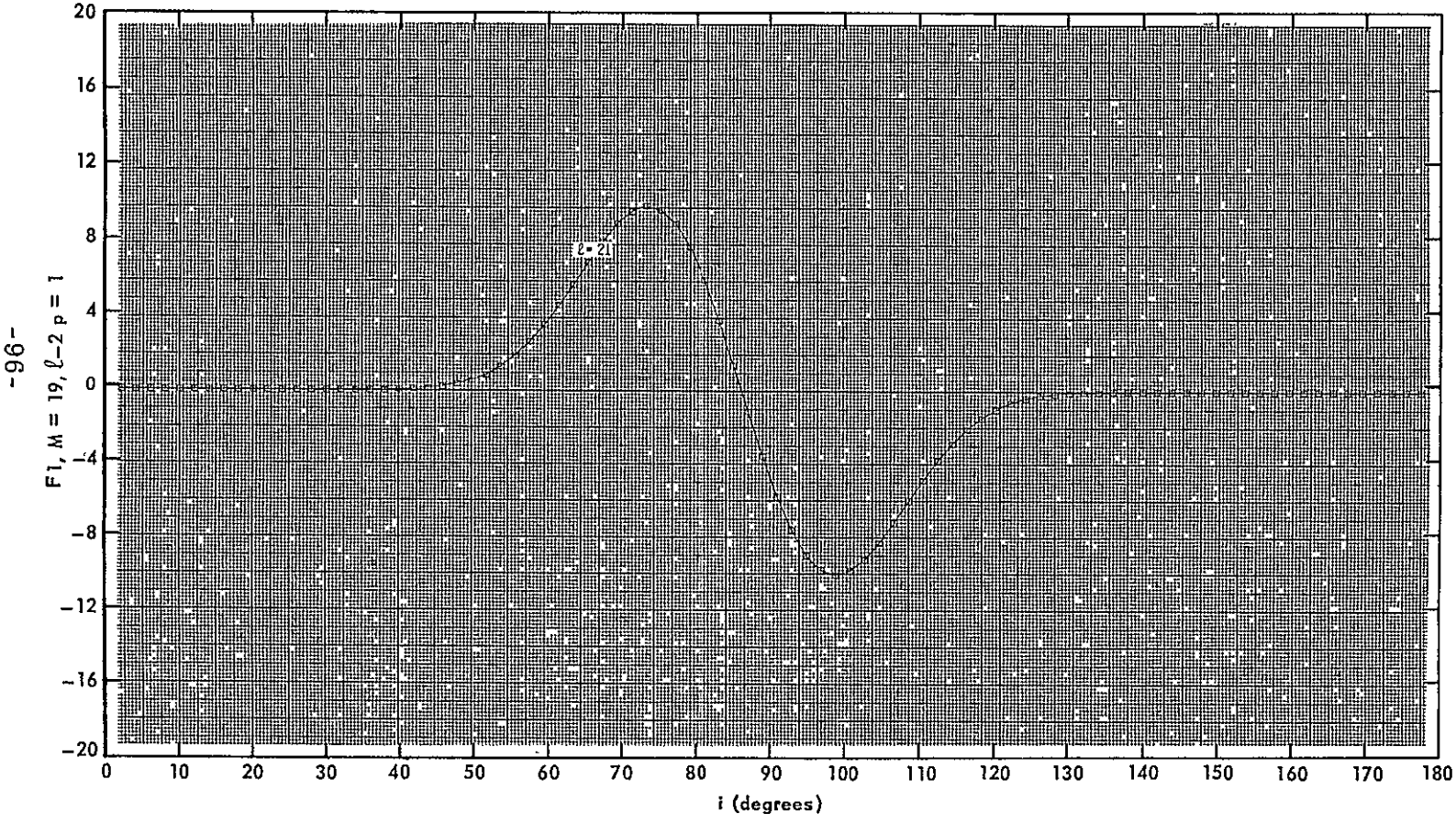
20
16
12
8
4
0
-4
-8
-12
-16
-20
0
10
20
30
40
50
60
70
80
90
100
110
120
130
140
150
160
170
180
i (degrees)
F1, M = 19, ℓ-2 p = 1
ℓ = 21

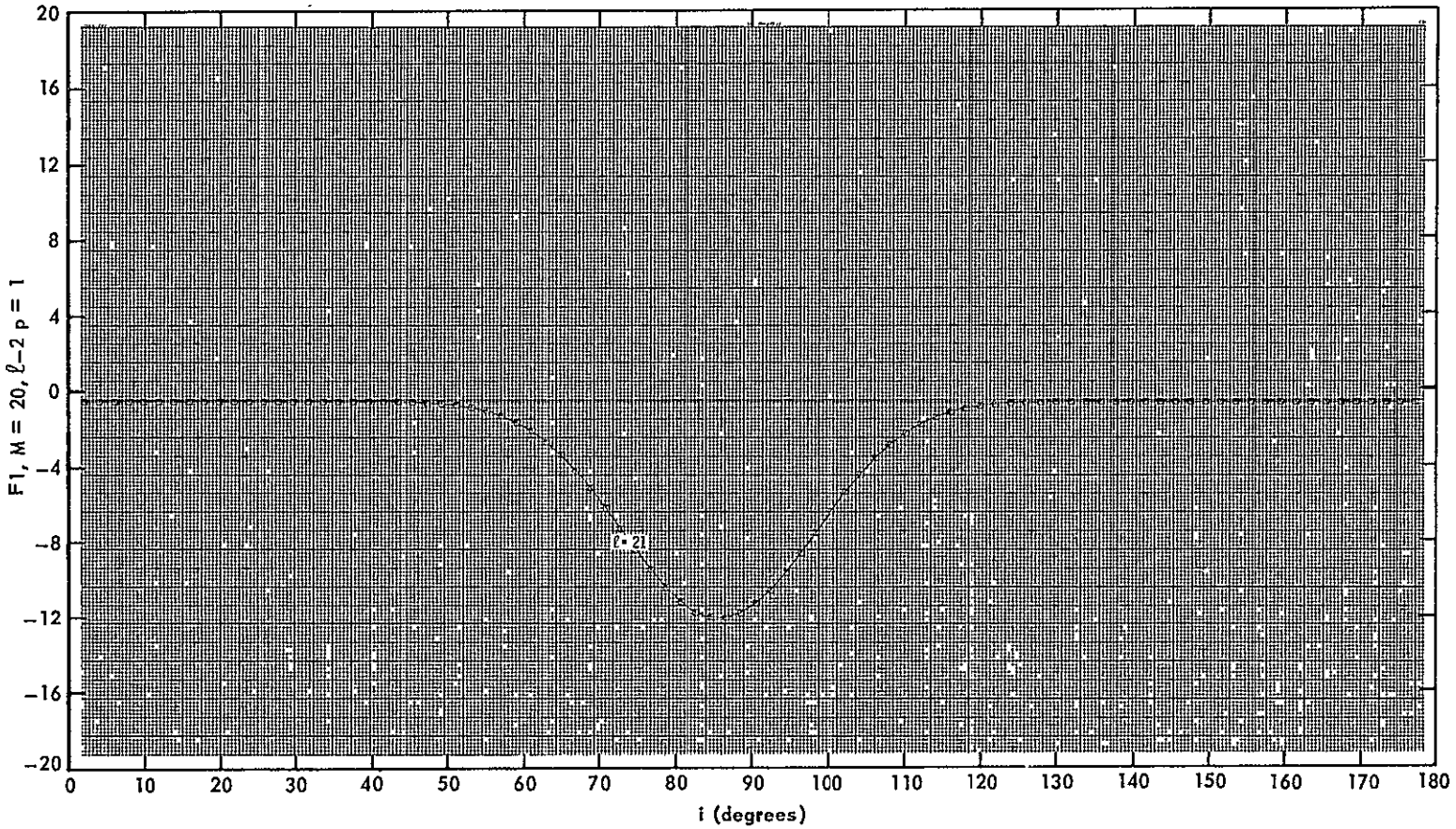
20
16
12
8
4
0
-4
-8
-12
-16
-20
F1, M = 20, ℓ-2 p = 1
ℓ = 21
0
10
20
30
40
50
60
70
80
90
100
110
120
130
140
150
160
170
180
i (degrees)

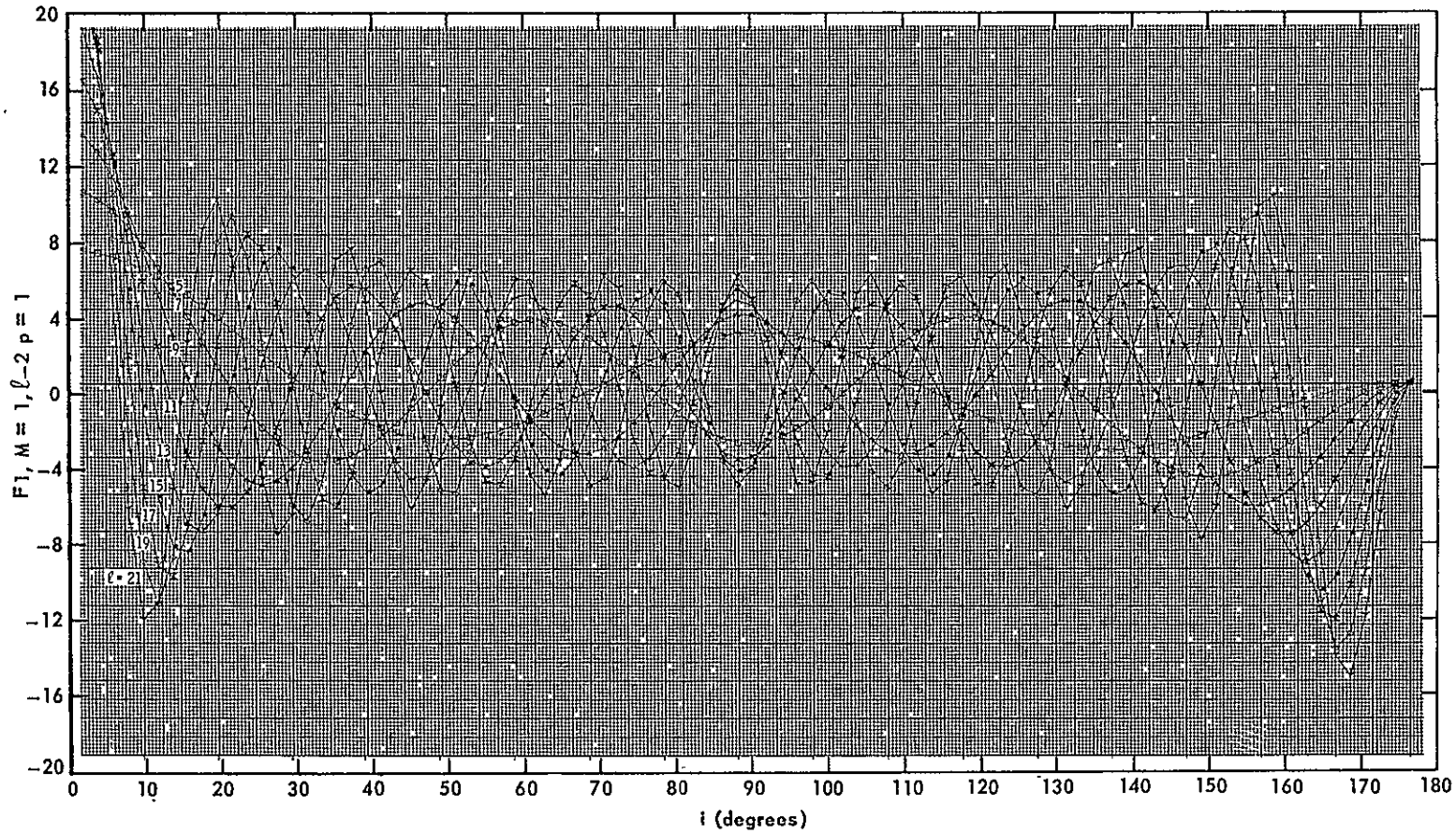
F1, M = 1, ℓ-2 p = 1
i (degrees)
20
16
12
8
4
0
-4
-8
-12
-16
-20
0
10
20
30
40
50
60
70
80
90
100
110
120
130
140
150
160
170
180
ℓ = 21

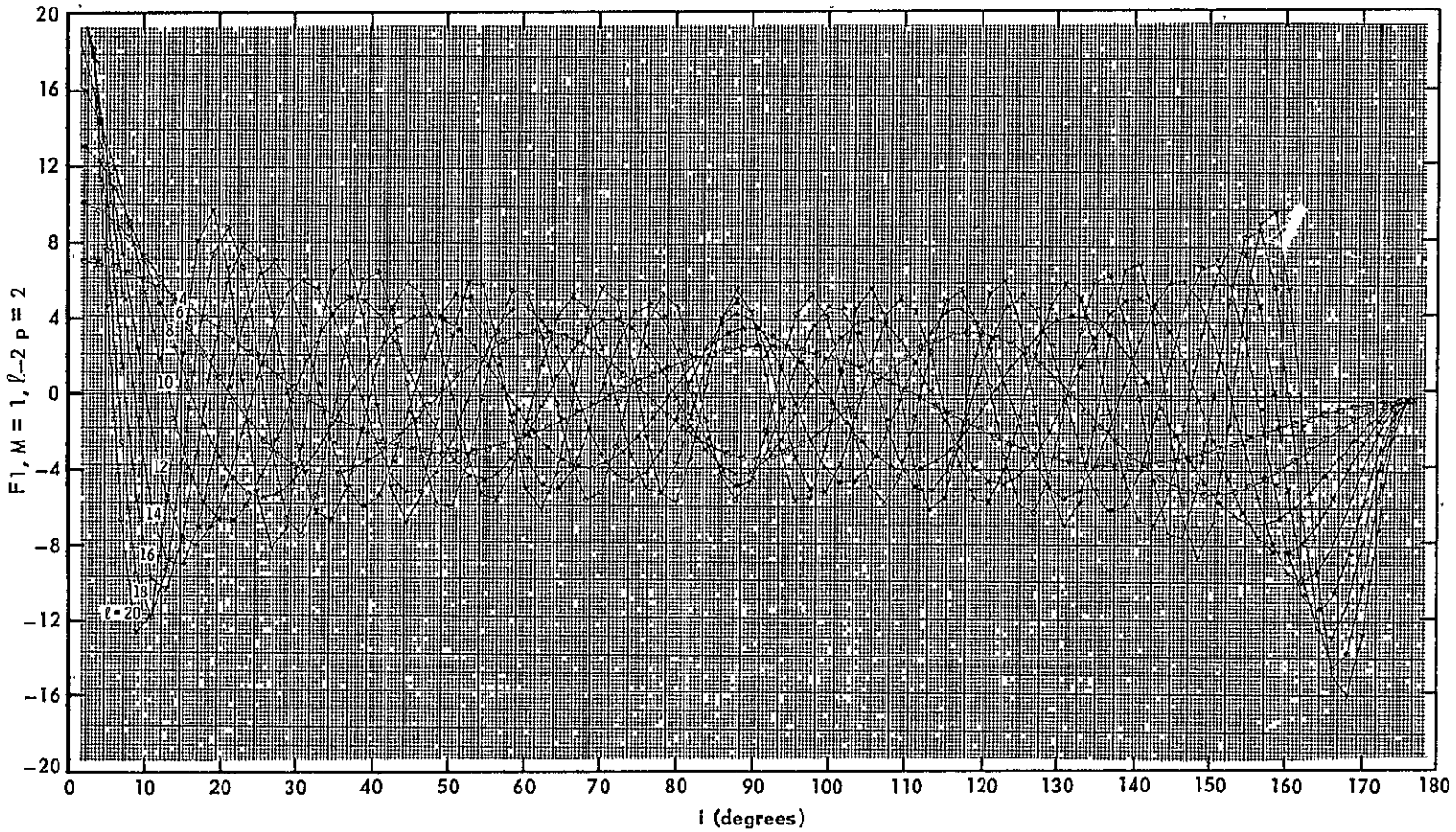
F1, M = 1, ℓ-2 p = 2
i (degrees)
ℓ = 20

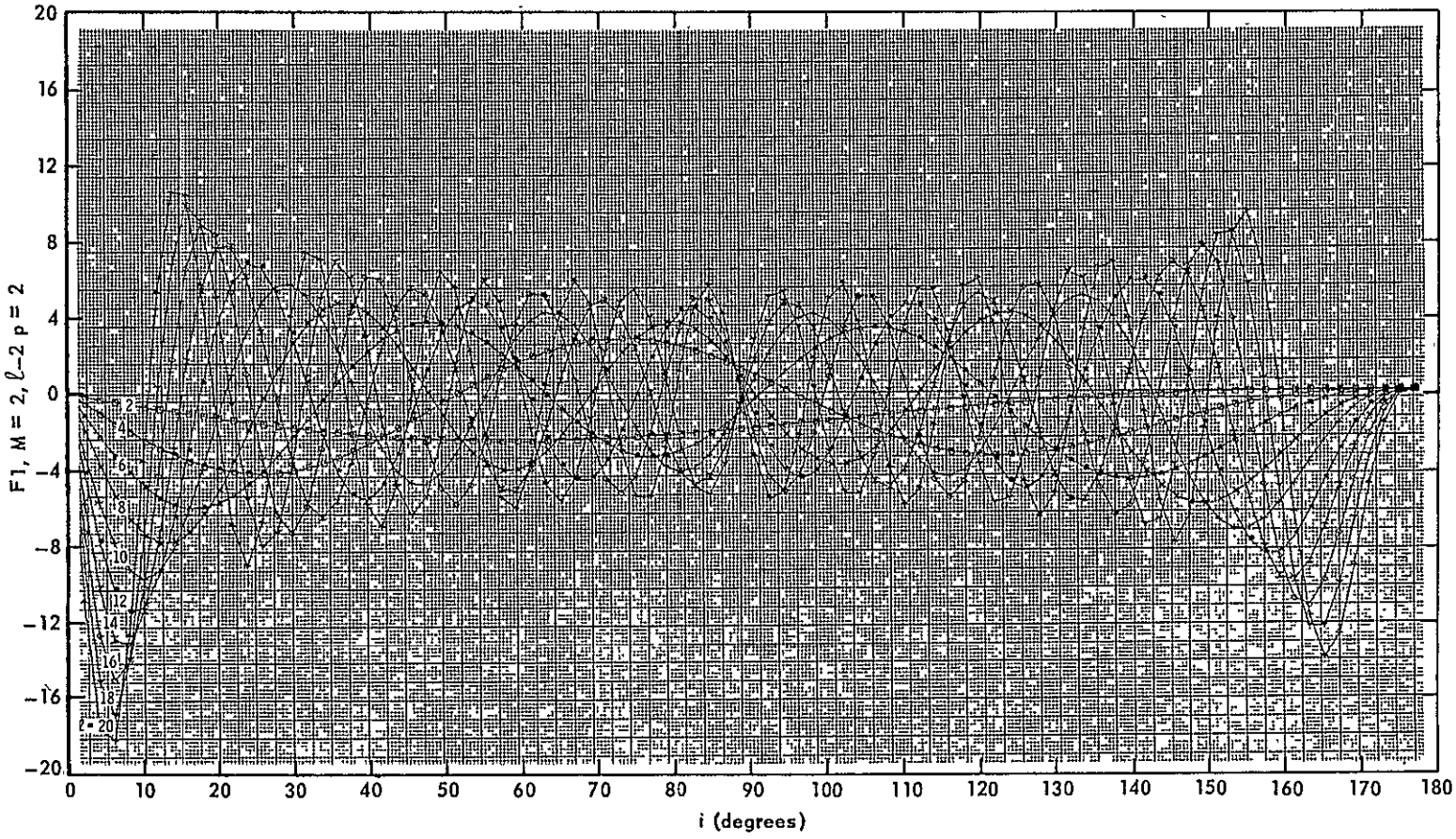
F1, M = 2, ℓ-2 p = 2
i (degrees)
20
16
12
8
4
0
-4
-8
-12
-16
-20
0
10
20
30
40
50
60
70
80
90
100
110
120
130
140
150
160
170
180
p = 2
4
6
8
10
12
14
16
18
20

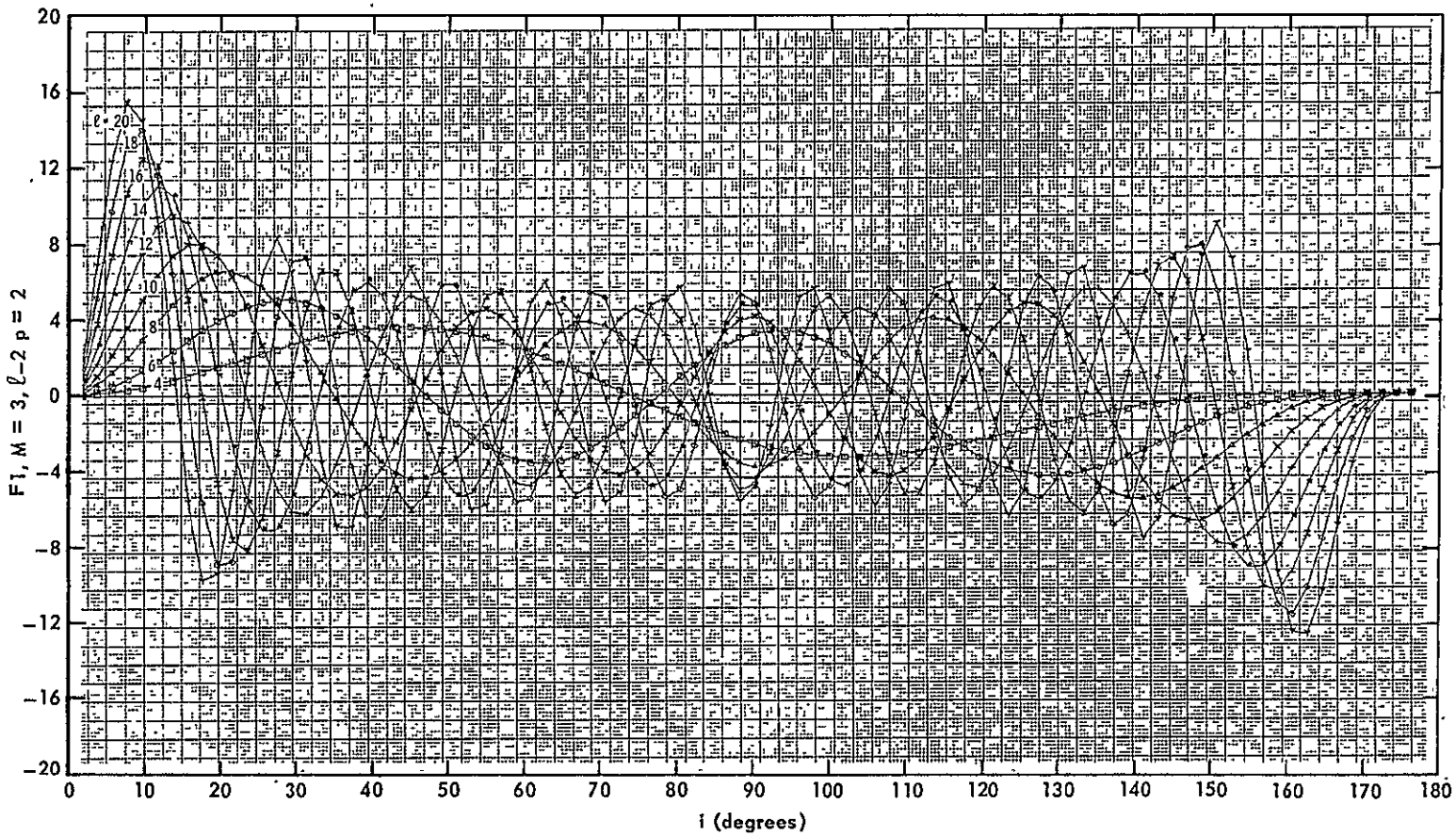
F1, M = 3, ℓ-2 p = 2
i (degrees)
ℓ = 20
18
16
14
12
10
8
6
4
20
16
12
8
4
0
-4
-8
-12
-16
-20
0
10
20
30
40
50
60
70
80
90
100
110
120
130
140
150
160
170
180

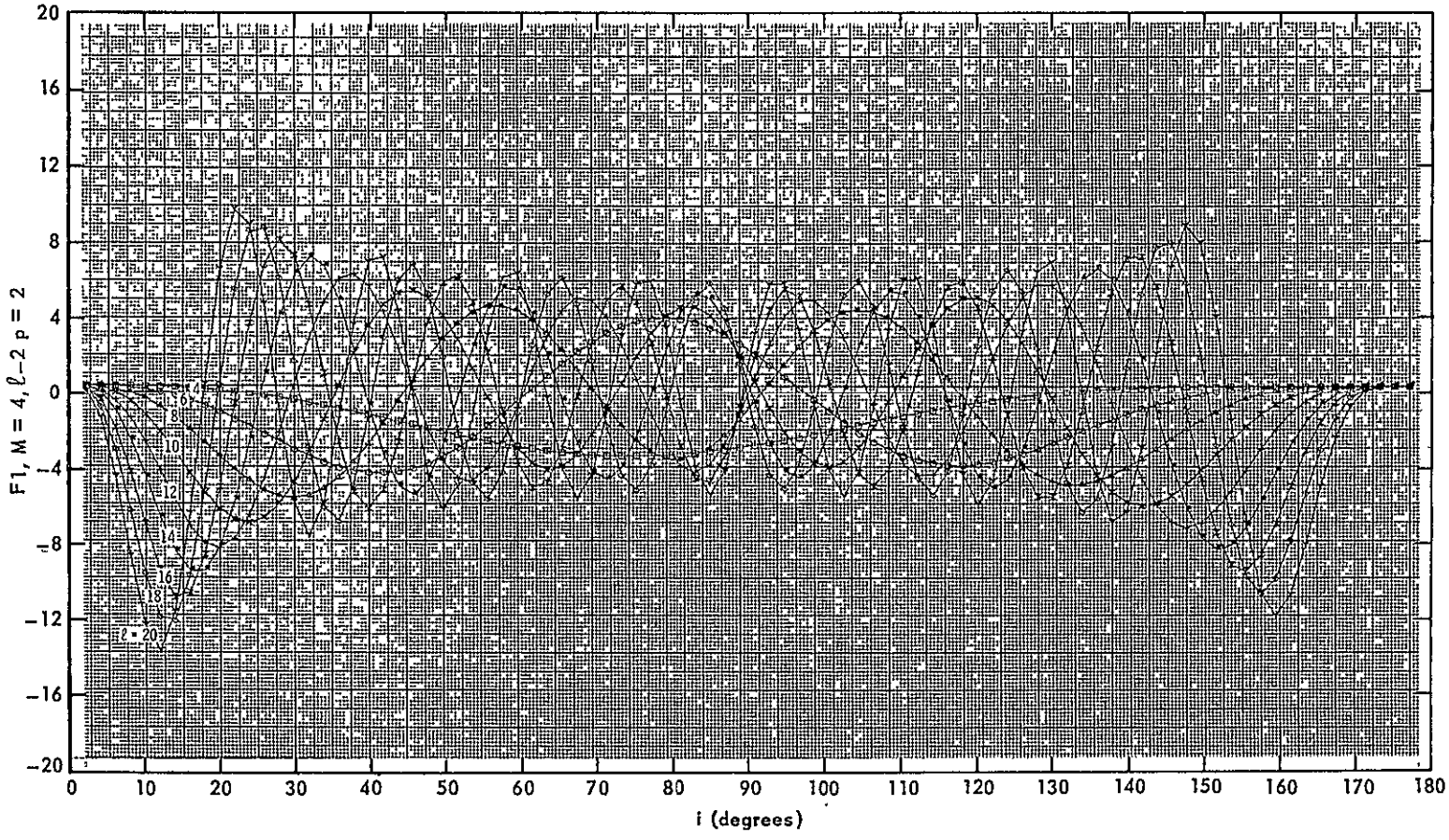
F1, M = 4, ℓ−2 p = 2
i (degrees)
20
16
12
8
4
0
−4
−8
−12
−16
−20
0
10
20
30
40
50
60
70
80
90
100
110
120
130
140
150
160
170
180
4
6
8
10
12
14
16
18
ℓ = 20

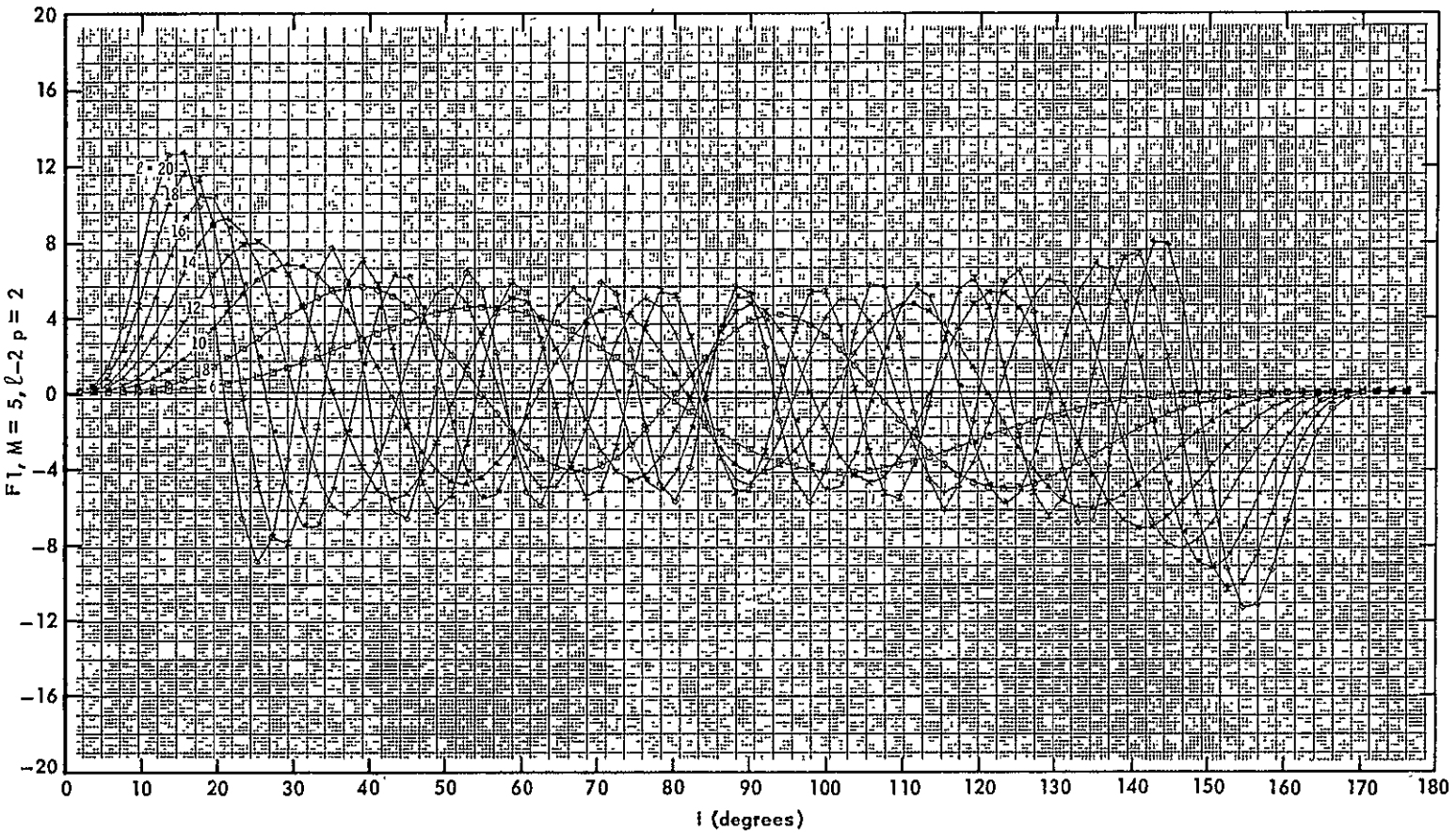
F l, M = 5, ℓ−2 p = 2
i (degrees)
20
16
12
8
4
0
−4
−8
−12
−16
−20
0
10
20
30
40
50
60
70
80
90
100
110
120
130
140
150
160
170
180
p = 20
18
16
14
12
10
8
6

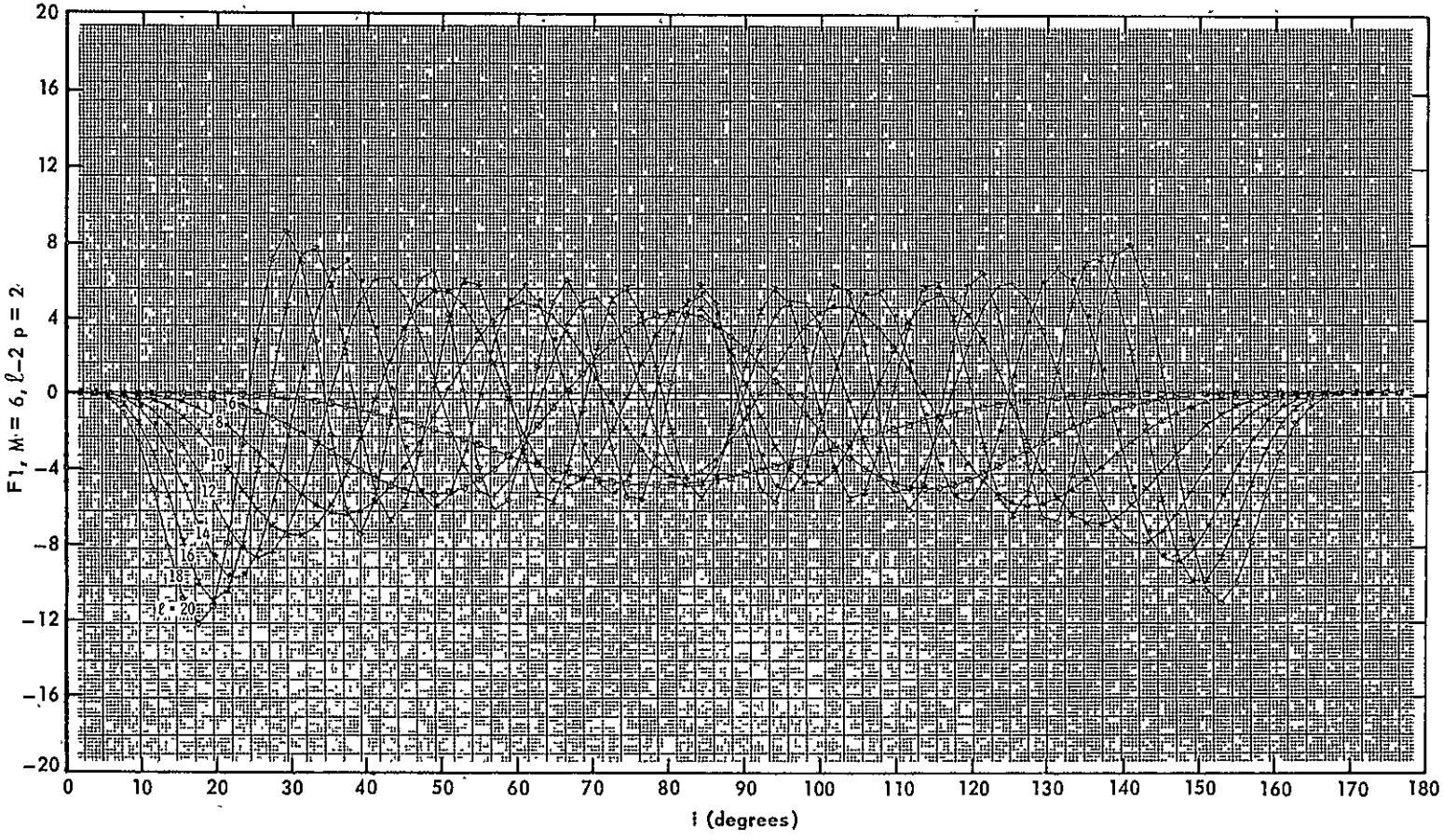
F1, M = 6, ℓ–2 p = 2
i (degrees)
20
16
12
8
4
0
-4
-8
-12
-16
-20
0
10
20
30
40
50
60
70
80
90
100
110
120
130
140
150
160
170
180
6
8
10
12
14
16
18
ℓ = 20

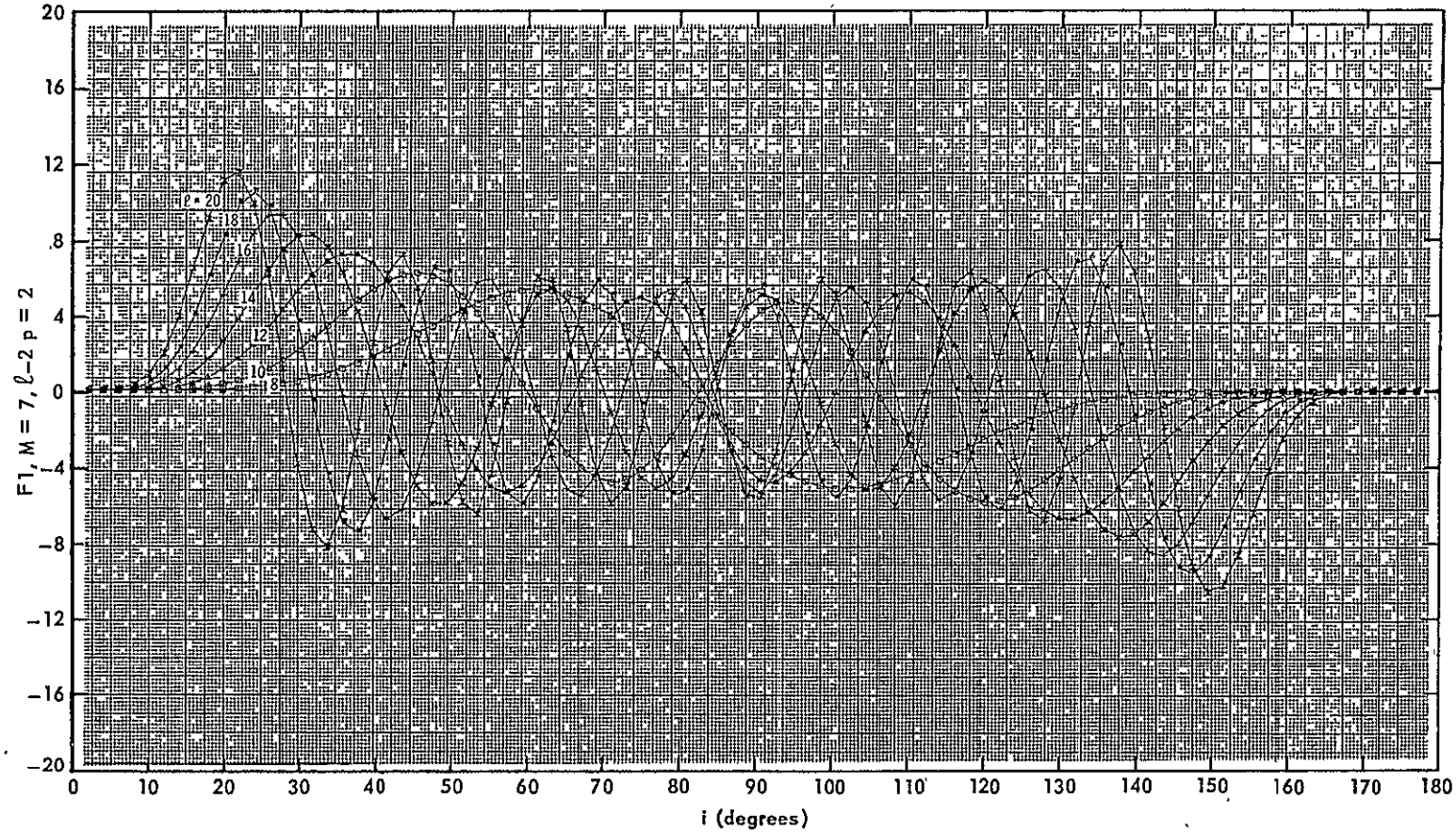
F1, M = 7, ℓ-2 p = 2
i (degrees)
20
16
12
8
4
0
-4
-8
-12
-16
-20
0
10
20
30
40
50
60
70
80
90
100
110
120
130
140
150
160
170
180
p = 20
18
16
14
12
10
8

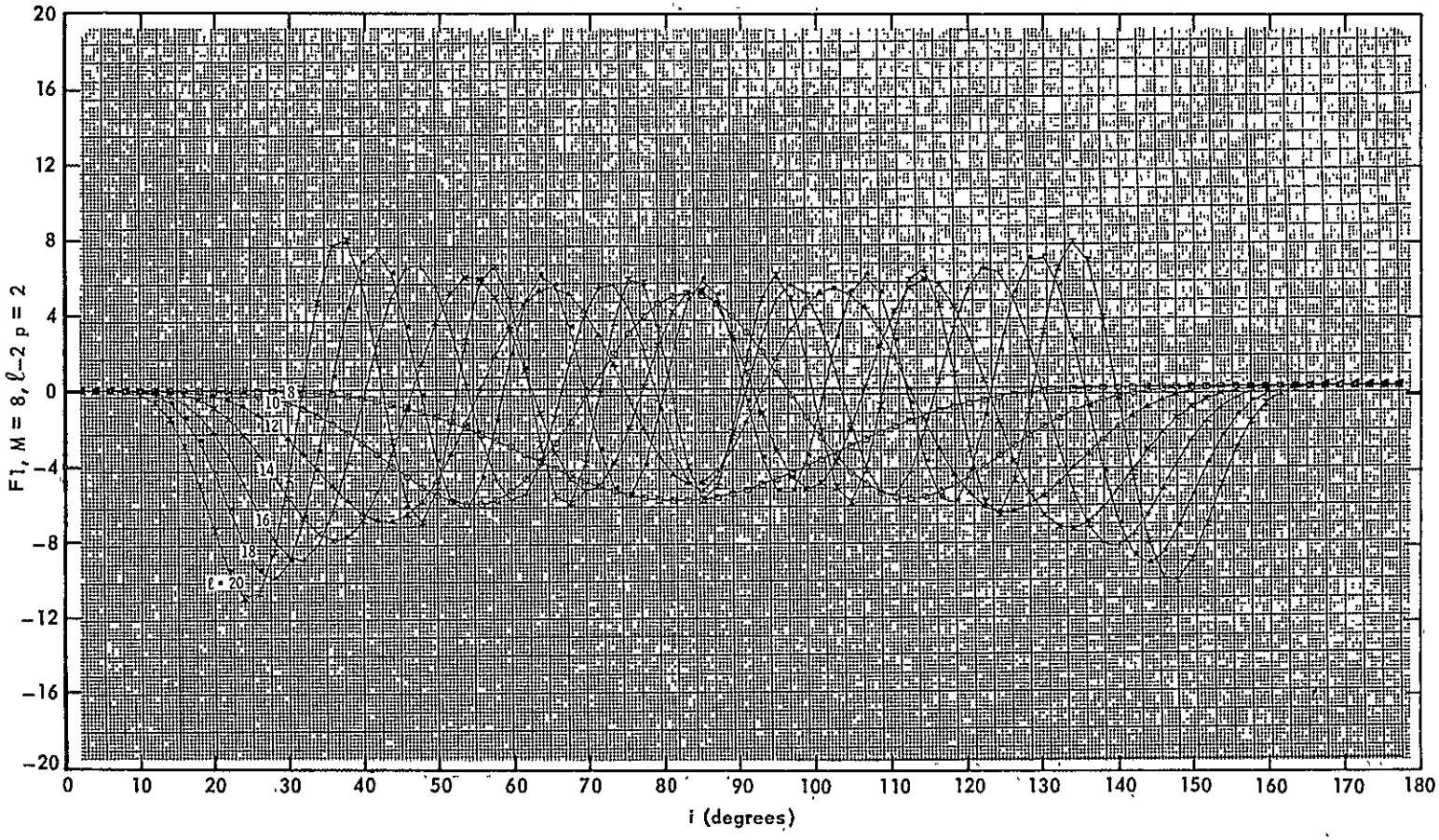
F1, M = 8, ℓ−2 p = 2
i (degrees)
20
16
12
8
4
0
−4
−8
−12
−16
−20
0
10
20
30
40
50
60
70
80
90
100
110
120
130
140
150
160
170
180
8
10
12
14
16
18
c = 20

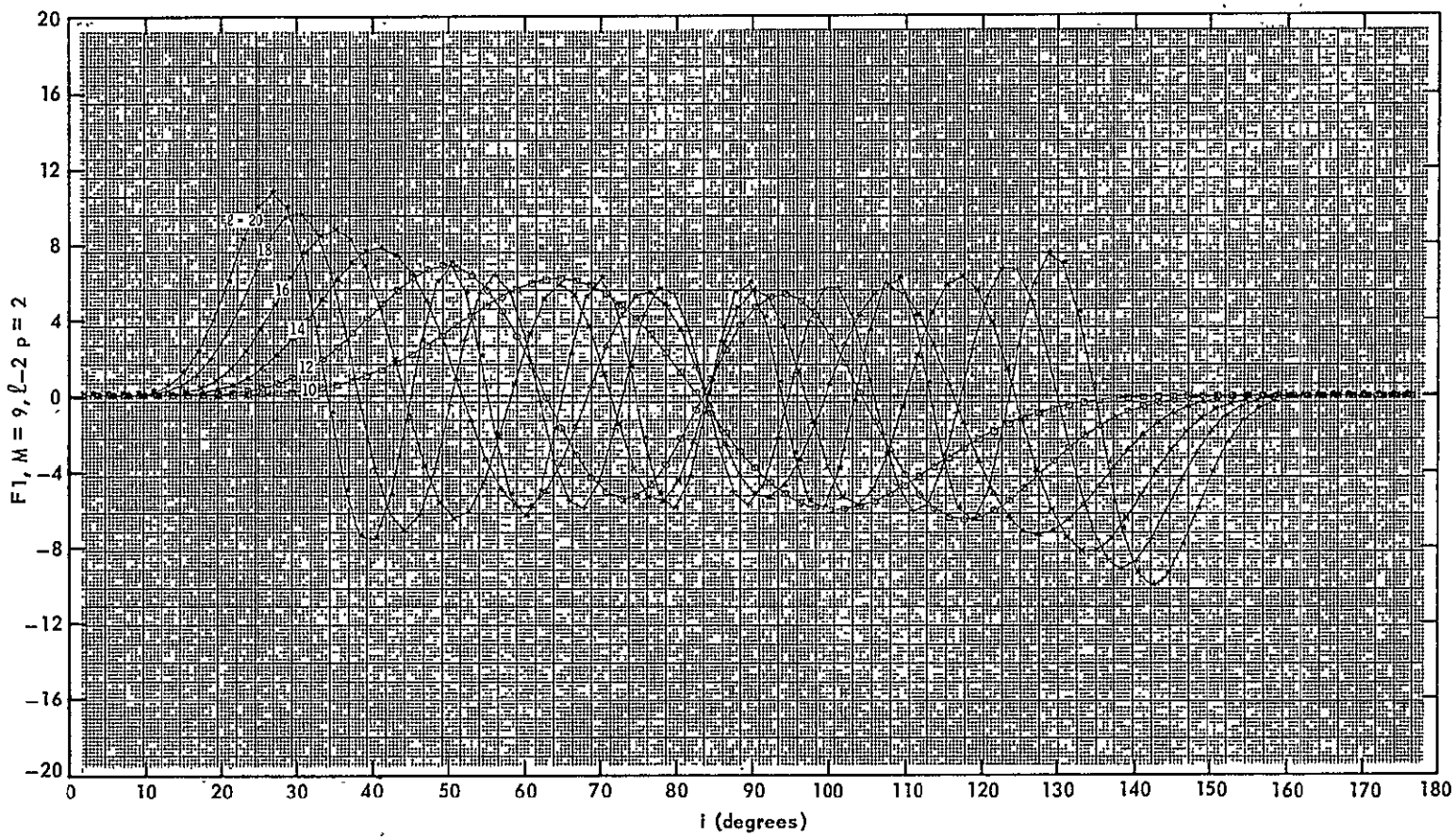
F1, M = 9, ℓ-2 p = 2
i (degrees)
ℓ = 20
18
16
14
12
10
11
20
16
12
8
4
0
-4
-8
-12
-16
-20
0
10
20
30
40
50
60
70
80
90
100
110
120
130
140
150
160
170
180

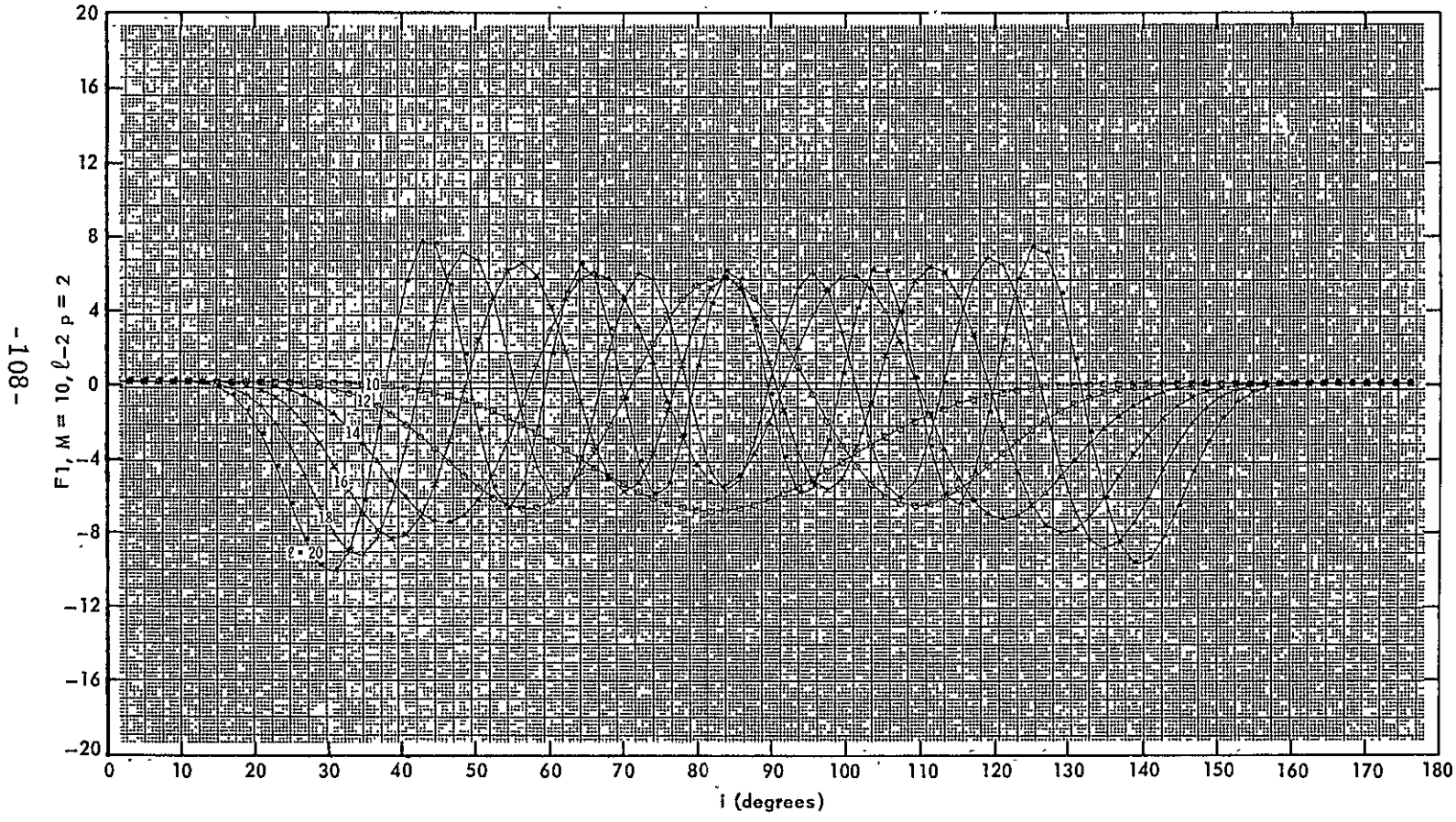
F1, M = 10, ℓ-2 p = 2
i (degrees)
20
16
12
8
4
0
-4
-8
-12
-16
-20
0
10
20
30
40
50
60
70
80
90
100
110
120
130
140
150
160
170
180
ℓ = 20

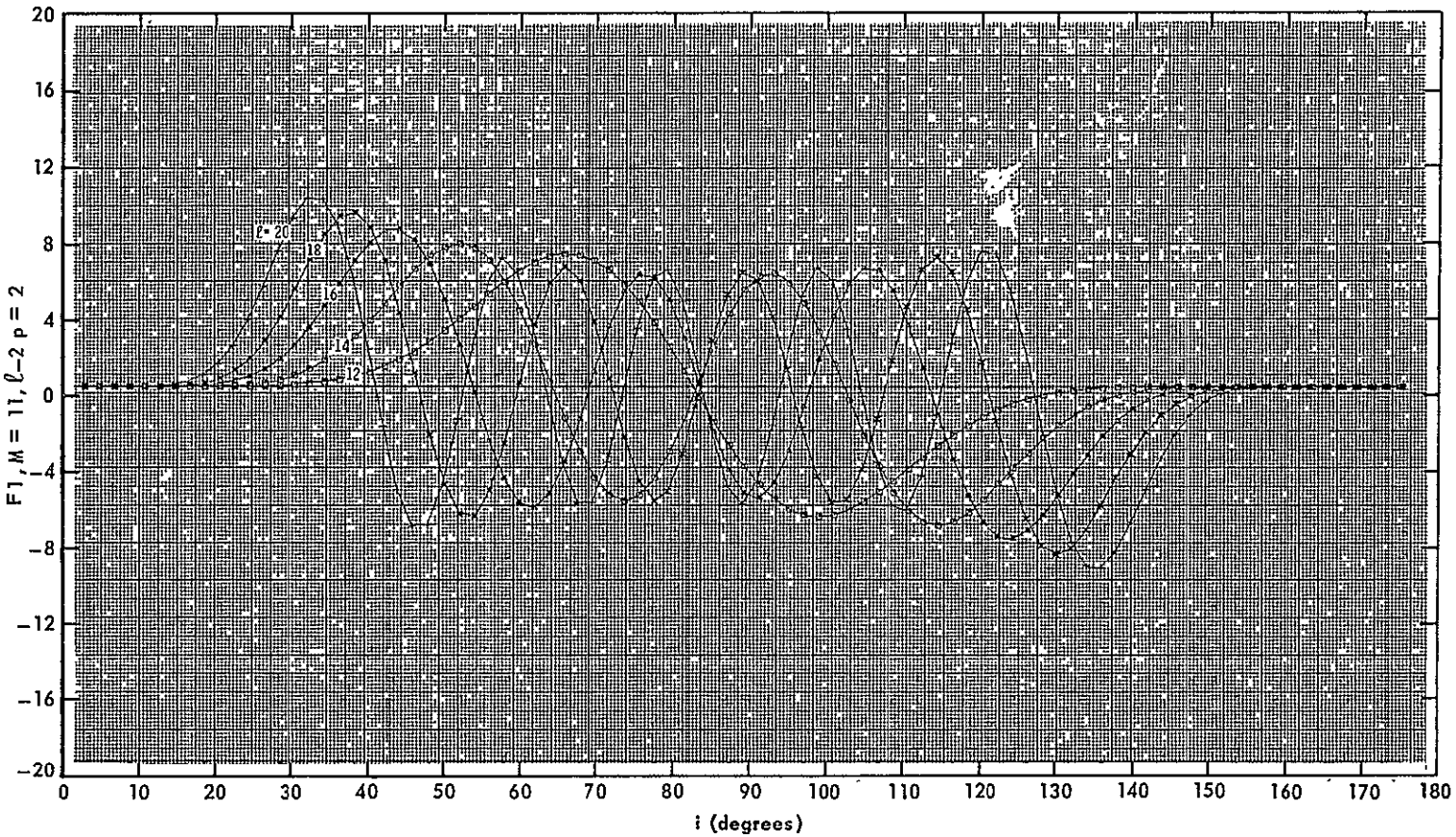
20
16
12
8
4
0
−4
−8
−12
−16
−20
0
10
20
30
40
50
60
70
80
90
100
110
120
130
140
150
160
170
180
i (degrees)
F1, M = 11, ℓ−2 p = 2
ℓ = 20
18
16
14
12

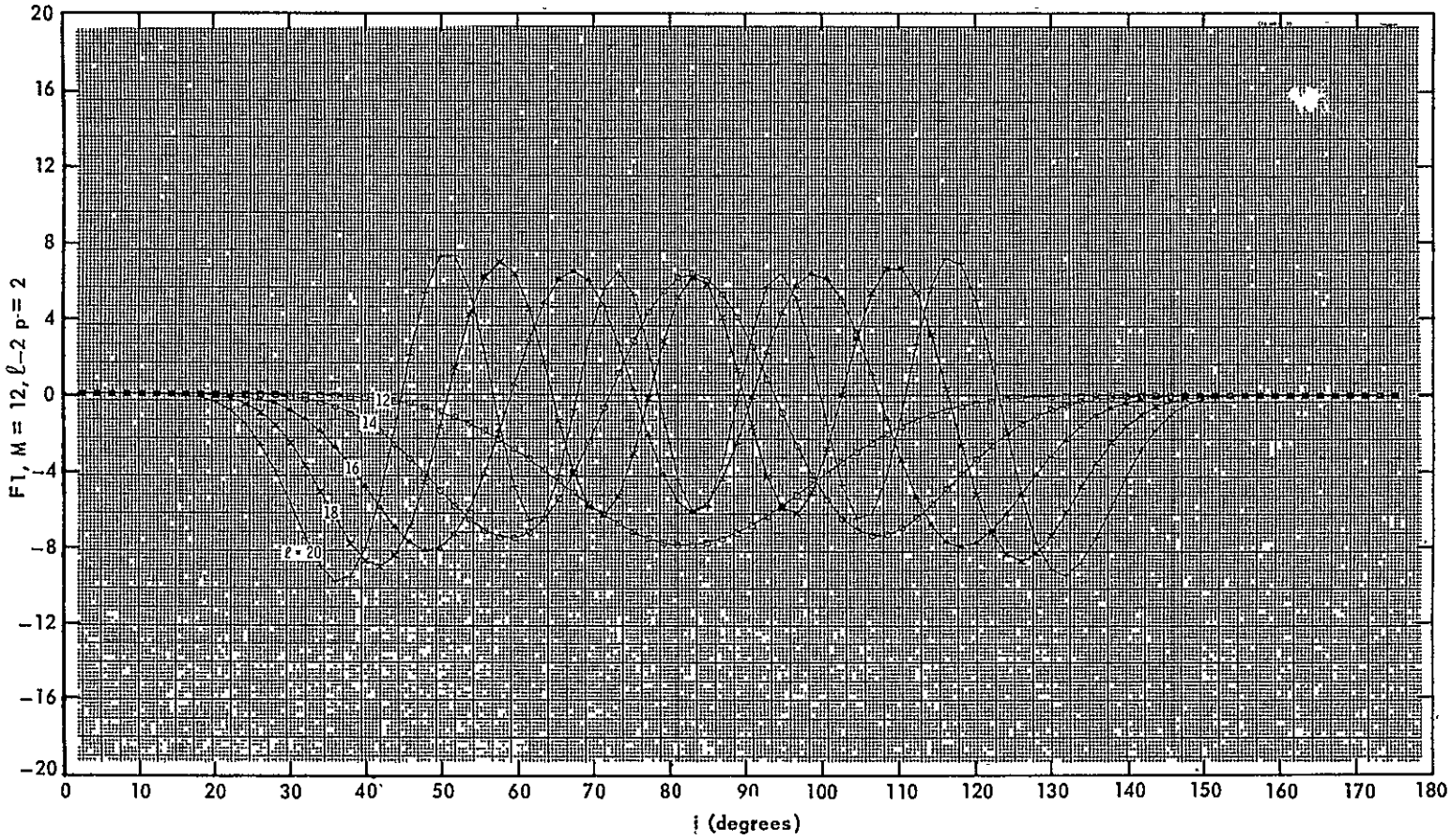
20
16
12
8
4
0
-4
-8
-12
-16
-20
0
10
20
30
40
50
60
70
80
90
100
110
120
130
140
150
160
170
180
F1, M = 12, ℓ-2 p= 2
i (degrees)
12
14
16
18
ℓ = 20

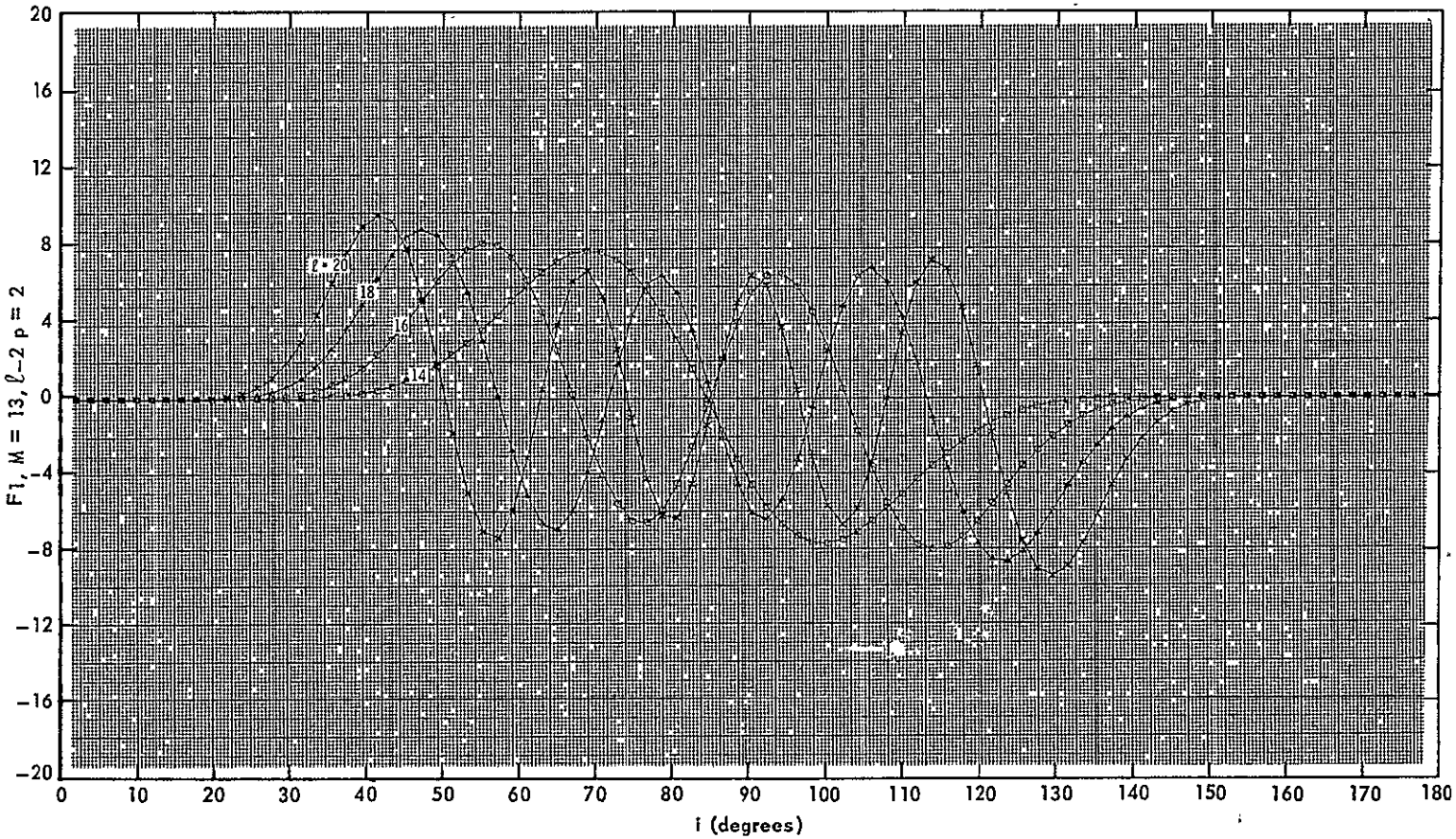
20
16
12
8
4
0
-4
-8
-12
-16
-20
0
10
20
30
40
50
60
70
80
90
100
110
120
130
140
150
160
170
180
i (degrees)
F1, M = 13, ℓ-2 p = 2
ℓ = 20
18
16
14

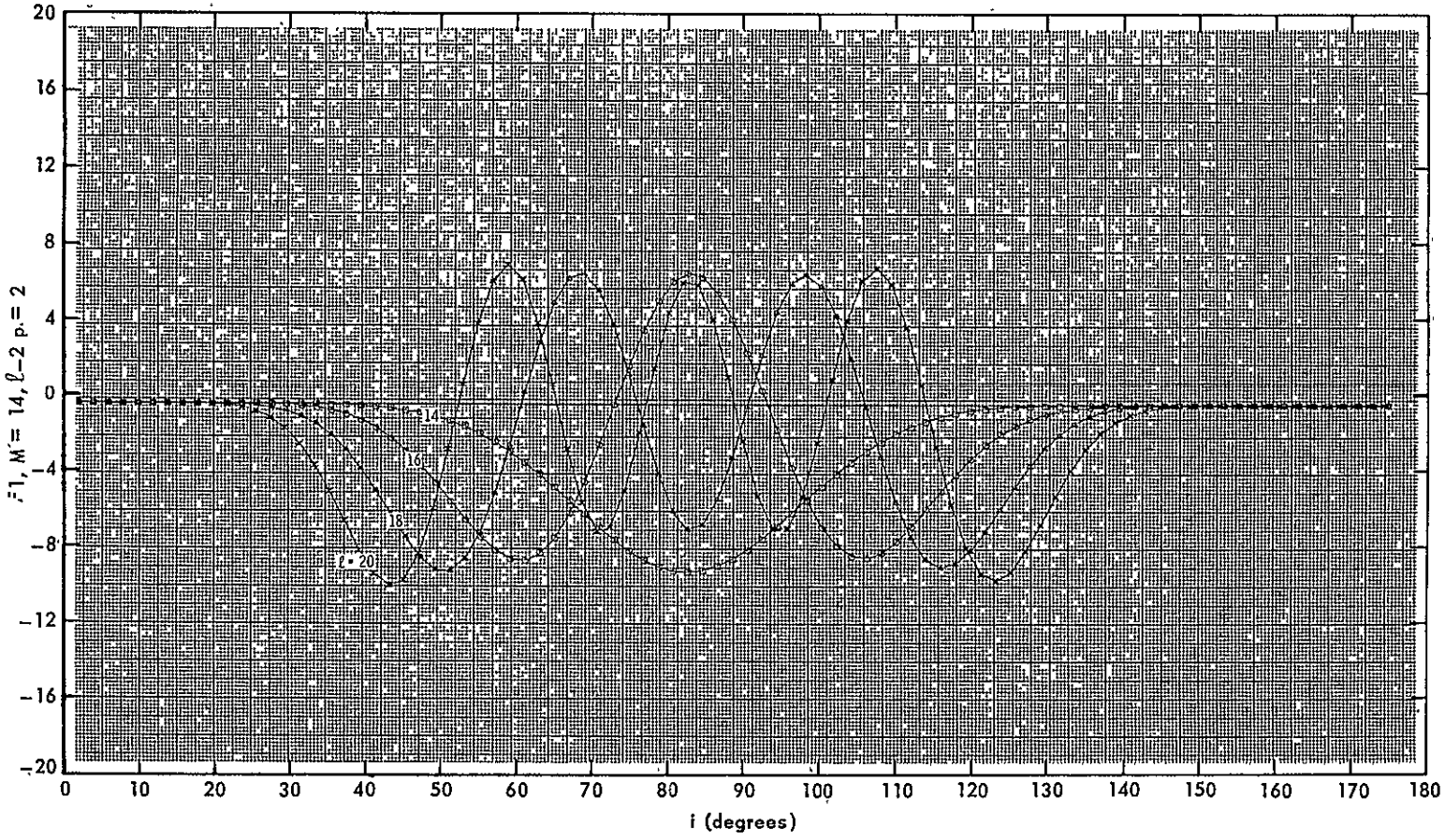
20
16
12
8
4
0
-4
-8
-12
-16
-20
0
10
20
30
40
50
60
70
80
90
100
110
120
130
140
150
160
170
180
i (degrees)
14
16
18
ℓ = 20

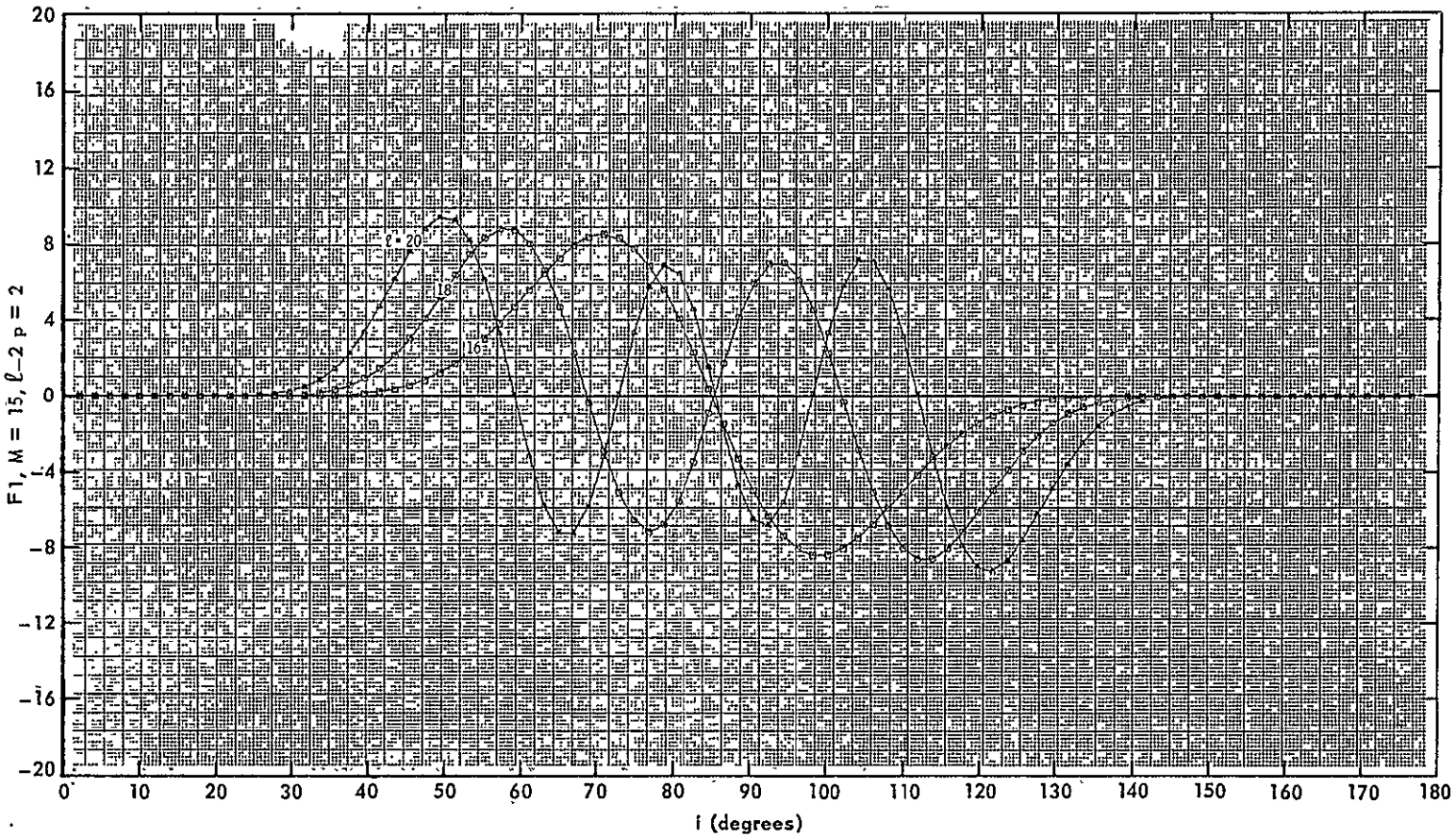
F1, M = 15, ℓ–2 P = 2
i (degrees)
20
16
12
8
4
0
-4
-8
-12
-16
-20
0
10
20
30
40
50
60
70
80
90
100
110
120
130
140
150
160
170
180
20
18
16

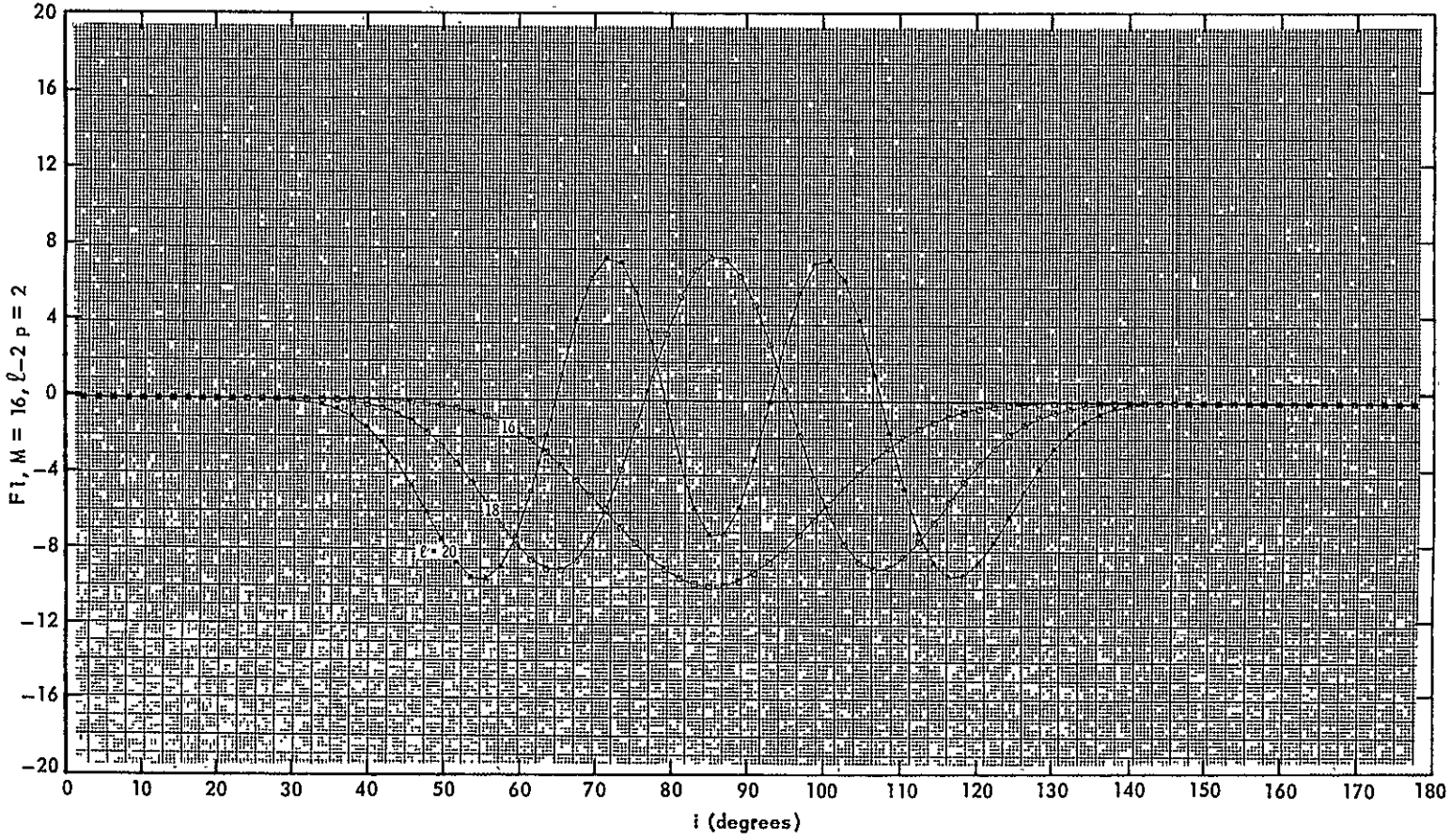
20
16
12
8
4
0
−4
−8
−12
−16
−20
0
10
20
30
40
50
60
70
80
90
100
110
120
130
140
150
160
170
180
i (degrees)
F1, M = 16, ℓ−2 p = 2
16
18
ℓ = 20

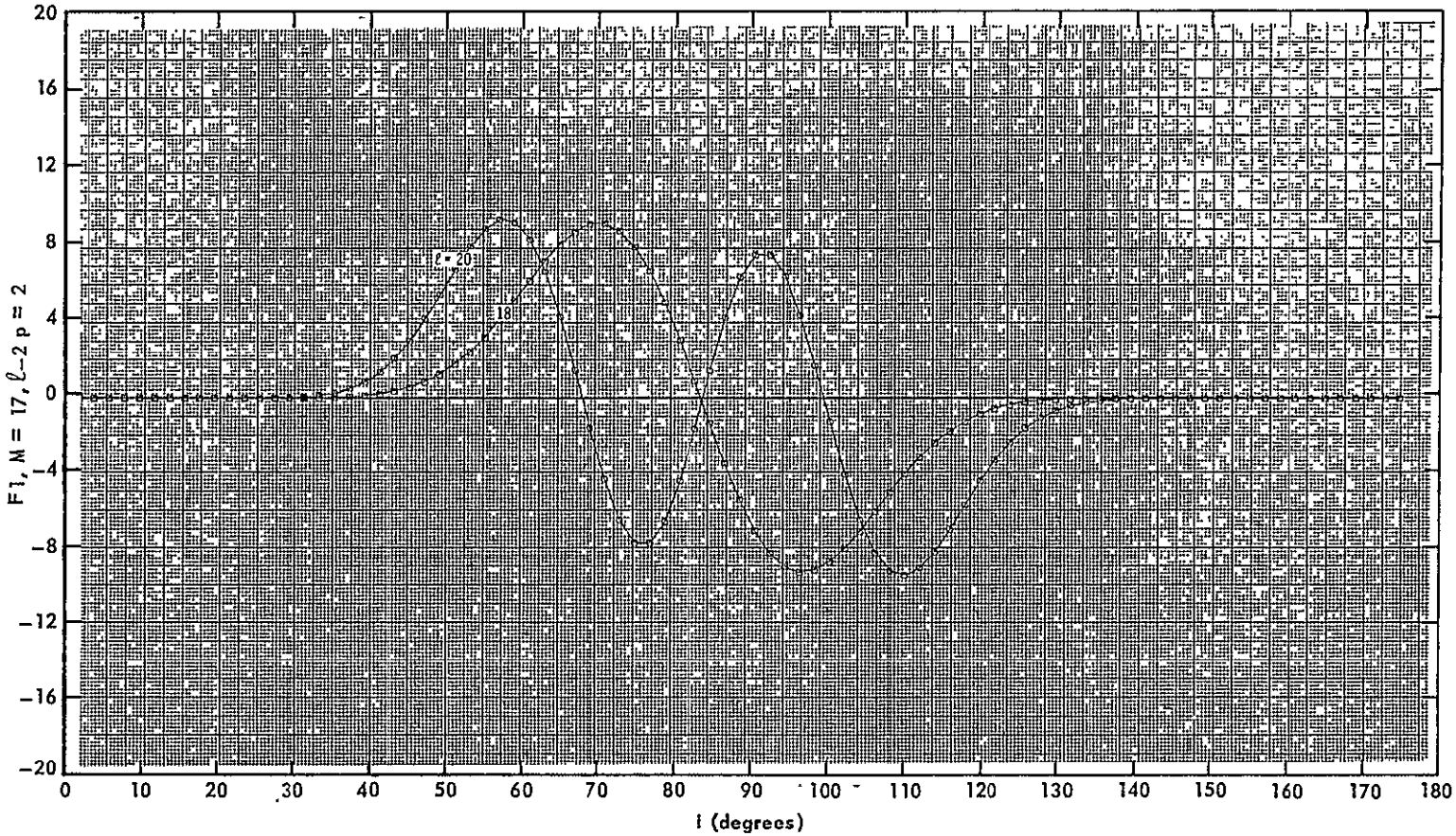
20
16
12
8
4
0
-4
-8
-12
-16
-20
0
10
20
30
40
50
60
70
80
90
100
110
120
130
140
150
160
170
180
i (degrees)
F1, M = 17, ℓ-2 p = 2
ℓ = 20
18

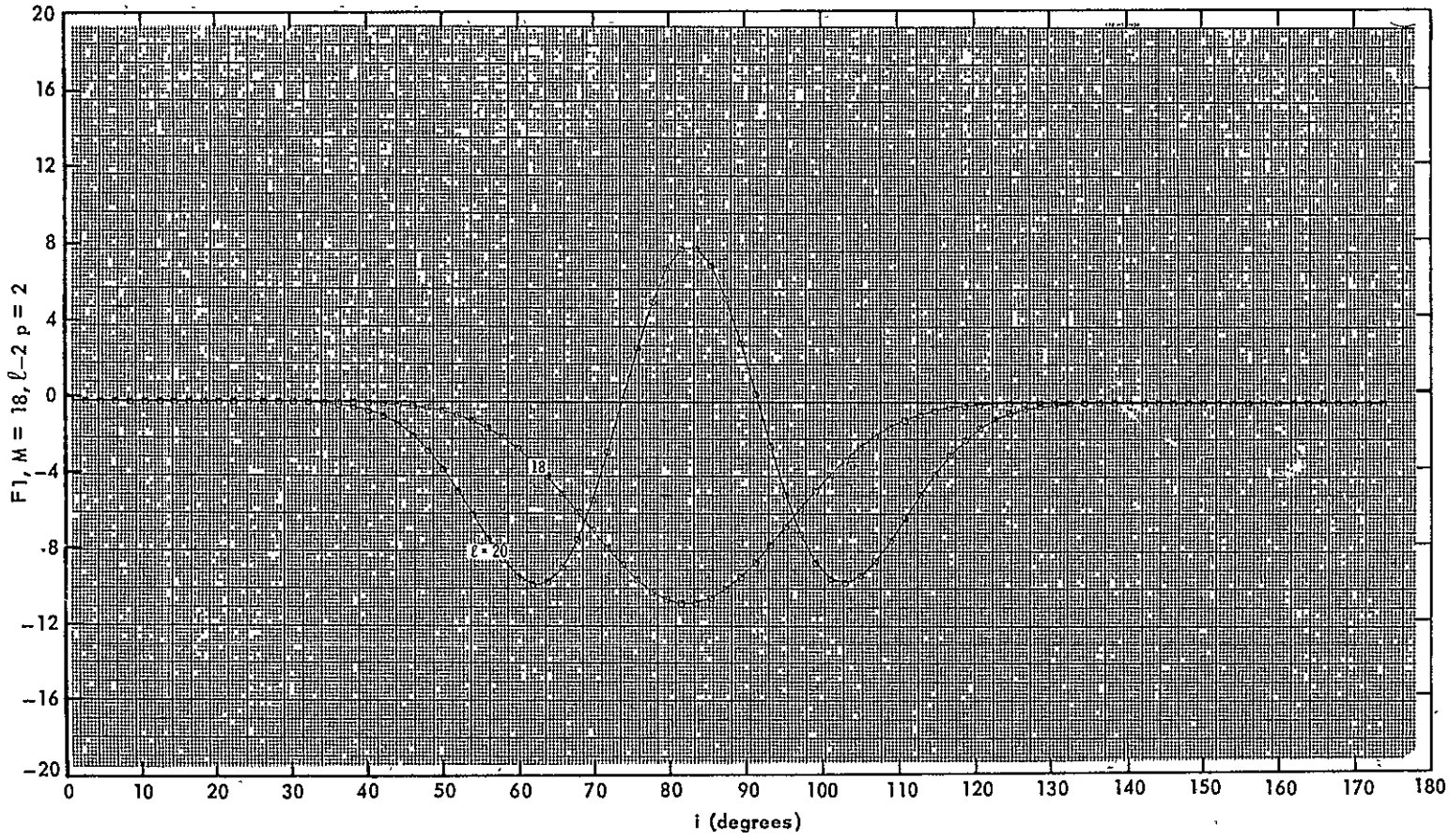
20
16
12
8
4
0
-4
-8
-12
-16
-20
0
10
20
30
40
50
60
70
80
90
100
110
120
130
140
150
160
170
180
i (degrees)
F1, M = 18, ℓ-2 p = 2
18
ℓ = 20

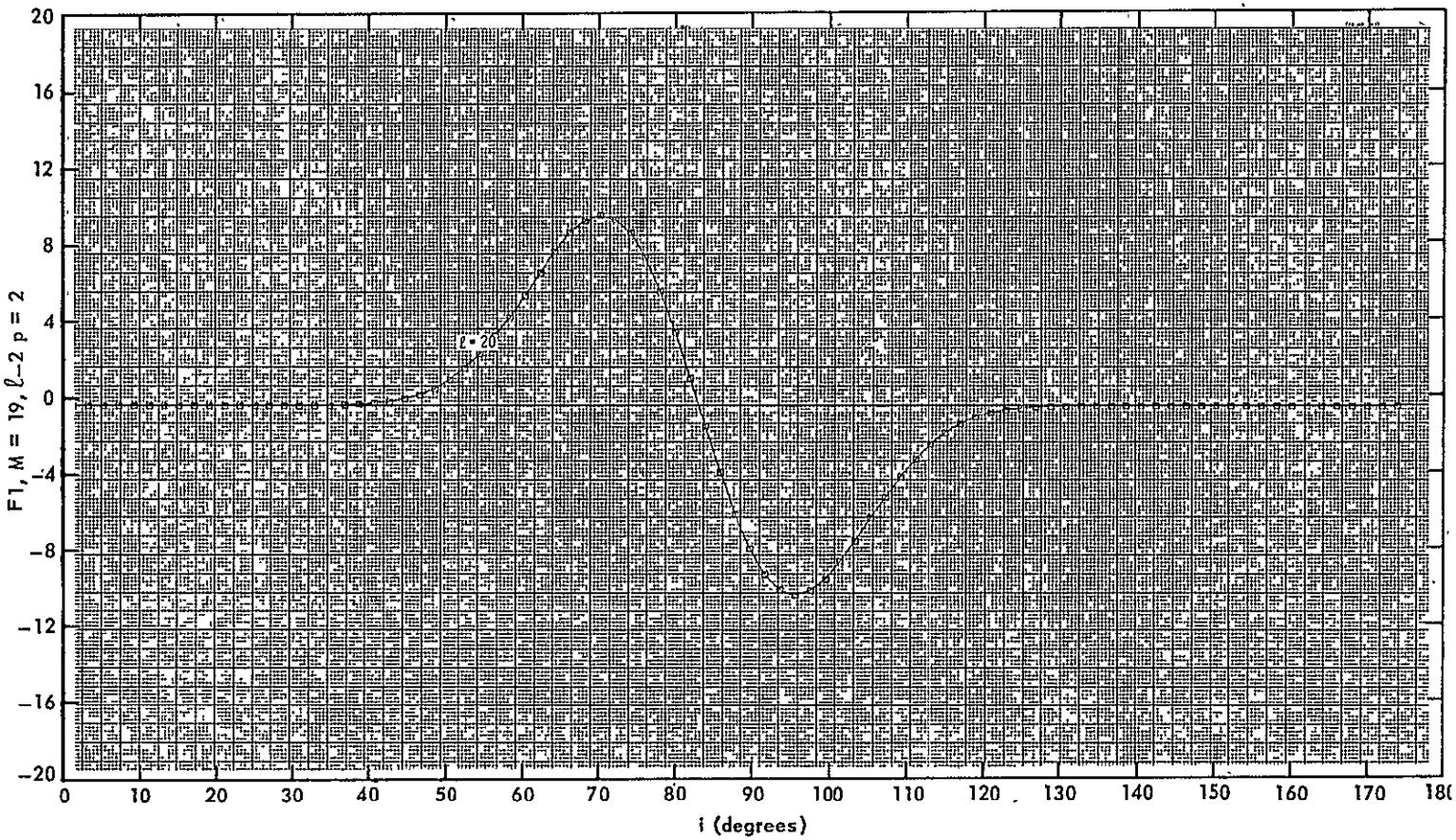
20
16
12
8
4
0
-4
-8
-12
-16
-20
0
10
20
30
40
50
60
70
80
90
100
110
120
130
140
150
160
170
180
F1, M = 19, ℓ-2 p = 2
i (degrees)
ℓ = 20

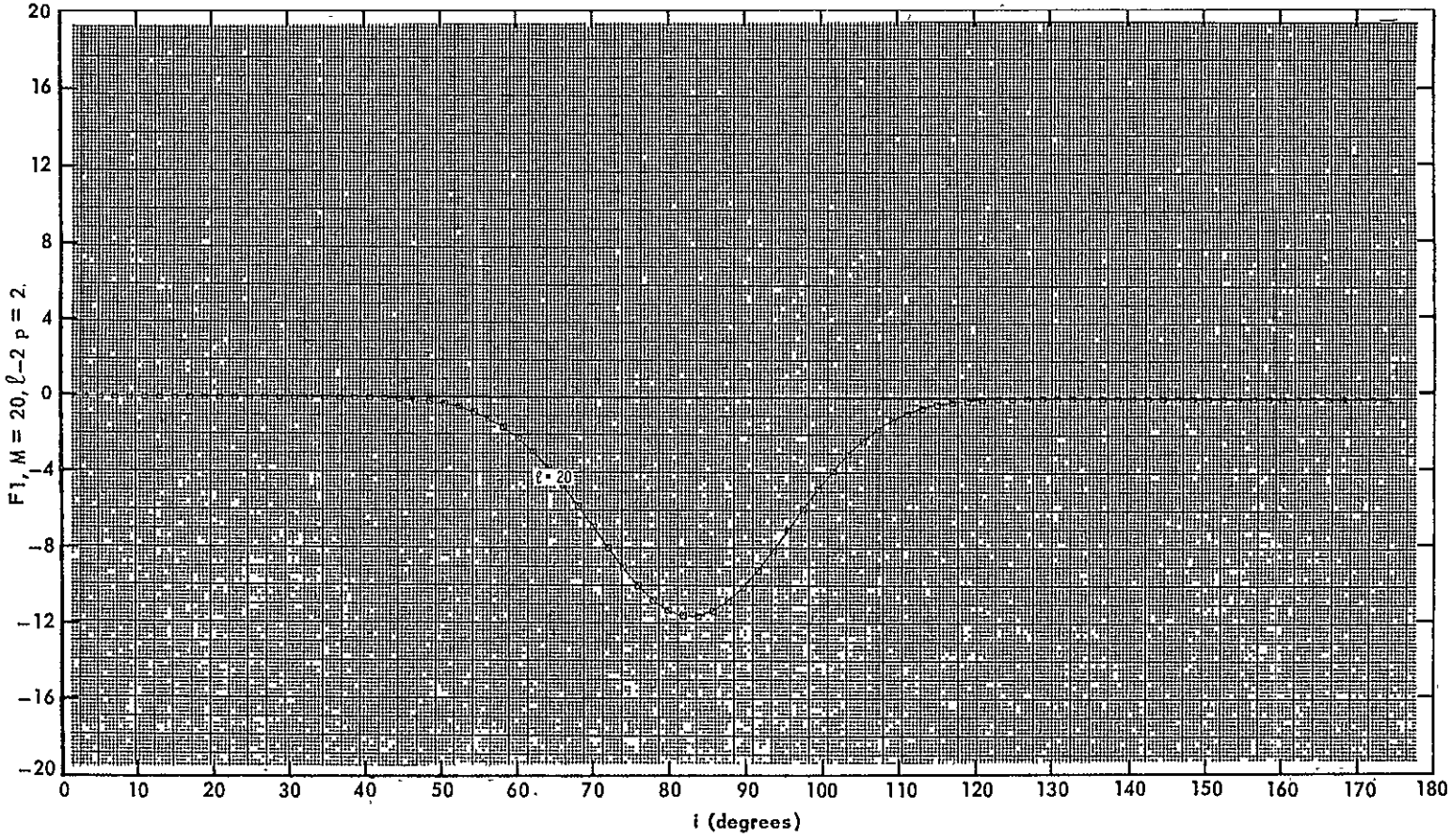
20
16
12
8
4
0
-4
-8
-12
-16
-20
F1, M = 20, ℓ-2 p = 2.
ℓ = 20
0
10
20
30
40
50
60
70
80
90
100
110
120
130
140
150
160
170
180
i (degrees)

APPENDIX E

Graphs of Eccentricity Function

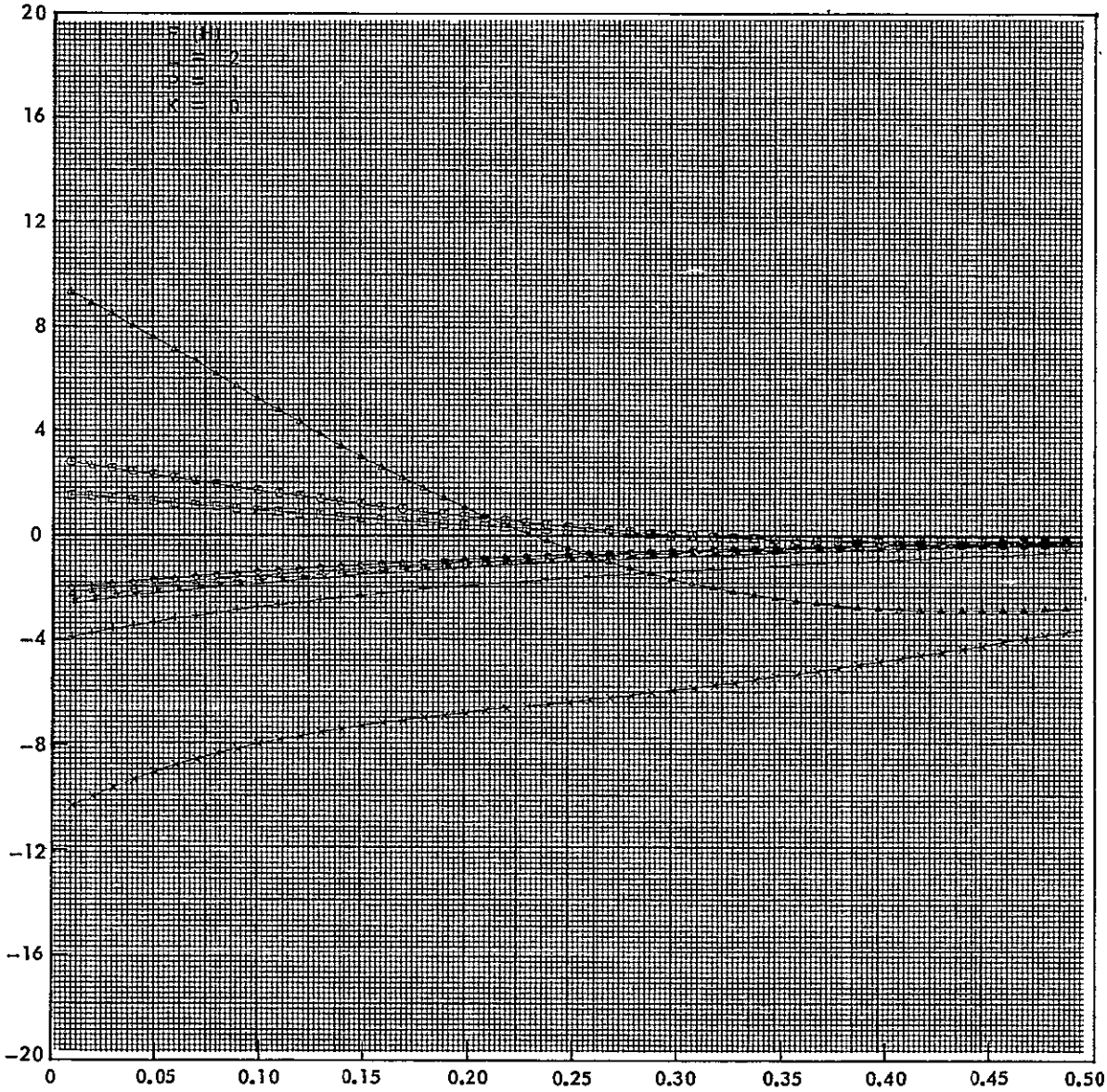

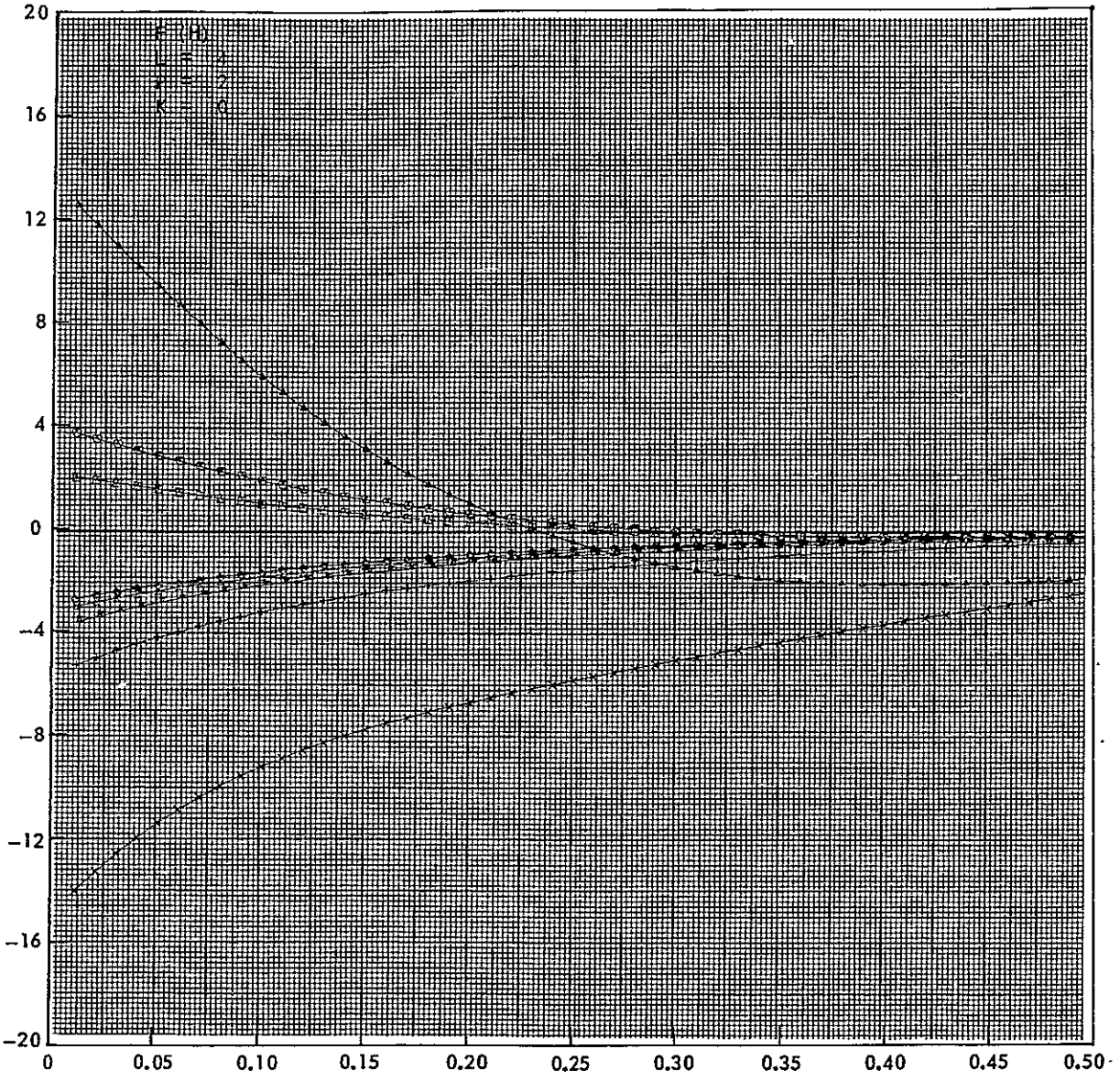
20
16
12
8
4
0
−4
−8
−12
−16
−20
0
0.05
0.10
0.15
0.20
0.25
0.30
0.35
0.40
0.45
0.50
ECCENTRICITY

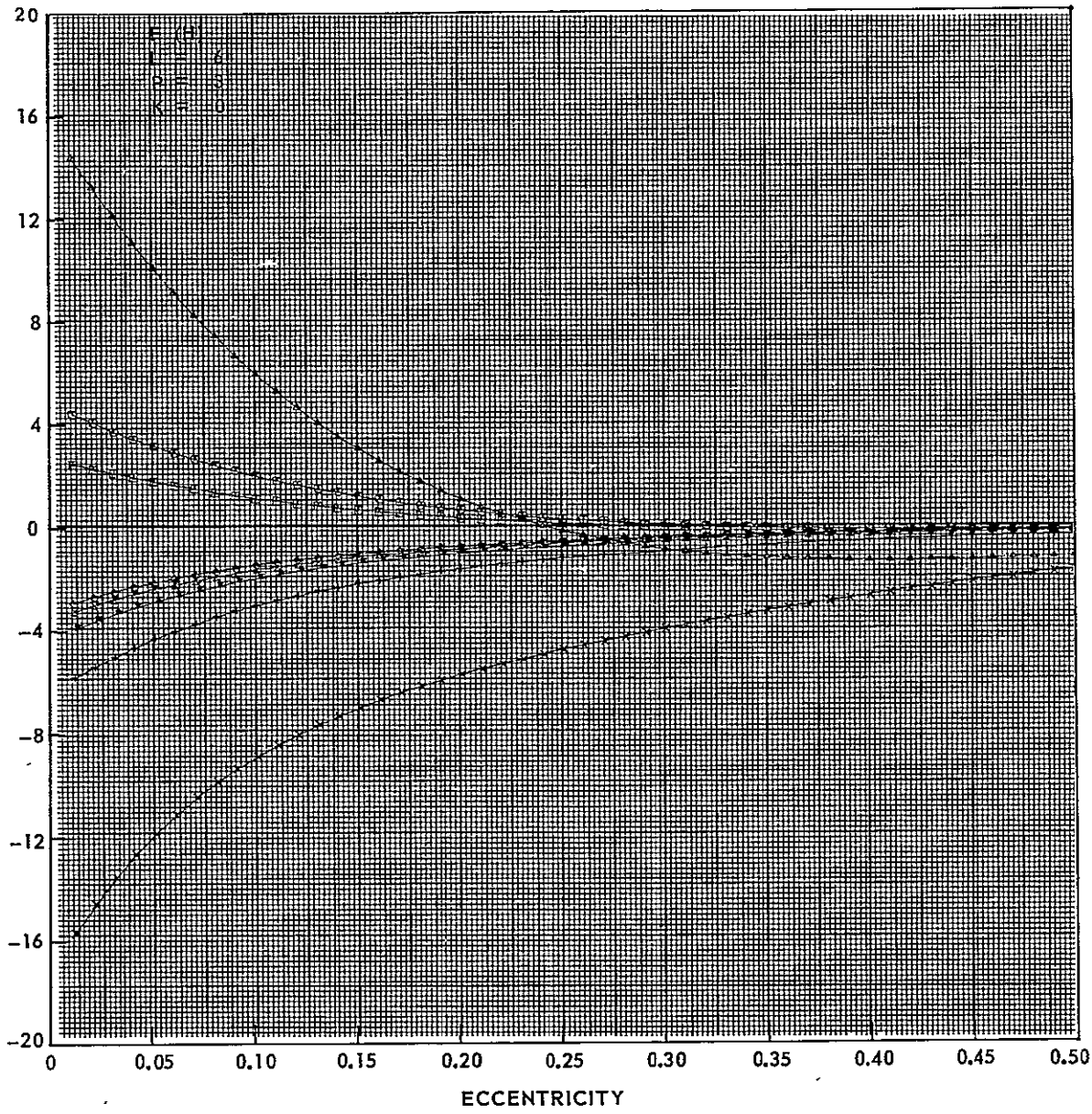
E (θ)
I = 4
θ = 3
K = 0
20
16
12
8
4
0
-4
-8
-12
-16
-20
0
0.05
0.10
0.15
0.20
0.25
0.30
0.35
0.40
0.45
0.50
ECCENTRICITY

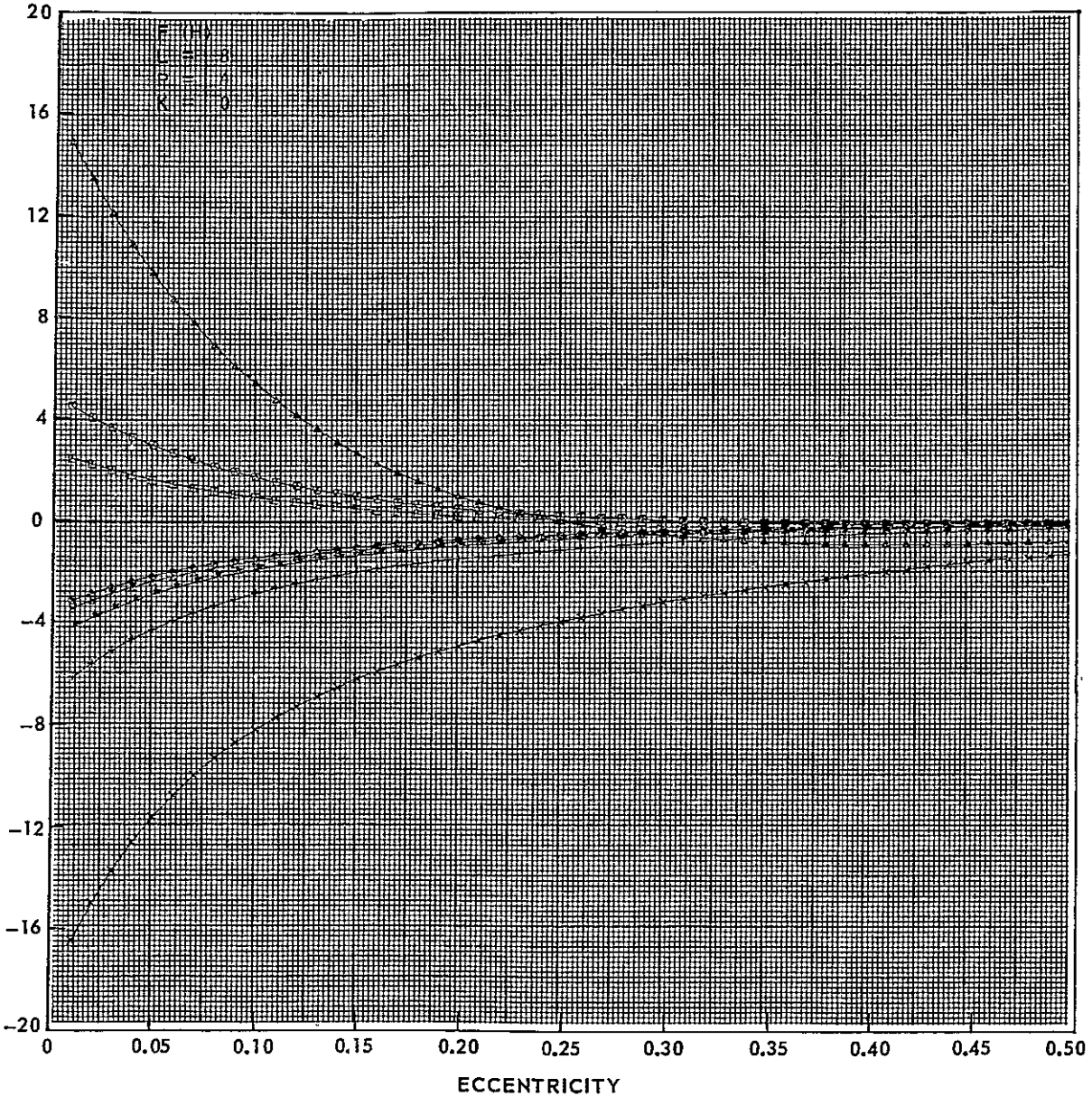
20
16
12
8
4
0
−4
−8
−12
−16
−20
0
0.05
0.10
0.15
0.20
0.25
0.30
0.35
0.40
0.45
0.50
ECCENTRICITY

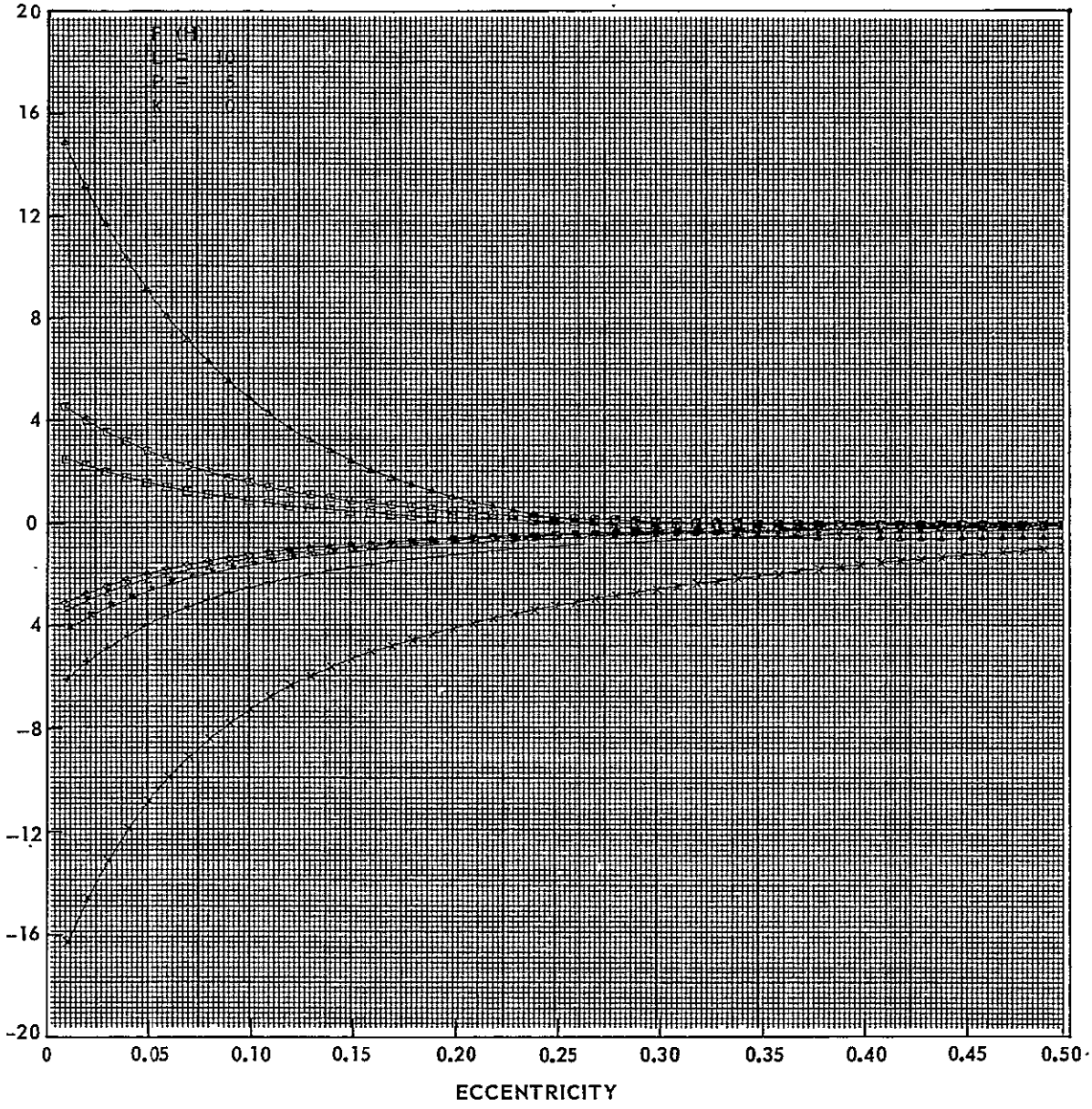
20
16
12
8
4
0
4
-8
-12
-16
-20
0
0.05
0.10
0.15
0.20
0.25
0.30
0.35
0.40
0.45
0.50
ECCENTRICITY

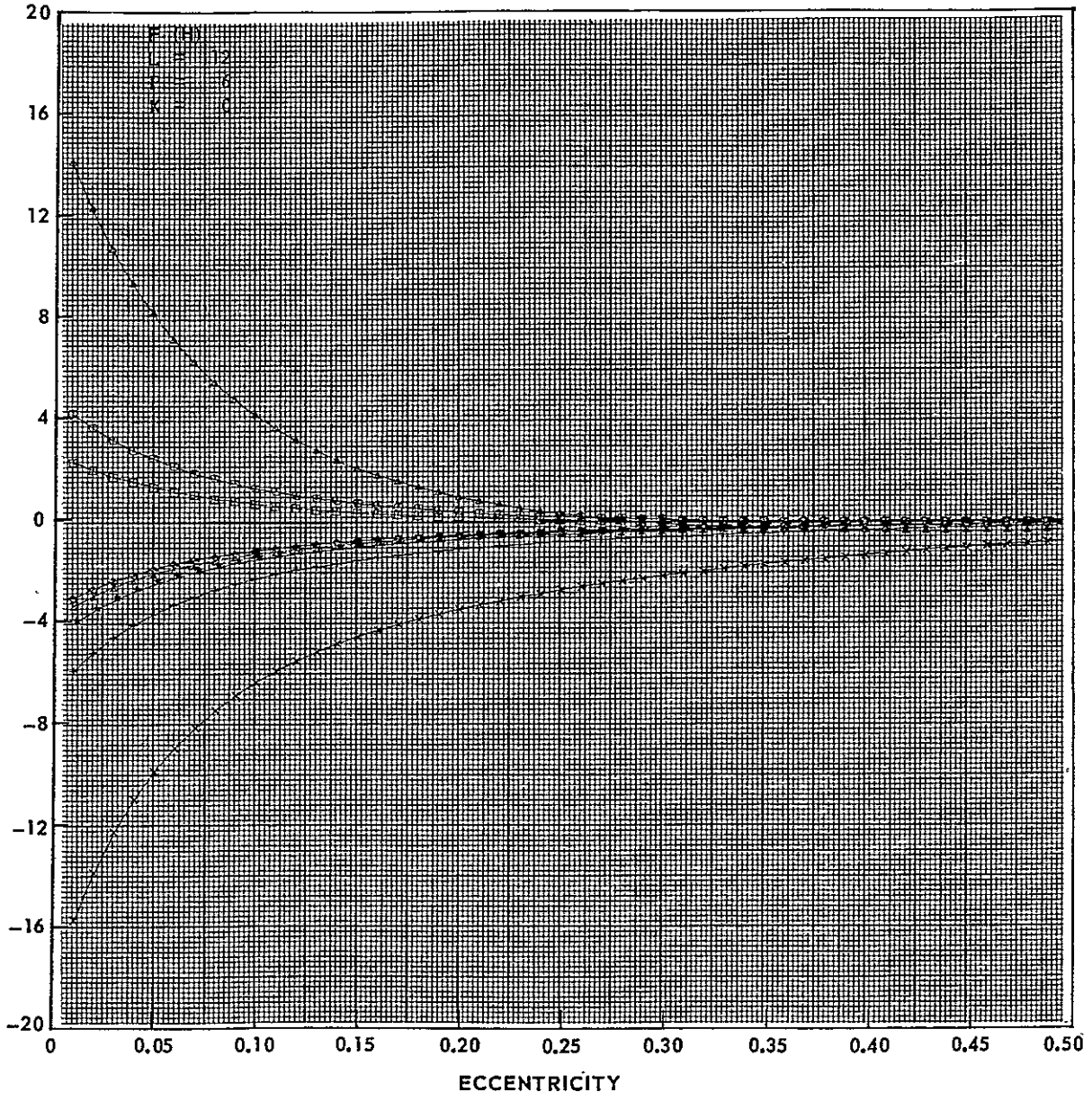
F (H)
C = 12
E = 6
K = 0
20
16
12
8
4
0
-4
-8
-12
-16
-20
0
0.05
0.10
0.15
0.20
0.25
0.30
0.35
0.40
0.45
0.50
ECCENTRICITY

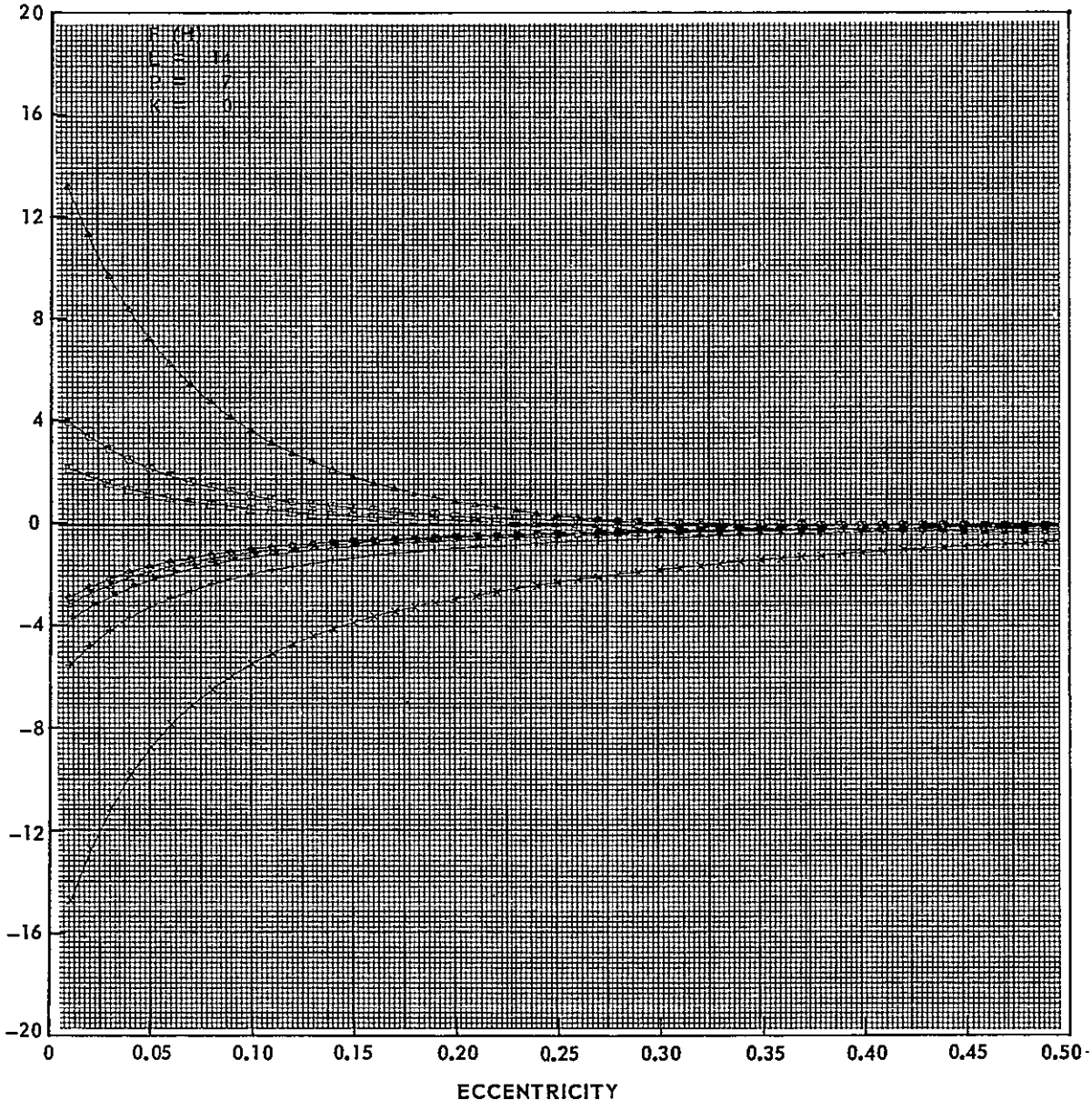
20
16
12
8
4
0
−4
−8
−12
−16
−20
0
0.05
0.10
0.15
0.20
0.25
0.30
0.35
0.40
0.45
0.50
ECCENTRICITY

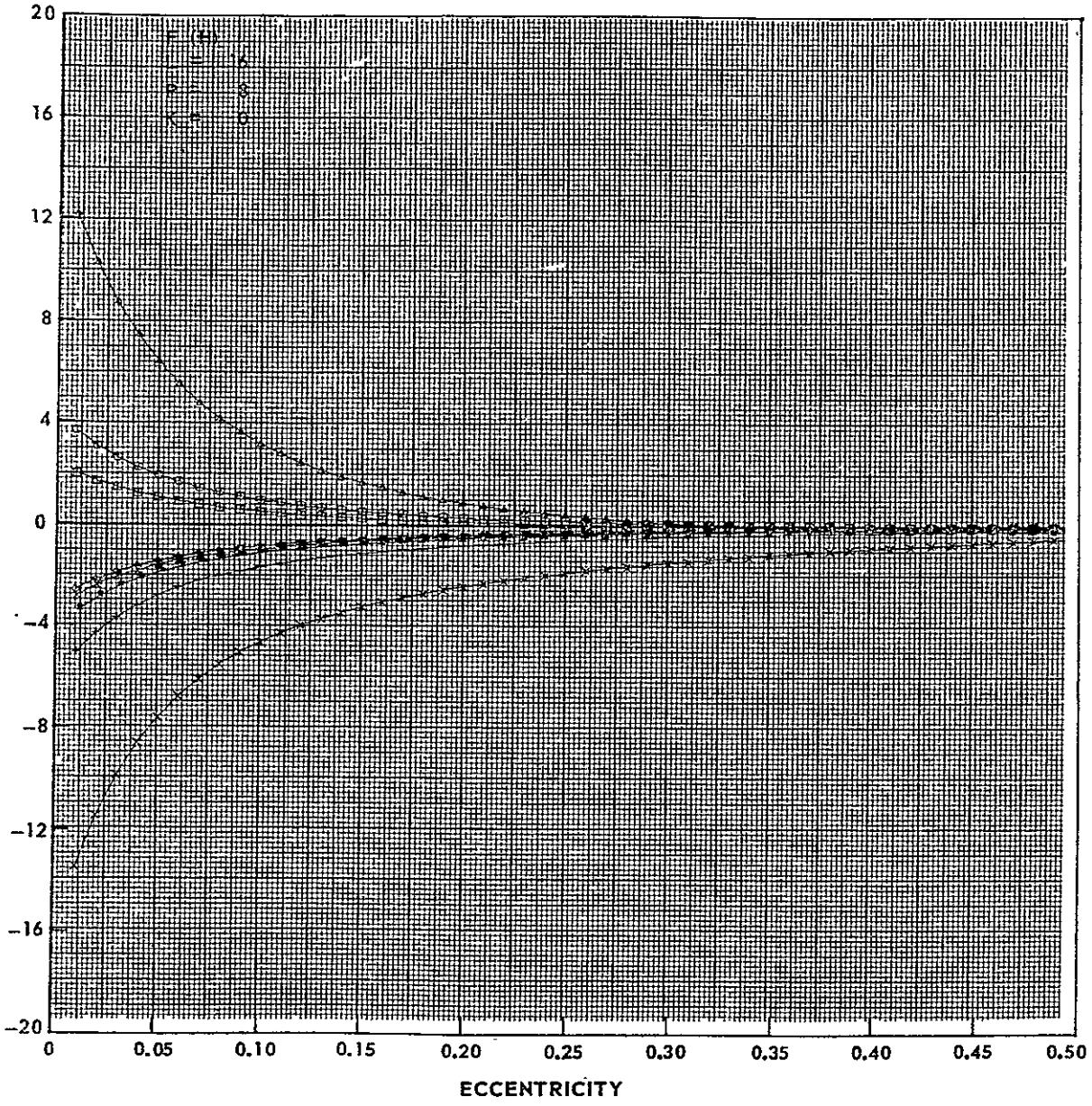
20
16
12
8
4
0
−4
−8
−12
−16
−20
0
0.05
0.10
0.15
0.20
0.25
0.30
0.35
0.40
0.45
0.50
ECCENTRICITY

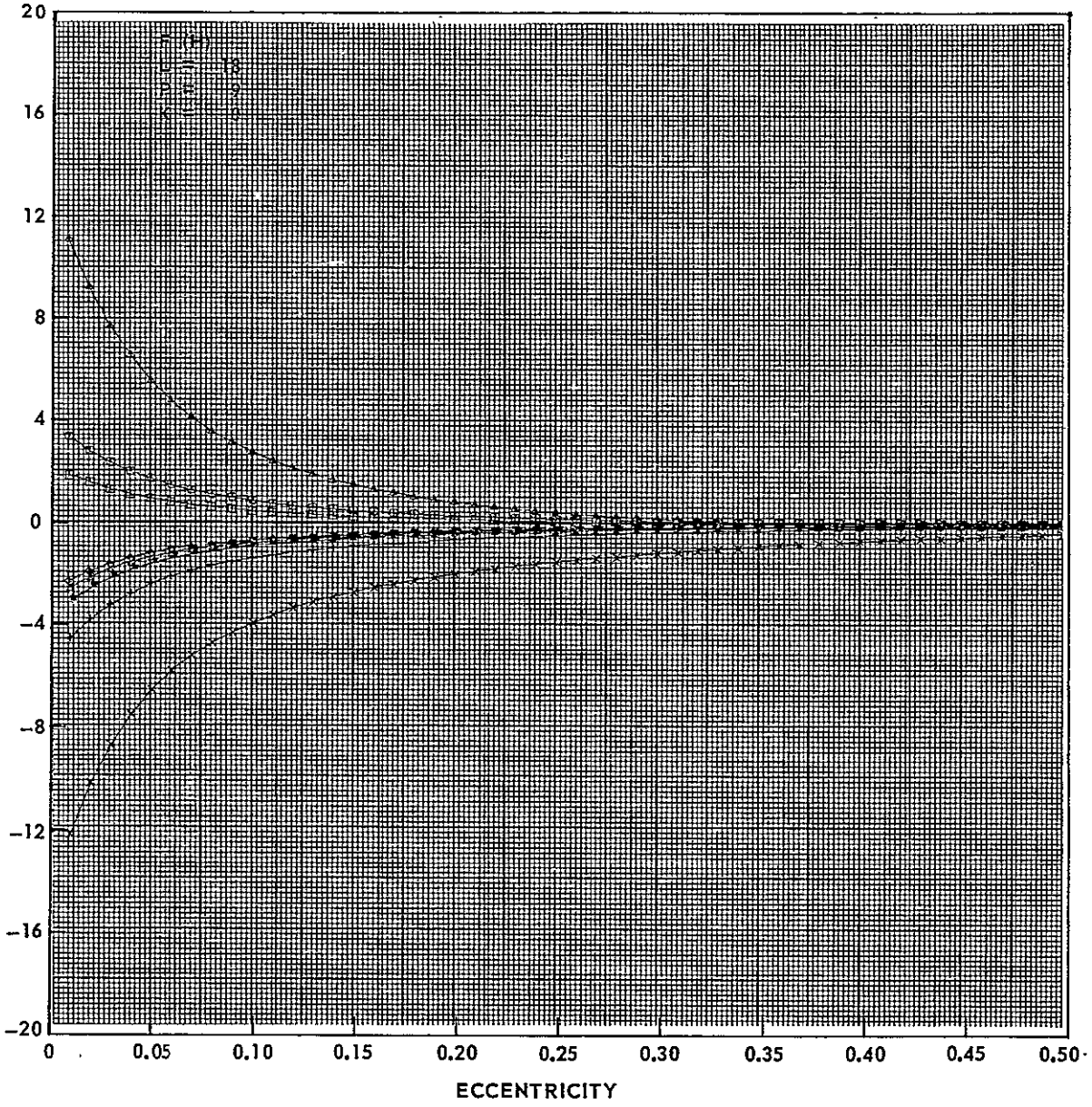
20
16
12
8
4
0
−4
−8
−12
−16
−20
0
0.05
0.10
0.15
0.20
0.25
0.30
0.35
0.40
0.45
0.50
ECCENTRICITY

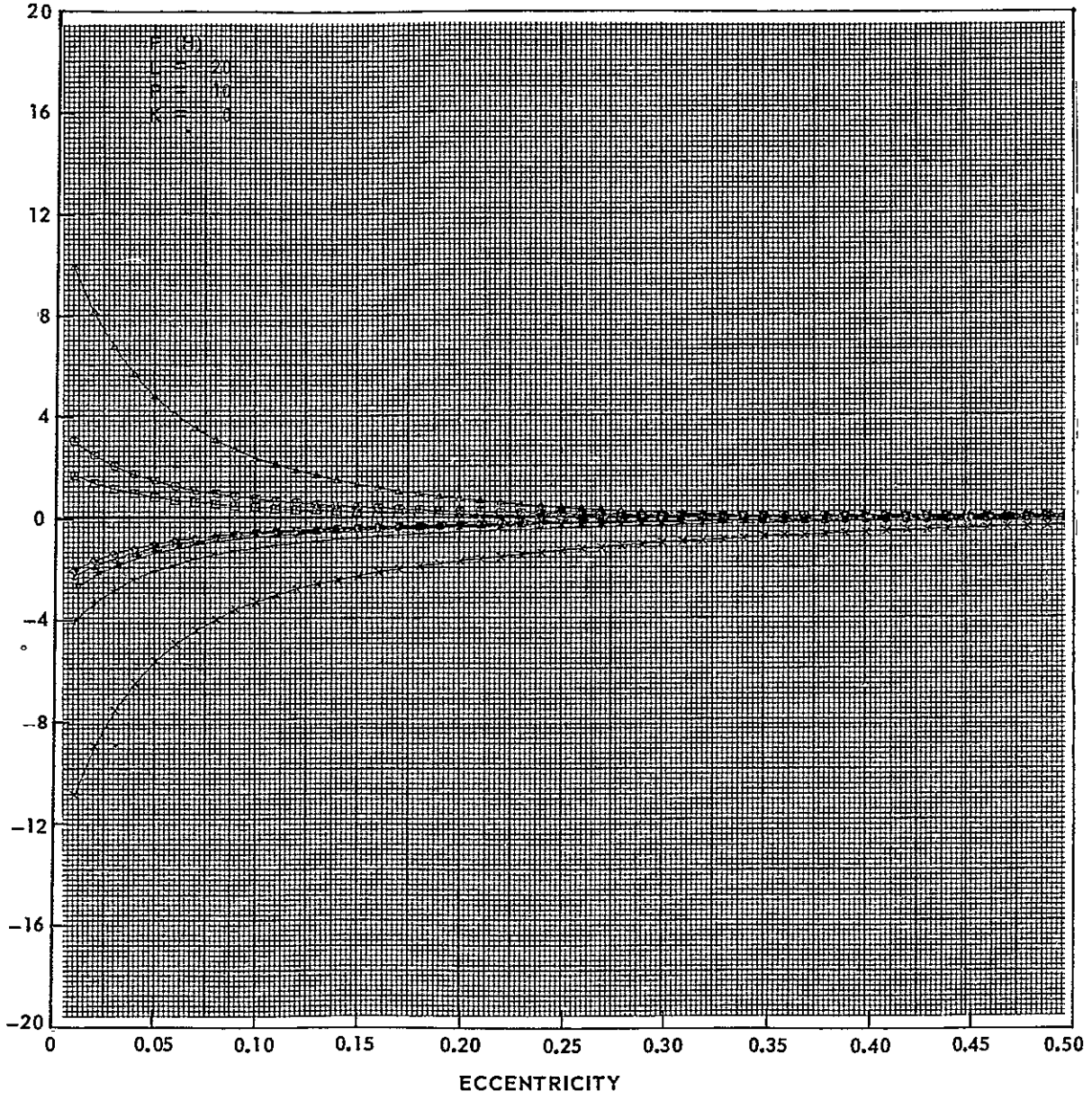
20
16
12
8
4
0
−4
−8
−12
−16
−20
0
0.05
0.10
0.15
0.20
0.25
0.30
0.35
0.40
0.45
0.50
ECCENTRICITY

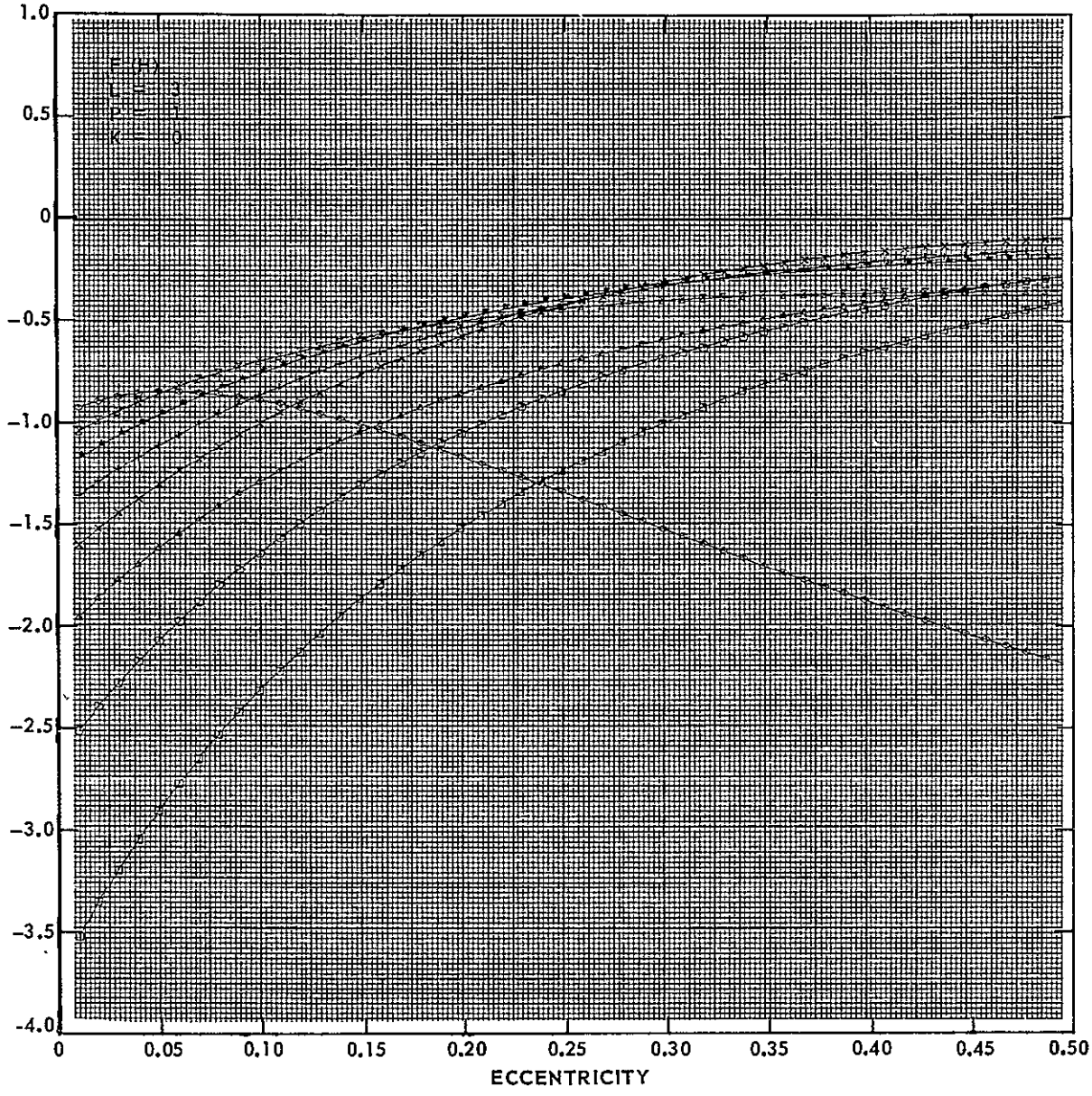
E (H)
L = 3
P = 1
K = 0
1.0
0.5
0
-0.5
-1.0
-1.5
-2.0
-2.5
-3.0
-3.5
-4.0
0
0.05
0.10
0.15
0.20
0.25
0.30
0.35
0.40
0.45
0.50
ECCENTRICITY

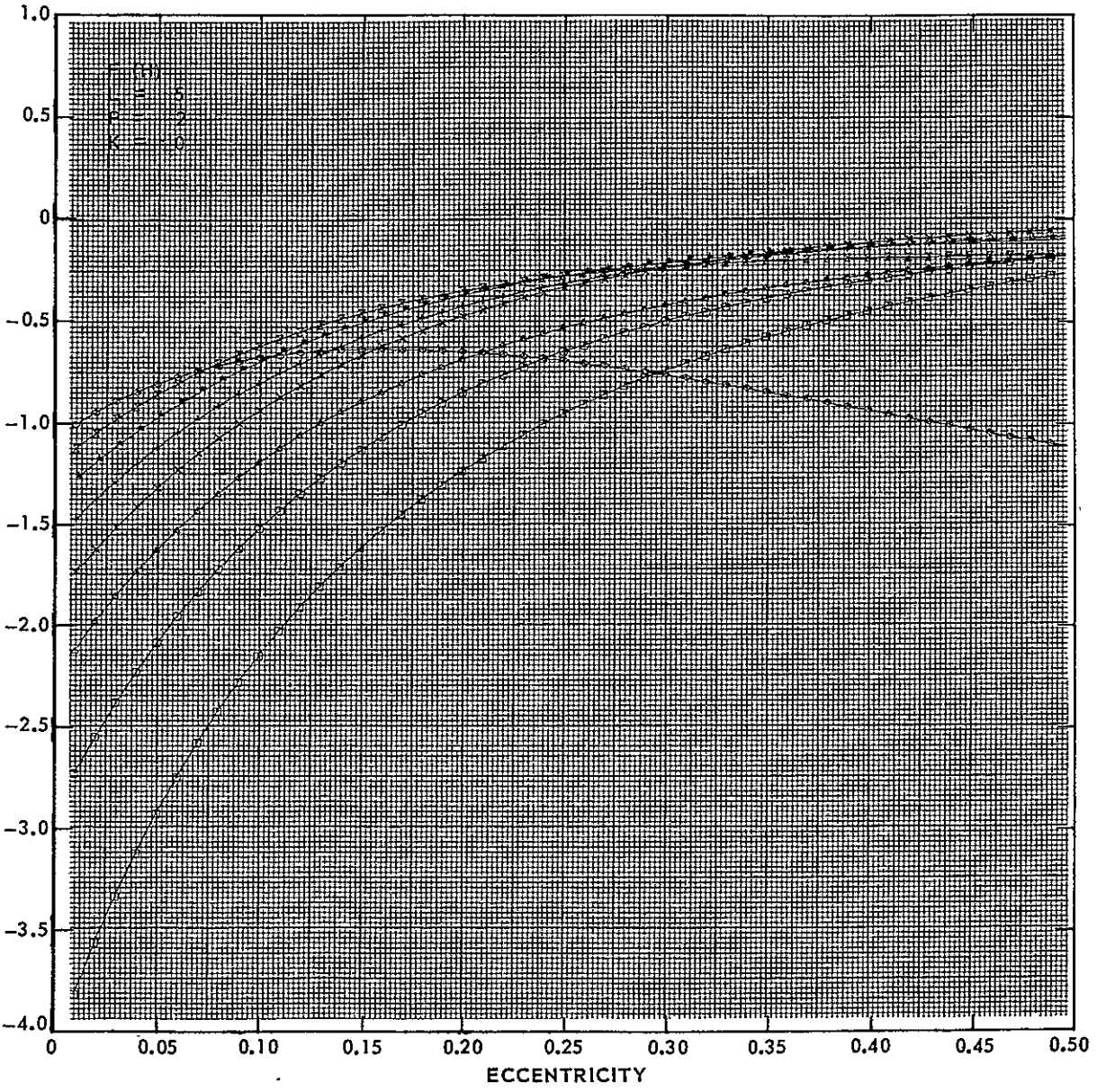
1.0
0.5
0
-0.5
-1.0
-1.5
-2.0
-2.5
-3.0
-3.5
-4.0
0
0.05
0.10
0.15
0.20
0.25
0.30
0.35
0.40
0.45
0.50
ECCENTRICITY

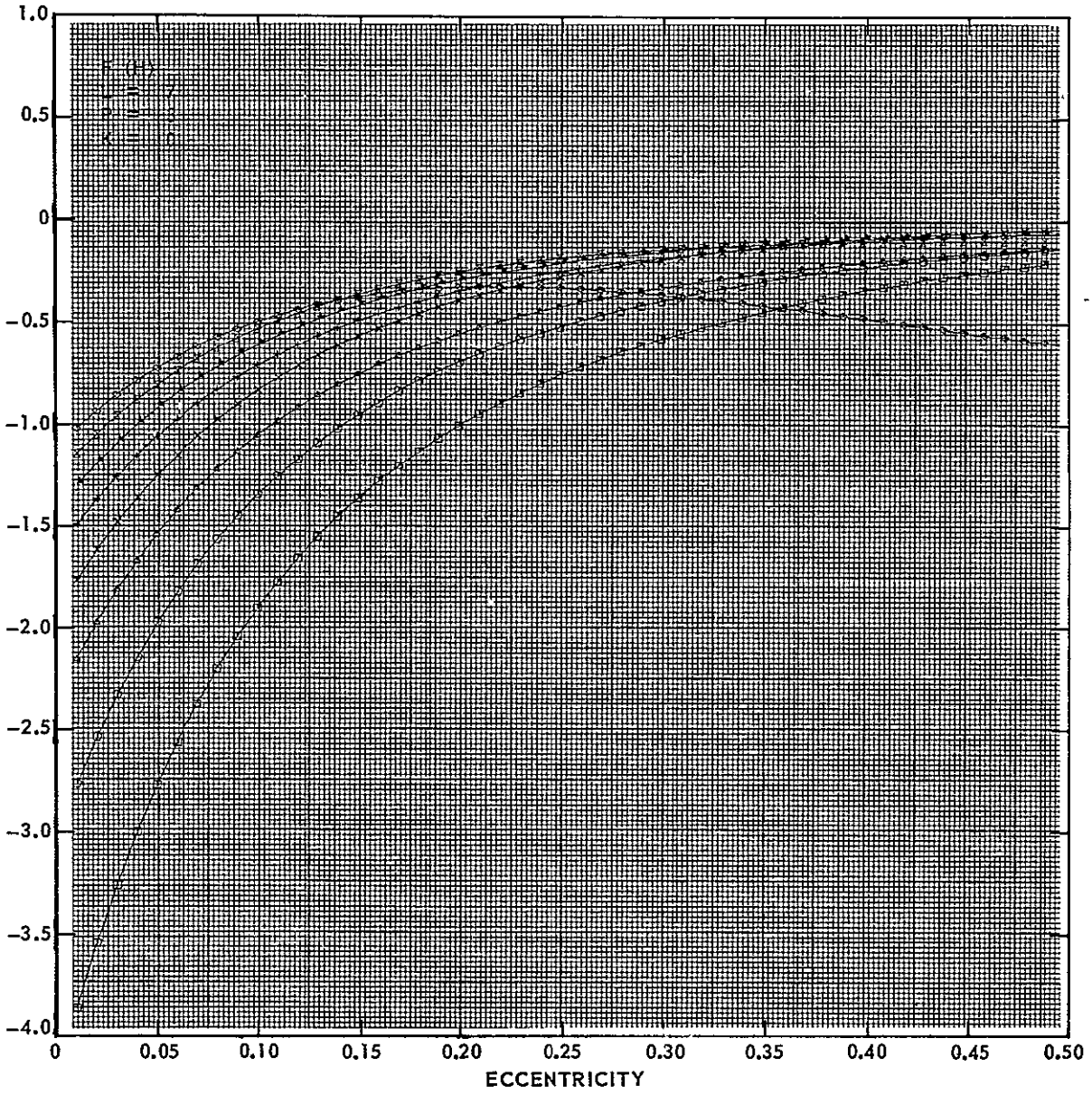
1.0
0.5
0
-0.5
-1.0
-1.5
-2.0
-2.5
-3.0
-3.5
-4.0
0
0.05
0.10
0.15
0.20
0.25
0.30
0.35
0.40
0.45
0.50
ECCENTRICITY

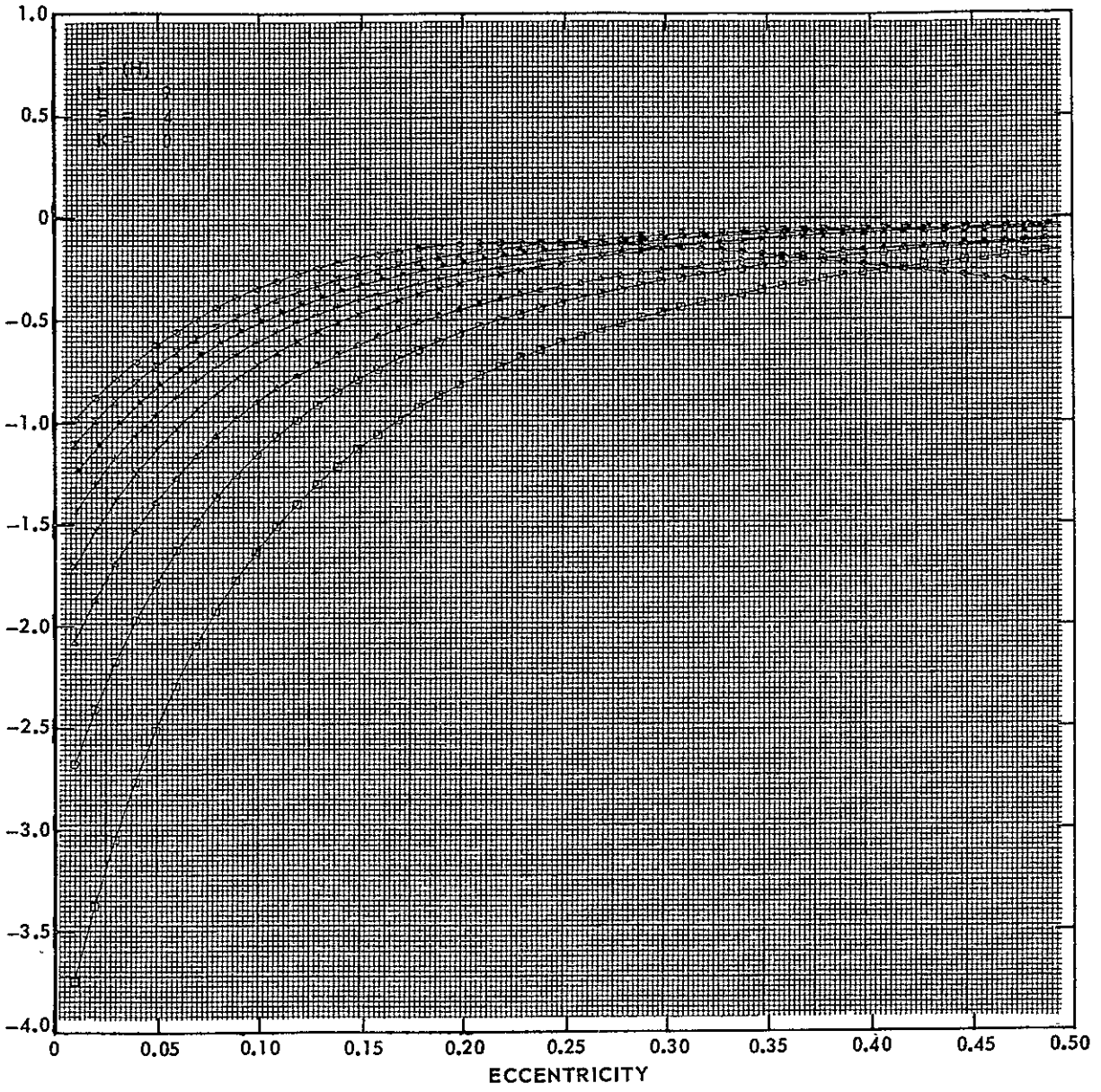
1.0
0.5
0
−0.5
−1.0
−1.5
−2.0
−2.5
−3.0
−3.5
−4.0
0
0.05
0.10
0.15
0.20
0.25
0.30
0.35
0.40
0.45
0.50
ECCENTRICITY

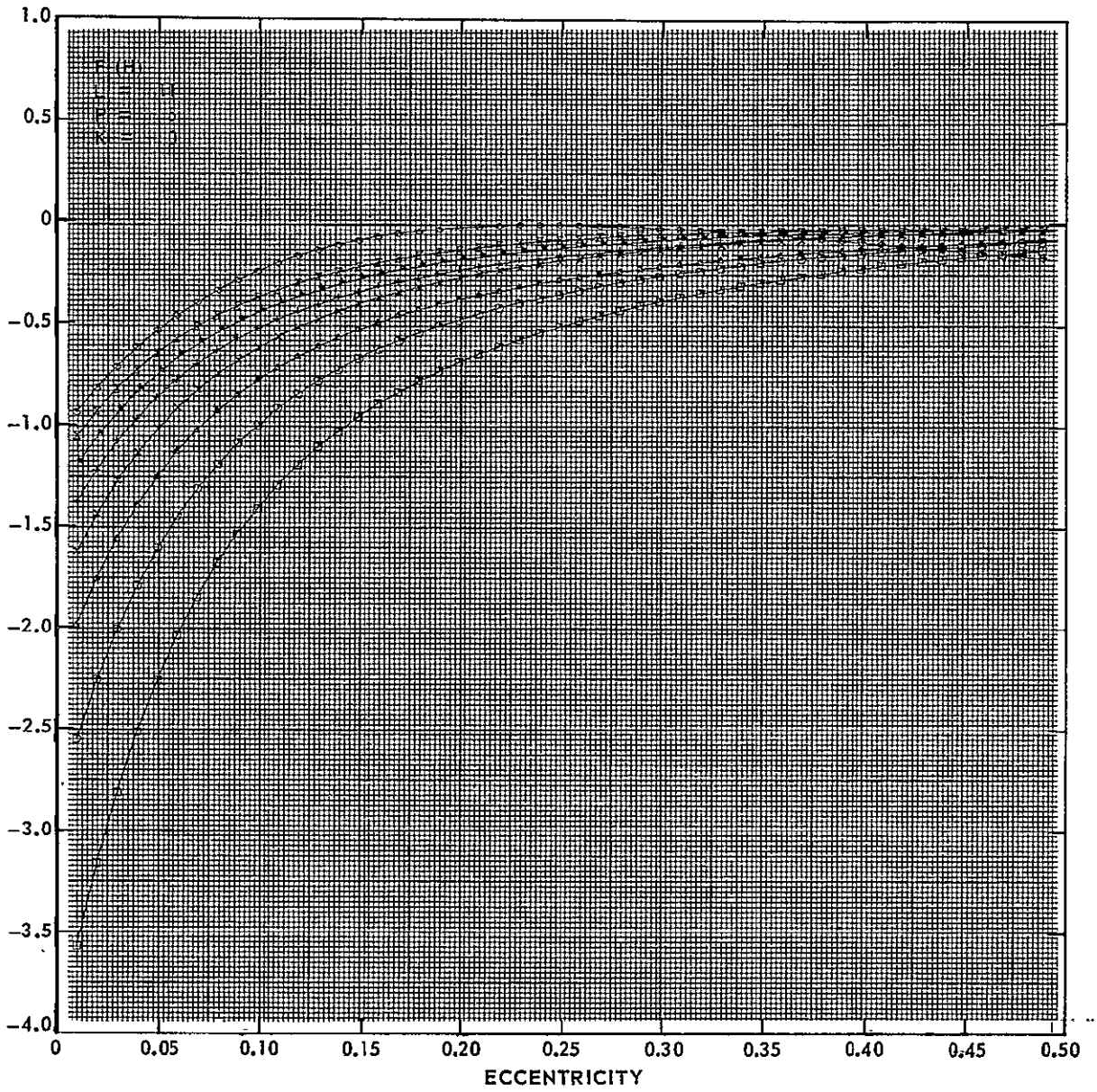
1.0
0.5
0
−0.5
−1.0
−1.5
−2.0
−2.5
−3.0
−3.5
−4.0
0
0.05
0.10
0.15
0.20
0.25
0.30
0.35
0.40
0.45
0.50
ECCENTRICITY

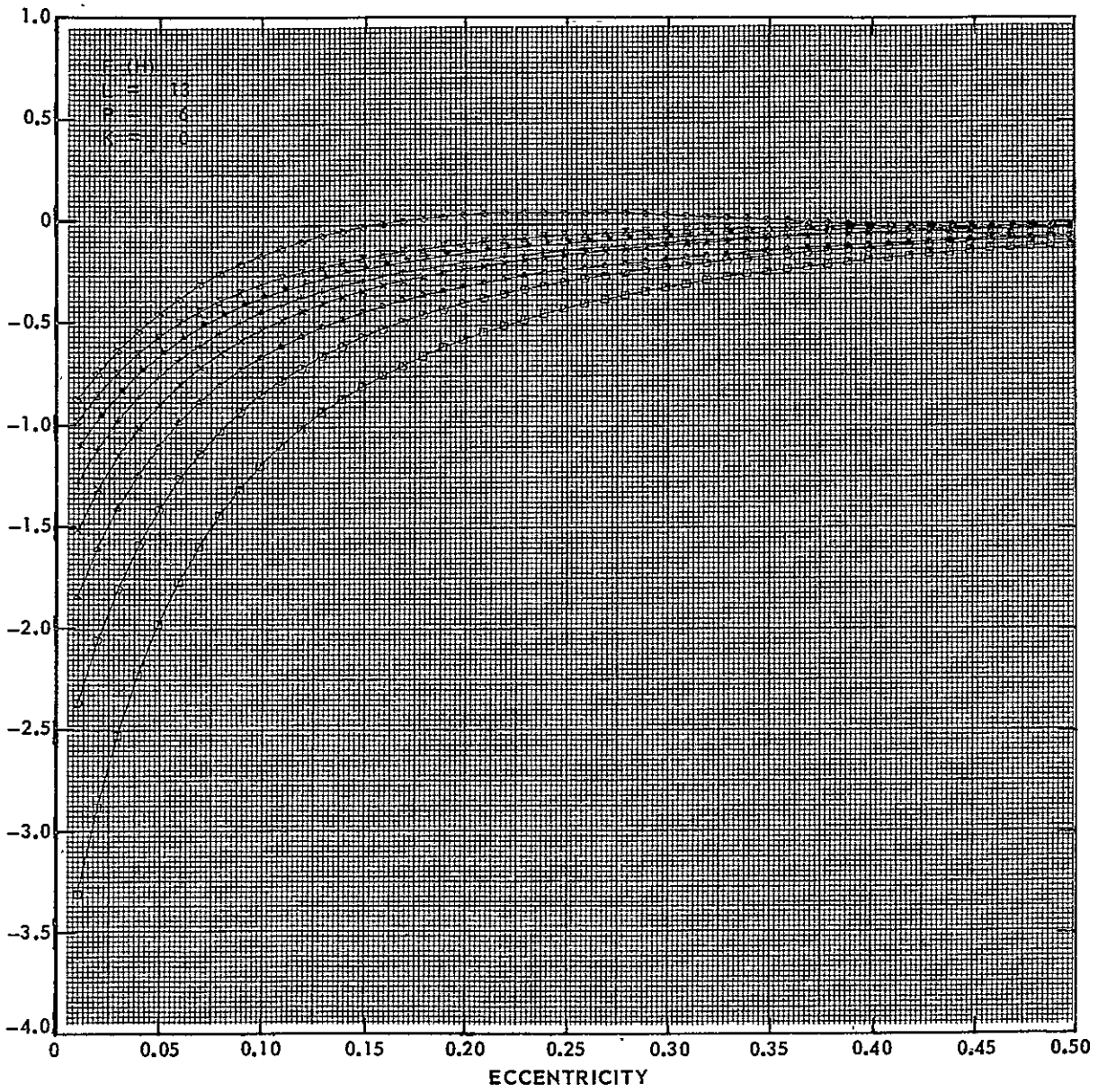
1.0
0.5
0
−0.5
−1.0
−1.5
−2.0
−2.5
−3.0
−3.5
−4.0
0
0.05
0.10
0.15
0.20
0.25
0.30
0.35
0.40
0.45
0.50
ECCENTRICITY

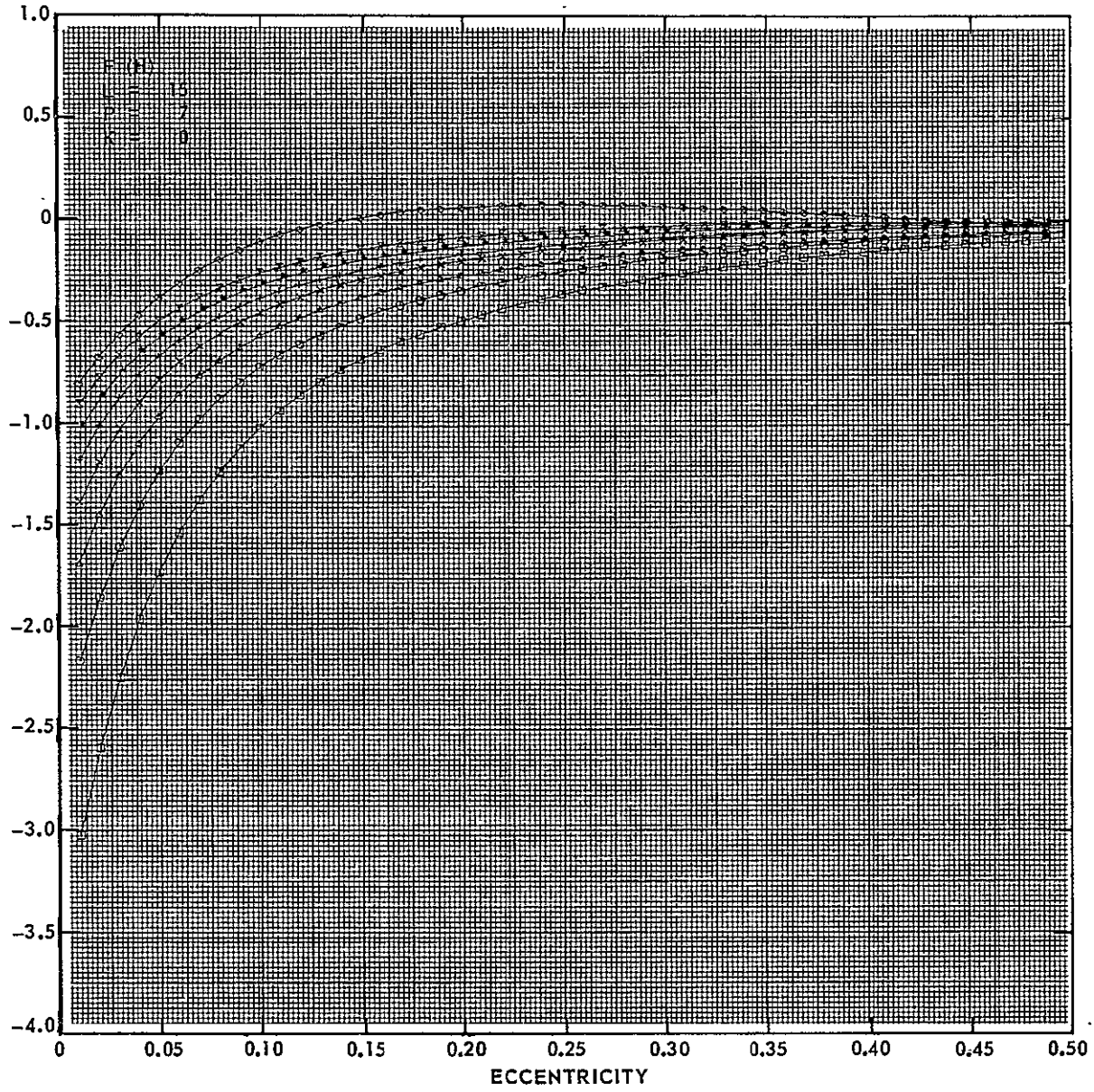
F (H)
L = 15
P = 7
K = 0
1.0
0.5
0
-0.5
-1.0
-1.5
-2.0
-2.5
-3.0
-3.5
-4.0
0
0.05
0.10
0.15
0.20
0.25
0.30
0.35
0.40
0.45
0.50
ECCENTRICITY

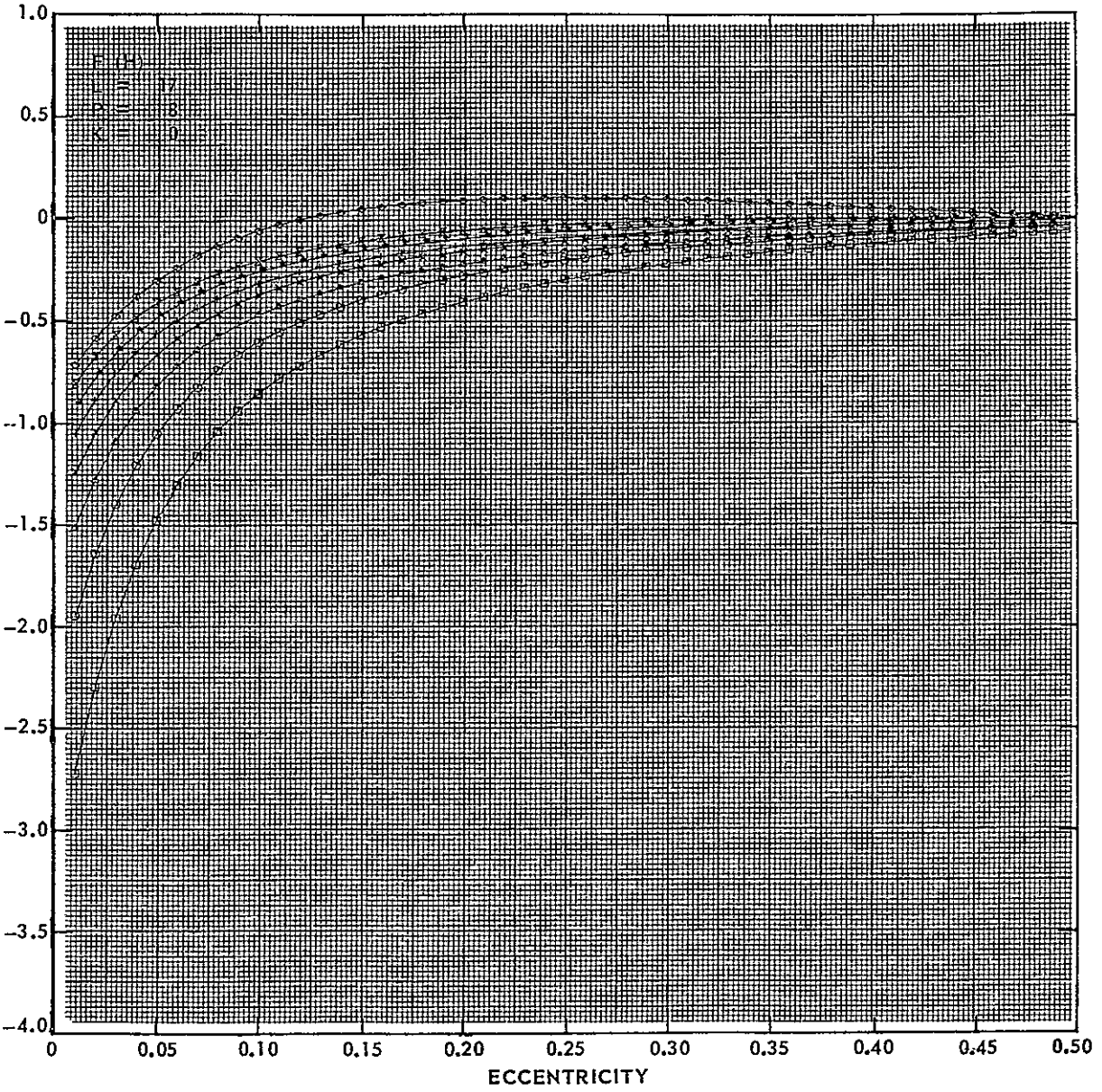
F (H)
L = 17
P = 8
K = 0
1.0
0.5
0
-0.5
-1.0
-1.5
-2.0
-2.5
-3.0
-3.5
-4.0
0
0.05
0.10
0.15
0.20
0.25
0.30
0.35
0.40
0.45
0.50
ECCENTRICITY

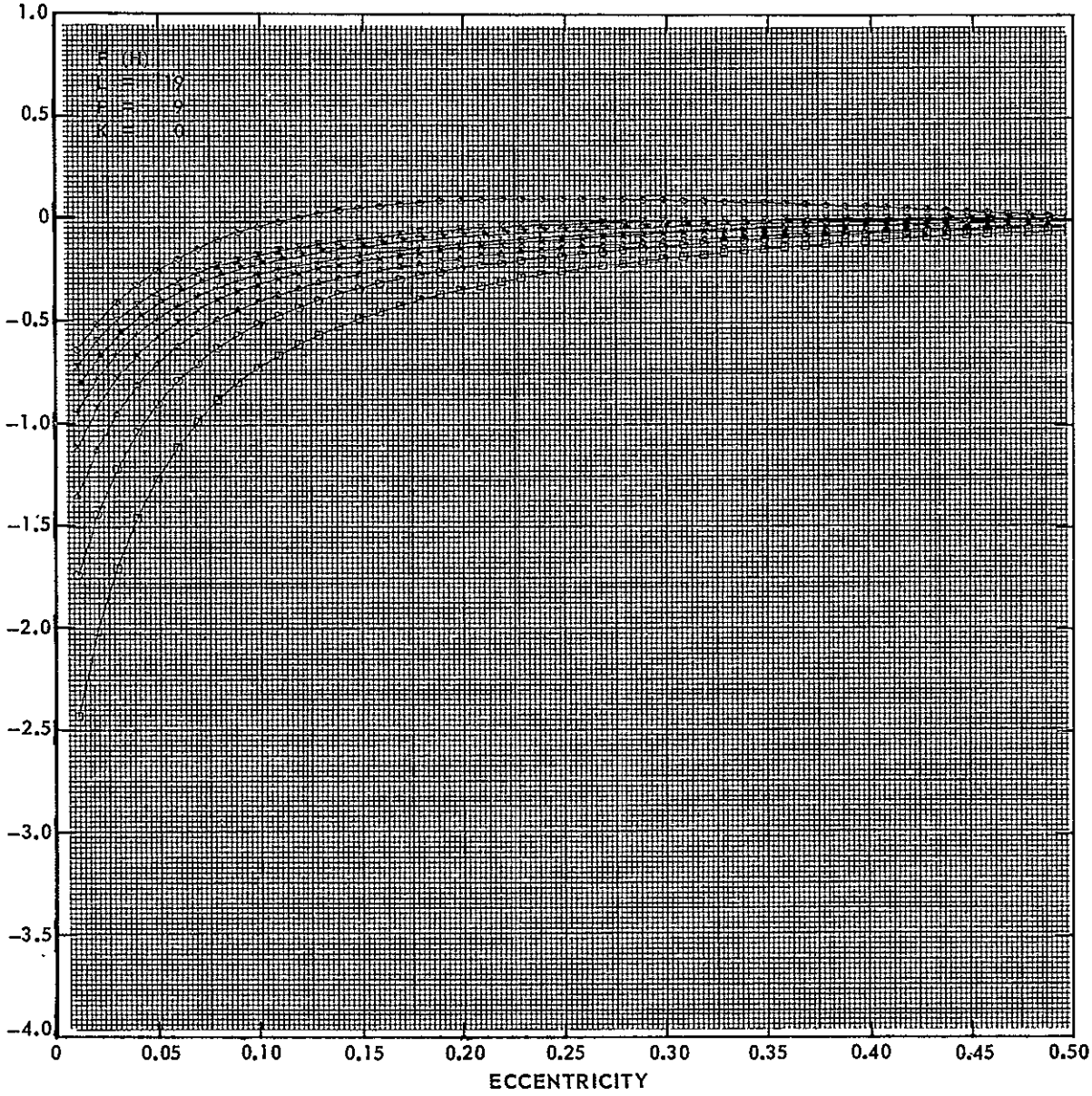
1.0
0.5
0
−0.5
−1.0
−1.5
−2.0
−2.5
−3.0
−3.5
−4.0
0
0.05
0.10
0.15
0.20
0.25
0.30
0.35
0.40
0.45
0.50
ECCENTRICITY

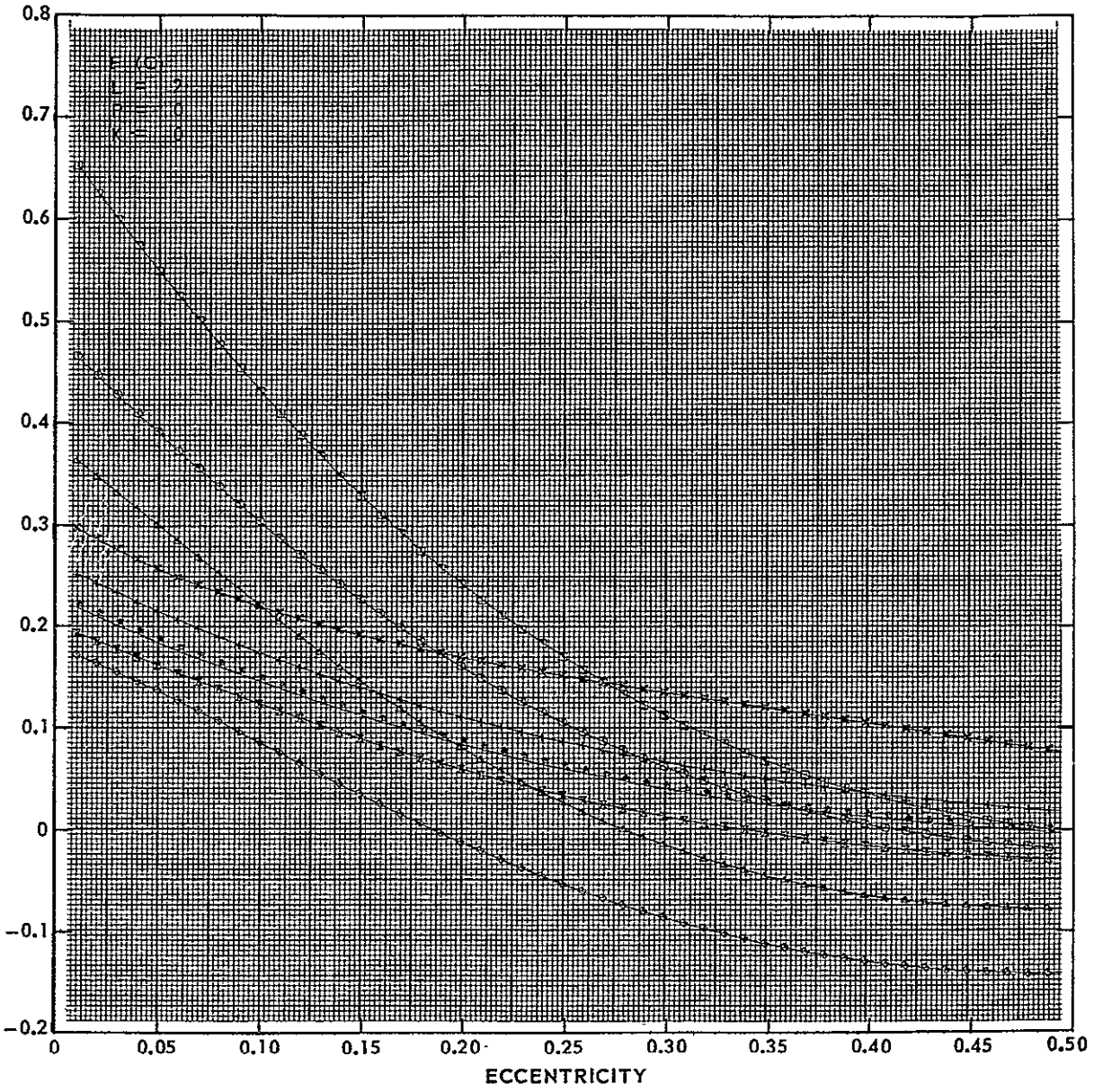
0.8
0.7
0.6
0.5
0.4
0.3
0.2
0.1
0
−0.1
−0.2
0
0.05
0.10
0.15
0.20
0.25
0.30
0.35
0.40
0.45
0.50
ECCENTRICITY

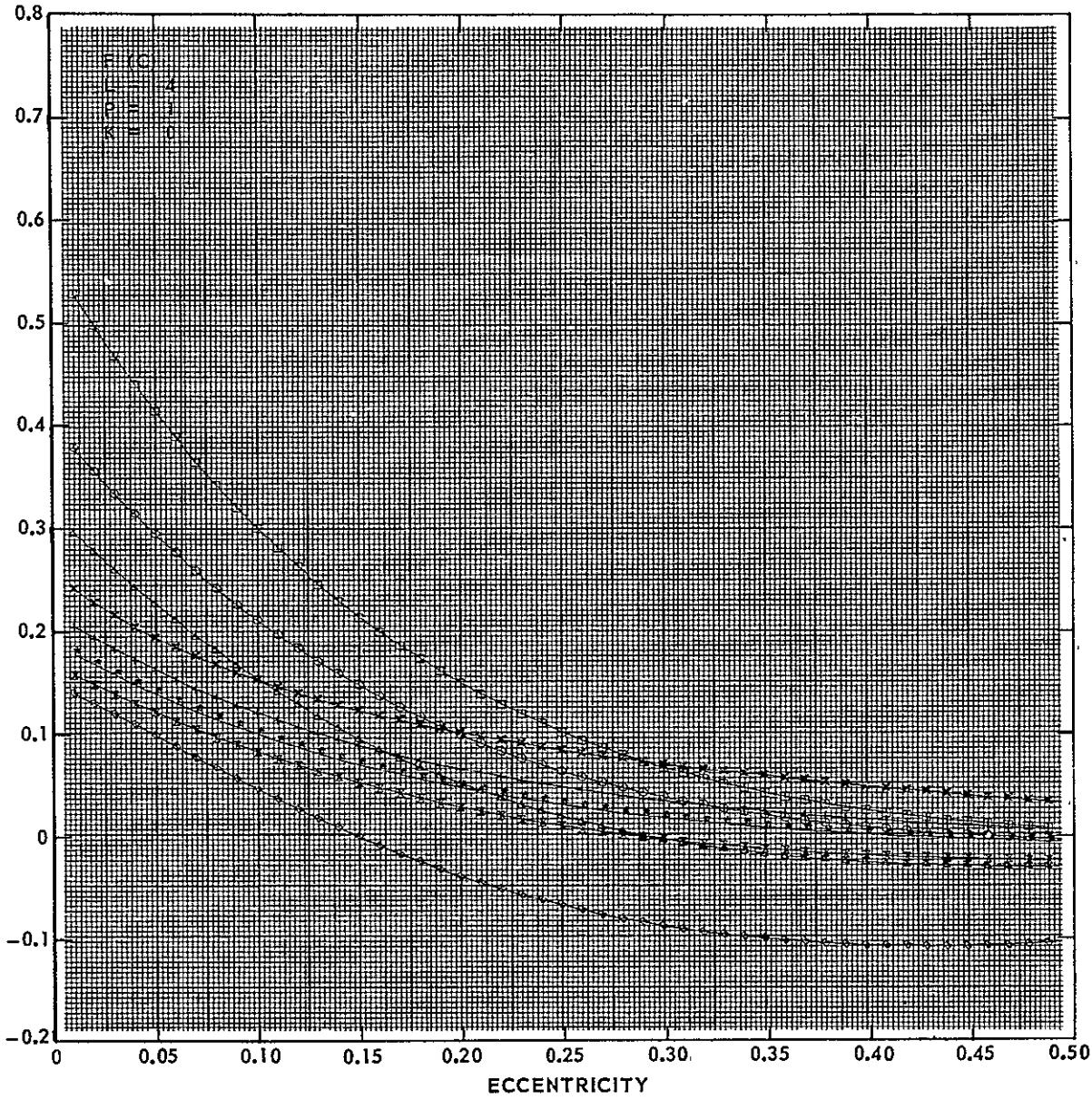
0.8
0.7
0.6
0.5
0.4
0.3
0.2
0.1
0
−0.1
−0.2
0
0.05
0.10
0.15
0.20
0.25
0.30
0.35
0.40
0.45
0.50
ECCENTRICITY

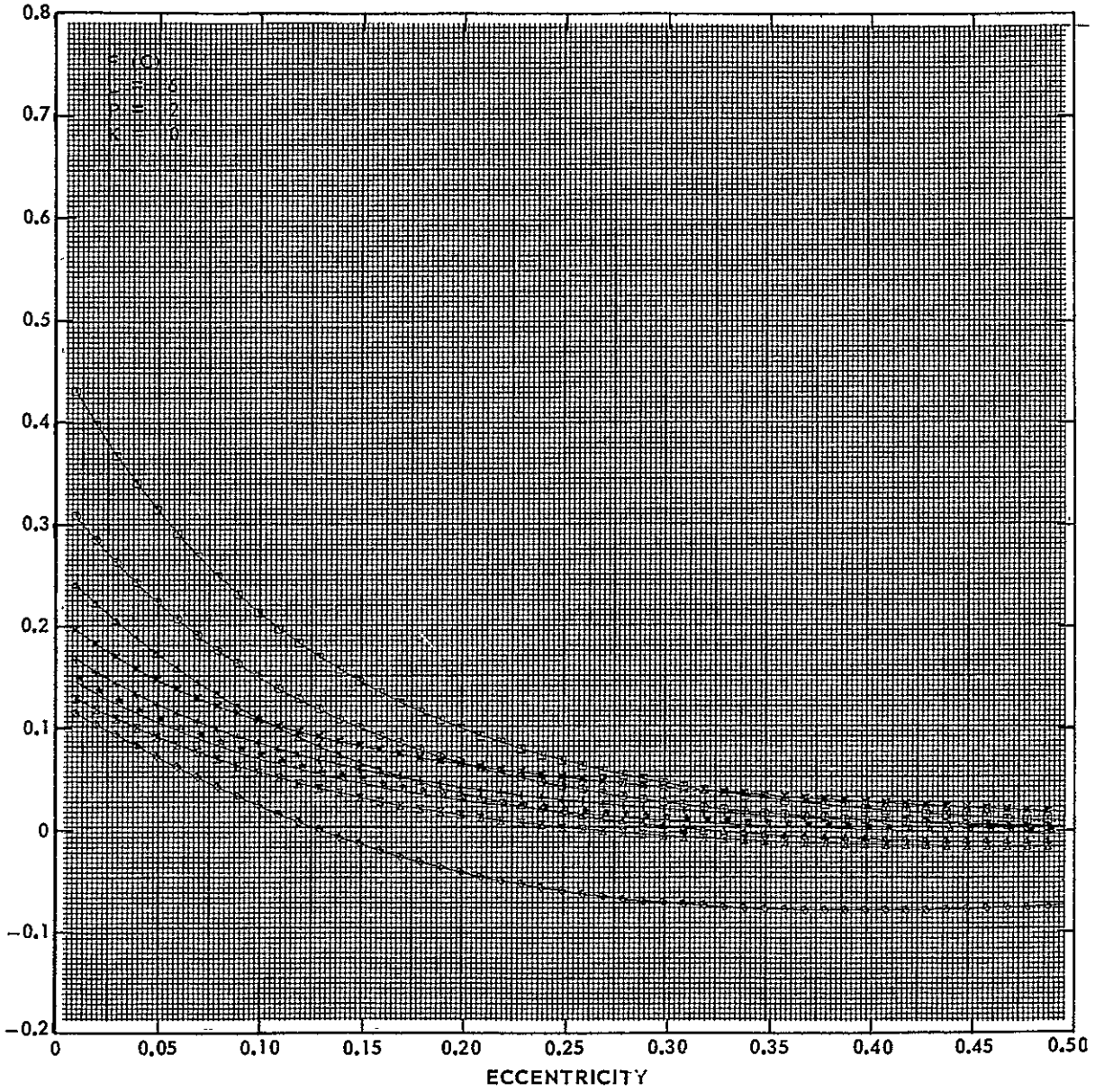
0.8
0.7
0.6
0.5
0.4
0.3
0.2
0.1
0
−0.1
−0.2
0
0.05
0.10
0.15
0.20
0.25
0.30
0.35
0.40
0.45
0.50
ECCENTRICITY

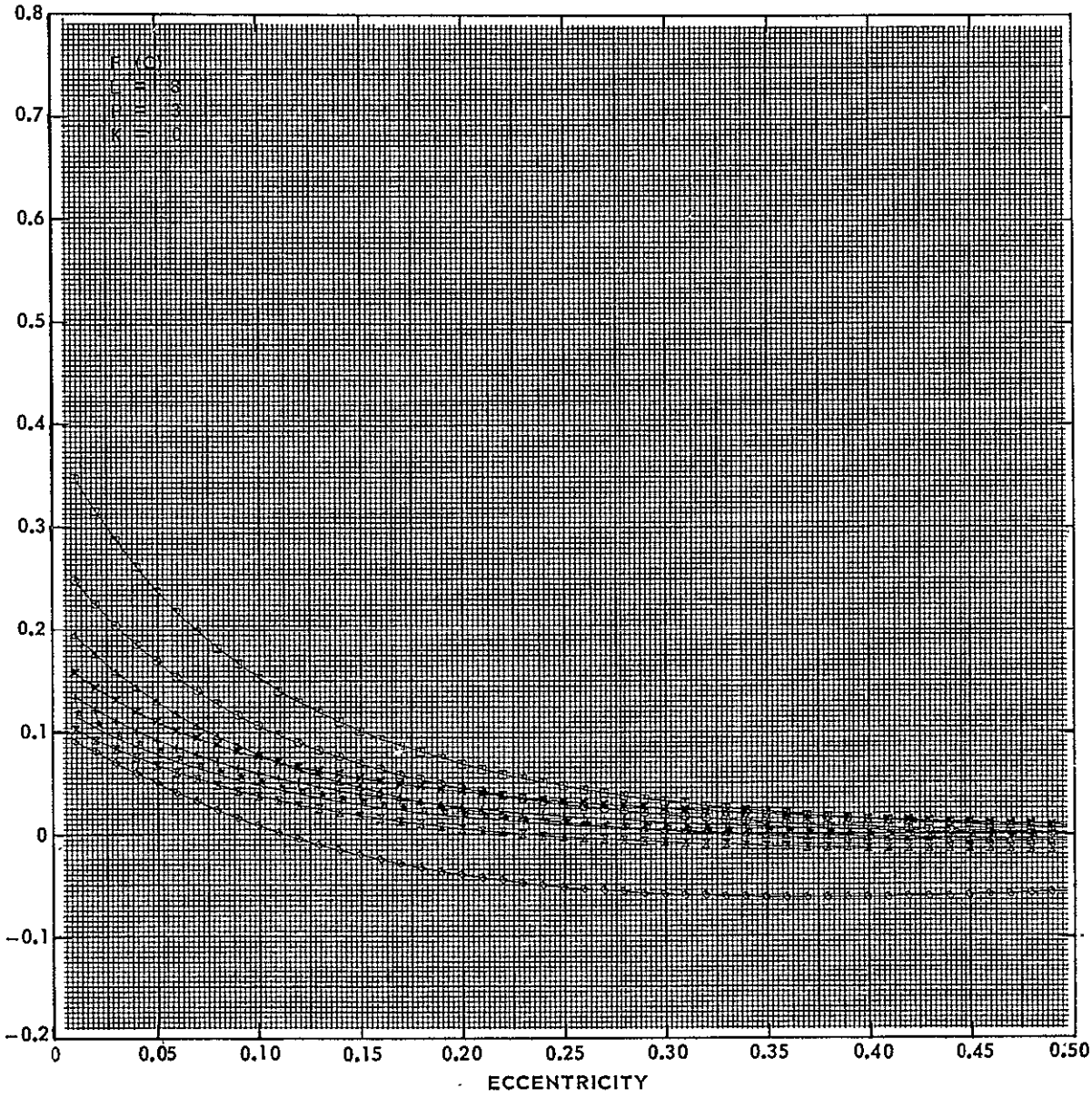
0.8
0.7
0.6
0.5
0.4
0.3
0.2
0.1
0
−0.1
−0.2
0
0.05
0.10
0.15
0.20
0.25
0.30
0.35
0.40
0.45
0.50
ECCENTRICITY

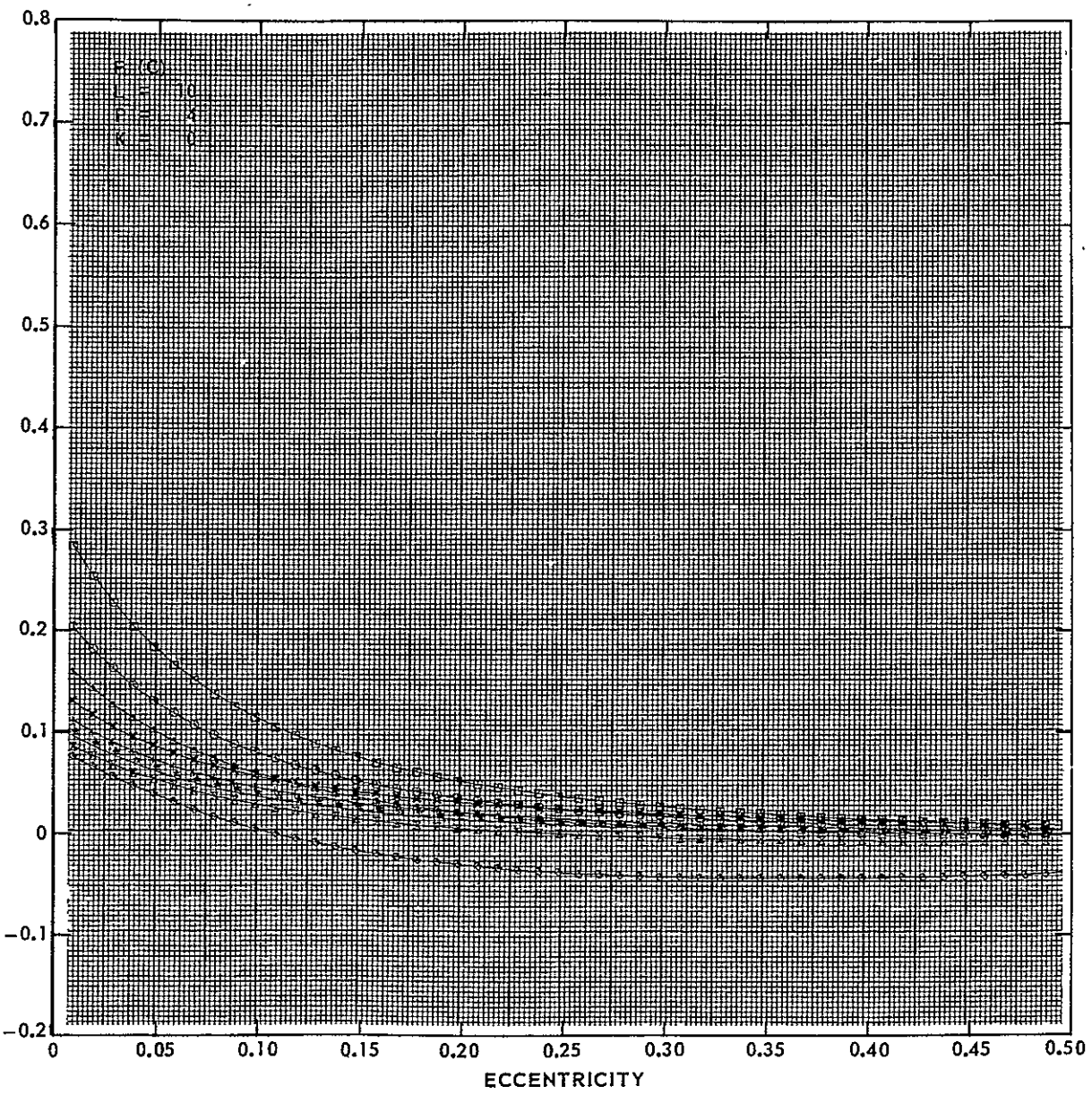
0.8
0.7
0.6
0.5
0.4
0.3
0.2
0.1
0
−0.1
−0.2
0
0.05
0.10
0.15
0.20
0.25
0.30
0.35
0.40
0.45
0.50
ECCENTRICITY

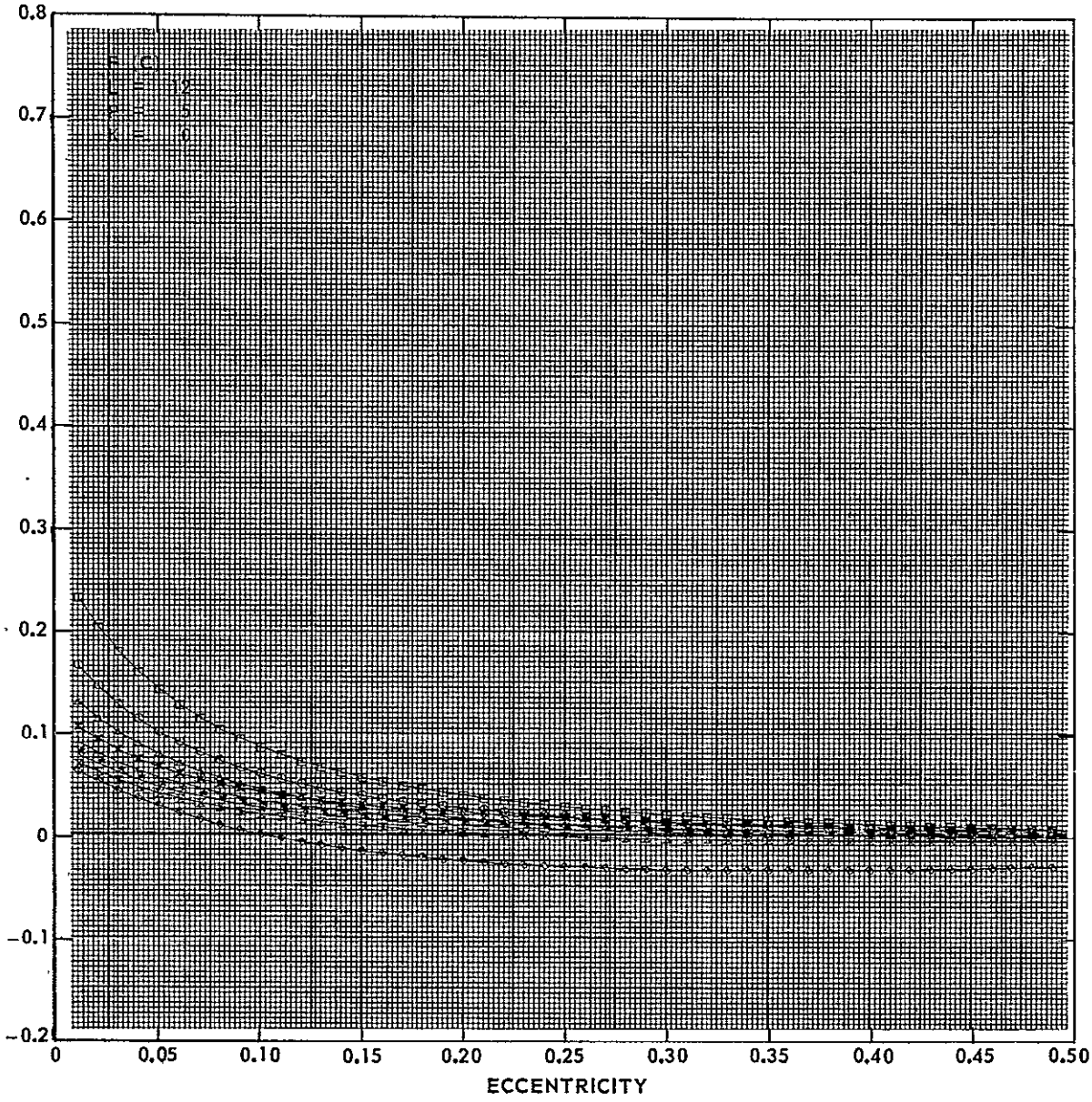
0.8
0.7
0.6
0.5
0.4
0.3
0.2
0.1
0
-0.1
-0.2
0
0.05
0.10
0.15
0.20
0.25
0.30
0.35
0.40
0.45
0.50
ECCENTRICITY

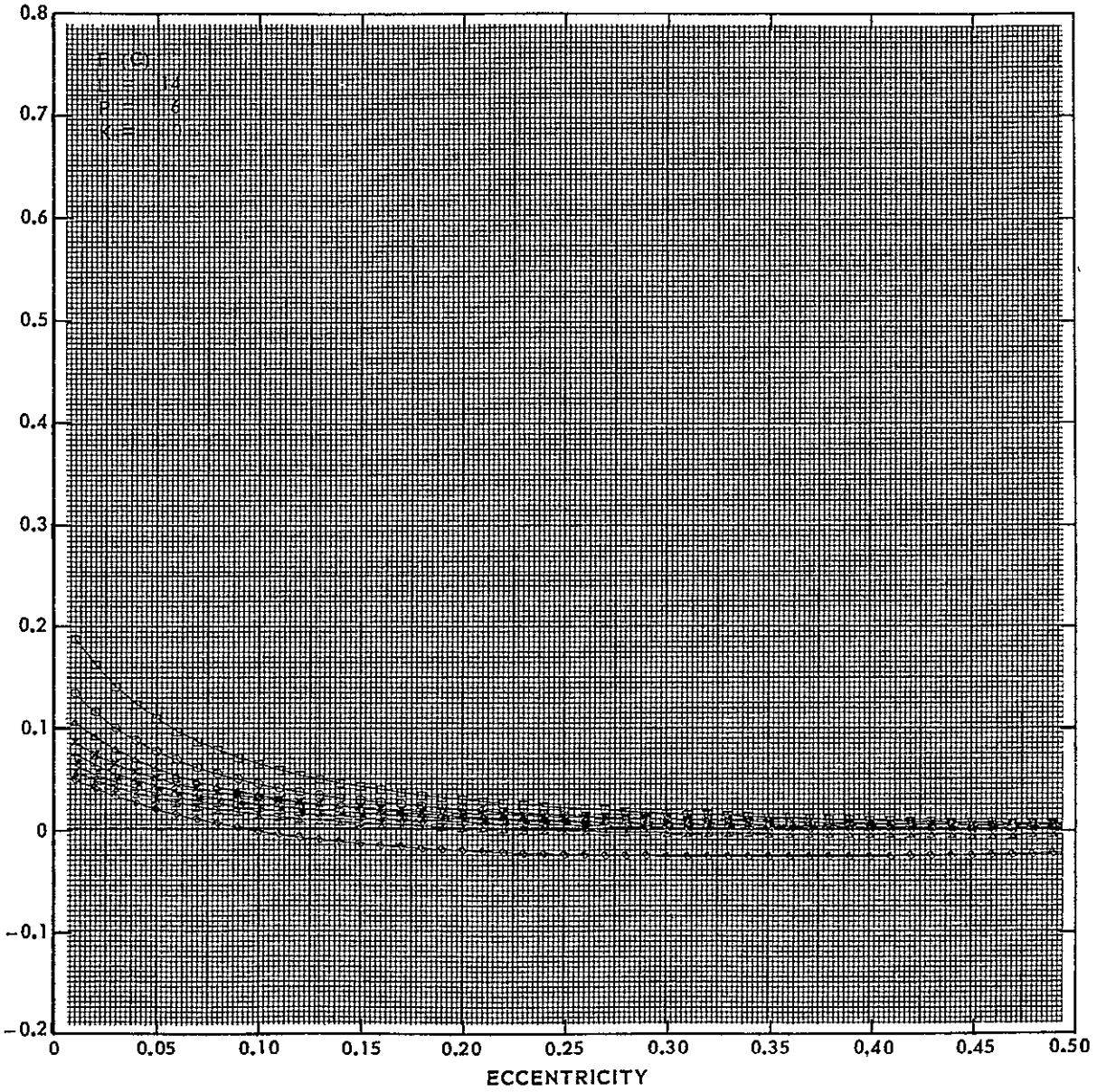
0.8
0.7
0.6
0.5
0.4
0.3
0.2
0.1
0
-0.1
-0.2
0
0.05
0.10
0.15
0.20
0.25
0.30
0.35
0.40
0.45
0.50
ECCENTRICITY

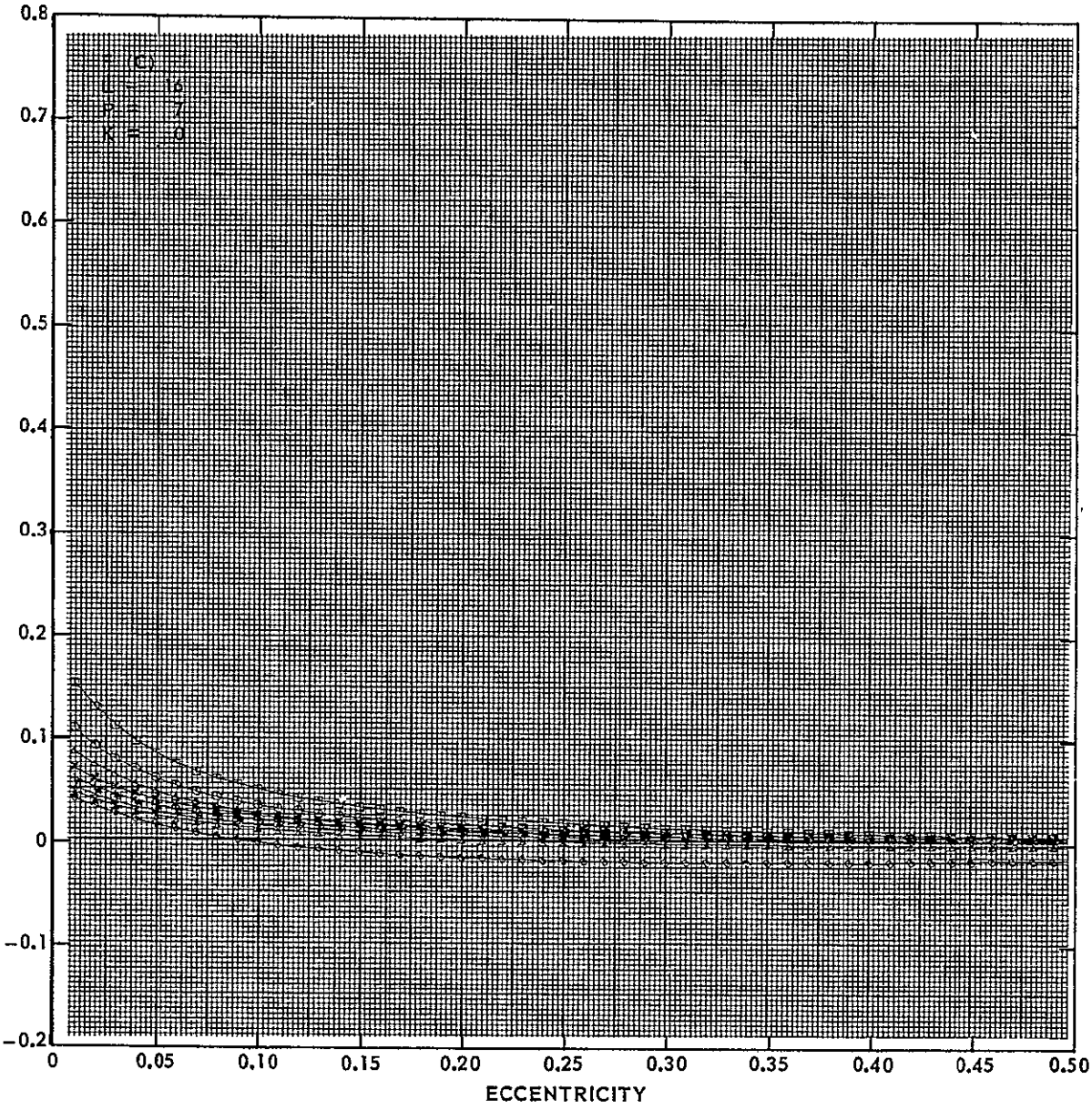
(C)
L = 16
P = 7
K = 0
0.8
0.7
0.6
0.5
0.4
0.3
0.2
0.1
0
-0.1
-0.2
0
0.05
0.10
0.15
0.20
0.25
0.30
0.35
0.40
0.45
0.50
ECCENTRICITY

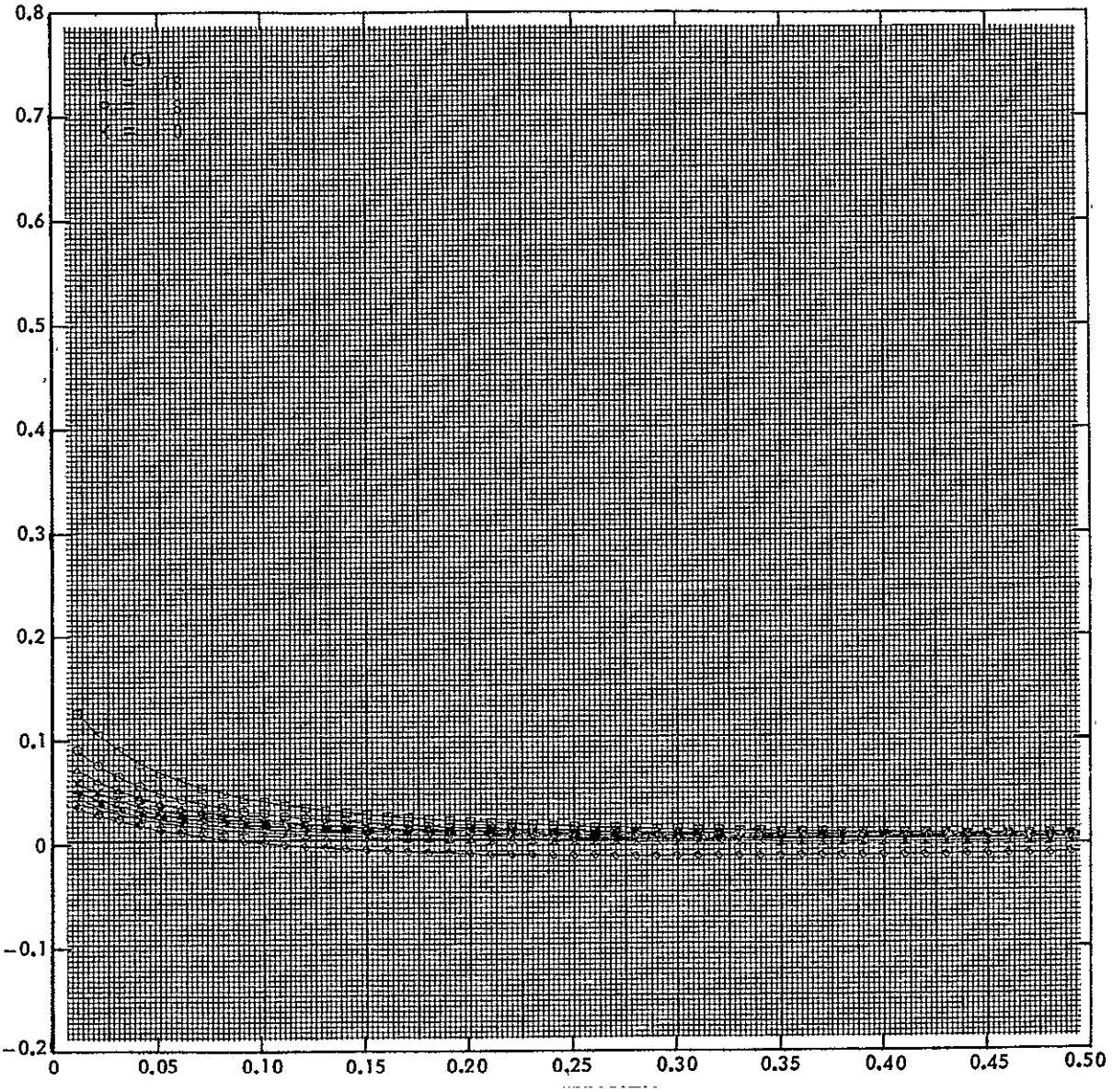
0.8
0.7
0.6
0.5
0.4
0.3
0.2
0.1
0
-0.1
-0.2
0
0.05
0.10
0.15
0.20
0.25
0.30
0.35
0.40
0.45
0.50

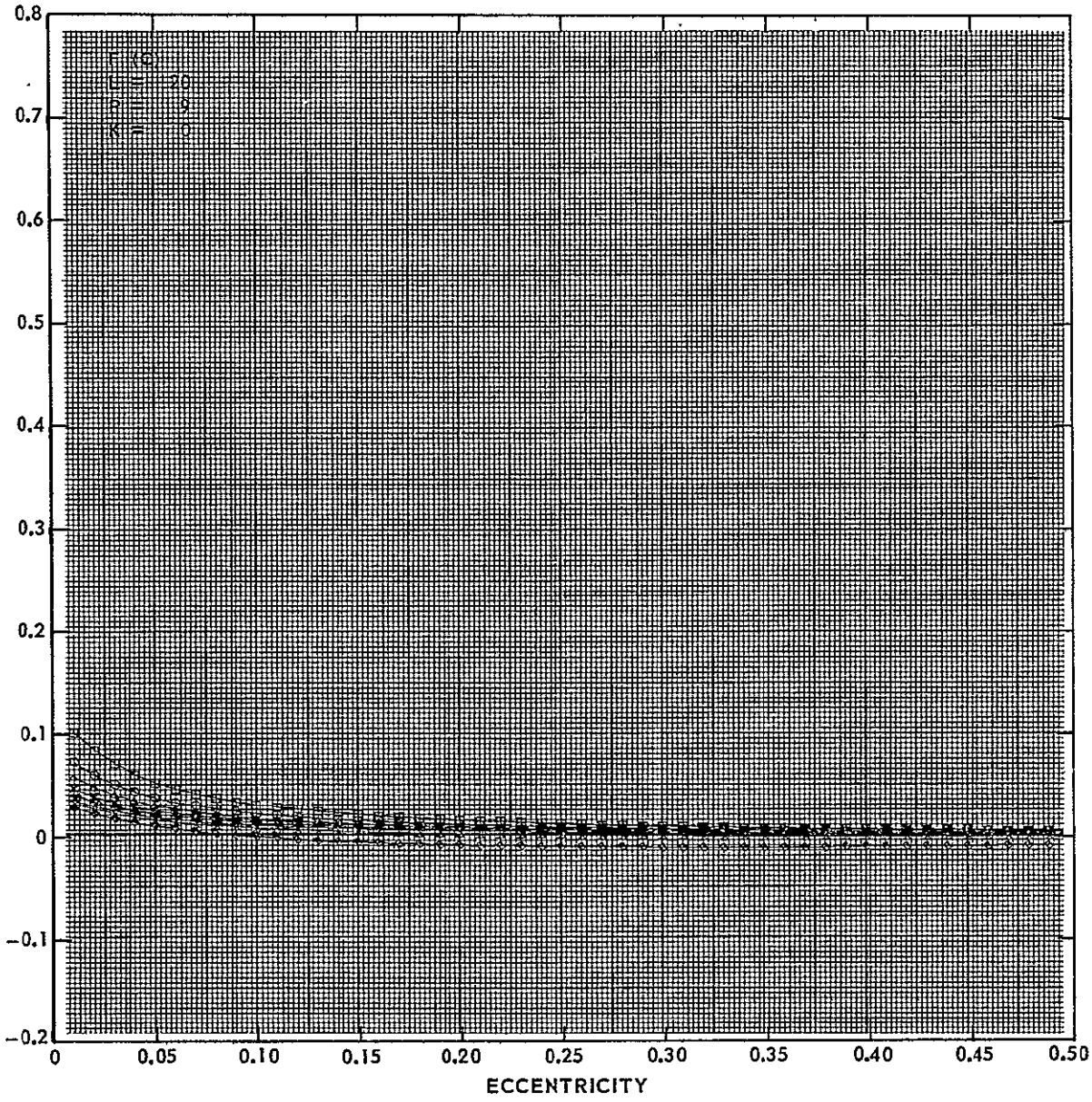
0.8
0.7
0.6
0.5
0.4
0.3
0.2
0.1
0
−0.1
−0.2
0
0.05
0.10
0.15
0.20
0.25
0.30
0.35
0.40
0.45
0.50
ECCENTRICITY

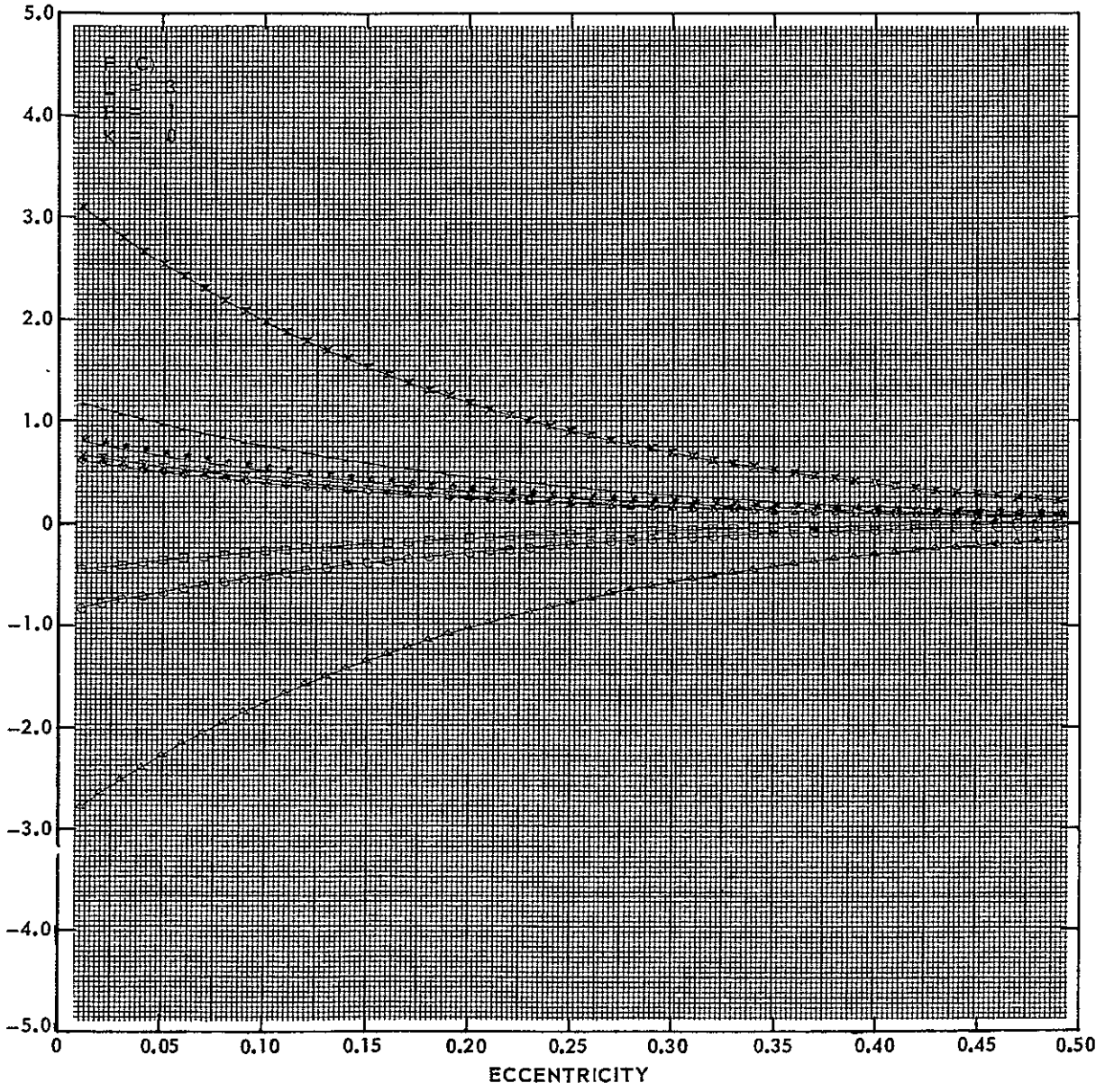
5.0
4.0
3.0
2.0
1.0
0
-1.0
-2.0
-3.0
-4.0
-5.0
0
0.05
0.10
0.15
0.20
0.25
0.30
0.35
0.40
0.45
0.50
ECCENTRICITY

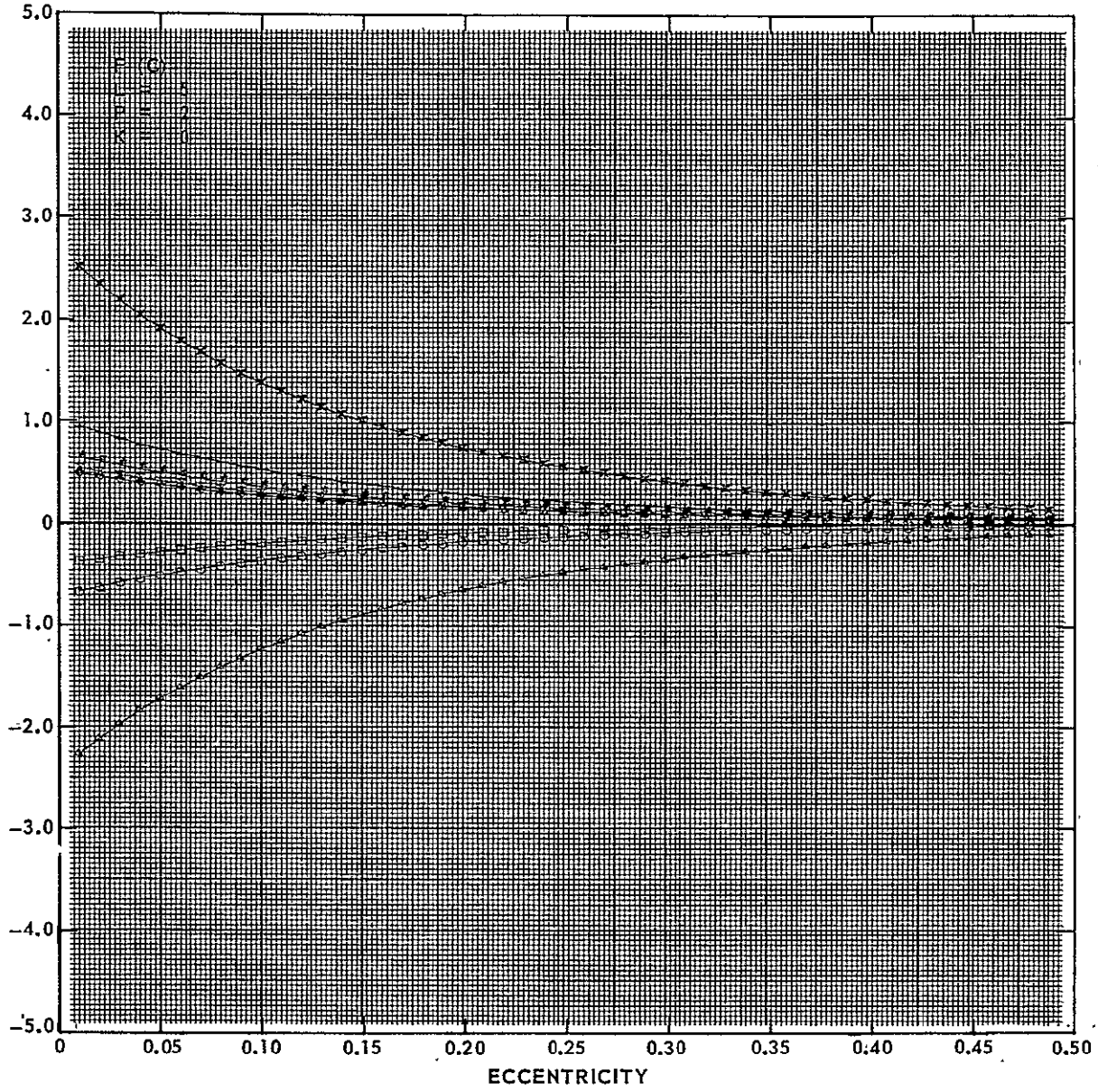
F (C)
L =
P =
K =
5.0
4.0
3.0
2.0
1.0
0
-1.0
-2.0
-3.0
-4.0
-5.0
0
0.05
0.10
0.15
0.20
0.25
0.30
0.35
0.40
0.45
0.50
ECCENTRICITY

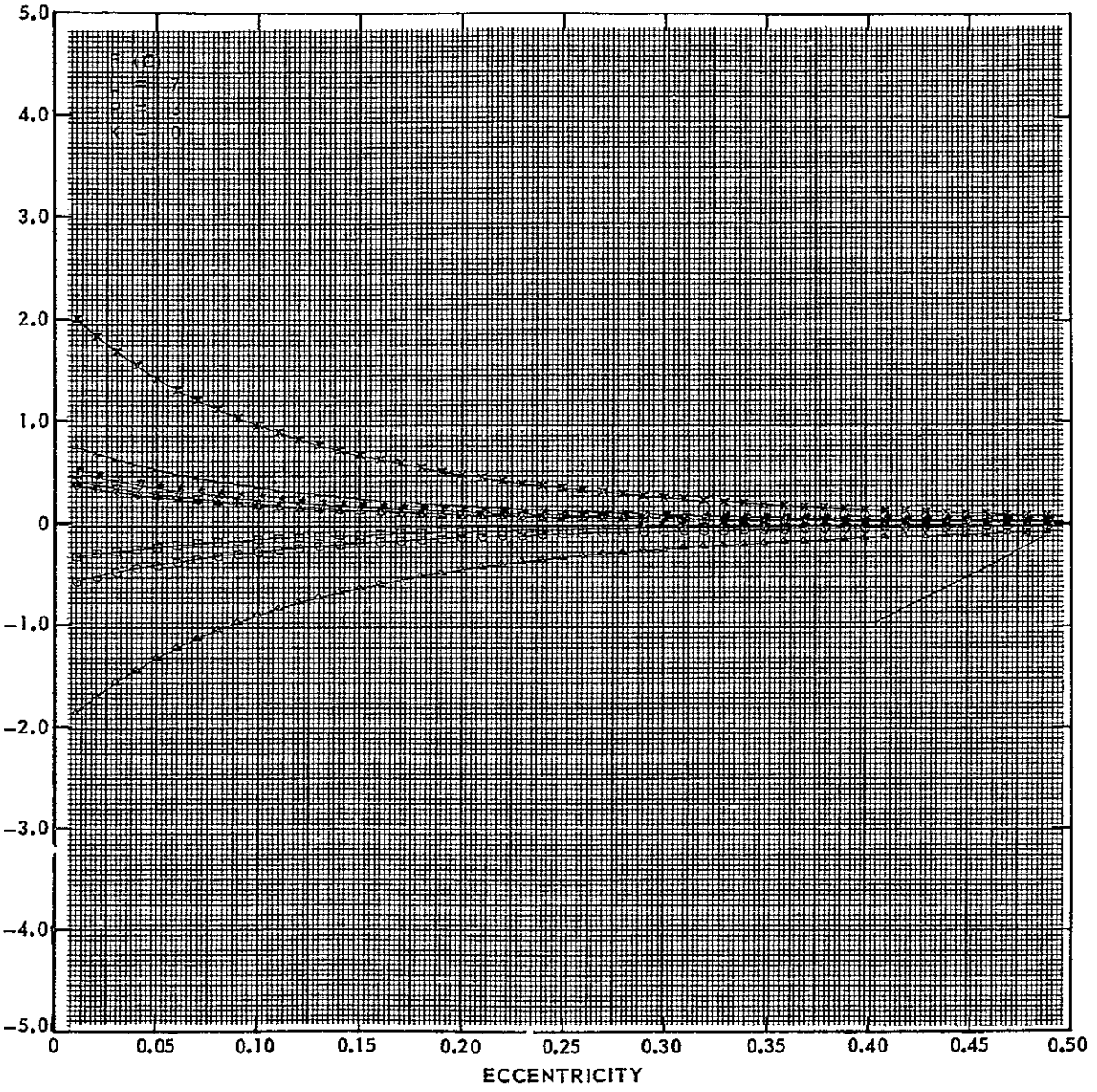
5.0
4.0
3.0
2.0
1.0
0
-1.0
-2.0
-3.0
-4.0
-5.0
0
0.05
0.10
0.15
0.20
0.25
0.30
0.35
0.40
0.45
0.50
ECCENTRICITY

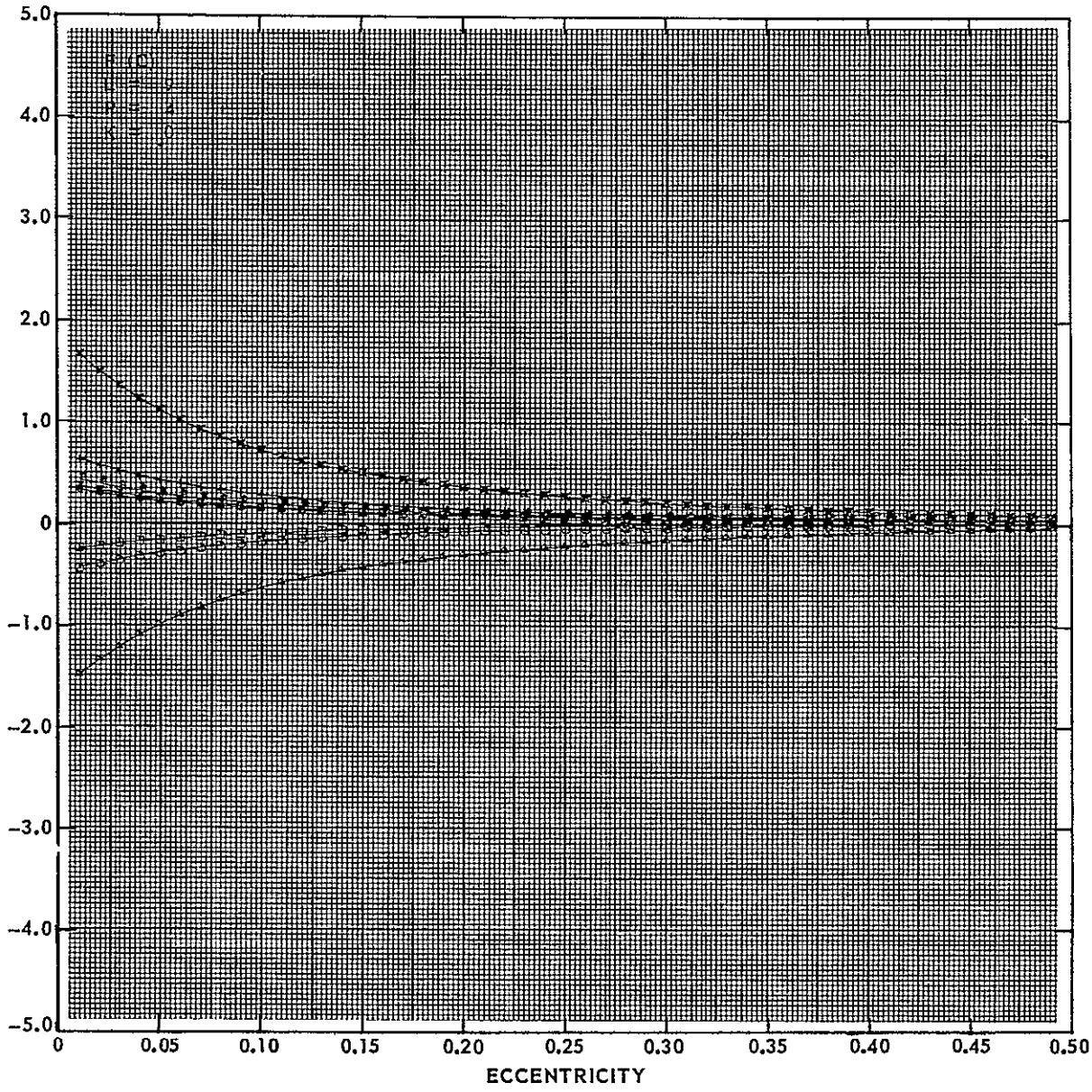
5.0
4.0
3.0
2.0
1.0
0
-1.0
-2.0
-3.0
-4.0
-5.0
0
0.05
0.10
0.15
0.20
0.25
0.30
0.35
0.40
0.45
0.50
ECCENTRICITY

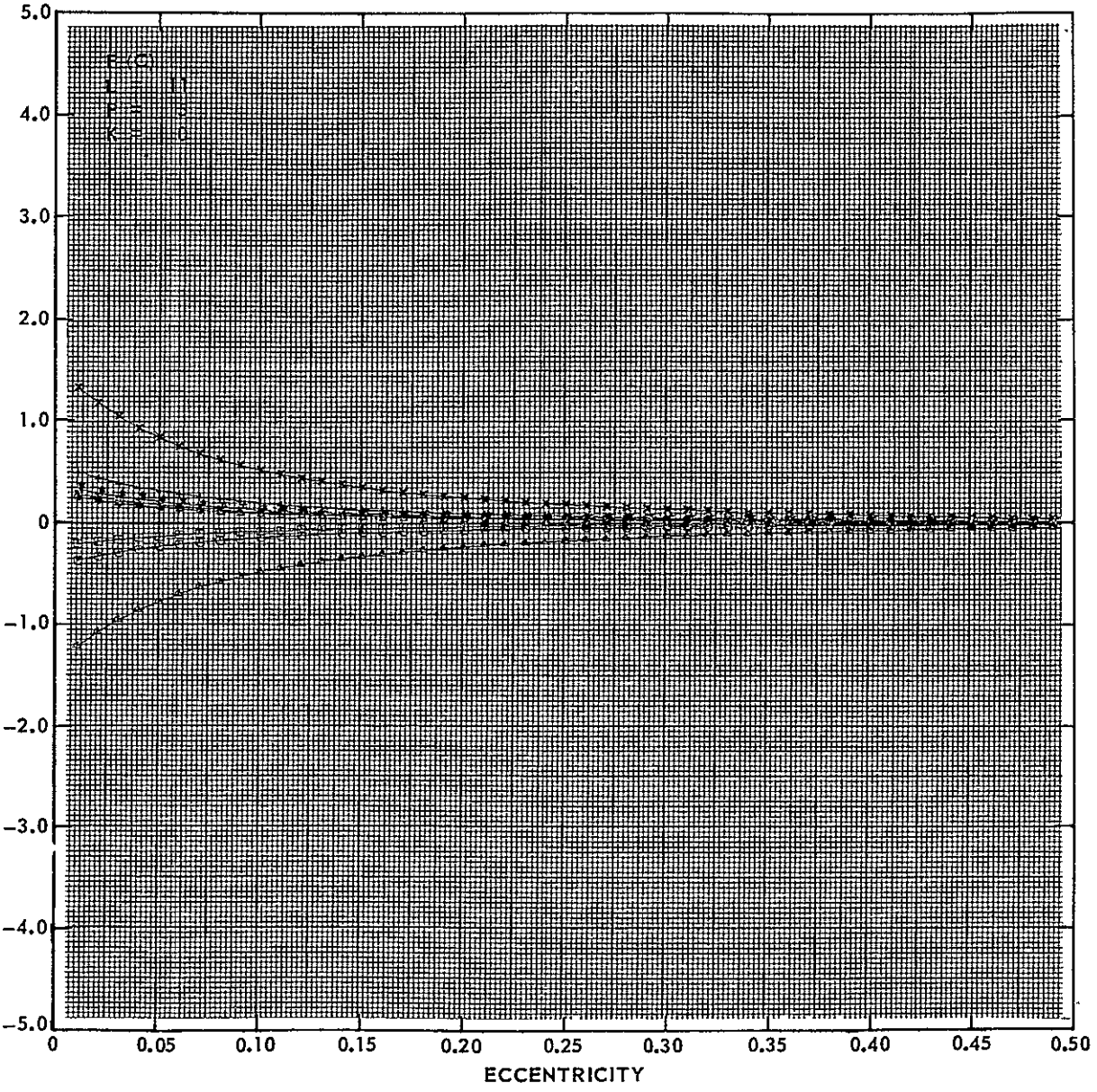
5.0
4.0
3.0
2.0
1.0
0
−1.0
−2.0
−3.0
−4.0
−5.0
0
0.05
0.10
0.15
0.20
0.25
0.30
0.35
0.40
0.45
0.50
ECCENTRICITY

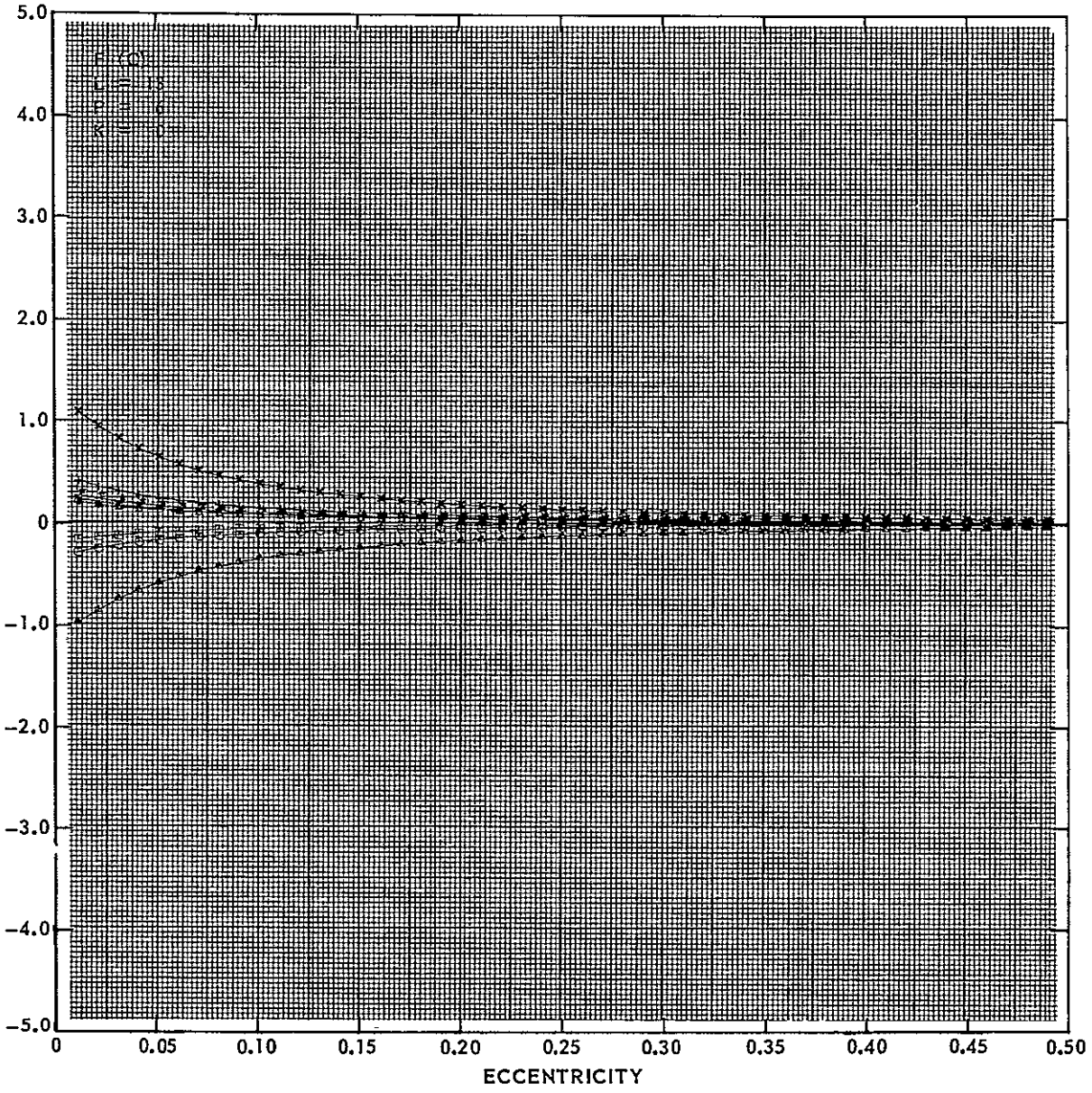
5.0
4.0
3.0
2.0
1.0
0
−1.0
−2.0
−3.0
−4.0
−5.0
0
0.05
0.10
0.15
0.20
0.25
0.30
0.35
0.40
0.45
0.50
ECCENTRICITY

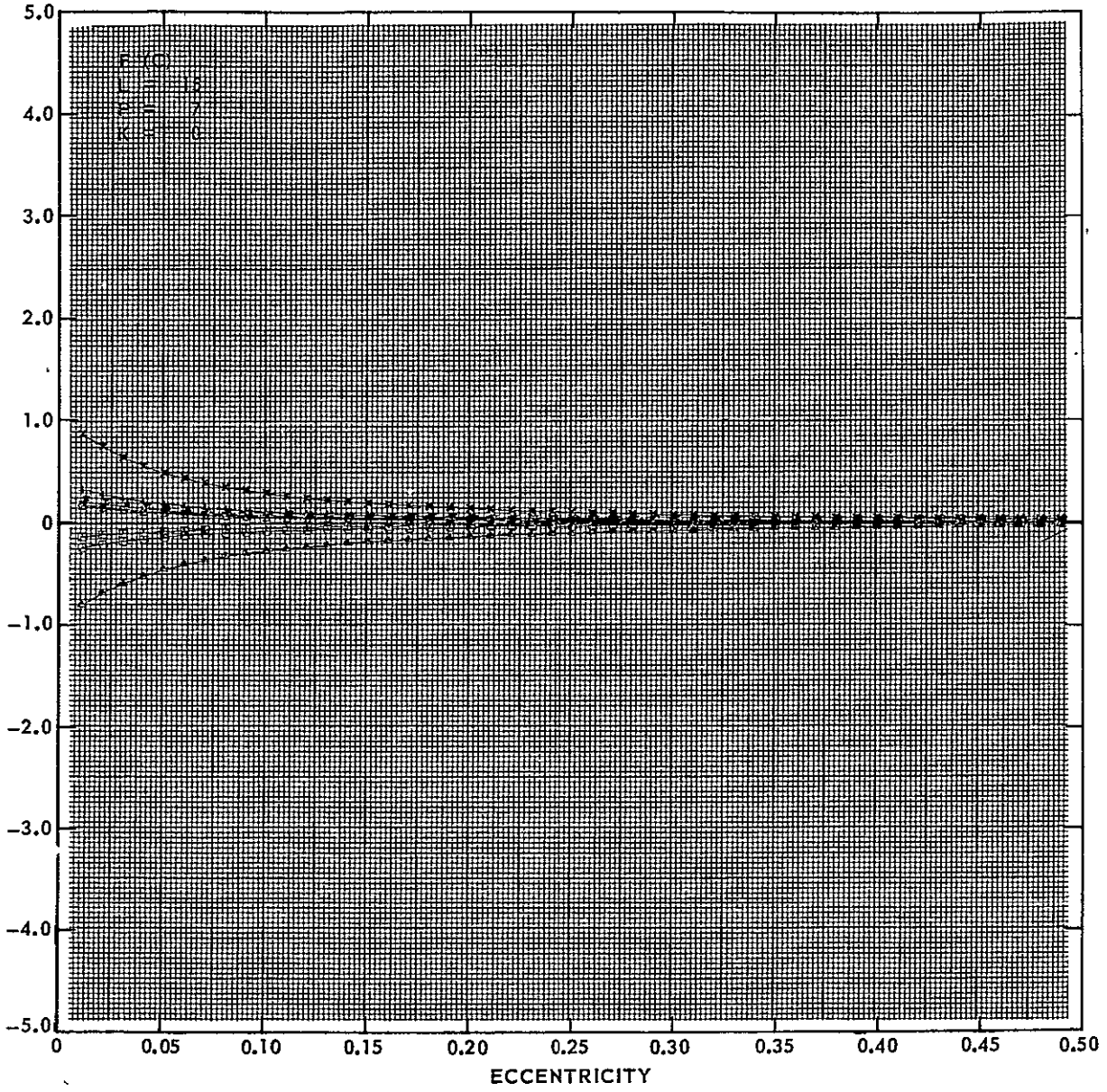
5.0
4.0
3.0
2.0
1.0
0
−1.0
−2.0
−3.0
−4.0
−5.0
0
0.05
0.10
0.15
0.20
0.25
0.30
0.35
0.40
0.45
0.50
ECCENTRICITY

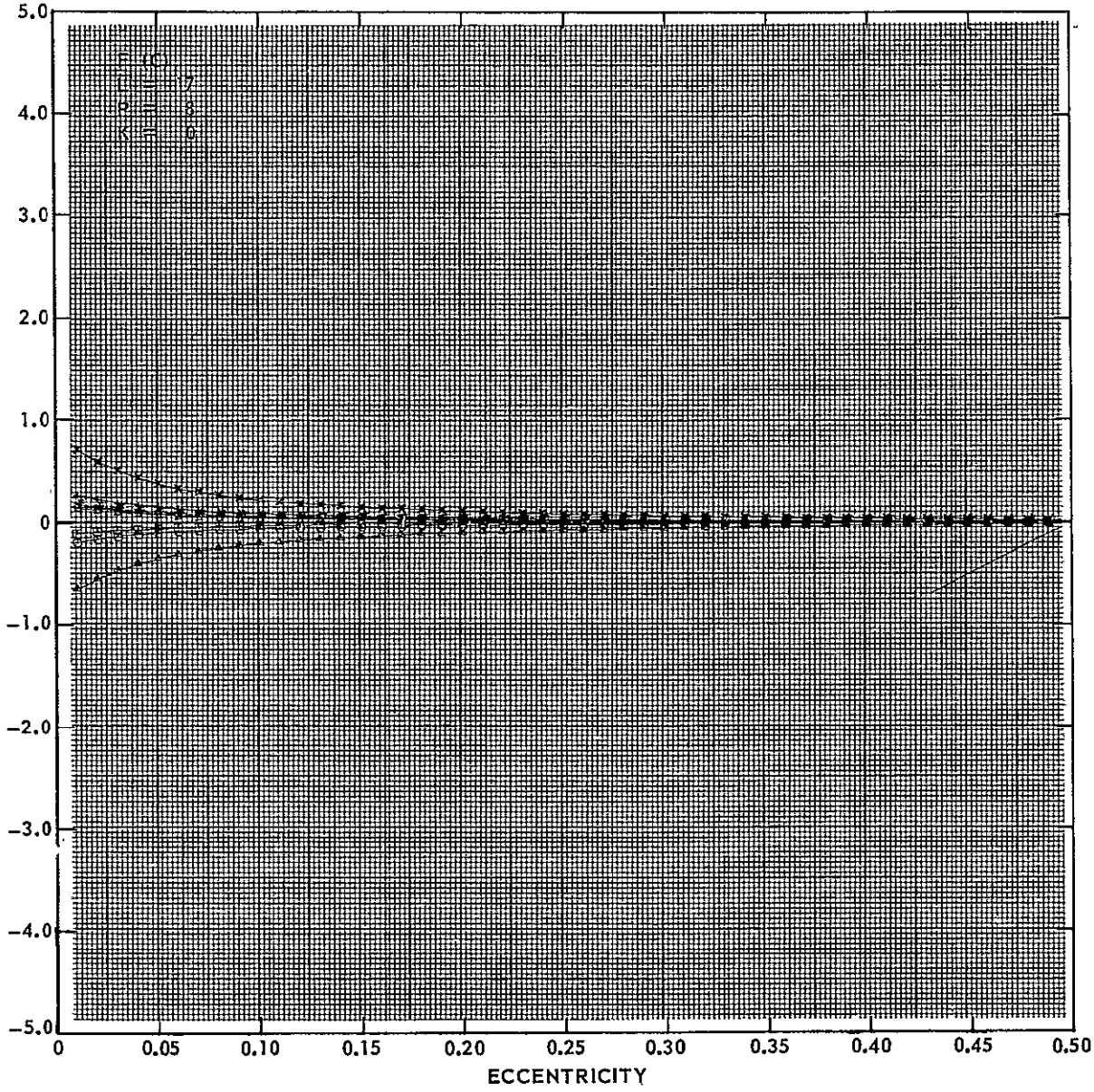
5.0
4.0
3.0
2.0
1.0
0
−1.0
−2.0
−3.0
−4.0
−5.0
0
0.05
0.10
0.15
0.20
0.25
0.30
0.35
0.40
0.45
0.50
ECCENTRICITY

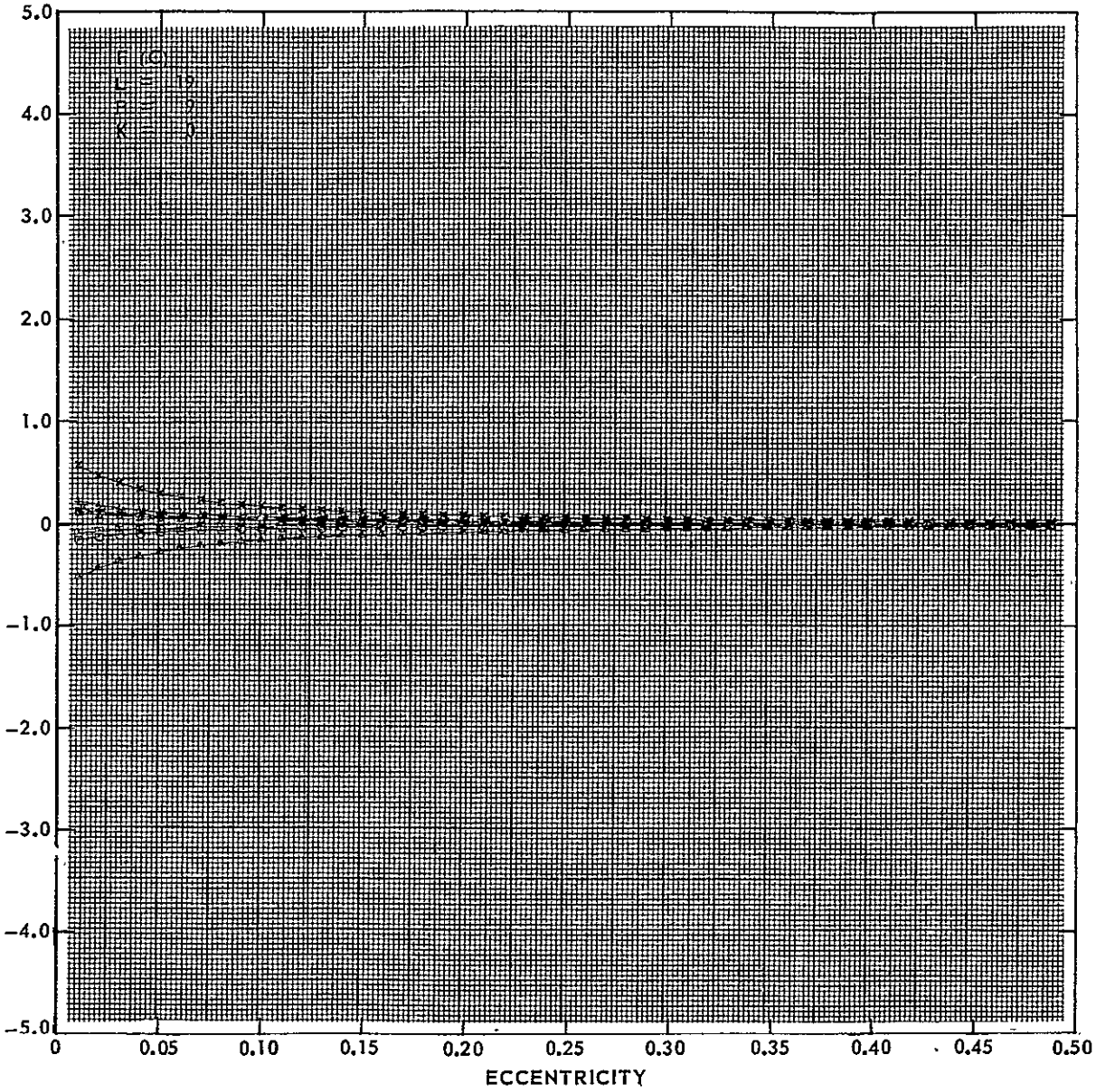
5.0
4.0
3.0
2.0
1.0
0
−1.0
−2.0
−3.0
−4.0
−5.0
0
0.05
0.10
0.15
0.20
0.25
0.30
0.35
0.40
0.45
0.50
ECCENTRICITY

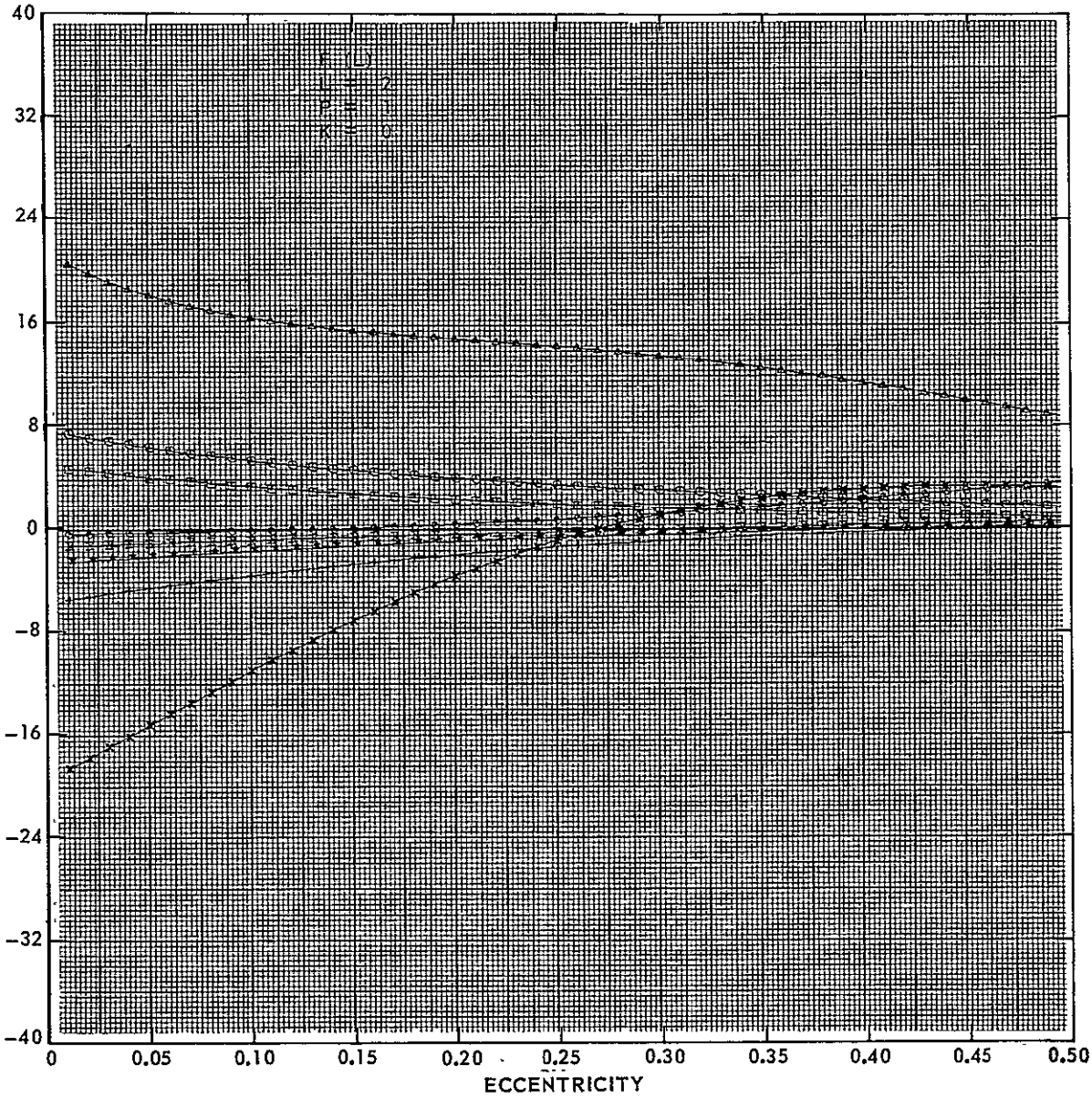
40
32
24
16
8
0
−8
−16
−24
−32
−40
0
0.05
0.10
0.15
0.20
0.25
0.30
0.35
0.40
0.45
0.50
ECCENTRICITY

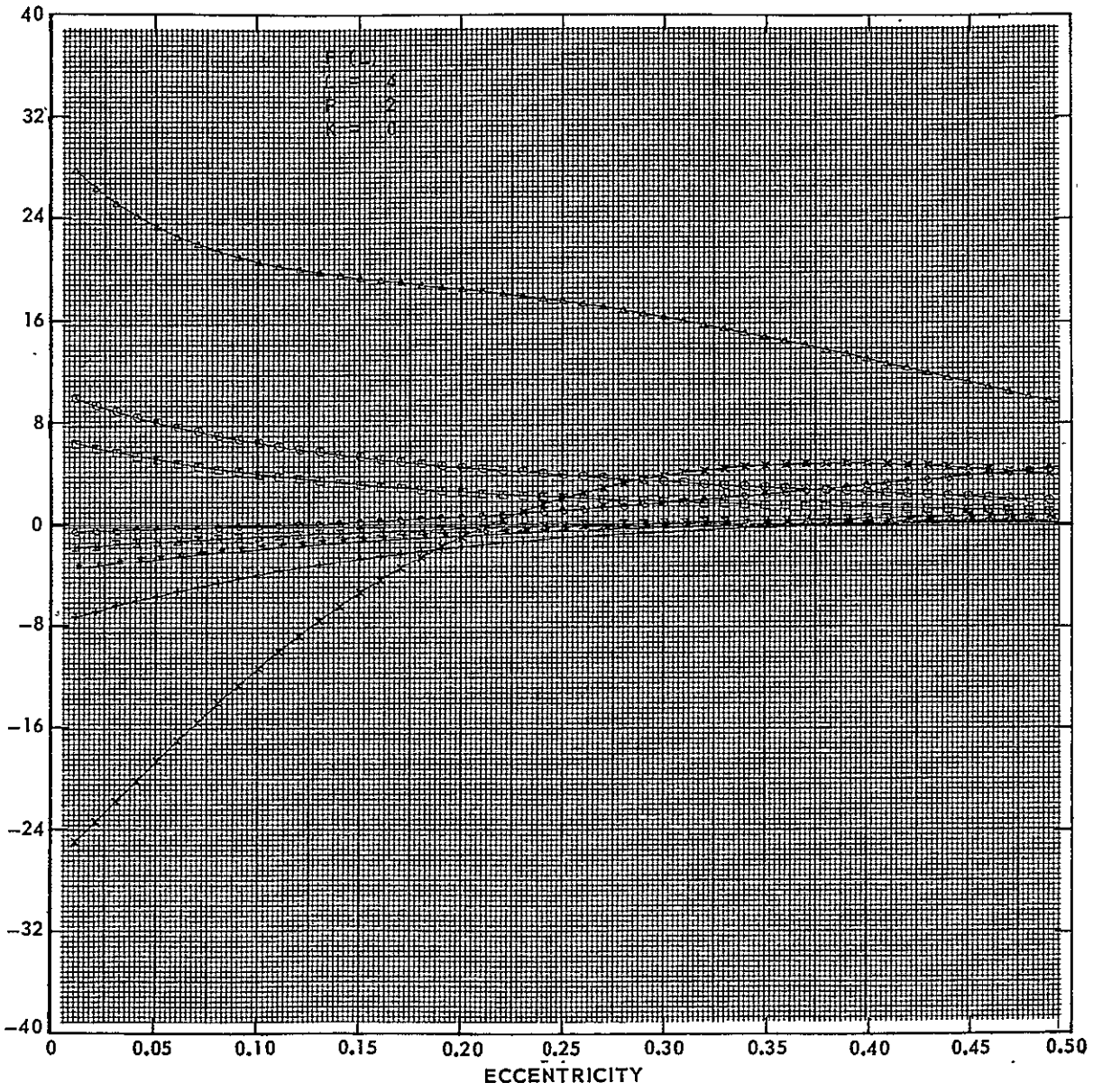
40
32
24
16
8
0
−8
−16
−24
−32
−40
0
0.05
0.10
0.15
0.20
0.25
0.30
0.35
0.40
0.45
0.50
ECCENTRICITY

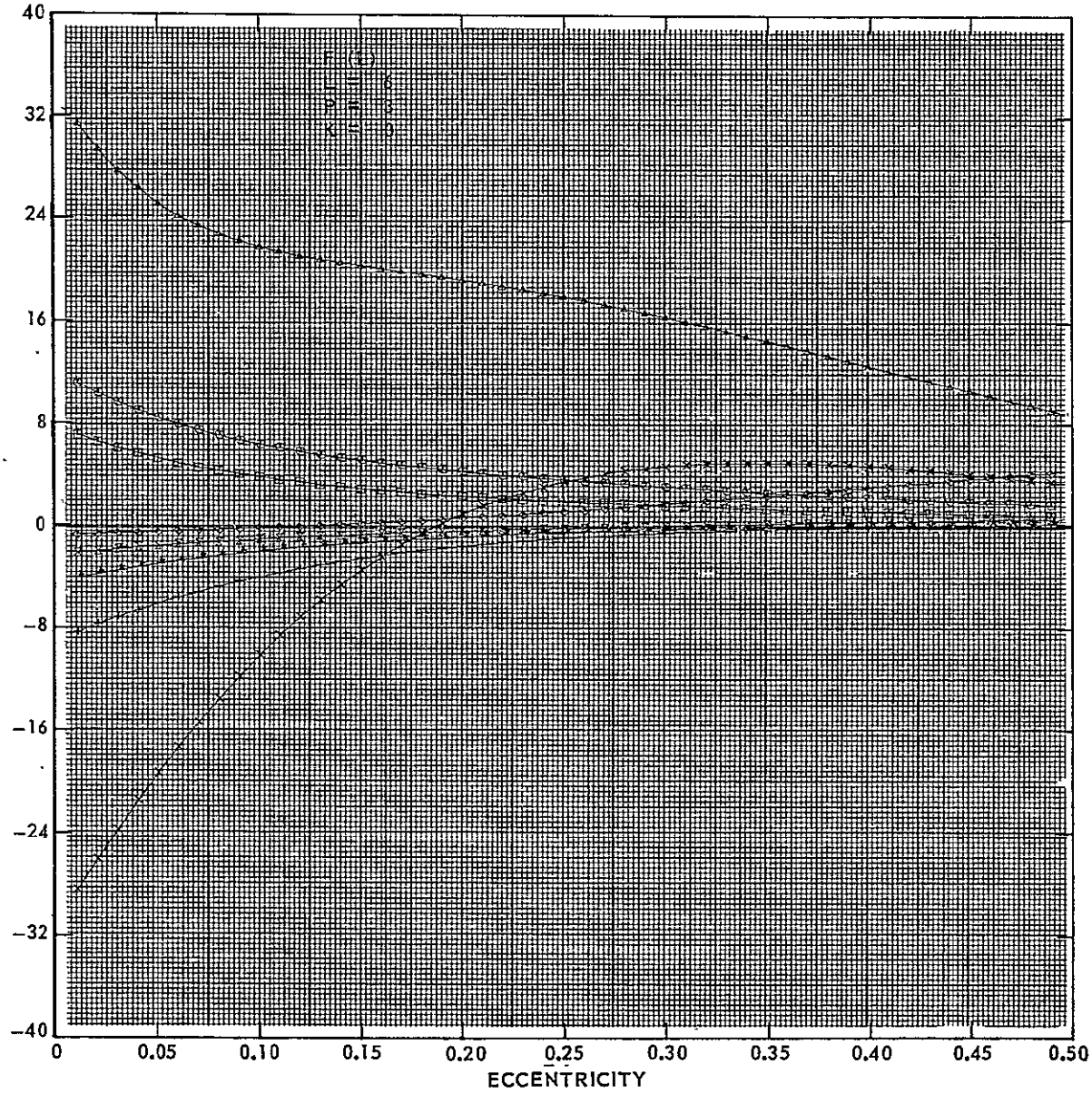
40
32
24
16
8
0
−8
−16
−24
−32
−40
0
0.05
0.10
0.15
0.20
0.25
0.30
0.35
0.40
0.45
0.50
ECCENTRICITY

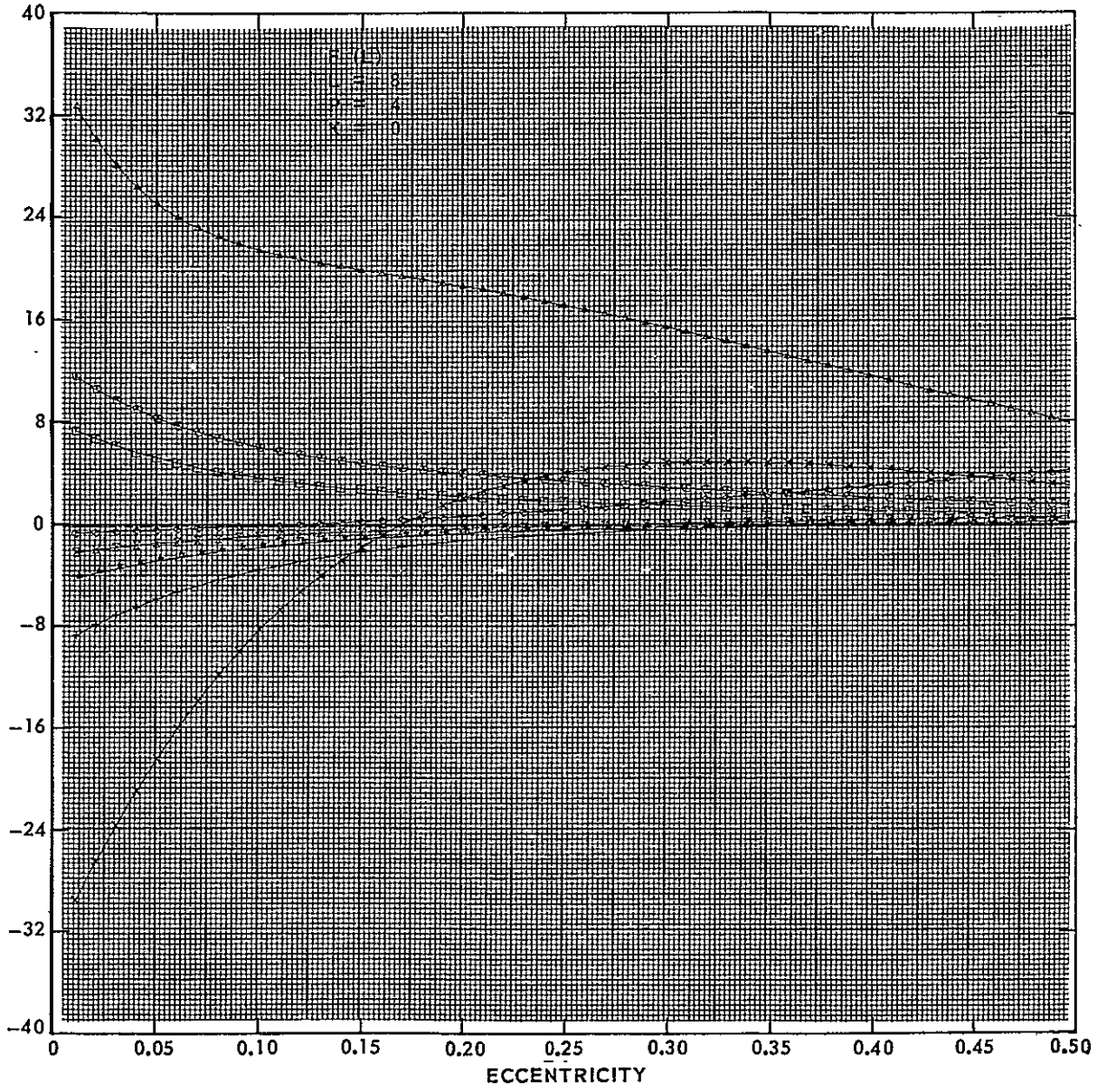
40
32
24
16
8
0
−8
−16
−24
−32
−40
0
0.05
0.10
0.15
0.20
0.25
0.30
0.35
0.40
0.45
0.50
ECCENTRICITY

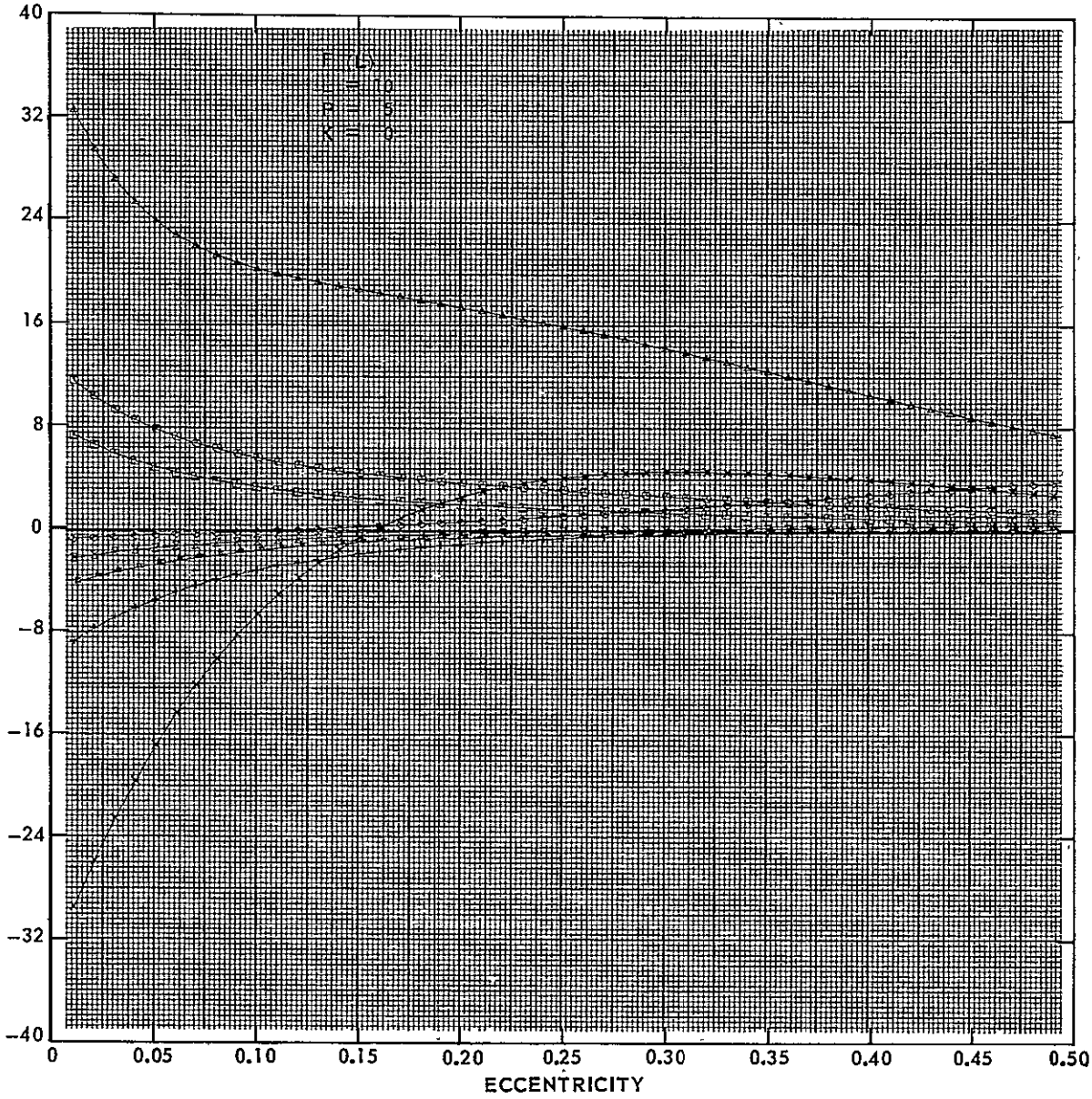
40
32
24
16
8
0
−8
−16
−24
−32
−40
0
0.05
0.10
0.15
0.20
0.25
0.30
0.35
0.40
0.45
0.50
ECCENTRICITY
T (D)
= 0
P = 5
K = 0

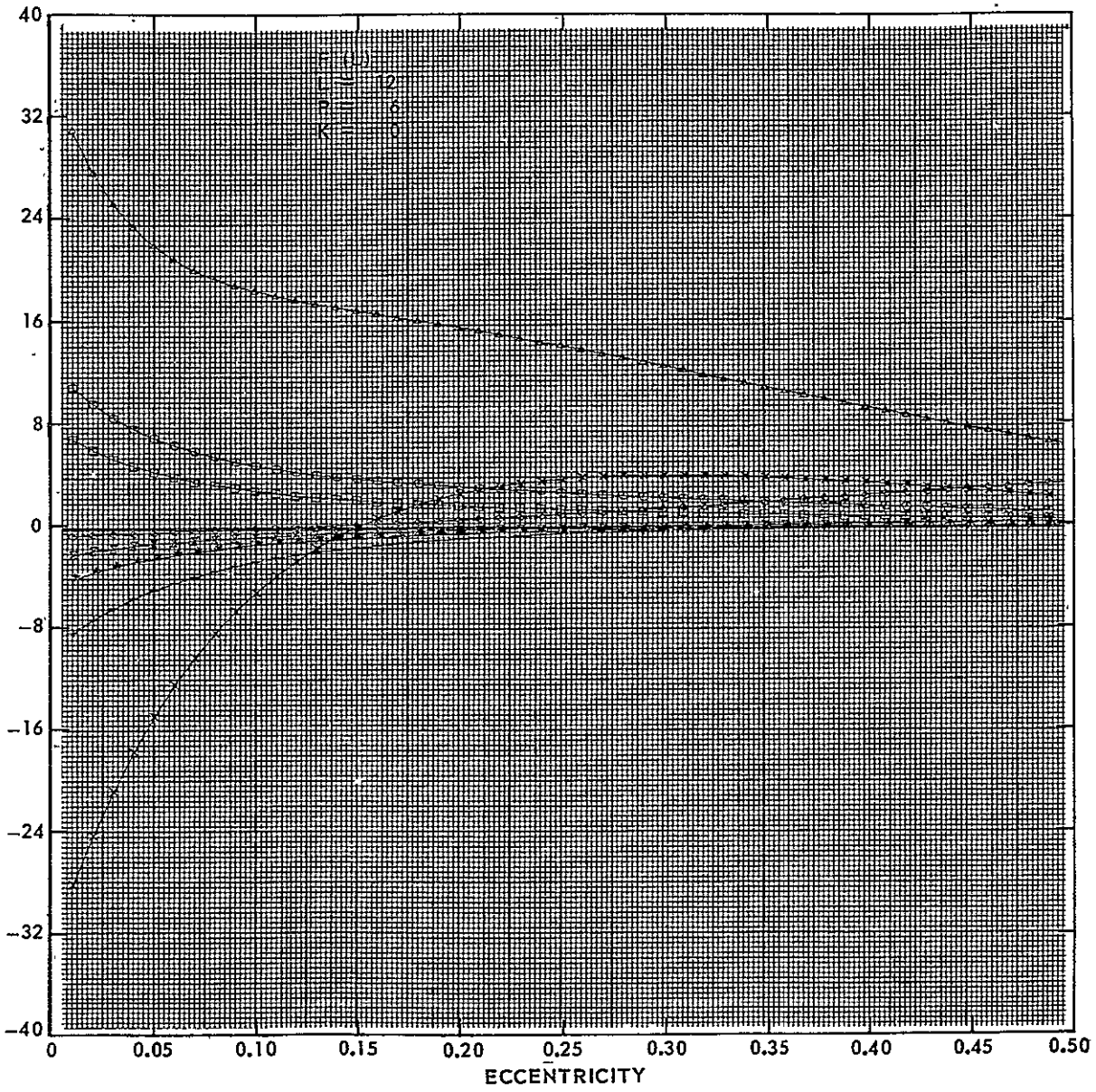
40
32
24
16
8
0
-8
-16
-24
-32
-40
0
0.05
0.10
0.15
0.20
0.25
0.30
0.35
0.40
0.45
0.50
ECCENTRICITY

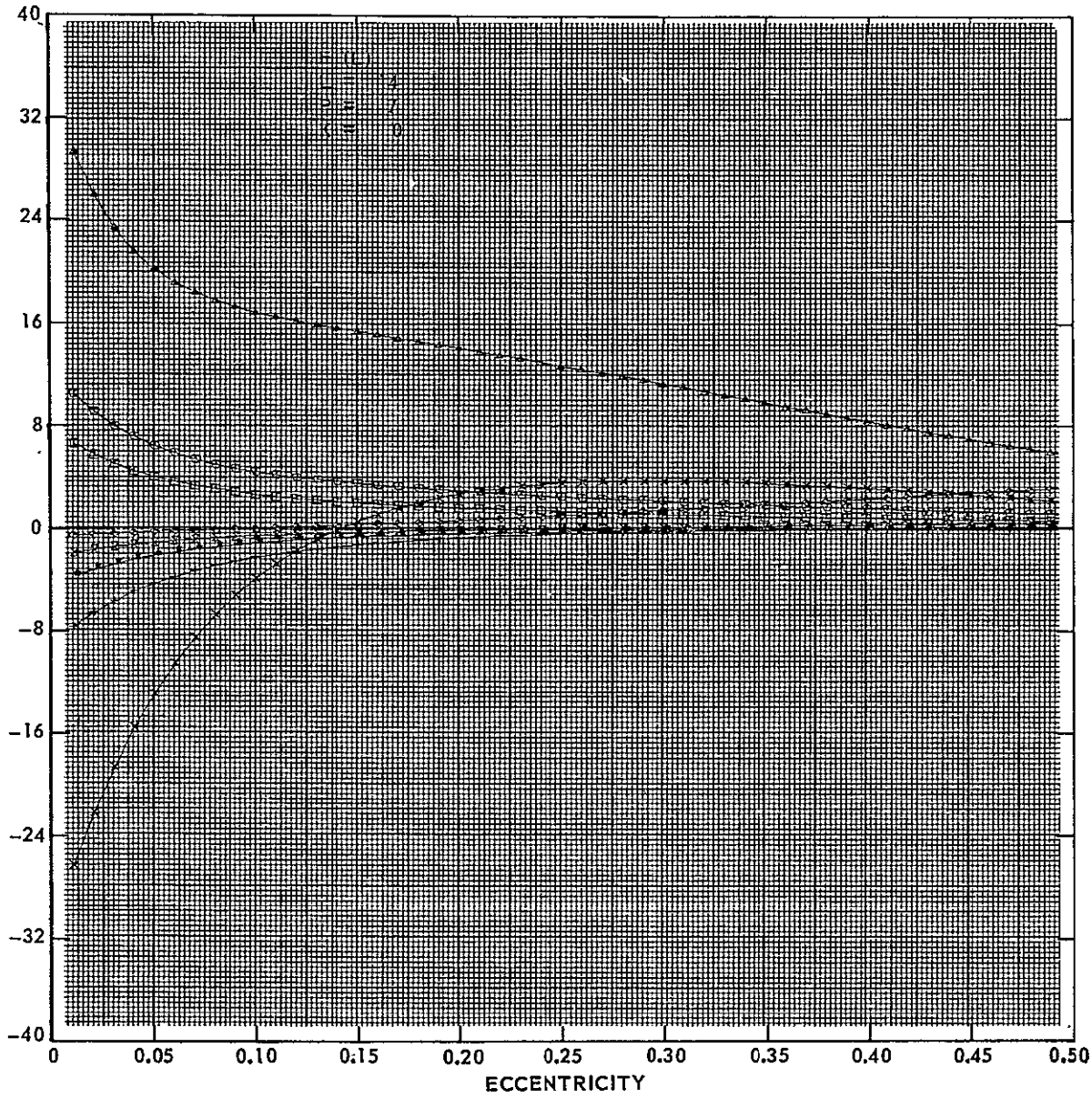
40
32
24
16
8
0
-8
-16
-24
-32
-40
0
0.05
0.10
0.15
0.20
0.25
0.30
0.35
0.40
0.45
0.50
ECCENTRICITY

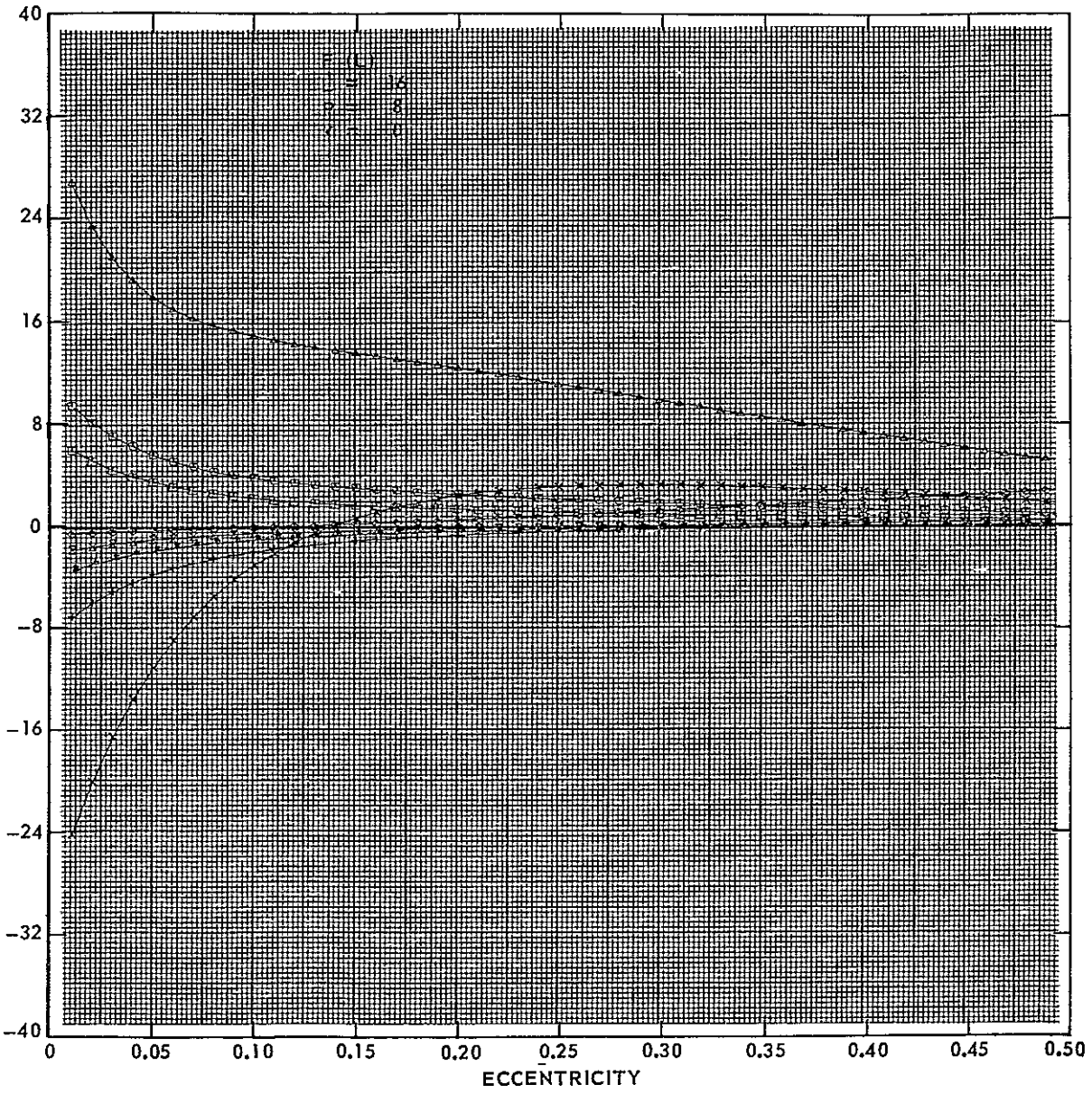
40
32
24
16
8
0
-8
-16
-24
-32
-40
0
0.05
0.10
0.15
0.20
0.25
0.30
0.35
0.40
0.45
0.50
ECCENTRICITY

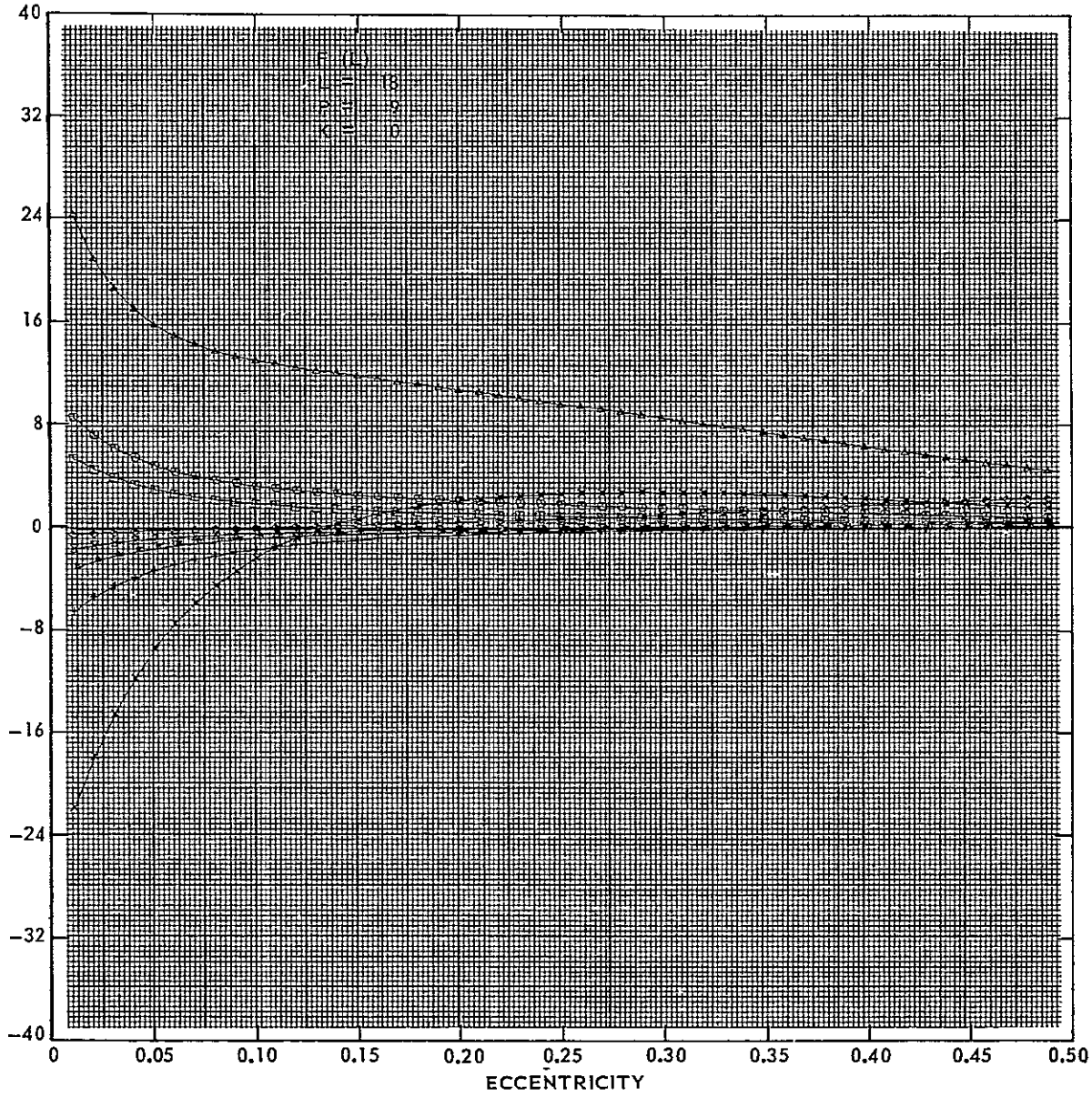
40
32
24
16
8
0
−8
−16
−24
−32
−40
0
0.05
0.10
0.15
0.20
0.25
0.30
0.35
0.40
0.45
0.50
ECCENTRICITY

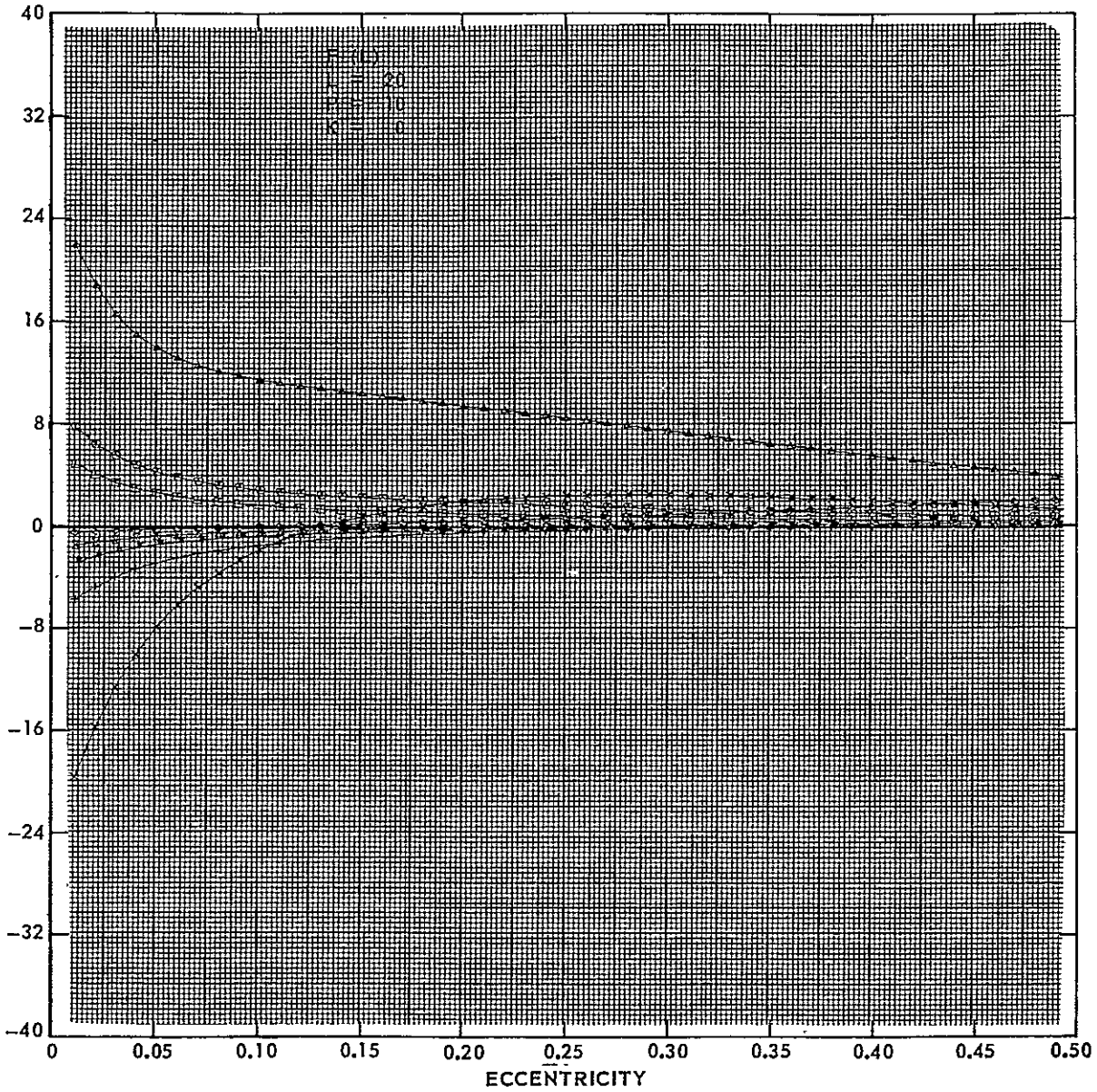
40
32
24
16
8
0
-8
-16
-24
-32
-40
0
0.05
0.10
0.15
0.20
0.25
0.30
0.35
0.40
0.45
0.50
ECCENTRICITY

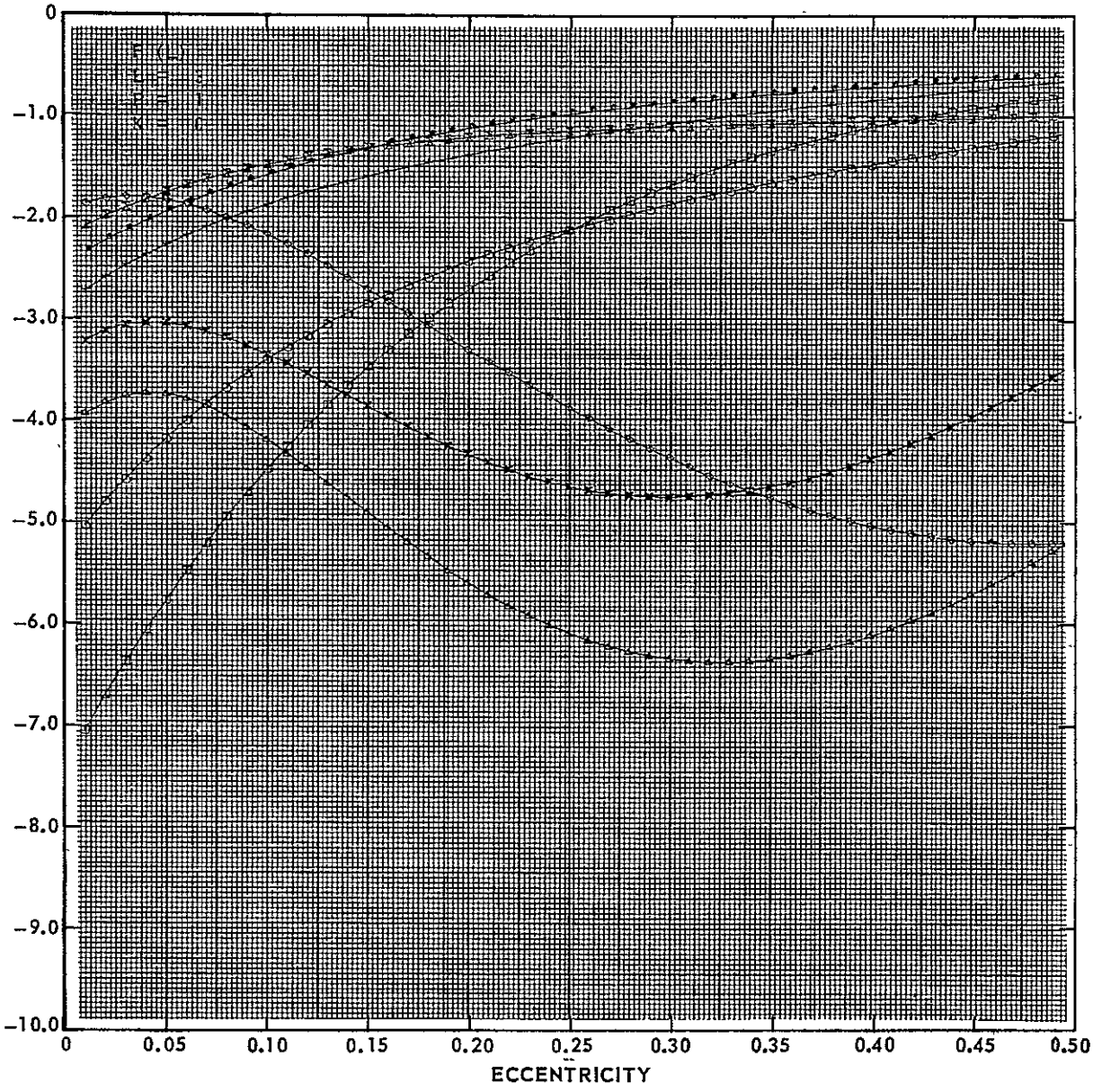
0
-1.0
-2.0
-3.0
-4.0
-5.0
-6.0
-7.0
-8.0
-9.0
-10.0
0
0.05
0.10
0.15
0.20
0.25
0.30
0.35
0.40
0.45
0.50
ECCENTRICITY

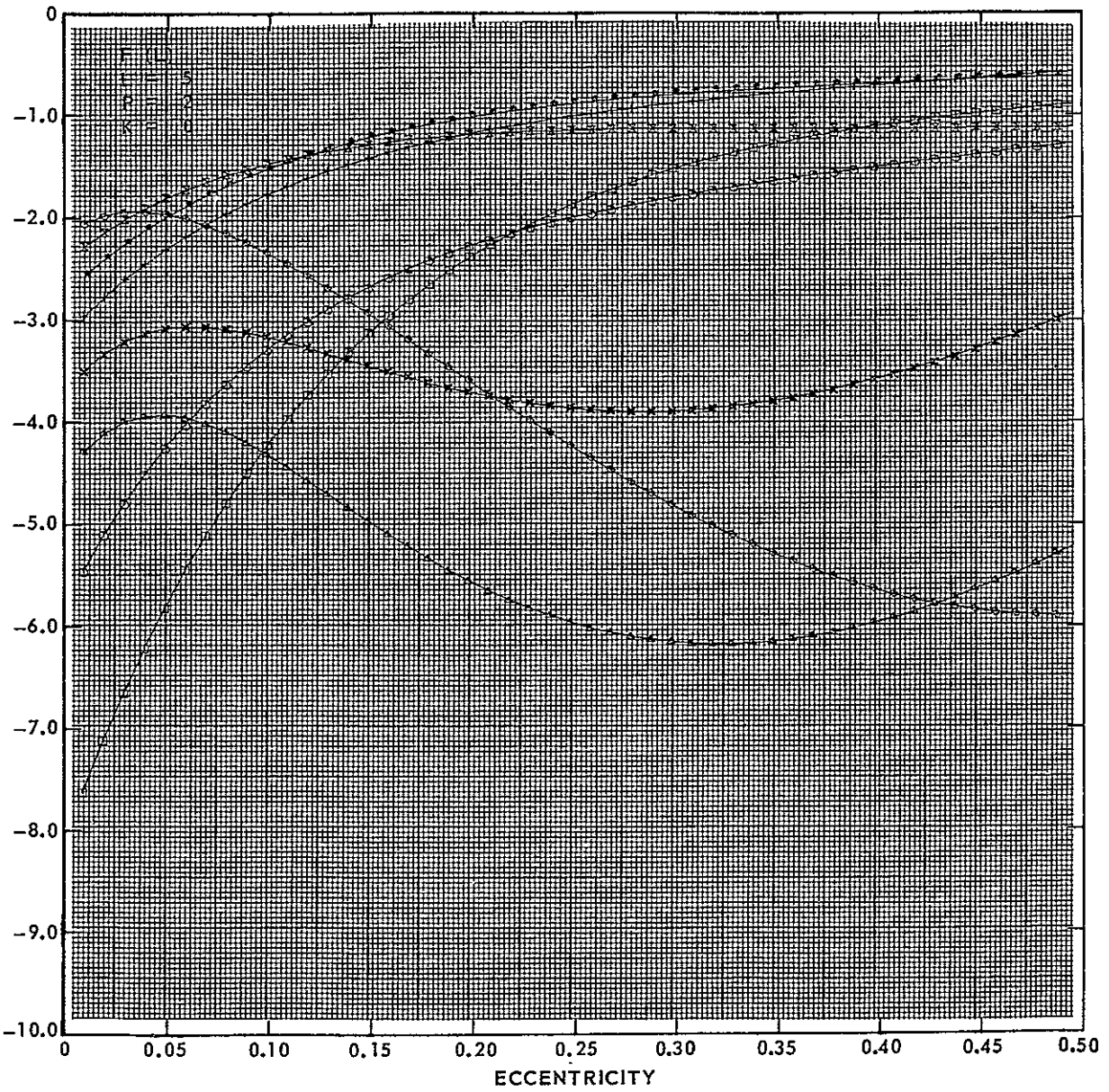
F (U)
E = .5
P = 2
K = 0
0
-1.0
-2.0
-3.0
-4.0
-5.0
-6.0
-7.0
-8.0
-9.0
-10.0
0
0.05
0.10
0.15
0.20
0.25
0.30
0.35
0.40
0.45
0.50
ECCENTRICITY

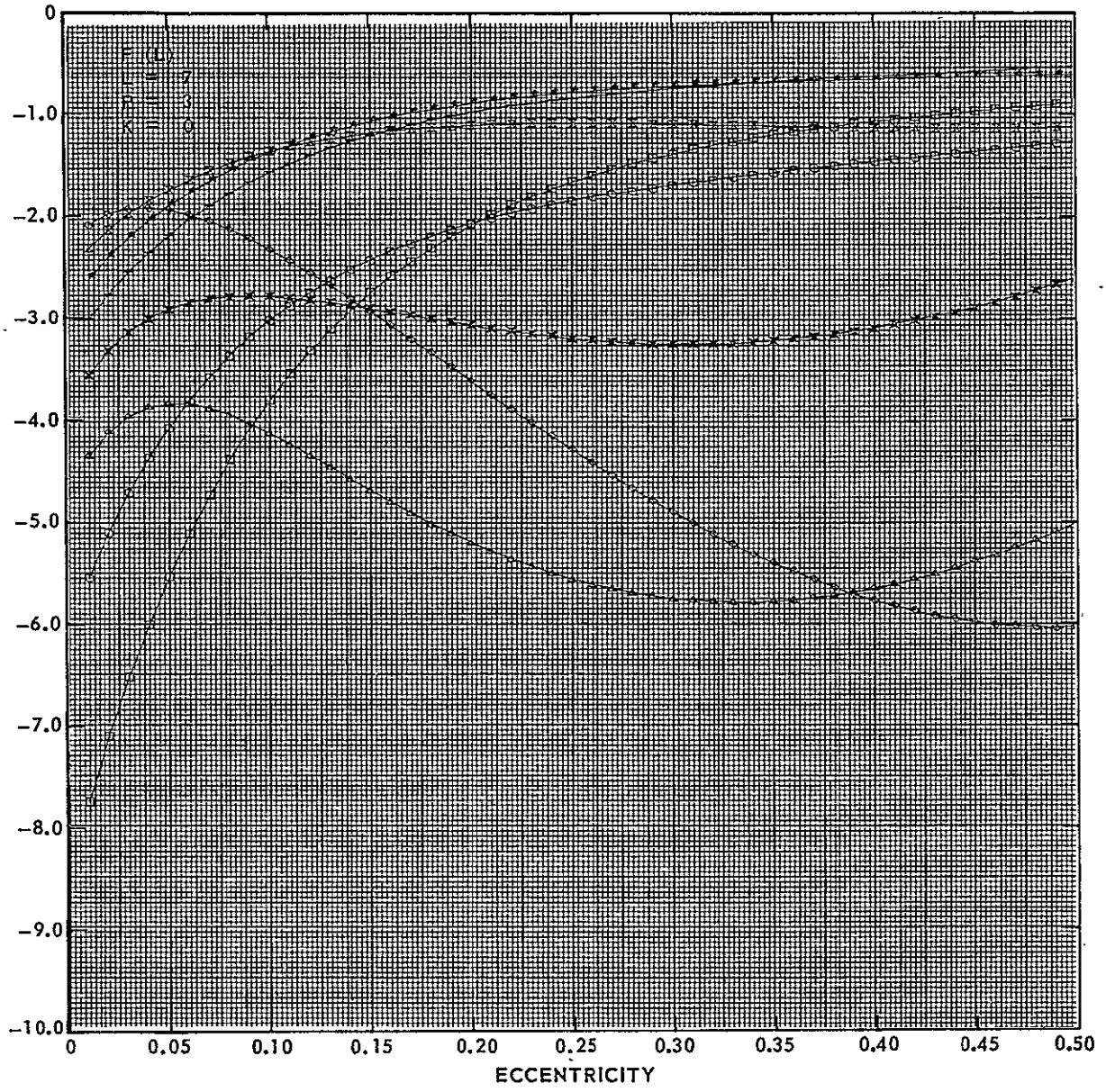
0
-1.0
-2.0
-3.0
-4.0
-5.0
-6.0
-7.0
-8.0
-9.0
-10.0
0
0.05
0.10
0.15
0.20
0.25
0.30
0.35
0.40
0.45
0.50
ECCENTRICITY

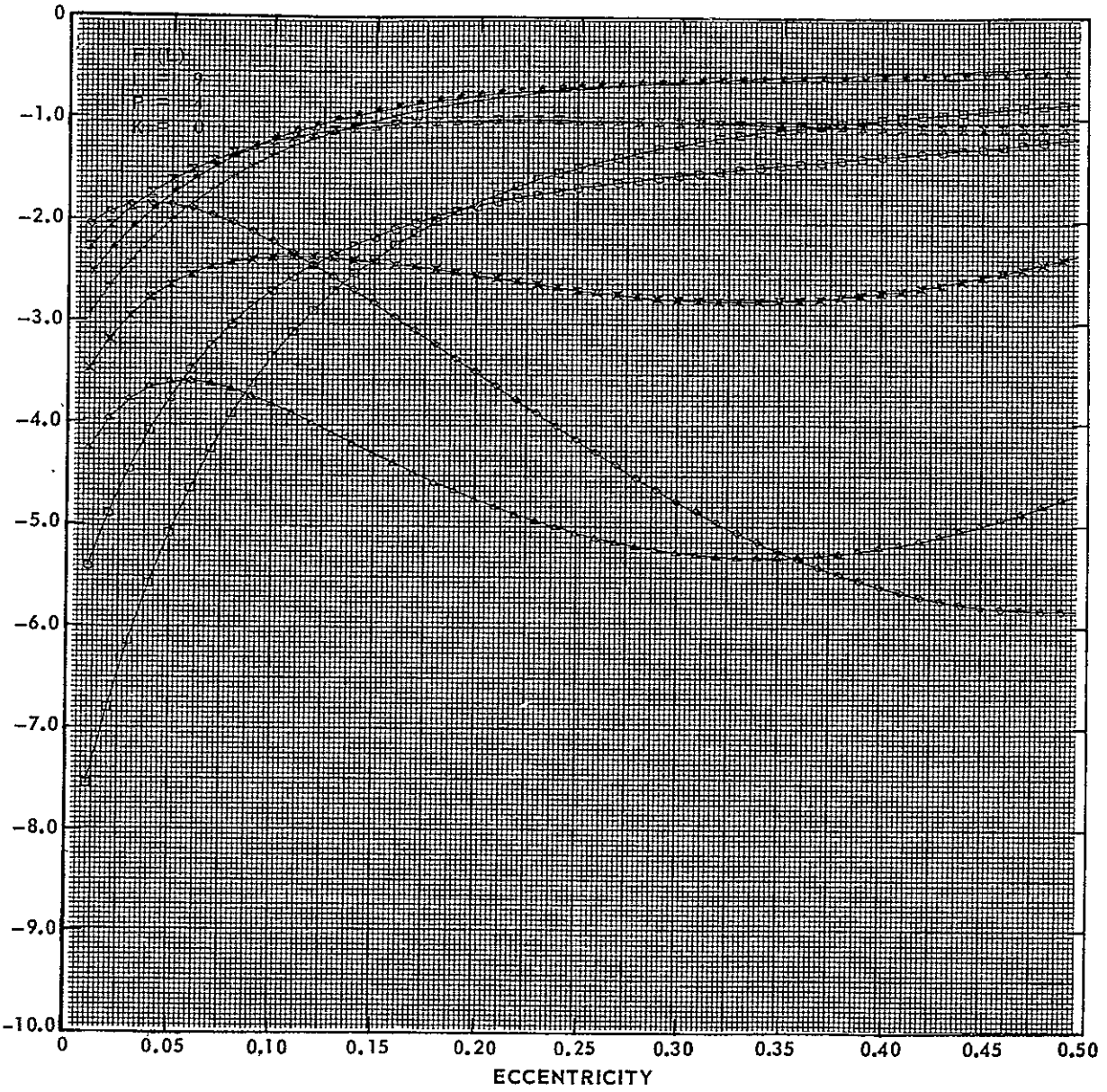
0
-1.0
-2.0
-3.0
-4.0
-5.0
-6.0
-7.0
-8.0
-9.0
-10.0
0
0.05
0.10
0.15
0.20
0.25
0.30
0.35
0.40
0.45
0.50
ECCENTRICITY

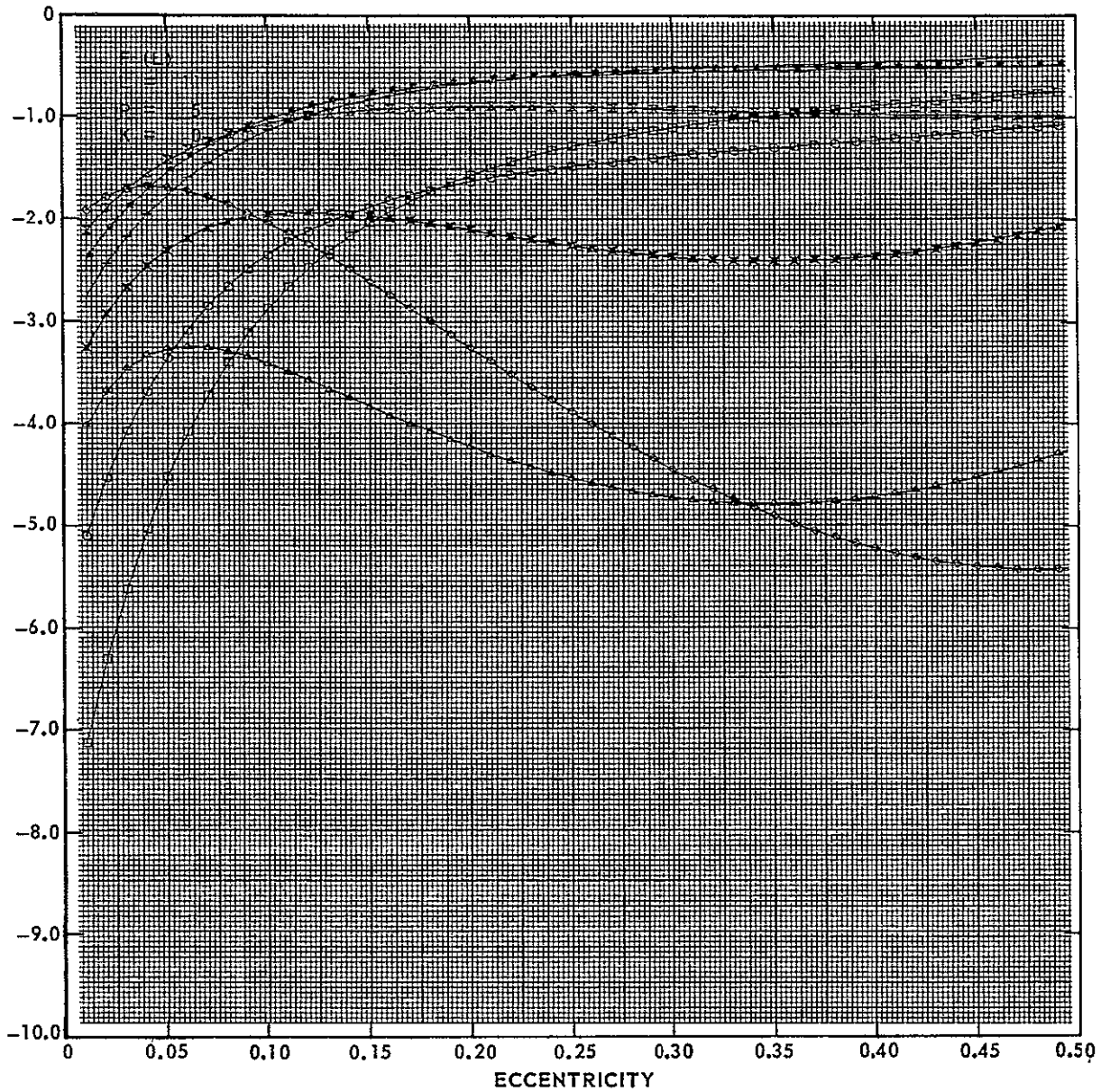
0
-1.0
-2.0
-3.0
-4.0
-5.0
-6.0
-7.0
-8.0
-9.0
-10.0
0
0.05
0.10
0.15
0.20
0.25
0.30
0.35
0.40
0.45
0.50
ECCENTRICITY

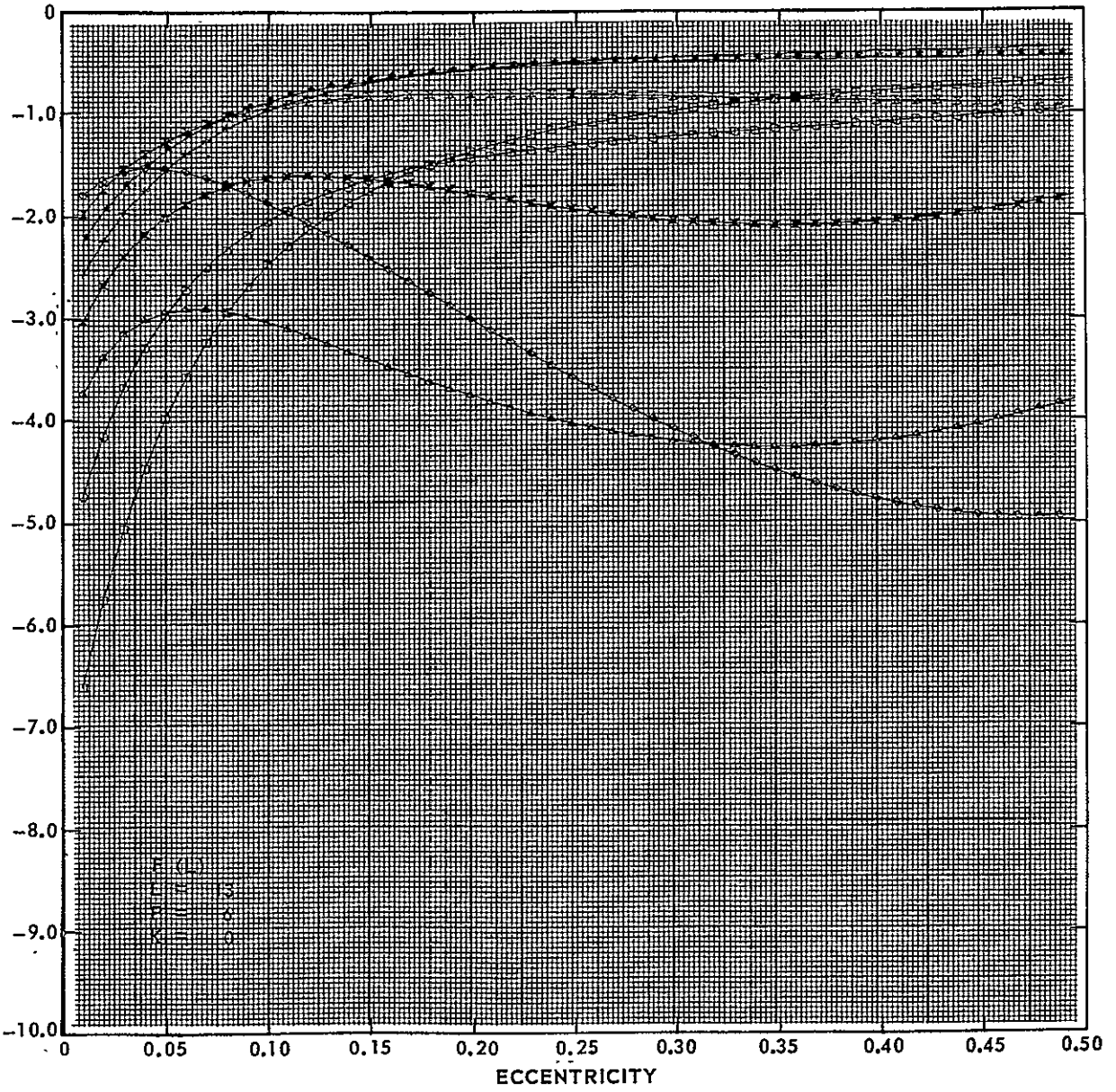
0
-1.0
-2.0
-3.0
-4.0
-5.0
-6.0
-7.0
-8.0
-9.0
-10.0
0
0.05
0.10
0.15
0.20
0.25
0.30
0.35
0.40
0.45
0.50
ECCENTRICITY

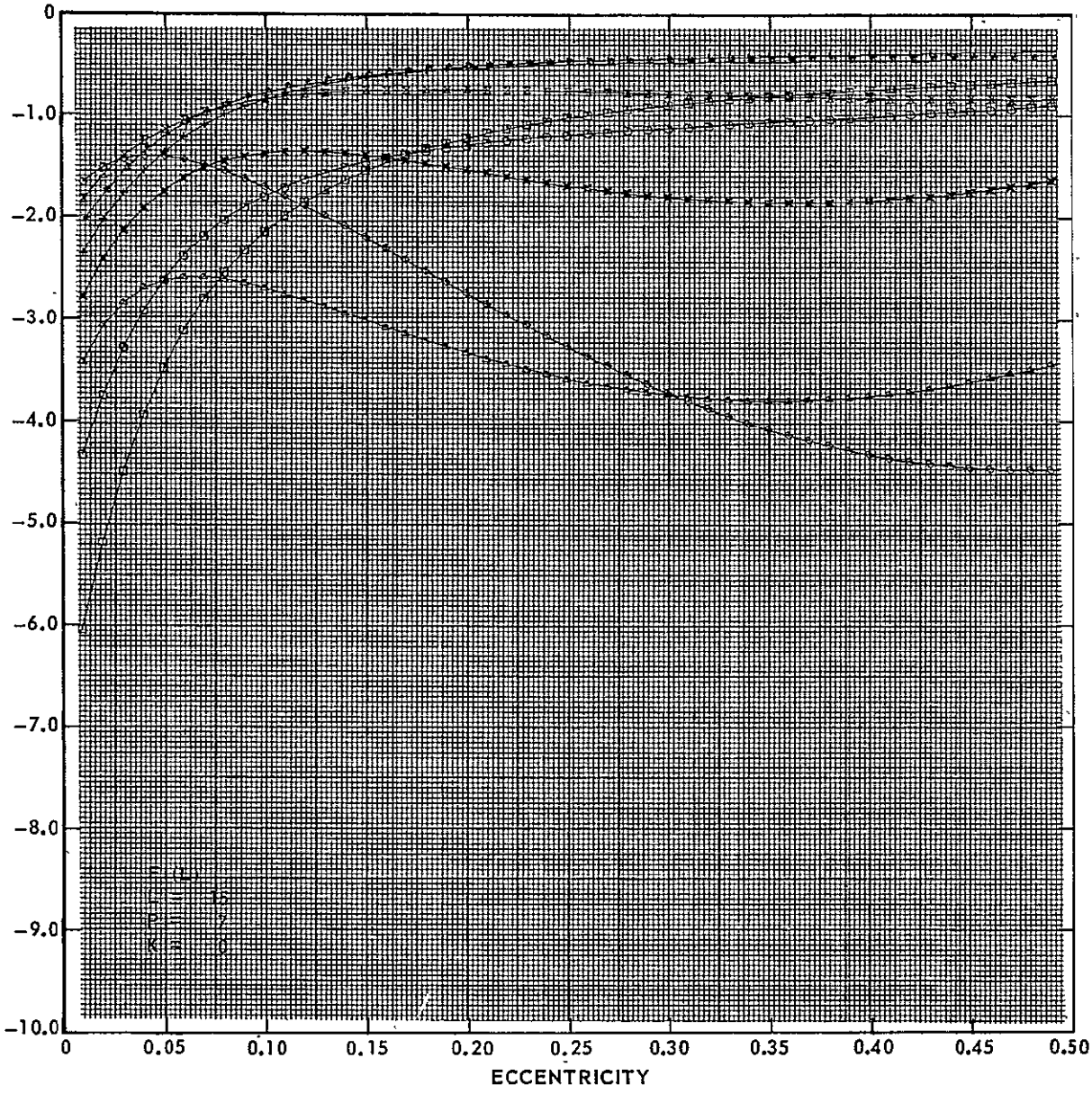
0
-1.0
-2.0
-3.0
-4.0
-5.0
-6.0
-7.0
-8.0
-9.0
-10.0
0
0.05
0.10
0.15
0.20
0.25
0.30
0.35
0.40
0.45
0.50
ECCENTRICITY

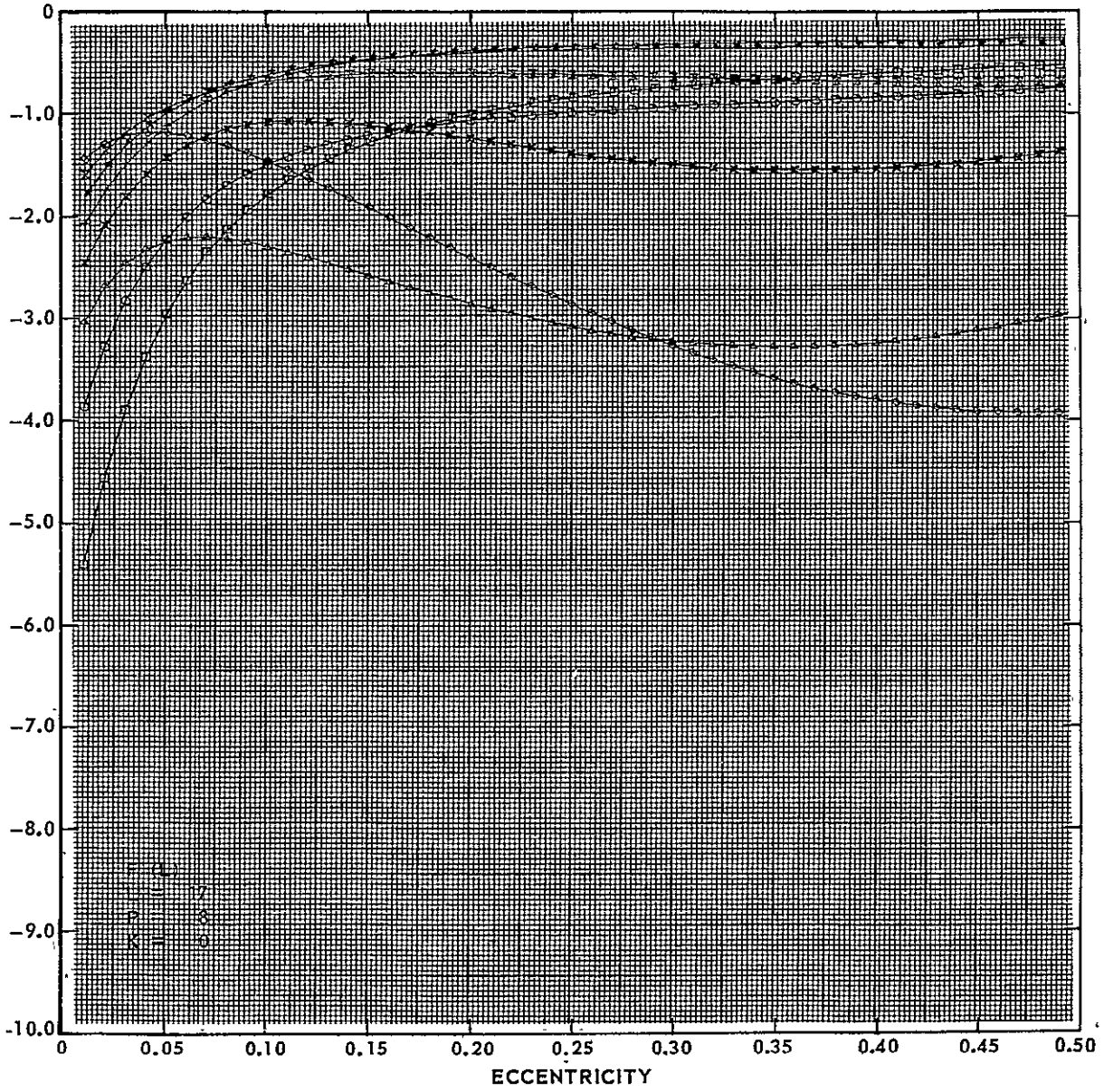
0
-1.0
-2.0
-3.0
-4.0
-5.0
-6.0
-7.0
-8.0
-9.0
-10.0
0
0.05
0.10
0.15
0.20
0.25
0.30
0.35
0.40
0.45
0.50
ECCENTRICITY

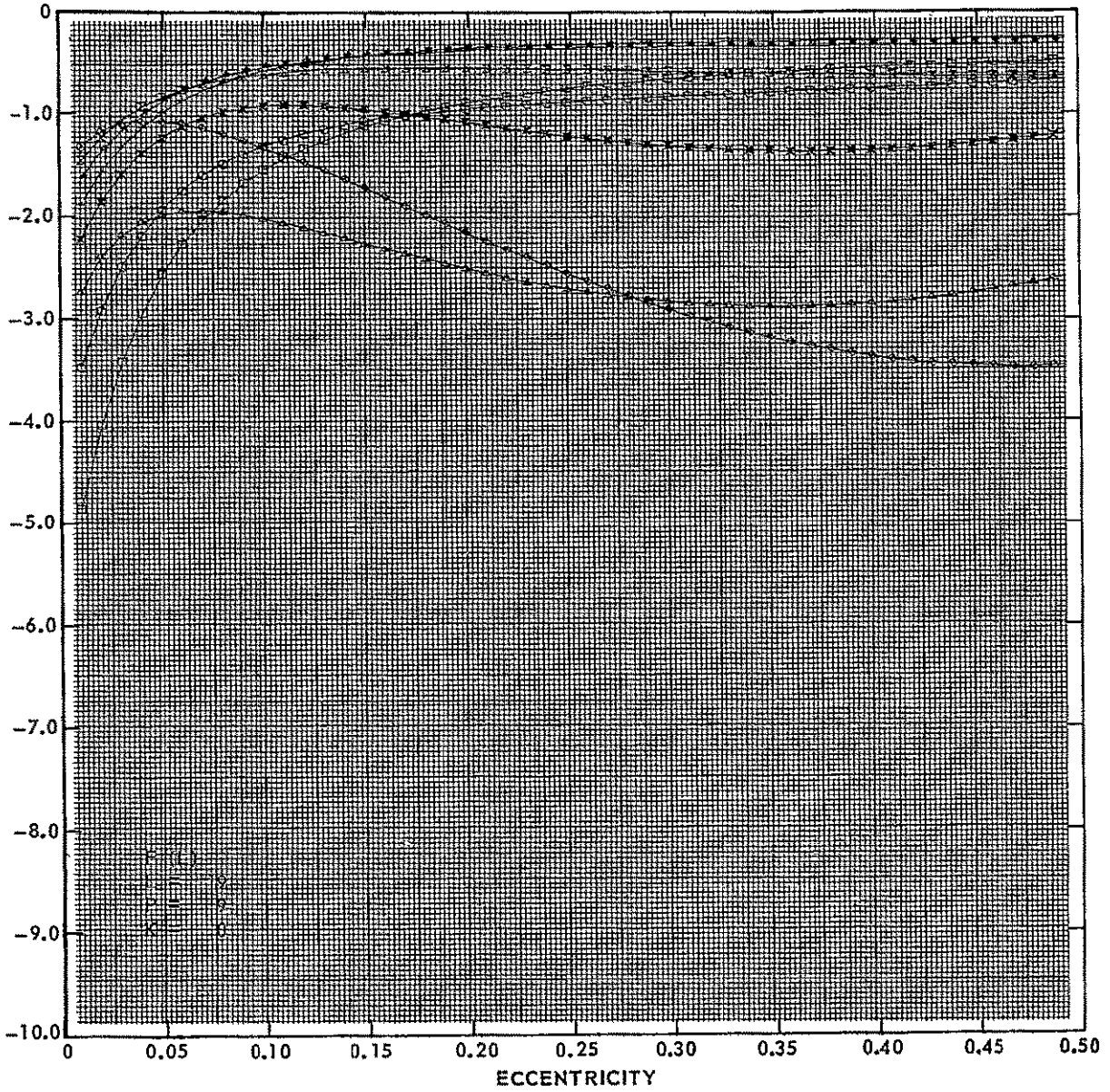
0
-1.0
-2.0
-3.0
-4.0
-5.0
-6.0
-7.0
-8.0
-9.0
-10.0
0
0.05
0.10
0.15
0.20
0.25
0.30
0.35
0.40
0.45
0.50
ECCENTRICITY

INITIAL DISTRIBUTION EXTERNAL TO THE APPLIED PHYSICS LABORATORY*

The work reported in TG-1069 was done under Navy Contract NOw 62-0604-c. This work is related to Task I44, which is supported by NASA.

ORGANIZATION	LOCATION	ATTENTION	No. of Copies
DEPARTMENT OF DEFENSE			
DDC	Alexandria, Va.		20
Department of the Navy			
NAVORDSYSCOM	Washington, D. C.	ORD-9132	2
NAVAIRSYSCOM	Washington, D. C.	AIR-604	2
		AIR-538	1
NAVPLANTREPO	Silver Spring, Md.		1
U. S. GOVERNMENT AGENCIES			
NASA	Washington, D. C.	Code SAG, J. D. Rosenberg	1

Requests for copies of this report from DoD activities and contractors should be directed to DDC, Cameron Station, Alexandria, Virginia 22314 using DDC Form 1 and, if necessary, DDC Form 55.

*Initial distribution of this document within the Applied Physics Laboratory has been made in accordance with a list on file in the APL Technical Reports Group.

UNCLASSIFIED

Security Classification

DOCUMENT CONTROL DATA - R & D

(Security classification of title, body of abstract and indexing annotation must be entered when the overall report is classified)

1 ORIGINATING ACTIVITY (Corporate author)	2a. REPORT SECURITY CLASSIFICATION
The Johns Hopkins University Applied Physics Lab. 8621 Georgia Ave. Silver Spring, Md. 20910	Unclassified
	2b. GROUP NA

3 REPORT TITLE

Investigation of the Earth's Gravitational Effects on the Motion of Near-Earth Satellites

4. DESCRIPTIVE NOTES (Type of report and inclusive dates)

Technical Memorandum

5 AUTHOR(S) (First name, middle initial, last name)

S. M. Yionoulis

6 REPORT DATE	7a. TOTAL NO OF PAGES	7b. NO OF REFS
June 1969	177	5

8a. CONTRACT OR GRANT NO.	9a. ORIGINATOR'S REPORT NUMBER(S)
NOw 62-0604-c b. PROJECT NO.	TG-1069
c.	9b. OTHER REPORT NO(S) (Any other numbers that may be assigned this report)
d.	

10. DISTRIBUTION STATEMENT

This document has been approved for public release and sale; its distribution is unlimited.

11 SUPPLEMENTARY NOTES	12 SPONSORING MILITARY ACTIVITY
This work was supported by the NASA Office of Space Science and Applications, under Task I of Contract NOw 62-0604-c.	NASA

13. ABSTRACT

The accuracy with which the Earth's gravitational field can be defined from an analysis of satellite data is strongly dependent upon the satellite constellation used. The constellation selected must satisfy several criteria. The objective of this study was to produce quantitative information on the effects of the geopotential harmonics on the motion of satellites for a large variety of orbits. These data can then be used to investigate satellite constellations that will yield useful geodetic information.

DD FORM 1 NOV 65 1473

UNCLASSIFIED

Security Classification

14. KEY WORDS

Geopotential

Satellite constellation